

**BIOTRANSFORMATION OF SYNTHETIC ABIETANE  
DITERPENES BY FILAMENTOUS FUNGI. NOVEL ROUTES  
TO THE FAMILY OF DITERPENES ISOLATED FROM  
*TRIPTERYGIUM WILFORDII***

by

Radka Koleva Milanova

B.Sc., Univ. of Plovdiv, Bulgaria, 1980

M.Sc., Univ. of Plovdiv, Bulgaria, 1982

THESIS SUBMITTED IN PARTIAL FULFILLMENT OF  
THE REQUIREMENTS FOR THE DEGREE OF  
DOCTOR OF PHILOSOPHY

in the Department

of

Biological Sciences

© Radka Koleva Milanova 1995

SIMON FRASER UNIVERSITY

January 1995

All rights reserved. This work may not be  
reproduced in whole or in part, by photocopy  
or other means, without permission of the author.

## APPROVAL

NAME: Radka Koleva Milanova

DEGREE: DOCTOR OF PHILOSOPHY

TITLE OF THESIS:

**BIOTRANSFORMATION OF SYNTHETIC ABIETANE DITERPENES BY  
FILAMENTOUS FUNGI. NOVEL ROUTES TO THE FAMILY OF DITERPENES  
ISOLATED FROM TRIPTERGIUM WILFORDII.**

Examining Committee:

Chair: Dr. B. Brandhorst

---

Dr. M. M. Moore, Assistant Professor, Senior Supervisor,  
Department of Biological Sciences, SFU

---

Dr. N. Haunerland, Associate Professor  
Department of Biological Sciences, SFU

---

Dr. ~~W~~Kutney, Professor  
Department of Chemistry, UBC

---

Dr. Z. Punja, Associate Professor  
Department of Biological Sciences, SFU

---

Dr. C. Oehlschlager, Professor  
Department of Chemistry, SFU  
Public Examiner

---

Dr. G. R. Pettit, Professor  
Department of Chemistry, Arizona State University  
External Examiner

Date Approved March 6, 1995

## PARTIAL COPYRIGHT LICENSE

I hereby grant to Simon Fraser University the right to lend my thesis, project or extended essay (the title of which is shown below) to users of the Simon Fraser University Library, and to make partial or single copies only for such users or in response to a request from the library of any other university, or other educational institution, on its own behalf or for one of its users. I further agree that permission for multiple copying of this work for scholarly purposes may be granted by me or the Dean of Graduate Studies. It is understood that copying or publication of this work for financial gain shall not be allowed without my written permission.

### Title of Thesis/Project/Extended Essay

BIOTRANSFORMATION OF SYNTHETIC ABIETANE

DITERPENES BY FILAMENTOUS FUNGI. NOVEL

ROUTES TO THE FAMILY OF DITERPENES

ISOLATED FROM TRIPTERYGIUM WILFORDII

Author: \_\_\_\_\_  
(signature)

\_\_\_\_\_  
(name)

March 6, 1995  
\_\_\_\_\_  
(date)

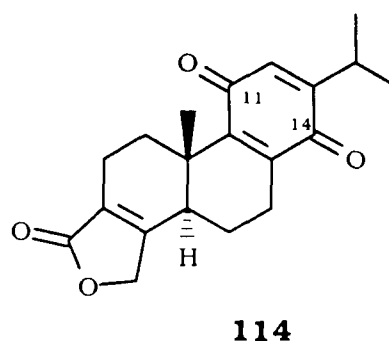
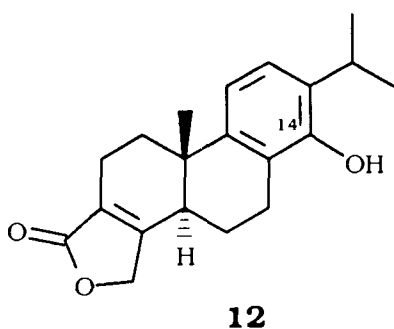
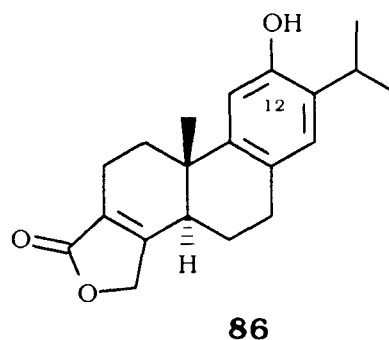
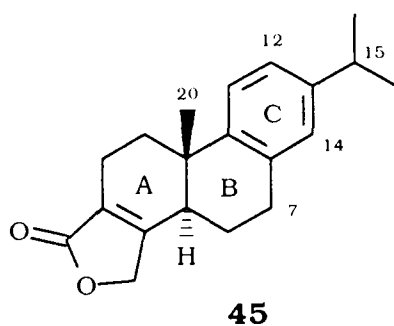
## Abstract

The studies presented in this thesis investigated the use of filamentous fungi in combination with synthetic chemistry to provide novel routes to the family of diterpenes isolated from the Chinese herbal plant, *Tripterygium wilfordii*. The isolated diterpene triepoxides, triptolide (**2**) and triptidiolide (**3**), which represent the first reported natural products containing the 18 (4->3) *abeo*-abietane skeleton, were of interest since they have been shown to possess significant anti-neoplastic and immunosuppressive activity. However, neither *T. wilfordii* plants nor plant cell cultures yield adequate material for the assessment of structure-activity relationships. Multi-step syntheses also failed to provide sufficient quantities. This thesis describes a series of experiments to functionalize the synthetic diterpene congeners, butenolide **45**, isotriptophenolide (**86**), and triptophenolide (**12**) by fungi in order to provide novel diterpene analogues which bear a close structural relationship to **2** and **3** and which may be of interest as biologically active compounds.

The substrates **45**, **86** and **12** were obtained in gram quantities via stepwise syntheses from dehydroabietic acid (**42**). These compounds were incubated with liquid cultures of the fungi *Syncephalastrum racemosum* (UBC#60), *Aspergillus fumigatus* (ATCC#13073), *Cunninghamella echinulata* (ATCC#9244), and *Cunninghamella elegans* (ATCC#20230), and the products were isolated and identified. With butenolide **45** as a substrate, the major site of fungal attack was on the B ring at C7 to afford 7-hydroxy (**101**) and 7-keto (**102**) analogues. Oxidation of C15 of the isopropyl side chain was less often observed. In contrast, the ring C "activated" substrates, isotriptophenolide (**86**) and

triptophenolide (**12**), were conjugated with glucose to yield the C12-glucosyl metabolite **112** as a major product (80%) with *C. echinulata*, and a C14-glucosyl metabolite **116** as a minor product with *C. elegans*, respectively. Selected yeast strains were unable to oxidize any of the diterpenes tested.

The major product (35%) of the oxidation of triptophenolide (**12**) by *C. elegans* resulted from the hydroxylation of the aromatic ring C which produced the 11,14-diphenolic metabolite; the latter rapidly converted to the corresponding 11,14-triptoquinone (**114**). Subsequent studies were performed to optimize the production of **114** by *C. elegans* using factorial design. The effects of medium composition and biotransformation time on triptoquinone (**114**) production were evaluated. Statistical analysis of the experimental data predicted 71% yield of triptoquinone (**114**) at optimum conditions which was verified by experiment (70% yield).



## **Acknowledgments**

I would like to express my sincere thanks to my supervisor, Dr. Margo Moore, for the opportunity to pursue this project and for her valuable advice, both during the progress of this research and in the preparation of the thesis. Her encouragement, understanding, and help in all circumstances made my life much easier and are greatly appreciated.

My gratitude is also extended to the members of her research group for their friendship, help and for making my time in the laboratory very pleasant. I would like to express my special thanks to my colleague Yousef Amaar who shared the excitement of my research and for many fruitful discussions. My thanks also to Linda, Loren, and the other colleagues for being kind and sincere to me.

I would like to thank my Committee members, Dr. Norbert Haunerland, Prof. James Kutney, and Dr. Zamir Punja, for their helpful suggestions.

My sincere thanks also go to Prof. James P. Kutney, who provided the opportunity to work in his laboratory during my study. His scientific help, assistance and excellent guidance made this endeavour very pleasant indeed. I would like to express my thanks to members of his research group (past and present) for their help, friendship and for making my time in the laboratory so enjoyable. I wish to address special thanks to Carlos Zetina-Rocha, Kang Han, and Rajina Naidu who patiently assisted my synthetic work in the Department of Chemistry, UBC.

My gratitude is also extended to Nikolay Stoynov for his constant and invaluable help, friendship and suggestions throughout my study and the writing of the thesis.

I wish to express many thanks to members of the Office of the Dean of Graduate Studies and the Department of Biological Sciences for awarding me Graduate Fellowships for five semesters of my study as well as to the Senate Graduate Awards Adjudication Committee, SFU, for awarding me the President's Ph.D. Research Stipend.

I would like to thank Dr. Jean Schmidt and Dr. Jean-Charles Chapuis at the Cancer Research Institute, Arizona State University, Tempe, Arizona for their efforts in evaluating some of the compounds obtained from this study for their cytotoxic activity.

The technical expertise of the staff in the NMR, Mass Spectroscopy, and Microanalytical Service Laboratories as well as the Mechanical, Electronics, and Glass Blowing Shops at SFU and UBC is very much appreciated.

Words cannot express my thanks to my loving son, Svetli, who has been very patient throughout the entire study and made my life so enjoyable.

Finally, I express my deep and sincere indebtedness to my parents and my sister who have always believed in me and encouraged me to pursue my studies even though it has been many miles away.

## Table of Contents

Approval .....	ii
Abstract .....	iii
Acknowledgments .....	v
Table of Contents .....	vii
List of Figures .....	xvi
List of Schemes .....	xix
List of Tables .....	xxi
List of Abbreviations .....	xxiii
Notes .....	xxvii
<b>CHAPTER I - INTRODUCTION</b> .....	1
1.1 General Introduction .....	1
1.2 Diterpenes from <i>Tripterygium species</i> .....	5
1.2.1 Isolation of Diterpenes from <i>Tripterygium species</i> .....	7
1.2.2 Biological and Pharmacological Properties of Products Derived from <i>T. wilfordii</i> .....	7
Diterpenes and Related Compounds .....	7
Preparations of Crude and Refined Extracts from <i>T. wilfordii</i> .....	16
Pharmacological Studies of Multi-Glycosides Extract (GTW) of <i>T. wilfordii</i> .....	17
Clinical Uses of Multi-Glycosides Extract (GTW) of <i>T.</i> <i>wilfordii</i> .....	18
Use of Multi-Glycosides Extract (GTW) of <i>T. wilfordii</i> as Male Contraceptive .....	19



1.2.3 Side Effects and Toxicity of Multi-Glycosides Extract (GTW) of <i>T. wilfordii</i> .....	21
Clinical Studies .....	21
Toxicity Effects on Male Fertility in Animals .....	22
1.2.4 Isolation of Diterpenes from Plant Tissue Cultures of <i>T.</i> <i>wilfordii</i> Hook F. ....	23
1.3 Microbial Transformations of Diterpenes .....	25
1.3.1 Aromatic Ring Hydroxylation and Degradation .....	26
Studies with Bacteria .....	26
Studies with Fungi .....	29
1.3.2 Fungal Oxidation of Abietane Diterpenes-Resin Acids	30
1.3.3 Oxidation of Compounds Other than Diterpenes by Fungi .....	33
1.3.4 Summary.....	39
<b>CHAPTER II - SYNTHESIS OF PRECURSORS FOR BIOTRANSFORMATION EXPERIMENTS</b> .....	40
2.1 Specific Research Objectives .....	40
2.2 Synthesis of Butenolide <b>45</b> .....	41
2.3 Synthesis of Triptophenolide ( <b>12</b> ) .....	45
2.4 Synthesis of Isotriptophenolide ( <b>86</b> ) .....	47
<b>CHAPTER III - MICROBIAL TRANSFORMATIONS OF SELECTED DITERPENE ANALOGUES</b> .....	50
3.1 General Procedure for Biotransformation Experiments	50
3.2 Studies with Butenolide <b>45</b> .....	51
Preliminary Screening Experiments .....	51
Studies with Yeast Strains .....	51
Studies with Filamentous Fungal Strains .....	53

Biotransformation of Butenolide <b>45</b> with	
<i>Syncephalastrum racemosum</i> .....	56
Effect of Growth Media on Biotransformation of	
Butenolide <b>45</b> .....	59
Time Course of Metabolism of the Butenolide <b>45</b> by	
<i>S. racemosum</i> Cultures .....	60
Effect of Cytochrome P-450 Inhibitors in Whole	
Cells on the Metabolism of Butenolide <b>45</b> to 7 $\beta$ -	
Hydroxy- and 15-Hydroxybutenolides .....	62
Biotransformation of Butenolide <b>45</b> with <i>Aspergillus</i>	
<i>fumigatus</i> .....	66
Influence of Growth Media on Biotransformation of	
Butenolide <b>45</b> .....	70
Biotransformation of Butenolide <b>45</b> with	
<i>Cunninghamella elegans</i> .....	71
3.3 Biotransformation of 7 $\beta$ -Hydroxybutenolide ( <b>101</b> ) with	
Fungi .....	78
3.4 Biotransformation of Isotriptophenolide ( <b>86</b> ) with	
<i>Cunninghamella echinulata</i> .....	78
Preliminary Screening Experiments .....	79
Detailed Studies of Isotriptophenolide	
Biotransformation by <i>C. echinulata</i> .....	79
3.5 Biotransformation of Triptophenolide ( <b>12</b> ) with	
<i>Cunninghamella elegans</i> .....	81
Preliminary Screening Experiments .....	81
Detailed Studies with <i>C. elegans</i> .....	82

Biotransformation of Triptophenolide ( <b>12</b> ) with <i>Cunninghamella echinulata</i> .....	85
Biotransformation of Triptophenolide ( <b>12</b> ) with Immobilized Cells of <i>Cunninghamella elegans</i> .....	86
3.6 Diterpene Quinones as Novel Interleukin-1 Inhibitors...	88
<b>CHAPTER IV - OPTIMIZATION OF TRIPTOQUINONE (114)</b>	
<b>PRODUCTION BY FACTORIAL DESIGN EXPERIMENT</b> .....	90
4.1 Experimental Design .....	94
Optimization Requirements of Biological Systems.....	95
Strategies for Optimization .....	97
Advantages of the Factorial Design .....	98
4.2 First Optimization of the Biotransformation of Triptophenolide ( <b>12</b> ) with <i>C. elegans</i> .....	99
Factors and Levels for Optimization .....	101
Matrix of the First Set of Experiments .....	102
Mathematical Model for Optimization .....	105
Influence of Medium Composition on Metabolite Production by <i>C. elegans</i> .....	106
Standard Curves .....	107
Time Course Experiments Relating to Metabolite Production - First Set of Experiments .....	107
Effect of Medium Composition on Biomass Production	134
4.3 Second Optimization of the Biotransformation of Triptophenolide ( <b>12</b> ) with <i>C. elegans</i> .....	140
Matrix of the Second Set of Experiments .....	141
Results from the Second Set of Experiments .....	142
4.4 A Verification Experiment .....	145

4.5 Conclusion .....	146
<b>CHAPTER V - PHARMACOLOGICAL DATA ON ANTI- NEOPLASTIC ACTIVITY OF <i>T. WILFORDII</i> CONGENERS</b> .....	
	147
<b>CHAPTER VI - SUMMARY AND OVERVIEW</b> .....	153
<b>CHAPTER VII - EXPERIMENTAL PROCEDURES</b> .....	158
7.1 Synthesis of Diterpene Analogues .....	158
7.1.1 General Experimental Procedures .....	158
7.1.2 Purification of Dehydroabietic Acid ( <b>42</b> ) .....	159
7.1.3 Synthesis of 18-Norabieta-4(19),8,11,13-tetraene ( <b>91</b> ) (Exo-olefin) .....	160
Acid Chloride <b>87</b> .....	160
Isocyanate <b>88</b> .....	161
Monomethylamine <b>89</b> .....	162
Dimethylamine <b>90</b> .....	163
Exo-olefin <b>91</b> .....	164
7.1.4 Synthesis of 18,19-Dinorabieta-8,11,13-trien-4-one ( <b>92</b> ) (Ketone) .....	165
7.1.5 Synthesis of 3-Dimethylthiomethylene-18,19- dinorabieta-8,11,13-trien-4-one ( <b>93</b> ) (Ketene Thioketal)	167
7.1.6 Synthesis of 19-Hydroxy-18 (4->3) <i>abeo</i> -abieta- 3,8,11,12-tetraen-18-oic Acid Lactone ( <b>45</b> ) .....	168
7.1.7 Synthesis of Triptophenolide ( <b>12</b> ) from Lactone <b>45</b> .....	170
Synthesis of 19-Hydroxy-12,14-dinitro-18 (4->3) <i>abeo</i> - abieta-3,8,11,13-tetraen-18-oic Acid Lactone ( <b>96</b> ) .....	170
Synthesis of 12-Amino-19-hydroxy-14-nitro-18 (4->3) <i>abeo</i> -abieta-3,8,11,13-tetraen-18-oic Acid Lactone ( <b>97</b> )	172

Synthesis of 14,19-Dihydroxy-12-iodo-18 (4->3) <i>abeo</i> -abieta-3,8,11,13-tetraen-18-oic Acid Lactone ( <b>98</b> ) .....	173
Synthesis of 14-Amino-19-hydroxy-12-iodo-18 (4->3) <i>abeo</i> -abieta-3,8,11,13-tetraen-18-oic Acid Lactone ( <b>99</b> ) .....	174
Synthesis of 14,19-Dihydroxy-12-iodo-18 (4->3) <i>abeo</i> -abieta-3,8,11,13-tetraen-18-oic Acid Lactone ( <b>100</b> ) ....	176
Synthesis of 14,19-Dihydroxy-18 (4->3) <i>abeo</i> -abieta-3,8,11,13-tetraen-18-oic Acid Lactone ( <b>12</b> ) (Tryptophenolide) .....	177
7.2 Biotransformation Studies .....	179
7.2.1 General Experimental Procedures .....	179
7.2.2 Experimental Procedure for Biotransformation of Butenolide <b>45</b> by <i>Syncephalastrum racemosum</i> .....	181
Fungal Material .....	181
Growth Conditions .....	181
Isolation and Purification of Metabolites .....	182
Identification of Metabolites .....	183
7 $\beta$ ,19-Dihydroxy-18 (4->3) <i>abeo</i> -abieta-3,8,11,13-tetraen-18-oic Acid Lactone ( <b>101</b> ) (7 $\beta$ -Hydroxybutenolide) .....	184
19-Hydroxy-7-oxo-18 (4->3) <i>abeo</i> -abieta-3,8,11,13-tetraen-18-oic Acid Lactone ( <b>102</b> ) (7-Ketobutenolide) .....	185
15,19-Dihydroxy-18 (4->3) <i>abeo</i> -abieta-3,8,11,13-tetraen-18-oic Acid Lactone ( <b>103</b> ) (15-Hydroxybutenolide) .....	185

7 $\alpha$ , 19-Dihydroxy- 18 (4->3) <i>abeo</i> -abieta-3,8, 11, 13-tetraen- 18-oic Acid Lactone ( <b>104</b> ) (7 $\alpha$ -Hydroxybutenolide) .....	186
Effect of Cytochrome P-450 Inhibitors on Hydroxylation of <b>45</b> .....	187
7.2.3 Experimental Procedures for Biotransformation of	
Butenolide <b>45</b> by <i>Aspergillus fumigatus</i> and <i>Cunninghamella elegans</i> .....	188
Fungal Material .....	188
Growth Conditions .....	188
Isolation and Purification of Metabolites .....	189
Identification of Metabolites .....	192
5 $\alpha$ , 7 $\alpha$ , 19-Trihydroxy- 18 (4->3) <i>abeo</i> -abieta-3,8, 11, 13-tetraen- 18-oic Acid Lactone ( <b>105</b> ) .....	192
5 $\alpha$ , 7 $\beta$ , 19-Trihydroxy- 18 (4->3) <i>abeo</i> -abieta-3,8, 11, 13-tetraen- 18-oic Acid Lactone ( <b>106</b> ) .....	193
5 $\alpha$ , 16, 19-Trihydroxy- 18 (4->3) <i>abeo</i> -abieta-3,8, 11, 13-tetraen- 18-oic Acid Lactone ( <b>107</b> ) .....	194
7 $\alpha$ , 15, 19-Trihydroxy- 18 (4->3) <i>abeo</i> -abieta-3,8, 11, 13-tetraen- 18-oic Acid Lactone ( <b>108</b> ) .....	195
7 $\beta$ , 15, 19-Trihydroxy- 18 (4->3) <i>abeo</i> -abieta-3,8, 11, 13-tetraen- 18-oic acid Lactone ( <b>109</b> ) .....	195
7 $\beta$ , 16, 19-Trihydroxy- 18 (4->3) <i>abeo</i> -abieta-3,8, 11, 13-tetraen- 18-oic Acid Lactone ( <b>110</b> ) .....	196
7 $\alpha$ , 16, 19-Trihydroxy- 18 (4->3) <i>abeo</i> -abieta-3,8, 11, 13-tetraen- 18-oic Acid Lactone ( <b>111</b> ) .....	197

7.2.4	Experimental Procedures for Biotransformation of Isotriptophenolide ( <b>86</b> ) by <i>Cunninghamella echinulata</i> and Triptophenolide ( <b>12</b> ) by <i>Cunninghamella elegans</i>	198
	Fungal Material .....	198
	Growth Conditions .....	198
	Isolation and Purification of Metabolites .....	199
	Identification of Metabolites .....	201
	12- $\beta$ -Glucosyl-19-hydroxy-18 (4->3) <i>abeo</i> -abieta- 3,8,11,13-tetraen-18-oic acid Lactone ( <b>112</b> ) (12- $\beta$ - Glucosyl Isotriptophenolide) .....	201
	19-Hydroxy-11,14-dioxo-18 (4->3) <i>abeo</i> -abieta-3,8,12- trien-18-oic Acid Lactone ( <b>114</b> ) (Triptoquinone) .....	202
	5 $\alpha$ ,14,19-Trihydroxy-18 (4->3) <i>abeo</i> -abieta-3,8,11,13- tetraen-18-oic Acid Lactone ( <b>115</b> ) (5 $\alpha$ ,14- Dihydroxybutenolide) .....	203
	14- $\beta$ -Glucosyl-19-hydroxy-18 (4->3) <i>abeo</i> -abieta- 3,8,11,13-tetraen-18-oic-acid Lactone ( <b>116</b> ) (14- $\beta$ - Glucosyl Triptophenolide) .....	204
7.2.5	Experimental Procedure for Immobilization of <i>C. elegans</i> in Polyurethane Foam .....	205
	Growth Conditions .....	205
	Metabolite Formation .....	206
7.2.6	Experimental Procedure for Optimization of Triptoquinone ( <b>114</b> ) Production by Factorial Design	
	Experiment .....	207
	Basic Experiment .....	207
	Media Preparation .....	207

HPLC Analyses .....	209
Materials .....	211
Standard Compounds .....	211
Sample Preparation for HPLC Analyses .....	211
<b>APPENDIX. FACTORIAL DESIGN</b> .....	213
A.1 Polynomial Models .....	215
A.2 Evaluation of the Coefficients in the Mathematical Model .....	216
A.3 Significant Coefficients .....	231
A.4 Optimization Procedure .....	232
A.5 Linear Regression for the Equations of the Standard Curves .....	233
<b>REFERENCES</b> .....	237



## List of Figures

Figure 1. TLC Analysis for the Time Course of Incubation of <b>45</b> with <i>S. racemosum</i> . (Schematic Presentation) .....	61
Figure 2. Influence of pH and Culture Age on the Biotransformation of Butenolide <b>45</b> with <i>Aspergillus fumigatus</i> .....	68
Figure 3. Yield of 7 $\beta$ -Hydroxylactone ( <b>101</b> ) after 48 Hours Incubation Using a Different Initial Concentration of Butenolide <b>45</b> .....	69
Figure 4. Standard Curve for Triptophenolide ( <b>12</b> ) .....	108
Figure 5. Standard Curve for Triptoquinone ( <b>114</b> ) .....	109
Figure 6. Standard Curve for 5 $\alpha$ ,14-Dihydroxybutenolide ( <b>115</b> ) .....	110
Figure 7. Standard Curve for 14- $\beta$ -Glucosyl Triptophenolide ( <b>12</b> ) .....	111
Figure 8. HPLC Profile of the Substrate <b>12</b> and the Products from the Biotransformation with <i>C. elegans</i> .....	112
Figure 9. Time Course of Biotransformation of Triptophenolide ( <b>12</b> ) to <b>114</b> , <b>115</b> and <b>116</b> in Medium Composition 1 .....	115
Figure 10. Time Course of Biotransformation of Triptophenolide ( <b>12</b> ) to <b>114</b> , <b>115</b> and <b>116</b> in Medium Composition 2 .....	116
Figure 11. Time Course of Biotransformation of Triptophenolide ( <b>12</b> ) to <b>114</b> , <b>115</b> and <b>116</b> in Medium Composition 3 .....	117
Figure 12. Time Course of Biotransformation of Triptophenolide ( <b>12</b> ) to <b>114</b> , <b>115</b> and <b>116</b> in Medium Composition 4 .....	118
Figure 13. Time Course of Biotransformation of Triptophenolide ( <b>12</b> ) to <b>114</b> , <b>115</b> and <b>116</b> in Medium Composition 5 .....	119

Figure 14. Time Course of Biotransformation of Triptophenolide ( <b>12</b> ) to <b>114</b> , <b>115</b> and <b>116</b> in Medium Composition 6	120
Figure 15. Time Course of Biotransformation of Triptophenolide ( <b>12</b> ) to <b>114</b> , <b>115</b> and <b>116</b> in Medium Composition 7	121
Figure 16. Time Course of Biotransformation of Triptophenolide ( <b>12</b> ) to <b>114</b> , <b>115</b> and <b>116</b> in Medium Composition 8	122
Figure 17. Time Course of Biotransformation of Triptophenolide ( <b>12</b> ) to <b>114</b> , <b>115</b> and <b>116</b> in Medium Composition 9	123
Figure 18. Time Course of Biotransformation of Triptophenolide ( <b>12</b> ) to <b>114</b> , <b>115</b> and <b>116</b> in Medium Composition 10	124
Figure 19. Time Course of Biotransformation of Triptophenolide ( <b>12</b> ) to <b>114</b> , <b>115</b> and <b>116</b> in Medium Composition 11	125
Figure 20. Time Course of Biotransformation of Triptophenolide ( <b>12</b> ) to <b>114</b> , <b>115</b> and <b>116</b> in Medium Composition 12	126
Figure 21. Time Course of Biotransformation of Triptophenolide ( <b>12</b> ) to <b>114</b> , <b>115</b> and <b>116</b> in Medium Composition 13	127
Figure 22. Time Course of Biotransformation of Triptophenolide ( <b>12</b> ) to <b>114</b> , <b>115</b> and <b>116</b> in Medium Composition 14	128
Figure 23. Time Course of Biotransformation of Triptophenolide ( <b>12</b> ) to <b>114</b> , <b>115</b> and <b>116</b> in Medium Composition 15	129
Figure 24. Influence of the Glucose Concentration and the Biotransformation Time on the Yield of Triptoquinone ( <b>114</b> ) at the Optimum Values of the Other Factors (Nutrient Broth and Malt Extract) .....	132

Figure 25. Influence of the Nutrient Broth and Malt Extract Concentrations on the Yield of Triptoquinone ( <b>114</b> ) at the Optimum Values of the Other Factors (Glucose Concentration and the Biotransformation Time) .....	133
Figure 26. Yield of Biomass (Fresh and Dry Weight) in Different Media .....	138
Figure 27. Influence of the Glucose Concentration and the Biotransformation Time on the Yield of Triptoquinone ( <b>114</b> ) at the Optimum Values of the Other Factors (Nutrient Broth and Malt Extract) .....	143
Figure 28. Compounds Tested for Potential Anti-neoplastic Activity .....	147
Figure 29. Thin Layer Chromatogram of the Metabolites Isolated from Biotransformation of <b>45</b> by <i>S. racemosum</i> .....	182
Figure 30. Thin Layer Chromatogram of the Metabolites Isolated from Biotransformation of <b>12</b> by <i>C. elegans</i> (Schematic Presentation) .....	200
Figure 31. Four-Factor, Single Response System .....	213

## List of Schemes

Scheme 1. Ideal Interactions Between Substrate and Cell .....	3
Scheme 2. Alkylation of Thiols by the Diterpene Triepoxides <i>via</i> Hydroxyl-assisted Epoxide Ring Opening .....	13
Scheme 3. Biodegradation of Dehydroabietic Acid ( <b>42</b> ) with <i>Flavobacterium resinovorum</i> .....	27
Scheme 4. Biodegradation of Methyl Dehydroabietate ( <b>54</b> ) with <i>Arthrobacter sp.</i> .....	28
Scheme 5. Biotransformation of Methyl Dehydroabietate ( <b>54</b> ) with <i>Corticium sasakii</i> .....	29
Scheme 6. Biotransformation of Methyl 7-Keto-Dehydroabietate ( <b>59</b> ) with <i>Corticium sasakii</i> .....	30
Scheme 7. Biotransformation of Dehydroabietic Acid ( <b>42</b> ) with <i>Mortierella isabellina</i> .....	31
Scheme 8. Oxidation of Benzene by Prokaryotic and Eukaryotic Organisms .....	36
Scheme 9. Aromatic Hydroxylation of Naphthalene ( <b>71</b> ) by Fungi .....	37
Scheme 10. Hydroxylation of Acenaphthene ( <b>80</b> ) by <i>Cunninghamella echinulata</i> .....	38
Scheme 11. Hydroxylation of Phenanthrene ( <b>83</b> ) by fungi .....	39
Scheme 12. Synthesis of Butenolide <b>45</b> from Dehydroabietic Acid ( <b>42</b> ) .....	42

Scheme 13. Synthesis of Triptophenolide ( <b>12</b> ) from Butenolide <b>45</b> .....	46
Scheme 14. The Synthesis of Isotriptophenolide ( <b>86</b> ) from Butenolide <b>45</b> .....	48
Scheme 15. Chromatographic Separation of Crude Ethyl Acetate Extract (Broth + Cell) of Biotransformation of <b>45</b> with <i>S. racemosum</i> .....	57
Scheme 16. Biotransformation of Butenolide <b>45</b> with <i>S.</i> <i>racemosum</i> .....	58
Scheme 17. Biotransformation of Butenolide <b>45</b> with <i>Aspergillus</i> <i>fumigatus</i> .....	67
Scheme 18. Chromatographic Separation of Crude Ethyl Acetate Extract (Broth) of Biotransformation of <b>45</b> with <i>C.</i> <i>elegans</i> .....	73
Scheme 19. Chromatographic Separation of Crude Ethyl Acetate Extract (Cells) of Biotransformation of <b>45</b> with <i>C.</i> <i>elegans</i> .....	74
Scheme 20. Biotransformation of Butenolide <b>45</b> with <i>Cunninghamella elegans</i> .....	75
Scheme 21. Biotransformation of Isotriptophenolide ( <b>86</b> ) with <i>Cunninghamella echinulata</i> .....	80
Scheme 22. Biotransformation of Triptophenolide ( <b>12</b> ) with <i>Cunninghamella elegans</i> .....	83, 100
Scheme 23. Extraction Procedure for <i>C. elegans</i> Suspension Culture .....	191

## List of Tables

Table 1. Reported Diterpenoids from <i>Tripterygium species</i> .....	9
Table 2. Yeasts Screened for Ability to Biotransform Butenolide <b>45</b> .....	52
Table 3. Filamentous Fungi Screened for Ability to Biotransform Butenolide <b>45</b> .....	54
Table 4. The Effects of Cytochrome P-450 Inhibitors on the Oxidation of Butenolide <b>45</b> by <i>S. racemosum</i> to 7 $\alpha$ - Hydroxy- ( <b>104</b> ) and 15-Hydroxylactone ( <b>103</b> ) .....	63
Table 5. Pertinent <sup>1</sup> H-NMR Data of Butenolide Metabolites Produced by <i>C. elegans</i> .....	77
Table 6. Factor Settings for the First Set of Experiments .....	103
Table 7. First Factorial Design Experiment Showing Selected Factors (Parameters) and Their Levels .....	104
Table 8. Summary of Optimum Conditions and Yields of Metabolites .....	134
Table 9. Experiments with Different Medium Composition .....	135
Table 10. Changes in pH During Growth of <i>C. elegans</i> and Final Biomass Yields .....	137
Table 11. Factor Settings for the Second Set of Experiments ....	142
Table 12. Second Factorial Design Experiment Showing Selected Factors (Parameters) and Their Levels .....	144
Table 13. Evaluation of Compounds in the Murine P388 Lymphocytic Leukaemia System .....	149

Table 14. Evaluation of Compounds for Activity in Human Cancer Cell Lines Grown <i>in vitro</i> .....	151
Table 15. Medium Preparation for the First Factorial Design Experiment .....	208
Table 16. Medium Preparation for the Second Factorial Design Experiment .....	210
Table 17. Factorial Design Showing the Factors (Parameters) and Their Levels .....	223
Table 18. Sums Necessary for Evaluation of the Coefficients of Equations 2 to 7 (Chapter IV) .....	229
Table 19. Coefficients of Equations 2 to 7 (Chapter IV) .....	230

## List of Abbreviations

Å	Angström
Ac	acetyl
br	broad
brd	broad doublet
brs	broad singlet
CIMS	chemical ionization mass spectrum
COSY	2-dimensional correlated NMR spectroscopy
d	doublet
dd	doublet of doublets
DHA	dehydroabiatic acid
DMF	dimethylformamide
EC <sub>50</sub>	median effective concentration (the concentration of a compound required to produce a specified effect in 50% of the population)
ED <sub>50</sub>	median effective dose (the dose of a compound required to produce a specified effect in 50% of the population)
eq	equivalent
Et	ethyl
Fr	fraction
g	gram
GI <sub>50</sub>	Concentration of compound required to cause 50% growth inhibition (µg/mL)
GTW	refined plant extract of <i>T. wilfordii</i> described as multi-glucoside extract



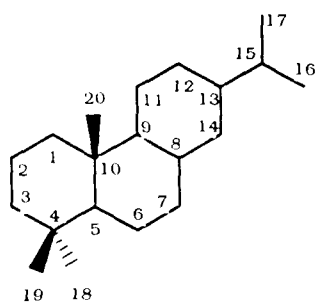
h	hour
hex.	generally a mixture of several isomers of hexane (C <sub>6</sub> H <sub>14</sub> ) predominantly n-hexane and methylcyclopentane (C <sub>6</sub> H <sub>12</sub> )
HPLC	high pressure liquid chromatography
HRMS	high resolution mass spectrum
IR	infra-red
J	coupling constant
KB	a tissue culture cell line derived from human epidermoid carcinoma of the nasopharynx-type 9KB-5
L	litre
L-1210	a tissue culture cell line derived from mice lymphoid leukaemia
LAH	lithium aluminum hydride
LD <sub>50</sub>	median lethal dose (effective dose at which 50% of animals are killed)
log ε	decimal log of extinction coefficient
m	multiplet
M	molar
M <sup>+</sup>	molecular ion
max	maximum
MCPBA	<i>meta</i> -chloroperbenzoic acid
Me	methyl
m.f.	molecular formula
mg	milligram
MHz	megahertz
min	minute

MNB	malt nutrient broth
mol	mole
mp	melting point
m/z	mass to charge ratio
nm	nanometer
NMR	nuclear magnetic resonance
NOE	nuclear Overhauser effect
P-388	a tissue culture cell line derived from mice leukaemia cells
PDA	potato-dextrose agar
PDB	potato-dextrose broth
ppm	parts per million
q	quartet
s	singlet
SSBF	soya bean flour containing 1% fat
t	triplet
TFA	trifluoroacetic acid
TGI	total growth inhibition
THF	tetrahydrofuran
TLC	thin-layer chromatography
TMS	tetramethylsilane
UV	ultraviolet
v/v	volume to volume ratio
YPD	yeast peptone dextrose agar
°C	degree Celsius
$[\alpha]_D^{20}$	specific rotation recorded at 20° C using sodium D-line

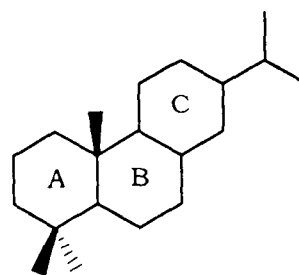
$\delta$	chemical shift
$\Delta$	heat
$\lambda$	wavelength
$\mu\text{L}$	microliter
$\mu\text{M}$	micromole
$\nu$	wave number ( $\text{cm}^{-1}$ )

## NOTES

The numbering system used throughout this thesis is that utilized by natural product chemists and is illustrated below. The lettering of the rings is given in alphabetical order and proceeds from left to right across the structure.

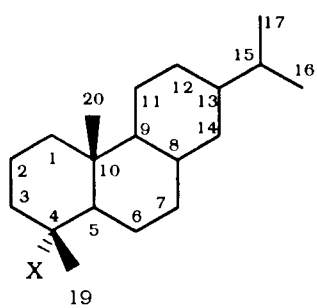


Abietane

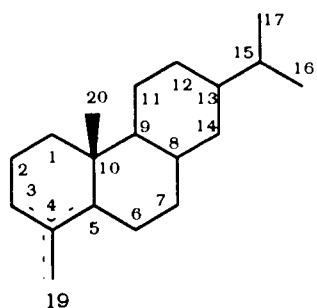


It should be noted that the classical abietane system possesses two methyl groups (C-18 and C-19) attached at C-4. However, natural diterpenes are known in which one of the C-4 methyl groups has been transferred to C-3 or eliminated from C-4. In these cases, the prefixes *nor* and *abeo* are utilized as shown below.

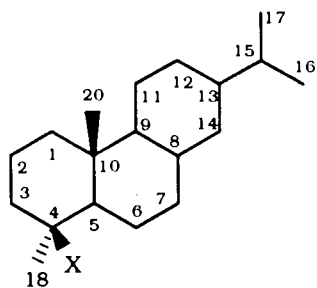
The abietane skeleton is designated as 18-nor if C-18 is absent or if a double bond is present at C-3 or C-4, and as 19-nor if the remaining methyl group at C-4 is  $\alpha$ . The rearranged abietane skeleton is designated as 18 (4->3) *abeo* except if the C-4 methyl group is  $\alpha$ , then the skeleton is designated as 19 (4->3) *abeo*.



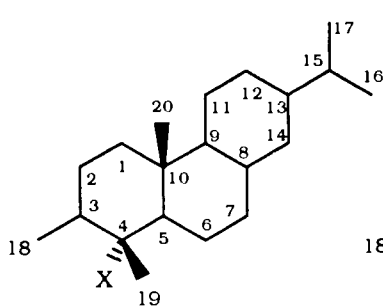
18-Nor



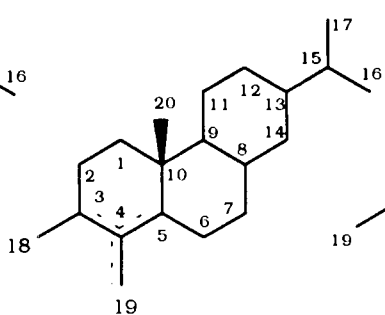
18-Nor



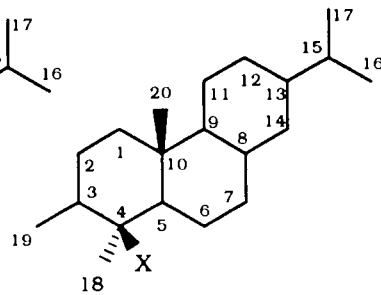
19-Nor



18 (4->3) abeo



18 (4->3) abeo



19 (4->3) abeo

# CHAPTER I -- INTRODUCTION

## 1.1 General Introduction

"Biotechnology is the integrated use of natural sciences (biology incl. molecular biology, biochemistry, chemistry, physics) and engineering sciences (chemical engineering, electronics) in order to achieve the application of microorganisms, plant and animal cells, parts thereof and molecular analogues so as to provide society with desirable goods and services" (Moser 1988).

Biotechnology has been widely used since the early days of mankind; microbial transformations in particular were used in the production of bread, dairy products, and alcoholic beverages. All of these early applications used mixed cultures of microorganisms and generally pertained to agriculture and human nutrition.

More recently, microorganisms have been employed in the production of industrially important materials, including fine chemicals (e.g. pharmaceuticals) and bulk chemicals, and the manufacture of single cell protein from diverse substrates. The research in this thesis concerned bioconversion, therefore, the following discussion will be confined to this area.

Although hundreds of different bioconversions have been described, they are only used commercially when conventional chemical approaches are too costly or difficult. For example, when a stereoselective transformation is required, often at a chemically inactive site, or when only one of many identical functional groups in a molecule is to be modified, the use of "biological" reagents versus direct chemical

conversions is a much preferred approach. Microorganisms are also used to effect transformations not conveniently achieved by chemical methods. In this case, the product is not a normal metabolite of the cell but is produced as a result of enzymatic conversion of an unusual substrate added to the culture medium. Often such substrates cannot support growth, they simply undergo bioconversion.

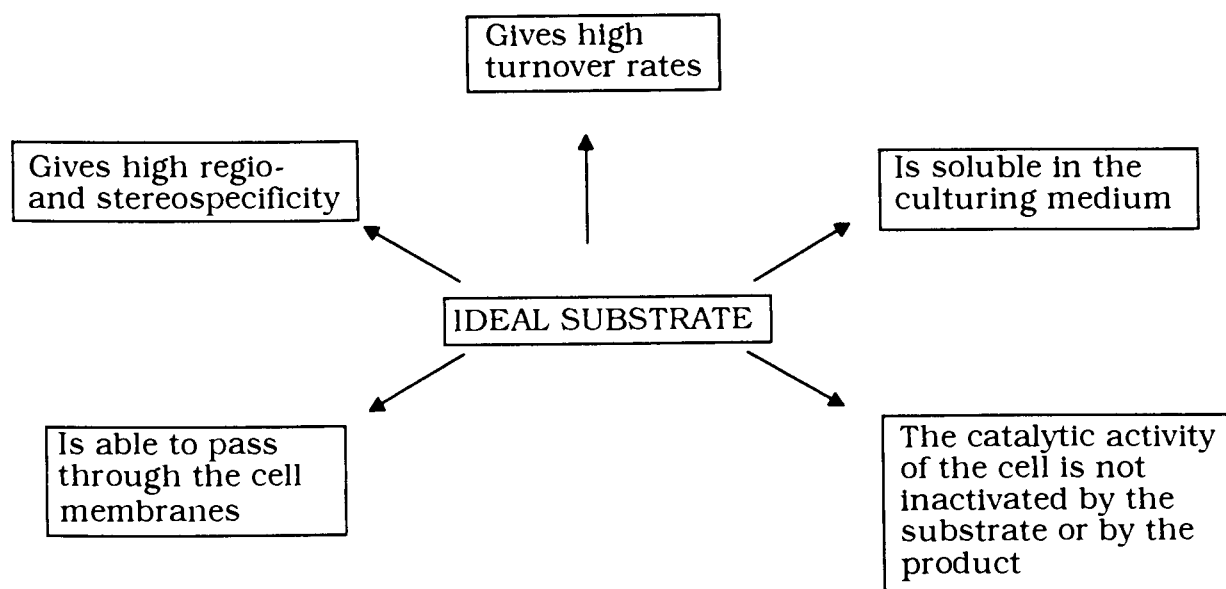
In contrast to the very early applications, biotransformations are presently carried out using pure cultures of microorganisms or plant cells or with purified enzymes and they are generally considered as a way to perform selective modifications of pure compounds into specific final products.

Of utmost importance in the successful application of microbial or plant bioconversion is the physicochemical nature of the substrate to be biotransformed. Many factors must be considered and Scheme 1 summarizes these in terms of an "ideal" substrate.

Microbial conversions (or biotransformations) are generally processes in which specific microorganisms convert a compound to a structurally-related product. They comprise only one or a small number of enzymatic reactions as opposed to the multi-reaction sequences of fermentations. In general, two different biotransformation systems, cells or isolated enzymes, are utilized. Availability of a certain organism can be a deciding factor for an organic chemist wishing to employ biotransformations in a synthetic route. Although bioconversions can be conducted with growing cells, many are carried out with resting cells or even spores (Finkelstein & Ball 1991). The advantages of using non-growing cells are threefold. First, very high substrate loadings can be used, e.g. tens of grams of substrate per liter, where such elevated

substrate levels usually inhibit growth. Second, if resuspended cells in buffer are used, there will be fewer contaminating compounds present. These two features allow for facile product isolation.

Scheme 1. Ideal Interactions Between Substrate and Cell.



Another attractive feature of bioconversions relates to their ease for scale-up since usually the only parameter of interest is the level of the enzyme mediating the transformation. Many enzymes have pH and/or temperature optima far removed from those of the intact cell. In bioconversions, these parameters can be optimized to increase the reaction rate. Techniques involving cell and/or enzyme immobilization to afford stable and long-acting systems for successful biotransformations are becoming increasingly important. Reactions by immobilized



microbial cells are advantageous when: (i) enzymes are intracellular; (ii) enzymes extracted from cells are unstable during and after immobilization.

Many publications and reviews on immobilization of microbial cells have been published (Chibata 1978, Chibata *et al.* 1983a, b). However, general methods which are ideally applicable to immobilization of all types of microbial cells have not been developed. In practice, it is necessary to choose suitable methods and conditions for immobilization of each type of cells. Three types of approaches to achieve immobilization are generally employed: physical binding to solid supports, cross linking and entrapment. In practice, combinations of these methods can be used. Physical binding is the oldest immobilization technique but is the least satisfactory. Cells or enzymes are mixed with an adsorbent and then packed in a column. The carrier-binding method is based on direct binding of cells to water-insoluble carriers by physical adsorption, ionic bonds, or covalent bonds. As carriers, water-insoluble polysaccharides (cellulose, dextran, and agarose derivatives), proteins (gelatin and albumin), synthetic polymers (ion-exchange resins and polyvinyl chloride), and inorganic materials (brick, sand, and porous glass) are used (Chibata *et al.* 1986). One of the first attempts to immobilize cells employed *Escherichia coli* and *Azotobacter agile* cells adsorbed to Dowex-1 for the oxidation of succinic acid (Hattory & Furusaka 1960, 1961). Silica and ceramics are the major inorganic carriers that have been used. *Saccharomyces carlbergensis* was immobilized on porous silica beads which had been treated with aminopropyltriethoxysilane and activated with glutaraldehyde (Navarro & Durand 1977). However, ease of adsorption also means ease of

desorption and this often occurs following substrate addition. Cells immobilized in this way have a tendency to autolyse and if enzymes are immobilized in this manner, activity is often partially or totally lost (Jack & Zajic 1977).

Enzymes and microbial cells can be immobilized by cross-linking them with bi- or multi-functional reagents, such as glutaraldehyde or toluene diisocyanate. This method is used to immobilize *E. coli* cells having high aspartase activity by cross-linking cell walls or cell membranes with the bifunctional reagents glutaraldehyde and toluene diisocyanate (Chibata *et al.* 1974). The most extensively used method of cell immobilization involves entrapment in a polymer matrix. Matrices which have been employed include collagen, gelatin, agar, alginate, carrageenan, polyacrylamide, cellulose triacetate, polystyrene and polyurethane (Chibata *et al.* 1986).

With entrapment methods, binding between the cells and the carrier should not occur, and a high retention of activity is expected. For practical applications, it is necessary to find an immobilization procedure that is simple and inexpensive and that achieves good retention of activity and operational stability. The use of immobilized cells for the production of useful organic compounds is expanded and could be an important addition to recombinant DNA technology.

## **1.2 Diterpenes from *Tripterygium Species***

For centuries, plants have provided a rich source of natural products, many of which have served as templates for the development of important pharmaceutical drugs. Within the broad area of natural products, the practice of herbal medicine has provided scientists with

significant leads for novel applications in clinical medicine. Of particular interest to the present study was the observation that certain diterpenes, initially isolated from the Chinese herbal plant, *Tripterygium wilfordii* Hook F., had considerable potential for the development of novel pharmaceutical agents (Qian 1987a; Li 1993; Matlin 1993).

Three *Tripterygium* species in the family Celastraceae, have been extensively investigated in China: *Tripterygium wilfordii* Hook F., a vine which grows in the mountainous areas of south-east and southern China, *T. hypoglaucum* Levl which occurs in south-western China, and *T. wilfordii* var. *regelii* Sprague et Takeda, found in the north-east of China. The most common species is *T. wilfordii*, and most of the research has been centered on this species. This herb is commonly known in China as Lei Gong Teng (Thunder God vine) or Mang Cao (rank grass) The plant is 2-3 meters high, twigs are reddish-brown, with longitudinal ridges and fine hairs. Leaves are alternated with serrated edges. The flowers are small, white coloured with 5 petals, 5 stamens and a high-positioned ovary. The samara is ellipsoid-shaped and is provided with 3 jutting wings. Each samara usually contains a single seed (Jiangsu 1977).

Crude preparations of *T. wilfordii* have been used for many centuries in traditional Chinese medicine. It is first mentioned in the Saint Peasant's Scripture of Materia Medica (Huang 1982), written about two thousand years ago, where it is described for use in the treatment of fever, chills, edema and carbuncle. Chinese gardeners used the powdered root to protect their crops from chewing insects. Crude water and alcohol extracts and refined extracts (a so-called multi-glycosides extract, or GTW) of *T. wilfordii* have been used increasingly to treat

diseases such as rheumatoid arthritis, ankylosing spondylitis, and a variety of dermatological disorders (Guo 1981; Yu 1983; Xu 1985). In the last two decades, many pharmacological applications of considerable significance, such as antitumor effect, anti-inflammatory effect and more recently, reversible male contraceptive activity, have been found.

### **1.2.1 Isolation of Diterpenes from *Tripterygium Species***

The chemistry of these plants has been studied for half a century. Approximately 150 natural products, including alkaloids, sesquiterpenoids, diterpenoids, and triterpenoids have been isolated from this plant and related species. From the large number of natural products isolated, only 33 diterpenes have been identified. The following detailed discussion of *T. wilfordii* derived products will be limited to the diterpenes found in this plant species. Table 1 and structures **1 - 33** summarize the characteristic features of these diterpenes.

### **1.2.2 Biological and Pharmacological Properties of Products Derived from *T. wilfordii***

#### **Diterpenes and Related Compounds**

Kupchan and coworkers isolated the novel diterpenoid triepoxides, triptonide (**1**), triptolide (**2**), and triptiolide (**3**) from the roots of *T. wilfordii* (Kupchan *et al.* 1972). These were the first reported natural products containing the 18 (4->3) abeo-abietane skeleton and the first recognized diterpenoid triepoxides.

Biological evaluations of these compounds showed that triptolide (**2**) and triptiolide (**3**) exhibited significant activity *in vivo* against the L-

1210 and P-388 leukaemias in the mouse, and *in vitro* against cells derived from human carcinoma of the nasopharynx (KB) (Kupchan *et al.* 1972; *Tripterygium* study group 1982; Zheng 1983a). Life-prolonging effects were demonstrated at the 0.1 mg/kg level for both compounds when tested *in vivo* in mice against the L-1210 lymphoid leukaemias, whereas cytotoxicity ( $ED_{50}$ ) against KB cells was demonstrated at  $10^{-3}$  to  $10^{-4}$  mg/mL. Triptonide (**1**), however, showed no anti-leukaemic activity at doses of up to 0.4 mg/kg (Kupchan *et al.* 1972). These results led to the proposal that the 14 $\beta$ -hydroxyl and 9,11-epoxide groups were necessary for the anti-leukaemic activity of the diterpene triepoxides (Kupchan *et al.* 1974), and that the 14 $\beta$ -hydroxyl group participated in the opening of the epoxide group during alkylation of thiol groups (Scheme 2).

Table 1. Reported Diterpenoids from *Tripterygium* species.

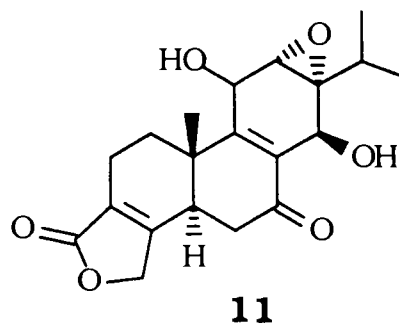
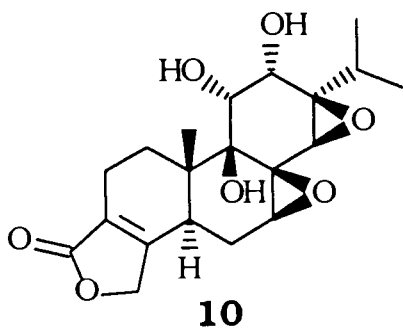
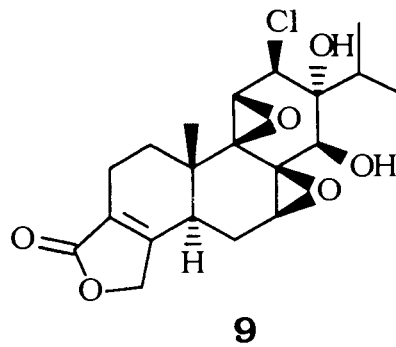
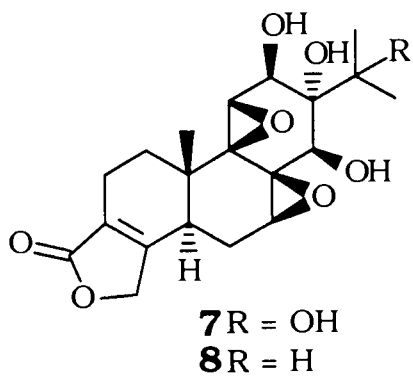
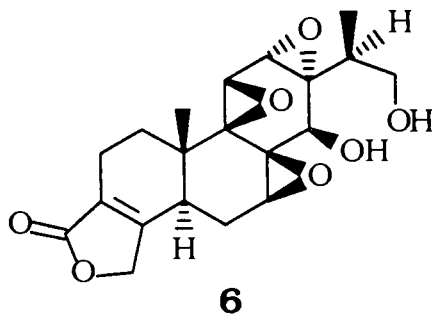
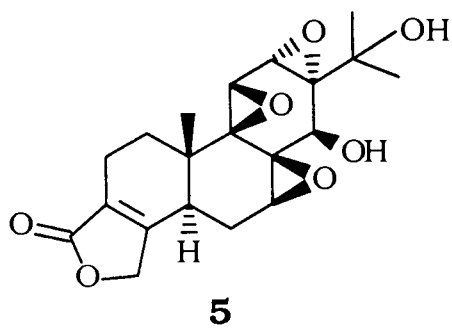
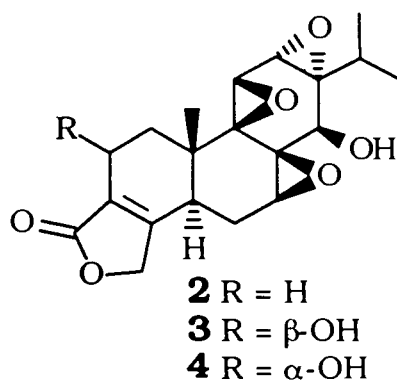
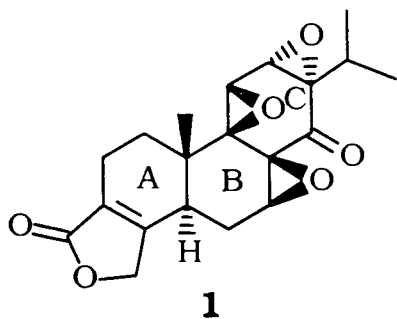
Compound	Molecular formula	mp (°C)	Plant	References
Triptonide (1)	C <sub>20</sub> H <sub>22</sub> O <sub>6</sub>	251-252	TW	Kupchan 1972
Triptolide (2)	C <sub>20</sub> H <sub>24</sub> O <sub>6</sub>	226-227	TW	Kupchan 1972
Tripdiolide (3)	C <sub>20</sub> H <sub>24</sub> O <sub>7</sub>	210-211	TW	Kupchan 1972
Tripterolide (4)	C <sub>20</sub> H <sub>24</sub> O <sub>7</sub>	225-228	TH	Wu 1979
Triptolidenol (5)	C <sub>20</sub> H <sub>24</sub> O <sub>7</sub>	193-194	TW	Deng 1985
16-Hydroxytriptolide (6)	C <sub>20</sub> H <sub>24</sub> O <sub>7</sub>	232-234	TW	Ma 1991
Tripteraolide (7)	C <sub>20</sub> H <sub>26</sub> O <sub>8</sub>	258-260	TW	Deng 1992
Triptriolide (8)	C <sub>20</sub> H <sub>26</sub> O <sub>7</sub>	260-262	TW	Ma 1991
Tripchlorolide (9)	C <sub>20</sub> H <sub>25</sub> O <sub>6</sub> Cl	256-258	TW	Lu 1990
13,14-Epoxy-9,11,12-trihydroxytriptolide (10)	C <sub>20</sub> H <sub>26</sub> O <sub>7</sub>	268-270	TW	Zhang 1993
Tripdioltonide (11)	C <sub>20</sub> H <sub>24</sub> O <sub>6</sub>	222-224	TW	Zhang 1993
Hypolide (Triptophenolide) (12)	C <sub>20</sub> H <sub>24</sub> O <sub>3</sub>	232-234	TH TW	Wu 1979 Deng 1982
Triptophenolide methyl ether (13)	C <sub>21</sub> H <sub>26</sub> O <sub>3</sub>	152-154	TW	Deng 1982
Triptonolide (14)	C <sub>20</sub> H <sub>22</sub> O <sub>4</sub>	214-215	TW	Deng 1981
Neotriptophenolide (15)	C <sub>21</sub> H <sub>26</sub> O <sub>4</sub>	189-191	TW	Deng 1982
Isonotriptophenolide (16)	C <sub>21</sub> H <sub>26</sub> O <sub>4</sub>	185-187	TW	Chen 1986
Triptonoterpene (17)	C <sub>20</sub> H <sub>28</sub> O <sub>2</sub>	153-155	TW	Deng 1985
Triptonoterpene methyl ether (18)	C <sub>21</sub> H <sub>30</sub> O <sub>3</sub>	209-211	TW	Deng 1985

Table 1. (Continued)

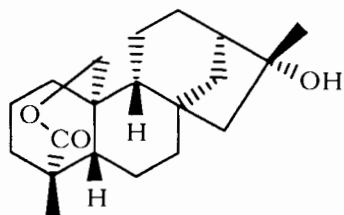
Compound	Molecular formula	mp (°C)	Plant	References
Neotriptonoterpene ( <b>19</b> )	C <sub>21</sub> H <sub>30</sub> O <sub>3</sub>	205-207	TW	Zhou 1988
Triptonoterpenol ( <b>20</b> )	C <sub>21</sub> H <sub>30</sub> O <sub>4</sub>	197-199	TW	Deng 1987
11-Hydroxy-14-methoxy-dehydroabietane ( <b>21</b> )	C <sub>21</sub> H <sub>32</sub> O <sub>2</sub>	194-195	TR	Sheng 1990
Tripterifordin ( <b>22</b> )	C <sub>20</sub> H <sub>30</sub> O <sub>3</sub>	255-256	TW	Chen 1992
Triptoditerpenic acid ( <b>23</b> )	C <sub>21</sub> H <sub>28</sub> O <sub>3</sub>	-	TH	Zhang 1991
Hypoglic acid ( <b>24</b> )	C <sub>21</sub> H <sub>28</sub> O <sub>4</sub>	219-224	TH	Zhang 1992a,b
Triptonoditerpenic acid ( <b>25</b> )	C <sub>21</sub> H <sub>28</sub> O <sub>4</sub>	189-191	TH	Zhang 1991
Triptoquinic acid A (Triptoquinone A) ( <b>26</b> )	C <sub>20</sub> H <sub>24</sub> O <sub>4</sub>	182-183 172-173	TR TH	Shen 1992 Takaishi 1992
Triptoquinic acid C ( <b>27</b> )	C <sub>20</sub> H <sub>24</sub> O <sub>5</sub>	202-203	TR	Sheng 1990
Triptoquinic acid B ( <b>28</b> )	C <sub>20</sub> H <sub>26</sub> O <sub>4</sub>	212-213	TR	Shen 1992
Triptoquinonal ( <b>29</b> )	C <sub>20</sub> H <sub>26</sub> O <sub>3</sub>	127-128	TR	Shen 1992
Triptoquinonol ( <b>30</b> )	C <sub>20</sub> H <sub>28</sub> O <sub>3</sub>	165-166	TR	Shen 1992
Triptoquinondiols ( <b>31</b> )	C <sub>20</sub> H <sub>28</sub> O <sub>4</sub>	183-184	TR	Shen 1992
3-Oxo-triptoquinonol (Triptoquinone B) ( <b>32</b> )	C <sub>20</sub> H <sub>26</sub> O <sub>4</sub>	135-136	TR	Shen 1992 Takaishi 1992
Wilforonide ( <b>33</b> )	C <sub>13</sub> H <sub>16</sub> O <sub>3</sub>	187-189	TW	Chen 1986

Plant: TW - *Tripterygium wilfordii*; TH - *Tripterygium hypoglaucum*;

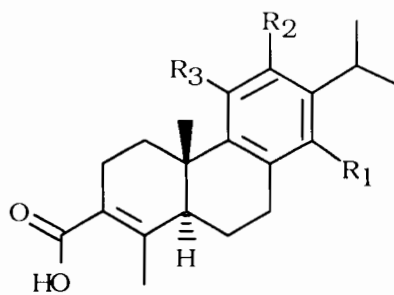
TR - *Tripterygium wilfordii* var. *regelii*







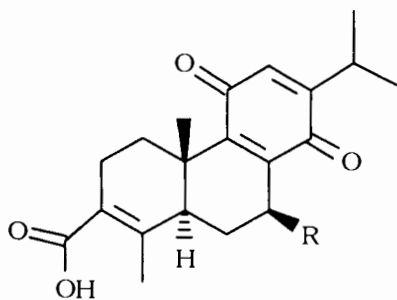
**22**



**23**  $R_1 = \text{OCH}_3$ ;  $R_2 = R_3 = \text{H}$

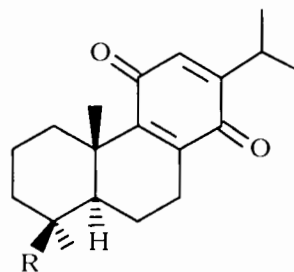
**24**  $R_1 = \text{OCH}_3$ ;  $R_2 = \text{H}$ ;  $R_3 = \text{OH}$

**25**  $R_1 = \text{OH}$ ;  $R_2 = \text{OCH}_3$ ;  $R_3 = \text{H}$



**26**  $R = \text{H}$

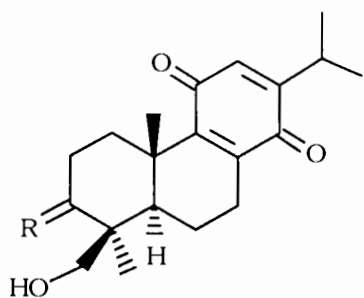
**27**  $R = \text{OH}$



**28**  $R = \text{COOH}$

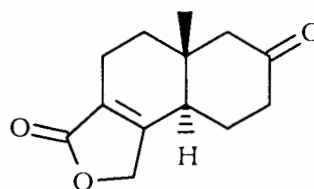
**29**  $R = \text{CHO}$

**30**  $R = \text{CH}_2\text{OH}$



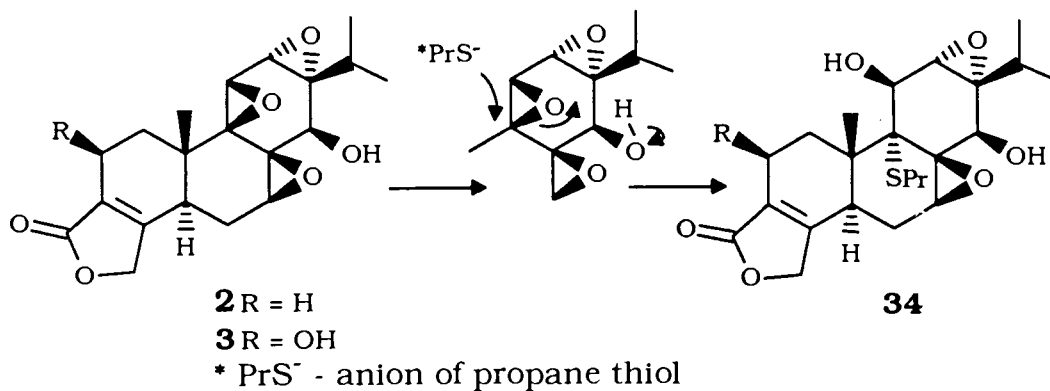
**31**  $R = \begin{array}{c} \text{OH} \\ \diagup \\ \text{H} \end{array}$

**32**  $R = \text{O}$

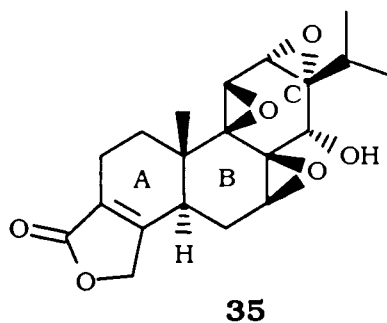


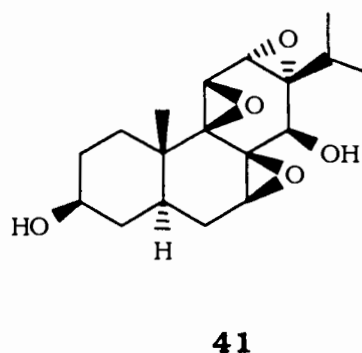
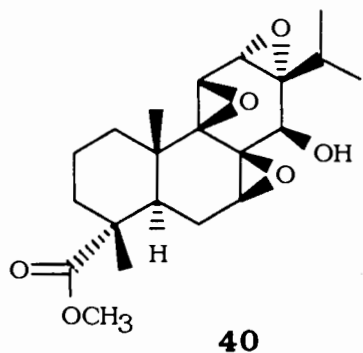
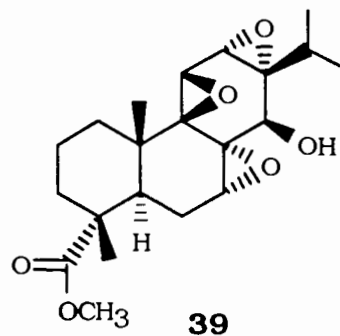
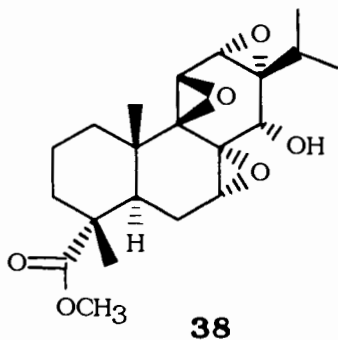
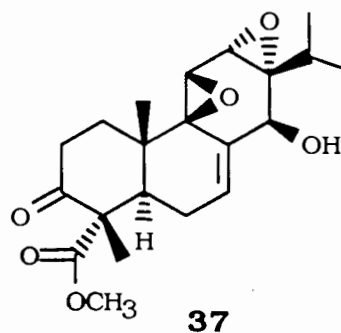
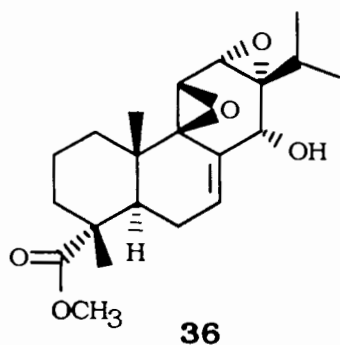
**33**

Scheme 2. Alkylation of Thiols by the Diterpene Triepoxides *via* Hydroxyl-assisted Epoxide Ring Opening.



This hypothesis is based on the proposal that plant-derived tumour inhibitors may act via selective alkylation of the thiol groups of growth regulation enzymes. The fact that triptonide (**1**) and 14-epitriptolide (**35**) showed no significant activity against the growth of L-1210 lymphoid leukaemia supported the proposal that intramolecular catalysis by the 14 $\beta$ -hydroxyl group was taking place (Kupchan *et al.* 1974).





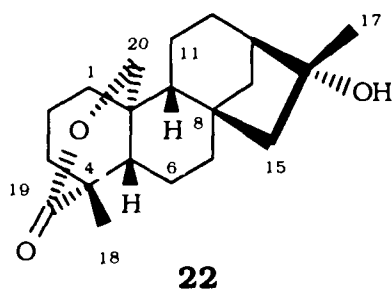
Analogues **36** to **40** of the above triepoxides were synthesized by Tokoroyama and coworkers and screened for antitumour activity against KB cells and L-1210 leukaemia in mice (Tokoroyama *et al.* 1981). The results indicated that the hydroxy-epoxide system in the B/C ring system and some functionality (possibly the butenolide ring) in ring A were necessary for the biological activities. Compound **41**, synthesized

by Berchtold and coworkers (Frieze *et al.* 1978) showed no antitumour activity, which further supports this conclusion (Lai *et al.* 1982).

More recent studies have shown that triptolide (**2**) prolonged the survival time of L615-bearing mice, with some mice surviving for longer than a month (Zhang *et al.* 1981). When these mice were rechallenged with leukaemic cells, there was no recurrence of the disease. Toxicity studies of triptolide (**2**) have shown that the LD<sub>50</sub> for mice was 0.8 mg/kg after intravenous administration. Dogs given triptolide intravenously, at 20-160 mg/kg/day, showed pathological or functional changes in the heart, liver, and gastrointestinal tract (Cheng *et al.* 1981).

Takaishi and coworkers (Takaishi *et al.* 1992a; Shishido *et al.* 1994) isolated triptoquinone A (**26**) and B (**32**) from the bark of *T. wilfordii* var. *regelii*. Subsequently, the chemical synthesis of triptoquinone A was described (Shishido *et al.* 1993). These triptoquinones are of clinical interest as they may be responsible, in part, for the anti-inflammatory effects of the crude plant extracts (Wang 1983). For example, micromolar quantities have been shown to inhibit the release of the inflammatory mediators, interleukin 1 $\alpha$  and 1 $\beta$ , from lipopolysaccharide-stimulated human peripheral monocytes (Shishido *et al.* 1994). A strong relationship between production of IL-1 by synovium and degree of inflammation of articular synovial membrane has been reported by Miyazaki and coworkers (Miyazaki *et al.* 1988).

The novel kaurane diterpene derivative tripterifordin (**22**) was isolated by Chen and coworkers from dry roots of *T. wilfordii* (Chen *et al.* 1992). The structure of **22** was elucidated by various spectroscopic methods. This compound showed anti-HIV replication activity in H9 lymphocyte cells with an EC<sub>50</sub> of 1 mg/mL.



Mori and Aki have developed a synthetic route to **22** and have determined the structures of the intermediates using spectroscopic analyses (Mori & Aki 1993).

### **Preparations of Crude and Refined Extracts from *T. wilfordii***

The herb is collected in summer or early autumn and the root xylem is obtained for medicinal use after removing the two layers of cortices. The root xylem is dried and cut into small pieces and then processed to obtain the following preparations:

- 1) The crude extract is composed of an aqueous decoction, with a daily dose of 15 - 20 g of the root cuttings and an alcoholic extract with a daily dose of 2 - 4 g of the root cuttings (Wang 1983).
- 2) The refined extract or the so-called "multi-glycosides (GTW) of the plant and the alkaloids. The alkaloid extract has not been used clinically because it had no definite therapeutic effect and showed severe side effects (Xu 1981). GTW was prepared by extraction of the root xylem with water and chloroform followed by column chromatography. Twenty-five g of the root xylem yields 1

mg of GTW. Commercial tablets containing 10 mg of GTW extract are available. The recommended dose for the treatment of rheumatoid arthritis and various skin diseases is 60 - 90 mg daily. The GTW extract has been reported to be much less toxic than that of the crude plant extracts (Xu 1981).

### **Pharmacological Studies of Multi-Glycosides Extract (GTW) of *T. wilfordii***

A comparison of the pharmacological effects of GTW with the crude extract from *T. wilfordii* has shown that a refined extract (GTW) contained the main anti-inflammatory constituents (Zheng *et al.* 1983a). GTW implies that some glycosides are present in the preparation; however, other constituents, such as pentacyclic triterpenes and some diterpenes, are also present and could be responsible for the pharmacological activity (Zheng *et al.* 1983a).

As an immunosuppressive agent, GTW of *T. wilfordii* Hook F. has significantly prolonged the mean survival time of cardiac allografts in rats, comparable with the well-known anti-rejection agent cyclosporine A (Li 1993). Immunological studies have also shown that GTW extract of *T. wilfordii* had an immunosuppressive action on humoral and cell-mediated immunity (Chang 1981). GTW was shown to inhibit antibody production in antigen-bound and antibody-secreting cells in mice.

Plaque-forming cell (PFC) tests and splenic cell immunospecific rosette-forming cell tests in mice demonstrated that GTW extract of *T. wilfordii* inhibited the primary antigen-antibody immune response. It was suggested that GTW extract might inhibit the activation of helper T-cells and B-cells. The crude preparation (total glycosides, total alkaloids,

and diterpenes) of *T. wilfordii* extracts were confirmed to have immunosuppressive action on humoral immunity (Xu *et al.* 1985).

An anti-inflammatory effect has been observed when aqueous decoction, ethyl acetate extracts or GTW was administered intraperitoneally in large dose in rats (Hou *et al.* 1980). In this experiment joint edema induced by agar-agar or formaldehyde was inhibited by these preparations.

Suppression of renal disease and arthritis and prolongation of survival of infected mice were observed when mice were treated with the GTW extract of *T. wilfordii* (Gu *et al.* 1992a). A further study by the same group (Gu *et al.* 1992b) on the inhibition of Type II collagen-induced arthritis in mice also revealed a strong immunosuppressive activity by *T. wilfordii* extract.

Finally a recent study has shown the induction of aneuploidy using a water extract of *T. hypoglaucom* in mouse bone marrow cells (Xu *et al.* 1993). This study indicated that this extract exhibited a colchicine-like activity by arresting cell division by inhibiting microtubule polymerization.

### **Clinical Uses of Multi-Glycosides Extract (GTW) of *T. wilfordii***

In the past 20 years the refined multy-glycosides extract (GTW) has been in clinical use in China. Various disorders have been treated, ranging from rheumatoid arthritis and ankylosing spondylitis (Guo *et al.* 1981; Yu 1983) to a variety of skin disorders including Behcet's disease, psoriatic arthritis, pustular psoriasis, systemic lupus erythematosus, allergic angiitis, Sweet's syndrome, lepra reactions, etc. (Xu *et al.* 1985).

These studies by Xu and coworkers showed that the extract used for skin disorders was more potent than the conventional non-steroidal antirheumatic agents such as salicylates, indomethacin and phenylbutazone. Moreover the GTW extract could be substituted for corticosteroids in some skin diseases and in some patients who were steroid-dependent or who had contraindications to steroids.

One recent report from Chinese physicians describes a patient suffering from severe lupus nephritis who went into clinical remission when treated with an extract of *T. wilfordii* (Kao *et al.* 1993). Li and Weir showed that the extract of *T. wilfordii* was capable of inhibiting several different immune functions including *in vitro* response of human peripheral blood mononuclear cells to both mitogen and alloantigen, and of generating cytotoxic T cells (Li & Weir 1990). They proposed that the inhibition was likely mediated through a reduction in both IL-2 production and IL-2 responsiveness. Similar studies were also reported by Tao and coworkers (Tao *et al.* 1991).

### **Use of Multi-Glycosides Extract (GTW) of *T. wilfordii* as Male Contraceptive**

Interest in *T. wilfordii* was renewed when the contraceptive properties of GTW were discovered (Qian 1987b). Preliminary results from the tests on the effects of this extract in male rats and in men have shown male antifertility effects. The observed effects have stimulated studies into the influence of GTW on the male reproductive system.

Study by Qian and coworkers on male and female rats, showed that at doses of 10 mg/kg per day of GTW, male rats became infertile at



the end of the eighth week of treatment. At these dose levels (much lower, for example, one-tenth than in the other studies), no damage to the seminiferous tubules was observed and no decrease in testosterone levels was observed (Qian *et al.* 1986a). In female rats, no effect on fertility was observed.

Some clinical data on the use of GTW as a male contraceptive agent is available. Qian and coworkers carried out a comparative study on the seminal indices and the blood hormonal profiles in rheumatoid arthritis patients with or without GTW therapy (Qian *et al.* 1986b). Twenty-two male patients, fertile, 22-40 years of age, suffering from a mild degree of rheumatoid arthritis were recruited. They were administered a low dose of GTW (20-30 mg/day), (one-third of the regular dose administered to arthritic patients), over a period of 1.5-5 months. The sperm motility of the treated patients was zero, indicating that they were infertile at the time of semen analysis. No significant side effect, at this low dose level, was observed. Fertility was regained after cessation of treatment (Qian *et al.* 1986b).

In studies on human males, infertility was observed at doses of one-third of those recommended for treatment of arthritis and skin disorders (Qian *et al.* 1986c). The libido and potency of treated patients were apparently not affected and infertility was reversible upon cessation of the drug treatment (Qian *et al.* 1986c). A decrease in the density of spermatozoa and a decrease in the sperm motility were thought to be the cause of the infertility. Reviews of the antifertility effect of GTW have been published by Qian (Qian 1987a, 1987b).

Zheng and coworkers carried out toxicity studies on GTW with emphasis on the effects on the male reproductive system (Zheng *et al.*

1983b). Their results showed that GTW caused damage of the seminiferous epidermis of the testis and inhibited spermatogonium mitosis in male mice which resulted in reduction or absence of reproductive cells of different stages. Subthreshold doses of GTW caused a reduction of the pregnancy rate and also sterility of mice. The observed effects were found to be reversible upon discontinuation of GTW use (Zheng *et al.* 1983b). A similar study on the effects of multiglycosides (GTW) of *T. wilfordii* on rat fertility showed that GTW caused a reversible reduction of the reproductive cells in male rats (Lan *et al.* 1992).

In a more recent study, Matlin and coworkers found that the diterpene epoxide, tripchlorolide (**9**, Table 1) had a higher antifertility potency than GTW. Unlike GTW, which caused relatively broad damage, especially to the sperm head (a potential source of mutation), tripchlorolide (**9**) only caused damage to the spermatozoa in the epididymis without significantly inducing sperm head anomalies or affecting other related organs such as seminiferous tubules (Matlin *et al.* 1993).

### **1.2.3 Side Effects and Toxicity of Multi-Glycosides Extract (GTW) of *T. wilfordii***

#### **Clinical Studies**

In the treatment of rheumatoid arthritis or dermatitis, the major side effects at regular clinical dose levels, i.e., a decoction from 15-25 g root xylem per day or GTW 60-90 mg/day (1.0-1.5 mg/kg/day), were gastrointestinal disturbances which include nausea, vomiting, anorexia, epigastric burning sensation, xerostomia, diarrhea and constipation.

Most of the effects were noted to subside in the course of treatment and the medication was not discontinued (Qian 1987). Leukopenia or thrombocytopenia was found in a few patients, but the cell counts recovered shortly after withdrawal of the drug. For example, in 698 patients taking GTW for the treatment of rheumatoid arthritis, fifteen (2.1%) developed leukopenia with a white blood cell count below  $3,000/\text{mm}^3$  and five (0.7%) developed thrombocytopenia without a bleeding tendency (Yu 1983). Li and coworkers indicated that in those cases where the white cell count had recovered after cessation of treatment, readministration of GTW did not cause any further leukopenia (Li *et al.* 1982). Qin showed that in patients with leukopenia, continuous use of GTW could decrease the white blood cell count (Qin 1981). Other side effects included menstrual disturbances, oligospermia, azoospermia, and a decrease in the size of the testis. The side effects of GTW were much less than those of the crude extracts and the former has been used in outpatients (Xu *et al.* 1985; Yu 1983).

### **Toxicity Effects on Male Fertility in Animals**

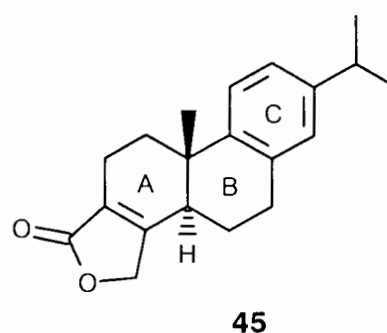
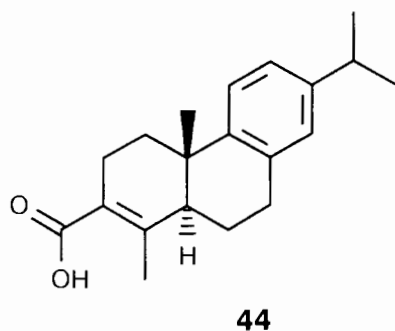
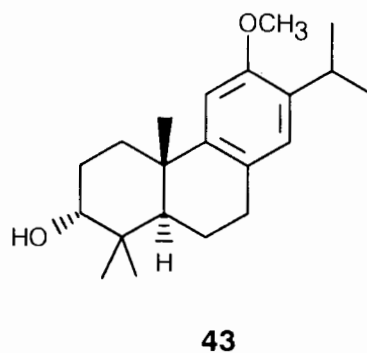
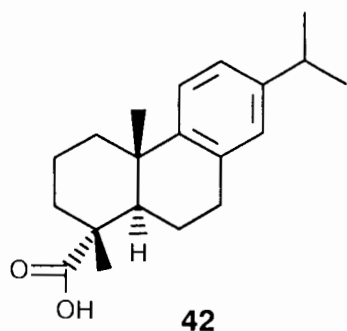
In the evaluation of the general toxicity of GTW, it was shown that when both the male and female hybrid mice were simultaneously fed a laboratory diet containing GTW for 4.5 months, the body weight growth, the birth rate and the litter size were decreased (Zheng 1983b). When rats were fed a laboratory diet containing GTW, at a dose of 30 mg/kg body weight per day for 35 or 80 days, marked seminiferous tubule damages were seen in the males together with a decrease in serum testosterone level in the 80 day group. Females showed disturbed

estrous cycle, decreased uterine weight and degenerative changes in the endometrium and myometrium (Zheng *et al.* 1985a, b).

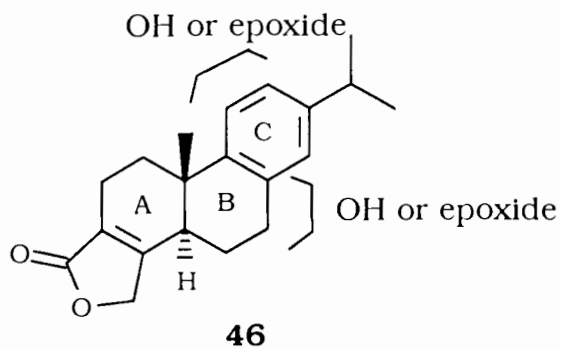
#### **I.2.4 Isolation of Diterpenes from Plant Tissue Cultures of *T. wilfordii* Hook F.**

In order to generate sufficient quantities of metabolites of *T. wilfordii* for pharmacological screening, a stable cell line of *T. wilfordii* has been developed (Kutney *et al.* 1981a, 1983a, 1992, 1993) and a total of 22 secondary metabolites belonging to the diterpene and triterpene families have been isolated and characterized. These included the diterpene triepoxides, triptolide (**2**), triptiolide (**3**) (produced in yields 36-40 times higher than in the plant) as well as three other compounds, dehydroabietic acid (**42**), the methoxylated abietane analogue **43**, and the unsaturated carboxylic acid **44**. In more recent further investigations, triptophenolide (**12**) and the butenolide **45** were also isolated (Han, unpublished data).

The extensive studies by Kutney and coworkers with *T. wilfordii* cell cultures have allowed the isolation of larger amounts of the diterpene compounds for a more detailed evaluation of their pharmacological activities. Their studies with plant cell cultures, when combined with chemistry, also provided another route to generating novel synthetic diterpene analogues.

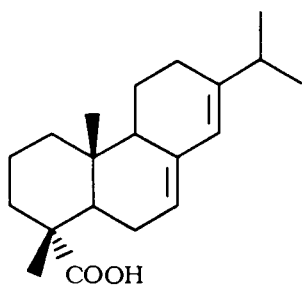


From the preliminary structure-activity data presented above (Tokoroyama *et al.* 1981), the most active systems bear the general structure **46**, that is, compounds possessing a lactone ring attached to ring A and particularly oxygen functions (hydroxyl or epoxide) in ring C.

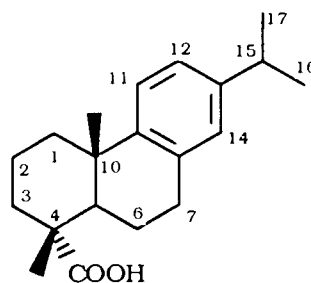


### 1.3 Microbial Transformation of Diterpenes

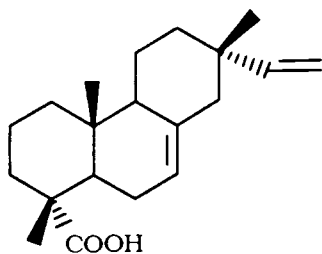
A large number of diterpenes have been isolated from living plants and microorganisms, but studies directed at their biotransformations are rather limited. The most pertinent studies related to the research herein concern the biotransformation of the abietane diterpenes which belong to the resin acid family. Compounds **47-49** represent typical structures in this series.



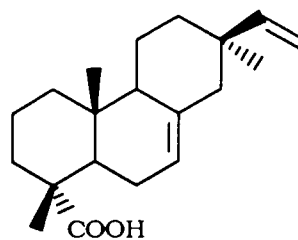
Abietic acid (**47**)



Dehydroabietic acid (**42**)



Pimaric acid (**48**)



Isopimaric acid (**49**)

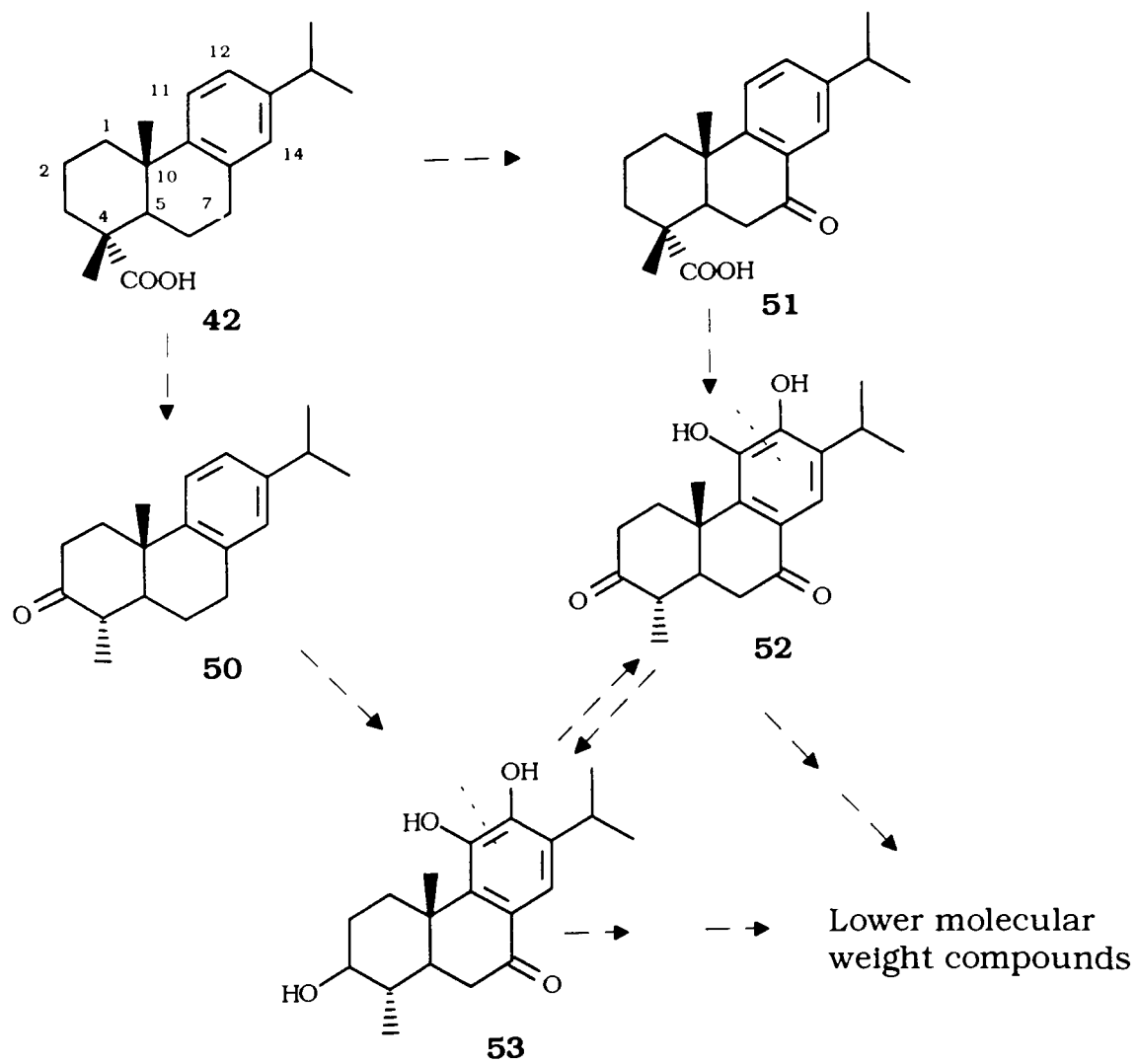
### 1.3.1 Aromatic Ring Hydroxylation and Degradation

#### Studies with Bacteria

The only published studies on the hydroxylation of the aromatic ring C of a resin acid have been described by Biellman and coworkers, who investigated the biodegradation of dehydroabietic acid (DHA, **42**) by the bacterium *Flavobacterium resinovorum* originally isolated from the soil of a *Pinus moritama* forest (Biellmann *et al.* 1968, 1970, 1973a). This organism was capable of utilizing the non-volatile portion of oleoresin from pine trees as the sole carbon source and the authors speculated that *F. resinovorum* may be responsible for the biodegradation of such natural products. Slow growing cultures of *F. resinovorum* were obtained either by omission of nitrogen, iron and magnesium or in the presence of a growth inhibitor  $\alpha',\alpha'$ -dipyridyl, and were shown to metabolize DHA to a series of metabolites.

A proposed pathway of the oxidation of DHA by *F. resinovorum* is shown in Scheme 3. Initial decarboxylation and oxidative attack at C-3 of ring A in dehydroabietic acid (**42**), could provide ketone **50** while benzylic oxidation at C-7 affords **51**. Either **50** or **51** could then undergo aromatic hydroxylation to allow the intermediates **52** and **53** to be formed. Subsequent degradation of **52** and/or **53** to smaller molecular weight compounds was observed. However, since these latter metabolites are not of direct relevance to the present study, they are not discussed here.

Scheme 3. Biodegradation of Dehydroabietic Acid (**42**) by *Flavobacterium resinovorum* (from Biellmann *et al.* 1973a).



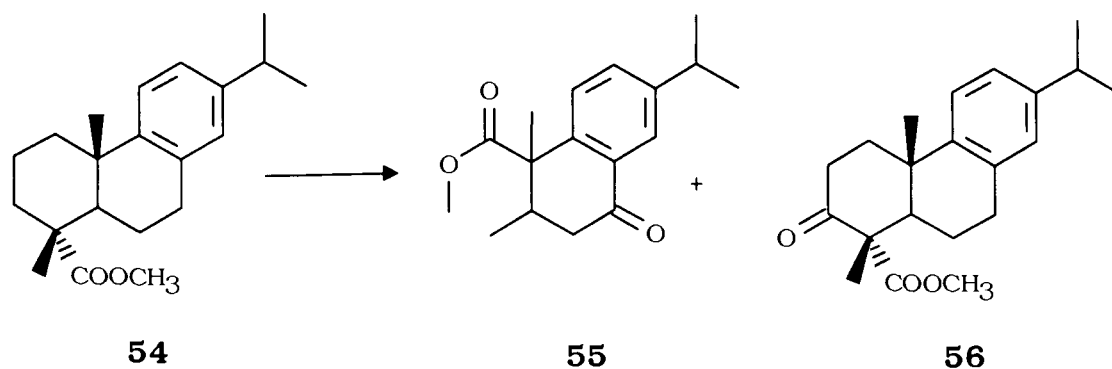


The above Scheme illustrates several types of interesting enzymatic processes: (i) aromatic hydroxylation; (ii) oxidation of saturated carbon systems; and (iii) carbon-carbon cleavage reactions.

Biellmann and coworkers also studied the biodegradation of DHA by *Pseudomonas* sp. and *Alcaligenes eutrophus*. They obtained similar results to those by *F. resinovorum*, that is, hydroxylation at C-7 followed by aromatic ring hydroxylation and finally cleavage of ring B (Biellmann *et al.* 1973b).

Levinson and Carter investigated the oxidation of the methyl ester of DHA, methyl dehydroabietate (**54**) by *Arthrobacter* sp. (Scheme 4) (Levinson & Carter 1968). This organism, in addition to achieving a similar oxidation of the C-3 position of ring A, also produced product **55**, in which a complete degradation of ring A of DHA (**42**) has occurred without any attack at rings C and/or B.

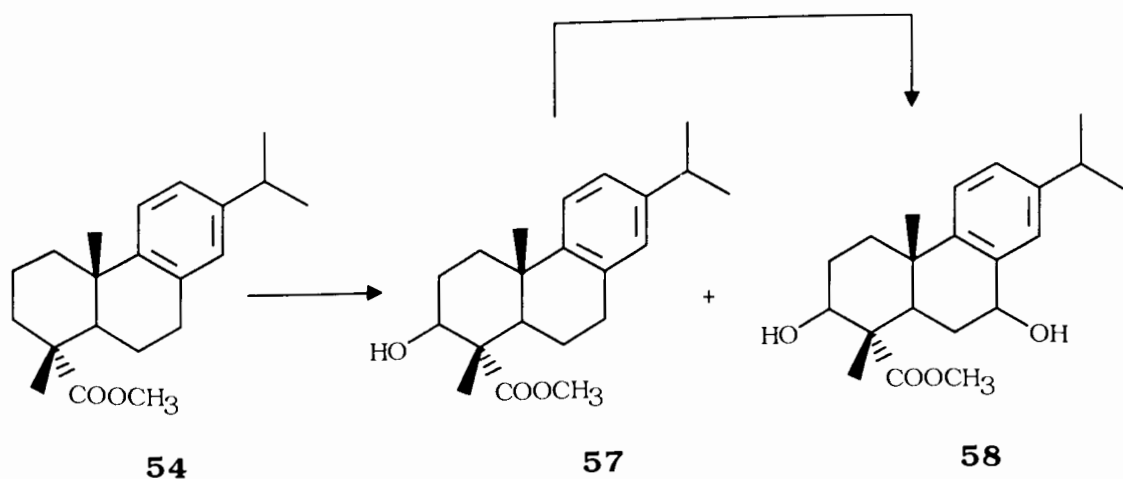
Scheme 4. Biodegradation of Methyl Dehydroabietate (**54**) by *Arthrobacter* sp. (from Levinson & Carter 1968).



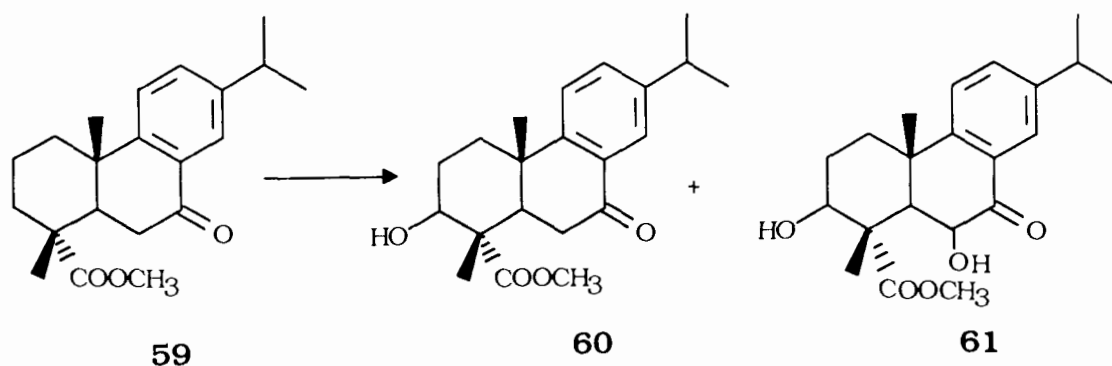
## Studies with Fungi

The first study involving the biodegradation of dehydroabietanes by fungi was published by Brannon and coworkers from the Lilly Research Laboratories (Brannon *et al.* 1968) (Scheme 5). Incubation of methyl dehydroabietate with the fungus *Corticium sasakii* resulted in hydroxylation at C-3 and at C-7 of the DHA system (Scheme 5). Initial attack occurred at C-3 to afford **57**. If the latter is incubated with the organism, the 3,7-dihydroxy analogue **58** was formed. When the 7-keto analogue **59** was incubated with the same fungus, hydroxylation occurred at C-3 (**60**) and at the activated C-6 position (**61**) (Scheme 6) (Brannon *et al.* 1968).

Scheme 5. Biotransformation of Methyl Dehydroabietate (**54**) by *Corticium sasakii* (from Brannon *et al.* 1968).



Scheme 6. Biotransformation of Methyl 7-Keto-Dehydroabietate (**59**) by *Corticium sasakii* (from Brannon *et al.* 1968).

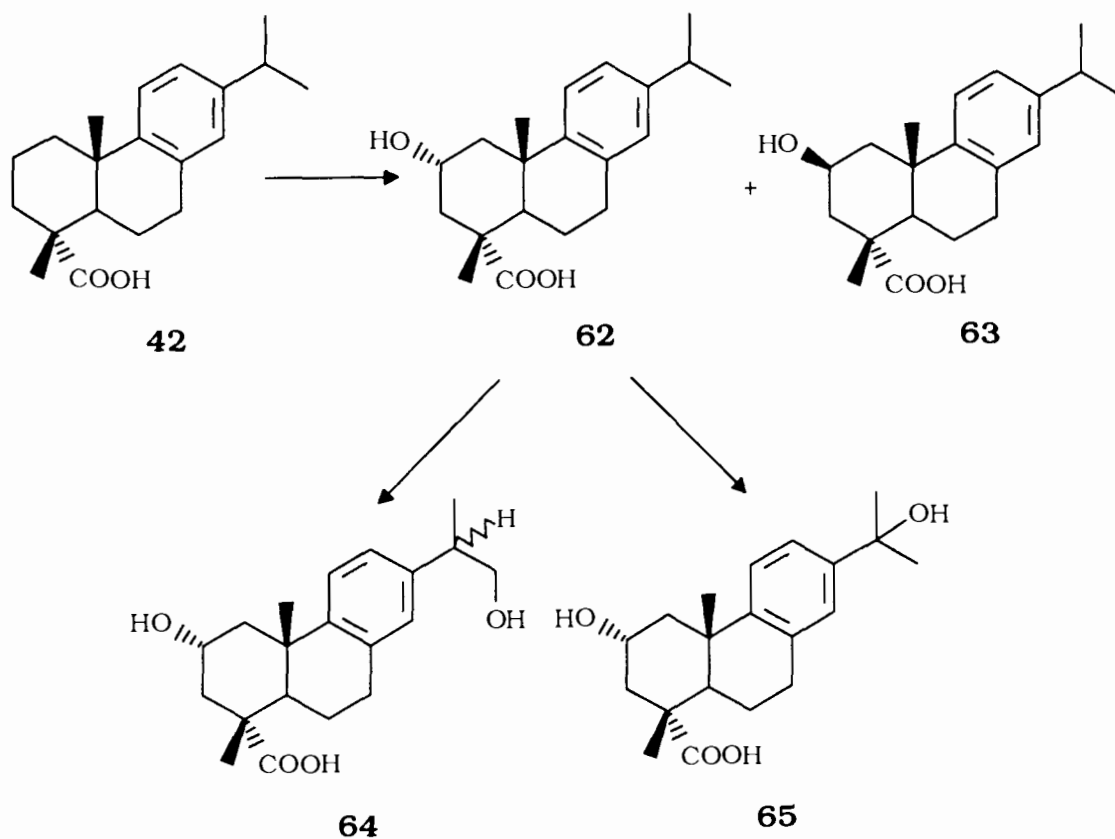


### 1.3.2 Fungal Oxidation of Abietane Diterpenes-Resin Acids

Research on the biodegradation of resin acids and related compounds was initiated by Kutney and coworkers in the early 1980's (Kutney *et al.* 1981b). They established that resin acids and their chlorinated analogues present in Kraft pulp mill effluent, were highly toxic to fish. It was therefore their objective to utilize biodegradation methods to obtain fish non-toxic compounds.

A series of microorganisms (fungi and bacteria) have been screened to metabolize DHA (**42**). *Mortierella isabellina* has been selected and the metabolites of the biotransformation were isolated and characterized. Fungal enzyme(s) were shown to attack ring A of DHA at the inactivated position, C-2, and the isopropyl side chain (structures **62-65**, Scheme 7).

Scheme 7. Biotransformation of Dehydroabietic Acid (**42**) by *Mortierella isabellina* (from Kutney *et al.* 1981b).



Aromatic ring hydroxylation was not observed. In contrast to the parent **42**, the hydroxylated metabolites **62-65** were non-toxic to fingerling salmon at concentrations simulating conditions in nature.

Subsequent studies revealed the sequence of metabolites of DHA formed by growing cultures of *M. isabellina*. The first metabolites formed were the C-2 hydroxy analogues **62** and **63**, which were then converted to **64** and **65** (Kutney *et al.* 1985).

To assess whether the bioconversion of DHA was catalyzed by intracellular (cell-associated) or secreted enzymes, mycelia were

separated from the media, the cells were washed and resuspended in Tris-hydrochloride buffer prior to addition of DHA. Metabolism of DHA was not observed in media alone whereas DHA was completely oxidized within 2 h by the washed cells of *M. isabellina*. Thus, the enzymes which metabolized DHA were shown to be cell-associated (Kutney *et al.* 1985).

Bioconversion of DHA (**42**) was also performed by immobilized on calcium alginate cultures of *M. isabellina* (Kutney *et al.* 1985). The immobilized cells were effective in the bioconversion of DHA to the above-illustrated metabolites with 94% bioconversion within 2.5 h. The enzymatic activity achieving this bioconversion remained for 110 days within this immobilized system, but since the experiment was terminated at this time, it was not known how long the activity could be maintained.

Immobilization of *M. isabellina* on polyurethane foam (Kutney *et al.* 1988) has shown that the cells immobilized in this way were similarly capable of efficient bioconversion of the resin acids: DHA (**42**), abietic (**47**) and isopimaric (**49**) acid to their respective hydroxylated metabolites. For example, DHA (**42**) was completely oxidized to such metabolites in 11 h (Scheme 7). Long lasting enzyme activity was also observed. After 87 days foam bound fungal cells still converted 52% of the added DHA to the hydroxylated products.

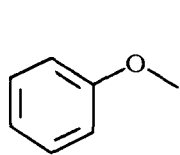
Other members of the resin acid series, that is, abietic (**47**), pimaric (**48**) and isopimaric (**49**) acids, as well as the 12-,14- and 12,14-chlorinated DHA analogues were also tested for biotransformation by *M. isabellina* and similar hydroxylations of ring A and side chain were observed (Kutney *et al.* 1981c; 1982a, b, c; 1983b, c).

### 1.3.3 Oxidation of Compounds other than Diterpenes by Fungi

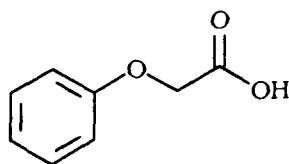
There are a large number of investigations concerning microbial transformation of various aromatic substrates. The present discussion summarizes selected biotransformations by fungi which are relevant to this thesis.

The hydroxylation of anisole (**66**), phenoxyacetic acid (**67**), phenylacetic acid (**68**), and benzoic acid (**69**) by the fungus *Aspergillus niger* has been shown (Bocks 1967). In this study, four strains of *A. niger* were evaluated and shown to convert **66-69** to the corresponding *ortho*-hydroxy metabolites. For example, *o*-hydroxy benzoic acid (**70**) was the product of benzoic acid oxidation.

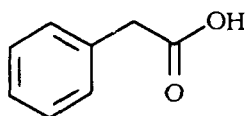
Experiments were carried out at varying pH values and substrate concentrations, and in the presence of additives like ascorbic acid, ethylenediaminetetraacetic acid and metal ions ( $\text{Cu}^{++}$ ,  $\text{Fe}^{++}$ ,  $\text{Mn}^{++}$ , and  $\text{Zn}^{++}$ ). Under all conditions, the *o*-isomer was the main mono-hydroxylated product. Hydroxylation was inhibited in incubation mixtures containing zinc sulfate and magnesium sulfate (Bocks 1967).



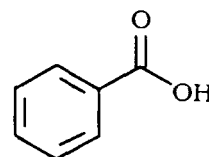
**66**



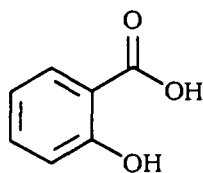
**67**



**68**

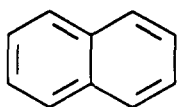


**69**

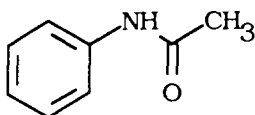


**70**

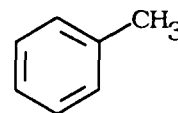
Rosazza and coworkers have published an extensive study on aromatic hydroxylation by a variety of microorganisms. For example, several strains of *Aspergillus*, *Rhizopus* and *Cunninghamella* species (Rosazza & Smith 1974) hydroxylated various substrates, including naphthalene (**71**), acetanilide (**72**), and toluene (**73**).



**71**



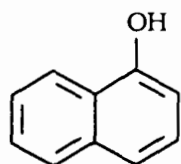
**72**



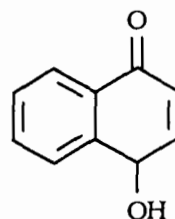
**73**

In most instances, the microbial model system yielded patterns of phenolic compounds such as **71-73** which were similar to those reported to occur with cytochrome P-450 monooxygenases either from mammalian or hepatic microsomes *in vivo*. However, specific isolation of such monooxygenases was not performed.

The metabolism of naphthalene by the fungus *Cunninghamella elegans* was reported by Gibson (Gibson *et al.* 1977), and major metabolites were 1-naphthol (**74**), and 4-hydroxy-1-tetralone (**75**).



74



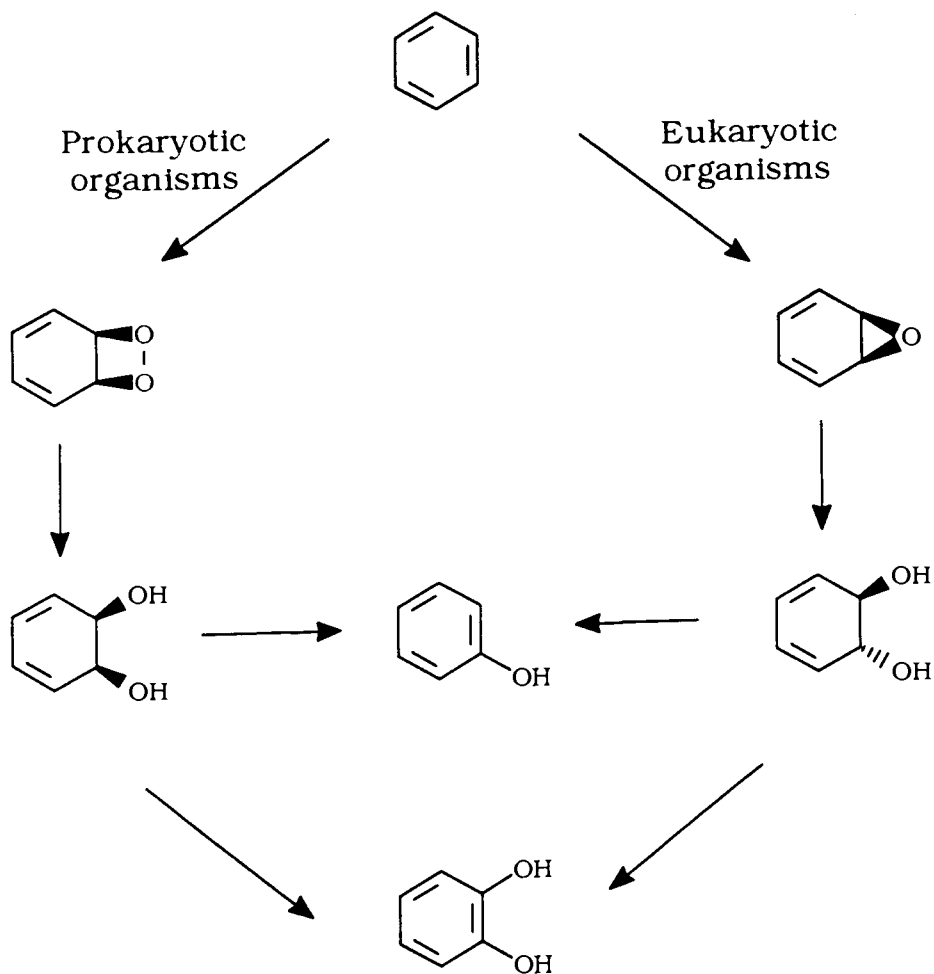
75

Direct epoxidation of the aromatic ring has been observed with some microorganisms (e.g. *Pseudomonas putida*) (Rosazza 1982) to afford the corresponding arene oxides (Scheme 8).

Eucaryotic organisms (fungi, yeasts, and higher organisms) utilize monooxygenases, such as cytochrome P-450, to give arene oxides which can be hydrolyzed to a *trans* diol. Oxidation of this diol yields a catechol, while loss of water results in the effective hydroxylation of the original aromatic ring (Rosazza 1982). Hydroxylation is often the initial step in the degradation of aromatic compounds by microorganisms in the environment and by the liver. In contrast, prokaryotic organisms (bacteria) hydroxylate aromatic compounds by dioxygenase enzymes, which catalyze a cycloaddition reaction with molecular oxygen to yield a dioxetane. This can be reduced to a *cis*-diol and/or catechol. The two pathways for the oxidation of benzene are compared in Scheme 8.

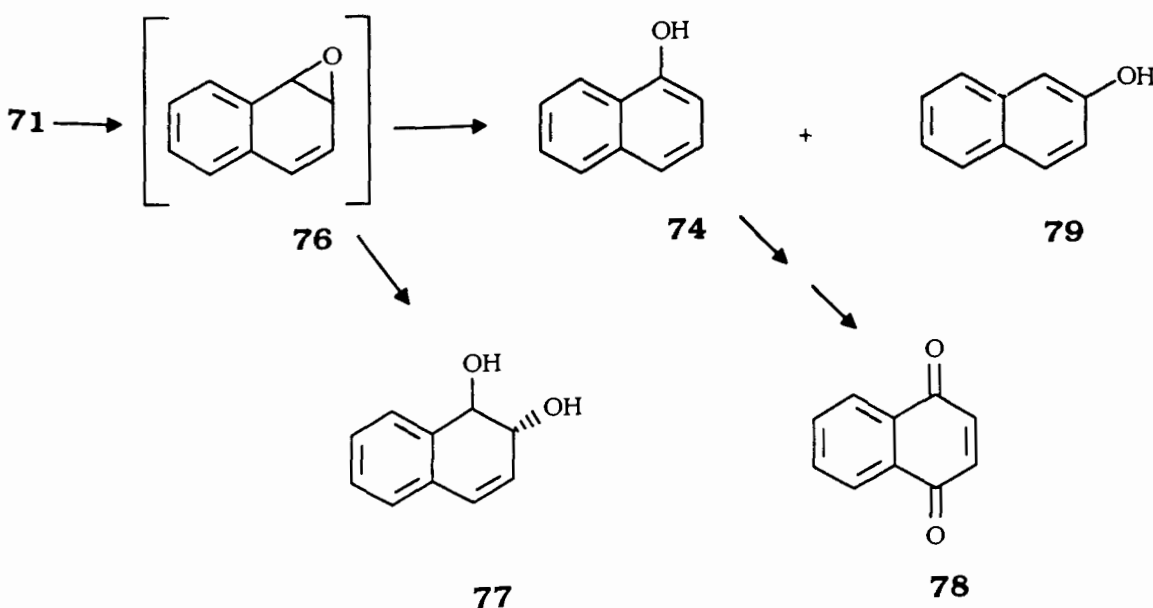


Scheme 8. Oxidation of Benzene by Prokaryotic and Eucaryotic Organisms (from Rosazza 1982).



Subsequent studies by Gibson (Gibson *et al.* 1978) with species of *Cunninghamella*, *Syncephalastrum* and *Mucor*, revealed that such fungi were capable of epoxidation of naphthalene (**76**) to afford unstable arene oxides which were rapidly converted to the more stable 1- and 2-naphthols (**74** and **79** respectively) and subsequently to naphthoquinones (**78**) (Scheme 9).

Scheme 9. Aromatic Hydroxylation of Naphthalene (**71**) by Fungi (from Gibson *et al.* 1978).

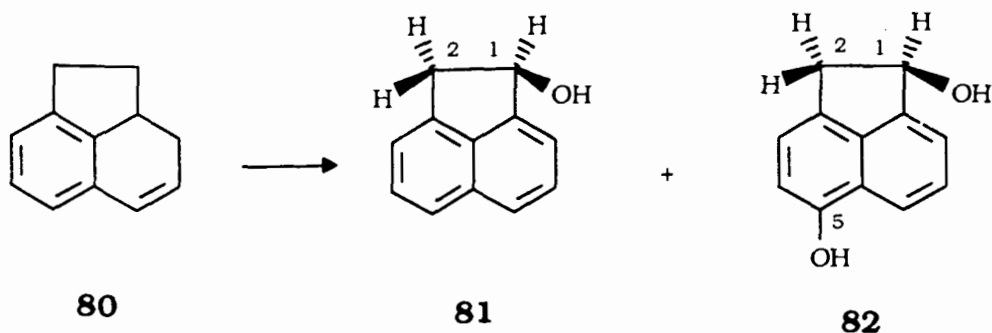


A major metabolite, *trans* 1,2-dihydroxy-1,2-dihydronaphthalene (**77**) was observed in approximately 35% of the fungal species tested. These authors therefore suggested that these fungi metabolized aromatic hydrocarbons in a manner similar to mammalian systems, i.e. a monooxygenase-catalyzed reaction (**71** → **76** → **74** → **78**).

*Cunninghamella echinulata* was also shown to be capable of metabolizing acenaphthene (**80**) to a series of hydroxylated analogues, for example, **81** and **82** (Cerniglia *et al.* 1992a) (Scheme 10).

The fungus *C. elegans* also metabolized acenaphthene via hydroxylation of both the aliphatic and aromatic rings to hydroxylated derivatives of acenaphthene (Cerniglia *et al.* 1992a).

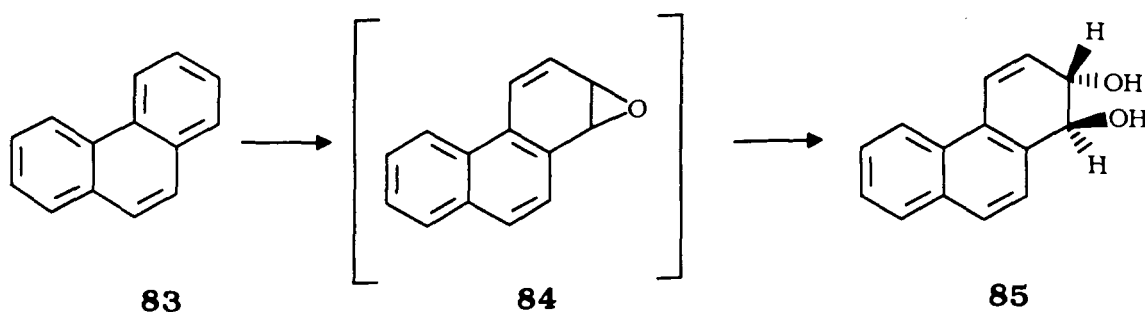
Scheme 10. Hydroxylation of Acenaphthene (**80**) by *Cunninghamella echinulata* (from Cerniglia *et al.* 1992a).



The authors proposed that the primary site of enzymatic attack by the fungus was on the C-1 - C-2 bridge which resulted in the formation of the secondary alcohol 1-acenaphthenol (**81**). Another proposal includes the hydroxylation at both C-1 and the aromatic ring of acenaphthene (**80**) to form 1,5-dihydroxyacenaphthene (**82**).

Another recent study (Cerniglia *et al.* 1993) has shown that phenanthrene (**83**) was also metabolized via the unstable epoxide **84** to the *trans* diol **85** and other metabolites by the fungi *Cunninghamella elegans*, *Syncephalastrum racemosum* and *Phanerochaete chrysosporium*. Although polycyclic aromatic hydrocarbons (PAHs) do not generally serve as carbon or energy sources for fungi it is apparent from these studies that many fungi can co-metabolize one or more PAHs to *trans*-dihydrodiols (Cerniglia *et al.* 1992b). These authors have found that there is interspecies variability among fungi in the regio- and stereoselectivity of the cytochromes P-450 and epoxide hydrolases involved in PAH metabolism.

Scheme 11. Hydroxylation of Phenanthrene (**83**) by Fungi (from Cerniglia *et al.* 1993).



#### 1.3.4 Summary

(A) The results of previous studies suggested that oxygen functions in ring B and/or C of selected abietane diterpenes were required for anti-tumour and anti-inflammatory activity. In particular, the presence of epoxide functionality, as in the natural products triptolide (**2**) and triptidiolide (**3**), was important for this type of activity.

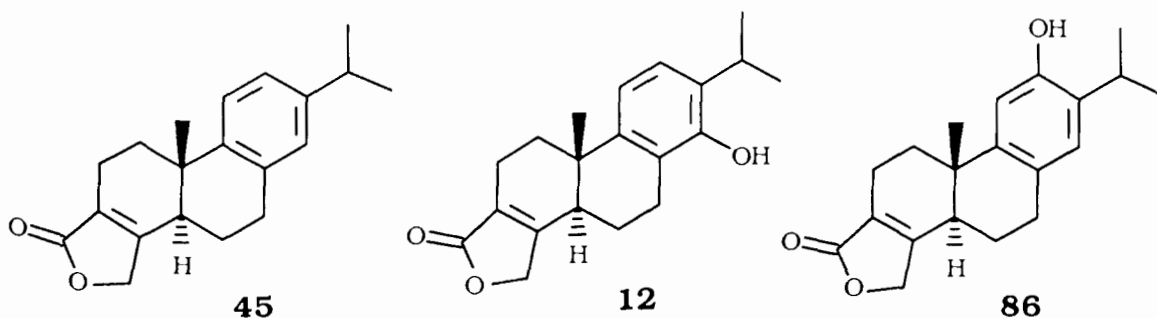
(B) Most of the research to date on fungal biotransformation of aromatic compounds has concentrated on the description of the biotransformation products. In a few cases enzymatic pathways have been proposed; however, evidence for the involvement of a particular enzyme exists for only a few fungi. Although the spectrum of microbial transformations of organic compounds is very broad, diterpene metabolism by fungi and bacteria was limited.

## CHAPTER II -- SYNTHESIS OF PRECURSORS FOR BIOTRANSFORMATION EXPERIMENTS

The main focus of this research was to develop efficient routes to selected diterpenes which may have useful pharmacological activity. The interdisciplinary approach which was considered involves chemical syntheses of appropriate substrates which, in turn, were then subjected to enzyme-catalyzed biotransformations to generate novel diterpene analogues of the abietane family.

### 2.1 Specific Research Objectives

- (i) Synthesis of sufficient quantities of abietane diterpene analogues, butenolide **45**, triptophenolide (**12**), isotriptophenolide (**86**), for biotransformation studies.



- (ii) To screen and select microorganisms (yeasts and fungi) for their ability to biotransform **45**, **86** and **12** as substrates.

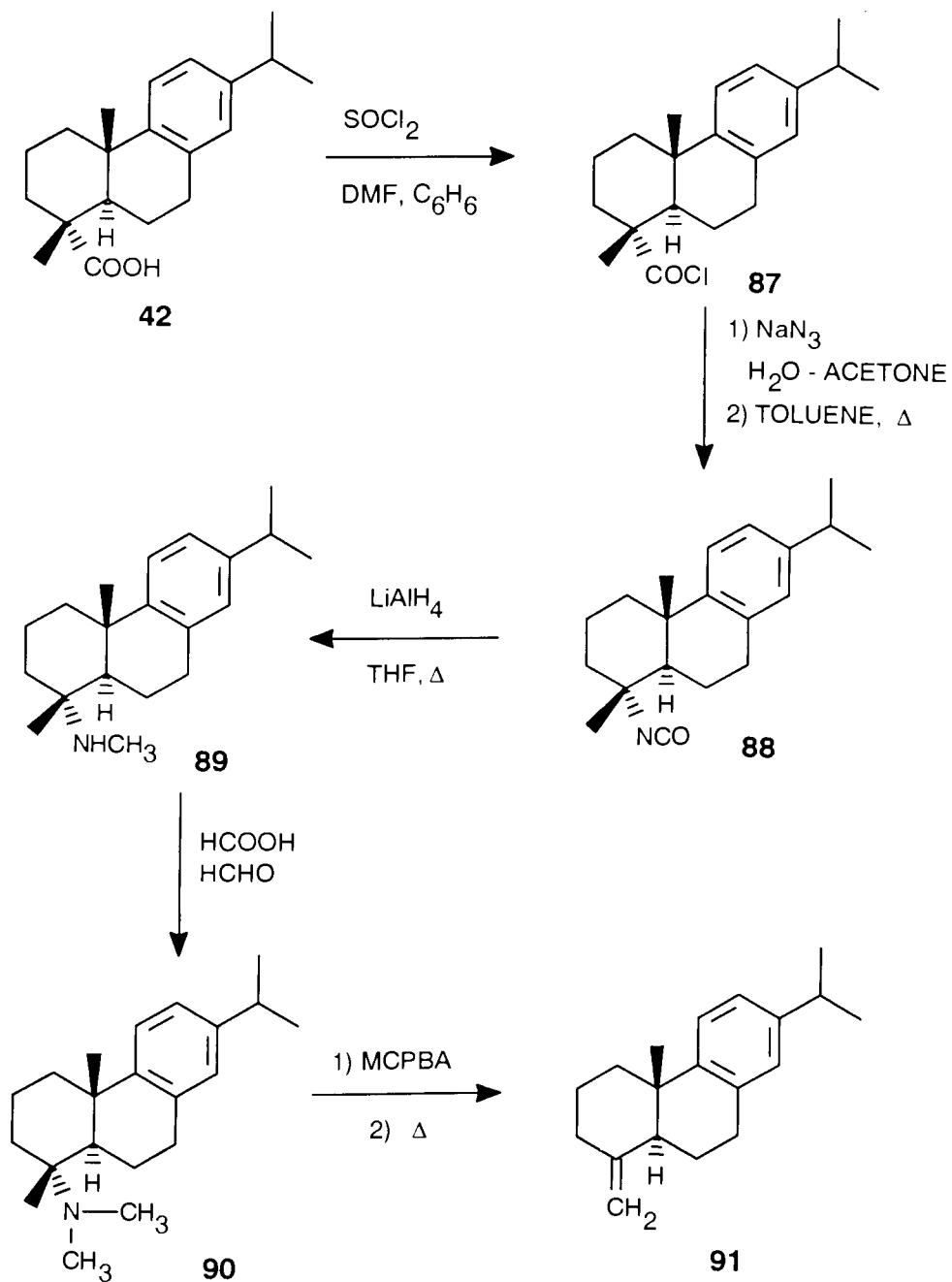
- (iii) To conduct scale-up experiments with selected microorganisms and obtain sufficient quantities of products for structural identification and eventually pharmacological studies.
- (iv) To optimize fermentation parameters using a factorial design experiment (growth media and incubation time) to obtain high yields of the desired products.
- (v) To employ cell immobilization on solid supports to afford stable and long-acting systems for biotransformations.

## 2.2 Synthesis of Butenolide 45

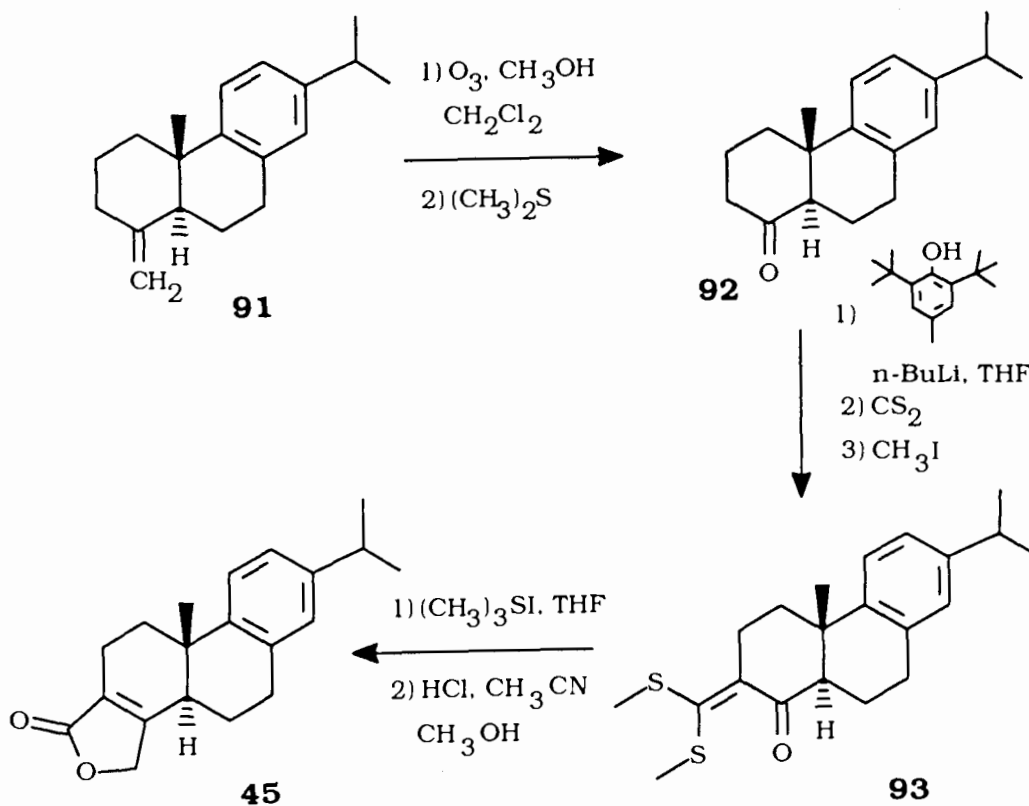
The original synthetic route developed by Roberts involved a lead tetraacetate decarboxylation of dehydroabietic acid (DHA) (**42**) to the exo-olefin **91** followed by conversion of **91** to butenolide **45** as outlined below (Roberts 1989). An improvement for the preparation of **91** to **45** was developed by Kuri-Brena and involves the sequence outlined in Scheme 12 (Kuri-Brena 1992). The conversion of exo-olefin **91** to butenolide **45**, in the latter study, involved the route developed by Roberts.

In the present study, which required the preparation of gram quantities of the substrates butenolide **45** and triptophenolide (**12**), larger scale synthetic transformations were performed. Using high quantities of DHA (**42**) (70 g), it was possible to investigate more fully the experimental details and to improve the yields in several reactions outlined in Scheme 12. Such improvements by the present author are cited in specific sections of the following discussion.

Scheme 12. Synthesis of Butenolide **45** from Dehydroabietic Acid (**42**).



Scheme 12. (Continued)



Treatment of pure DHA (**42**) (obtained after extensive purification of the commercial product) with thionyl chloride in a solution of dimethyl formamide and benzene, afforded the acid chloride **87**. Monitoring of this reaction by infrared spectroscopy with the characteristic carbonyl absorption band of **87** ( $1780\text{ cm}^{-1}$ ) indicated an essentially quantitative conversion of **42** to **87**. The latter, without purification, was converted to the acid azide ( $1720\text{ cm}^{-1}$ ) by treatment with sodium azide and directly heated to afford the rearranged product, the isocyanate **88** ( $2250\text{ cm}^{-1}$ ). The latter after isolation, but without further purification, was reduced with lithium aluminum hydride to the amine **89** (disappearance of



isocyanate absorption band at  $2250\text{ cm}^{-1}$ ) and crude **89** was treated with formic acid-formaldehyde to afford the dimethylamine **90**. Finally, reaction of **90** with *m*-chloroperbenzoic acid and pyrolysis of the resulting amine oxide provided the exocyclic olefin **91**. Purification of **91** by flash column chromatography afforded an overall yield of 52% from the starting acid **42**.

Removal of the methylene unit in the exocyclic olefin **91** was achieved by ozonolysis to the ketone **92** (82% yield). Previous workers were unable to maintain high and constant (80-90%) yields in the ozonolysis process when larger quantities (25 g, for example) of olefin **91** were involved. With careful monitoring of the reaction by TLC, and temperature control at  $-78^{\circ}\text{C}$ , the present study showed that large scale reactions were possible without loss in yield.

In contrast to the above series of reactions which were performed from dehydroabiatic acid (**42**) to exocyclic olefin **91** without purification of intermediates, it was important to perform an extensive chromatographic purification of exo-olefin **91**, which was then converted to ketone **92**. In similar fashion, **92** must be pure so as to obtain optimum yields of the subsequent products. It was clear that the lower yields of **45**, reported by the previous workers, were due, at least in part, to the utilization of ketone **92** which contained trace quantities of impurities from the earlier conversions.

The crystalline ketone **92** was converted to the desired anion by careful treatment with the sterically hindered phenoxide as base. It is important to note that removal of the more accessible C-3 proton, in contrast to the tertiary C-5 proton, is the exclusive reaction. Reaction of the C-3 anion with carbon disulfide and methyl iodide afforded the

ketene thioketal **93**. Careful chromatographic purification provided **93** as a crystalline compound. The interesting conversion of **93** to the butenolide **45** completed the synthesis.

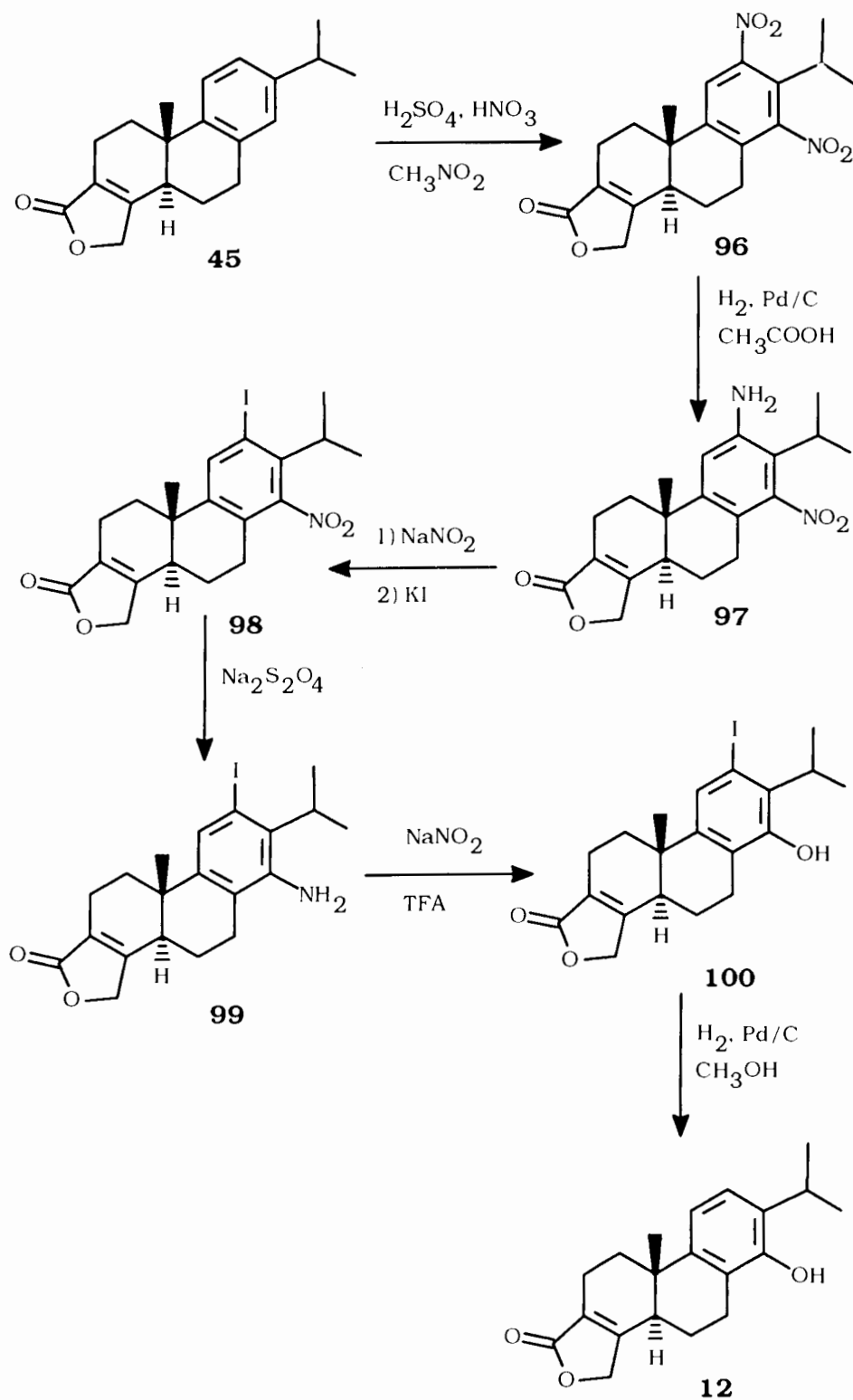
It is particularly important to emphasize that high yields in the overall conversion of **92** to **45**, via the intermediate ketene thioketal **93**, were again only possible when careful monitoring of the reaction by TLC and purification of intermediate **93** (95% yield) was carried out. For example, failure to purify the oily product mixture in the conversion of **92** to **93**, to afford **93** as a crystalline solid, invariably leads to a low yield of **45**.

Under the carefully controlled conditions noted above, an overall yield of 20% of **45** was obtained from **42** when a large scale reaction sequence starting with 70 grams of **42** was conducted. A total of 14 grams of butenolide **45** was prepared by the present author for the synthesis of triptophenolide (**12**) and for the biotransformation experiments with fungi discussed in Chapter III.

### **2.3 Synthesis of Triptophenolide (12)**

Preliminary experiments indicated that **12** was a substrate for the fungus *Cunninghamella elegans* and large scale incubations necessitated the synthesis of gram quantities of this compound. An original synthetic route from butenolide **45** had been developed by Han (Han 1995). Our requirement for larger amounts of **12** demanded that this synthesis be repeated by the present author. For this purpose, the originally developed route (Scheme 13) which had been previously performed on small scale, was now modified by the present author for gram scale synthesis of triptophenolide (**12**).

Scheme 13. Synthesis of Triptphenolide (**12**) from Butenolide **45**.



Nitration of the aromatic ring in butenolide **45** with excess nitric acid afforded the 12,14-dinitro butenolide (**96**) (90% yield). Selective reduction of **96** with hydrogen and a palladium catalyst allows reduction of the 12-nitro function and an excellent yield (87%) of the 12-amino-14-nitro butenolide (**97**) was obtained. Replacement of the amino group by iodide was accomplished via diazotization and displacement of the diazonium function by reaction with potassium iodide to afford 12-iodo-14-nitro butenolide (**98**) in an overall 69% yield.

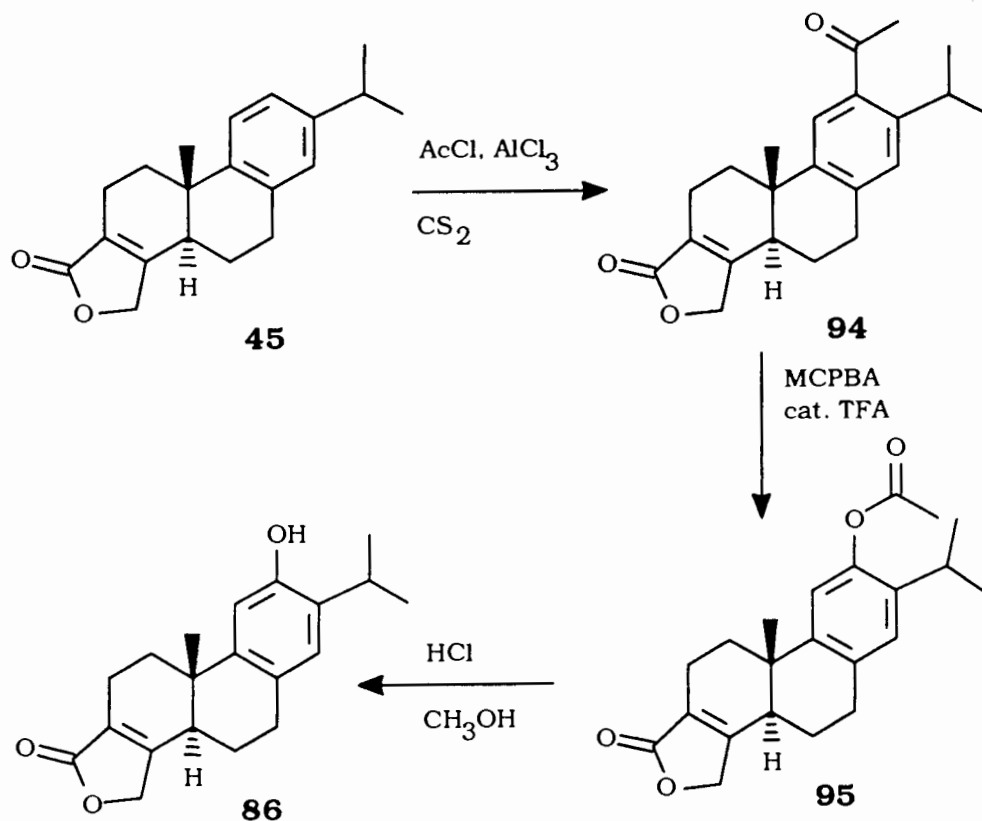
Reduction of the 14-nitro group was then achieved by reaction of **98** with sodium dithionite and the resulting 12-iodo-14-amino butenolide (**99**) (83% yield) was again converted to the 14-hydroxy derivative **100** via diazotization. The final step in the sequence involved removal of the iodine function in **100** to afford the desired triptophenolide (**12**) (94% yield).

The overall yield of triptophenolide (**12**) obtained from butenolide **45** was 30%. In the present study, 1.8 g of **12** were prepared by the author and used for biotransformation experiments with *C. elegans* as outlined in Chapter III. Triptophenolide (**12**) was also used for the immobilization experiments as well as a factorial design experiment discussed in Chapter IV.

#### **2.4 Synthesis of Isotriptophenolide (86)**

Scheme 14 illustrates the conversion of butenolide **45** to the phenolic analogue isotriptophenolide (ITP, **86**). This compound, with a phenolic function in the aromatic ring, was postulated to provide an "activated" system which could result in a more facile bioconversion to desired end products.

Scheme 14. The Synthesis of Isotriptophenolide (**86**) from Butenolide **45**.



The original synthetic route developed by Kuri-Brena involved a conversion of butenolide **45** to ketone **94** by Friedel-Crafts acylation at the more reactive C-12 position of the starting material (Kuri-Brena 1993). Reaction of **94** with *m*-chloroperobenzoic acid provided **95** which upon hydrolysis generated the desired isotriptophenolide (**86**). This synthesis was repeated by Han (Dept. of Chemistry, UBC) and a generous sample (450 mg) of **86** was used for the present study. Biotransformation experiments with yeasts and fungi were conducted using the substrate **86**, and the results are presented in Chapter III.

In conclusion, the synthetic studies discussed above completed the synthesis of the three target molecules, butenolide **45**, triptophenolide (**12**) and isotriptophenolide (**86**), in sufficient amounts for the biotransformation experiments.

## CHAPTER III -- MICROBIAL TRANSFORMATIONS OF SELECTED SYNTHETIC DITERPENE ANALOGUES

The literature survey summarized in Chapter I showed that diterpenes which possess the abietane skeleton can be biotransformed by various microorganisms to novel end products. The purpose of this research was to evaluate specific microorganisms for their ability to oxidize the synthetic diterpenes butenolide **45**, isotriptophenolide (**86**), and triptophenolide (**12**). Specifically, the studies were directed to the introduction of oxygen functionalities without degradation of the structure. For this reason, attention was focussed on the use of eukaryotic microorganisms - yeasts and filamentous fungi.

### 3.1 General Procedure for Biotransformation Experiments

In all cases, experiments were first conducted in Erlenmeyer flasks with a substrate concentration of 0.1 mg/mL of culture volume and with varying incubation times (24-144 h). The biotransformation was monitored by TLC to determine the optimum time to harvest the culture. In order to obtain more quantitative data, with respect to yields, and analytical samples of high purity for the final spectroscopic results and elemental analyses etc., a larger scale experiment involving several hundred milligrams of substrate was then conducted. The reaction mixture was extracted with ethyl acetate and the crude extract chromatographed on silica gel. The pure products were then subjected to spectroscopic analysis (UV, IR, NMR and MS, see Experimental).

A more details on the various experiments undertaken with the specific substrates are shown below.

### **3.2 Studies with Butenolide 45**

As noted above, initial experiments were conducted on small scale and these were followed with larger quantities of butenolide **45** in order to isolate and characterize the products formed.

#### **Preliminary Screening Experiments**

Butenolide **45** was initially incubated in small scale experiments (generally 5 mg of **45** at a concentration of 0.1 mg/mL of culture volume) and the bioconversion monitored by TLC. The conditions employed in these initial studies and also in subsequent larger scale experiments, where appropriate, were as follows:

#### **Studies with Yeast Strains**

Yeasts (Table 2) were generally grown on solid YPA medium consisting of the following (g/L): yeast extract (10 g), Bacto peptone (20 g), glucose (20 g), and agar (20 g). The pH of the medium was adjusted to 6.5.

Several parameters were varied to assess their effect on the extent of biotransformation. These are:

- (1) incubation time (24-144 h).
- (2) pH (4-7).
- (3) growth media components.

The following liquid media were employed (g/L):

- (1) glucose (20 g), Bacto peptone (20 g), and yeast extract (10 g), pH 6.5.



(ii) soybean fat (5 g), glucose (20 g), yeast extract (5 g), NaCl (5 g), K<sub>2</sub>HPO<sub>4</sub> (5 g), pH 6.5.

Table 2. Yeasts Screened for Ability to Biotransform Butenolide **45**.

YEASTS	Conversion of Substrate <b>45</b>
<i>Saccharomyces cerevisiae</i> WT D 273 10B	-
<i>Debaryomyces casteleii</i> CBS #2923	-
<i>Trichosporon aquatile</i> CBS #5973	-
<i>Rhodotorula muciliginosa</i> SFU #1	-
<i>Candida tropicalis</i> CBS #94	-
<i>Rhodosporidium toruloides</i> UBC #659	-
<i>Rhodotorula rubra</i> ATCC #2503	-
<i>Rhodotorula</i> sp. ATCC #18101	-

Legend:

CBS - Centraalbureau voor Schimmelcultures, Amsterdam,  
The Netherlands

SFU - Simon Fraser University, Burnaby, Canada

UBC - Dr. R. Bandoni, University of British Columbia,  
Vancouver, Canada

ATCC - American Type Culture Collection, Rockville,  
Maryland, USA

*S. cerevisiae* - University of Amsterdam, gift of C. Westerbeek-  
Marres

(iii) soybean grits (5 g), glucose (20 g), yeast extract (5 g), NaCl (5 g),  $K_2HPO_4$  (5 g), pH 6.5.

(iv) soybean flour (5 g), glucose (20 g), yeast extract (5 g), NaCl (5 g),  $K_2HPO_4$  (5 g), pH 6.5.

Biotransformation experiments of butenolide **45** by each of the yeast strains shown in Table 2 in the different media (i) - (iv) were performed. The substrate **45** was added at different ages and pH of the growing cultures, and the incubation time of **45** was varied from 24 to 144 h. All of the experiments were done in the presence of control flasks without substrate addition and monitored by TLC.

The results showed that yeast strains were unable to biotransform the abletane analogue **45**.

### **Studies with Filamentous Fungal Strains**

As discussed in Chapter 1, various studies on introduction of hydroxyl groups into aromatic ring systems by fungi (*Aspergillus*, *Rhizopus*, *Syncephalastrum* and *Cunninghamella* species) have been described. For this reason, the filamentous fungi listed in Table 3 were selected for the present study.

Filamentous fungi were grown on PDA medium containing the following (g/L): potato extract (an aliquot of 230 ml of an extract prepared from 100 g of potato autoclaved in 300 mL of water), yeast extract (0.5 g), glucose (20 g), and agar (20 g). The pH of the medium, prior to autoclaving, was 6.5. Cultures were stored at 4<sup>o</sup> C under a layer of sterile mineral oil.

Table 3. Filamentous Fungi Screened for Ability to Biotransform Butenolide **45**.

FUNGI	Conversion of Substrate <b>45</b>
<i>Syncephalastrum racemosum</i> UBC #60	+
<i>Cunninghamella echinulata</i> UBC #92	-
<i>Cunninghamella</i> sp. UBC #95	-
<i>Cunninghamella echinulata</i> ATCC #9244	+
<i>Cunninghamella elegans</i> ATCC #20230	+
<i>Aspergillus niger</i> ATCC #9141	-
<i>Aspergillus fumigatus</i> ATCC #13073	+

Legend:

UBC - Dr. R. Bandoni, University of British Columbia,  
Vancouver, Canada

ATCC - American Type Culture Collection, Rockville,  
Maryland, USA

As in the experiments with yeasts, the following parameters were evaluated:

- (1) age of culture (time at which substrate added),
- (2) incubation times (24-96 h),
- (3) effect of pH (2.5-7.0),
- (4) growth media components.

The following liquid media were employed ( g/L):

- (i) PDB: glucose (20 g), potato extract (23 g), and yeast extract (0.5 g), pH 6.5.
- (ii) SSBF: glucose (20 g), soya bean flour containing fat (10 g), NaCl (5 g),  $\text{KH}_2\text{PO}_4$  (5 g), and yeast extract (5 g), pH 7.0.
- (iii) MNB: glucose (10 g), malt extract (20 g), and nutrient broth ( 8 g), pH 6.2.

The fungal strains presented in Table 3 were evaluated for their ability to biotransform **45** under the varying growth conditions listed above. Cultures were grown for 48-72 h after the butenolide **45** was added at a concentration of 0.1 mg/mL (5 mg to 50 mL volume of culture). Incubation times with **45** varied from 74-96 h and the progress of the bioconversion was again monitored by TLC. From these screening tests for biotransformation of butenolide **45** by the filamentous fungi, it was concluded that some strains were unable (shown as minus sign in Table 3) to convert this substrate, whilst others (positive signs in Table 3) could and were used for further studies.

**Conclusion:** In contrast to yeast strains, certain filamentous fungi converted **45** to products. The ability to oxidize **45** was not uniform within a species or genus. In a number of the experiments, the complexity of the product mixture, as determined by TLC monitoring, required that a selection of the most encouraging data be made. On this basis, *Syncephalastrum racemosum*, *Cunninghamella elegans*, *C. echinulata*, and *Aspergillus fumigatus* were selected for further study.

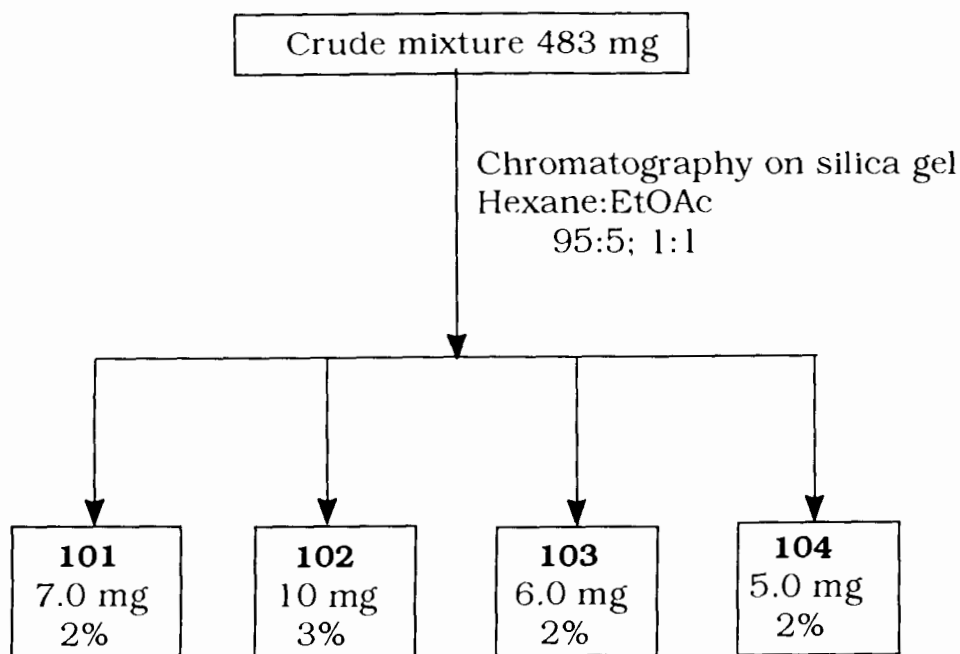
## **Biotransformation of Butenolide 45 with *Syncephalastrum racemosum***

In order to assess the extent of biotransformation of **45** with *S. racemosum*, larger scale experiments (300 mg of **45**) were conducted under the various conditions noted above. The primary culture was then used as an inoculum for a secondary culture (10% v:v). Cultures were incubated on a rotary shaker at 240 rpm at 28° C. To maintain adequate aeration, the ratio of cell suspension volume to flask volume was always 1:5. Butenolide **45** was added as an ethanolic solution to a final concentration of 0.1 mg/mL. As a control, ethanol alone was added to cells in PDB; the volume of ethanol in either control or lactone containing flasks never exceeded 1% of the total volume of the suspension.

Incubation times of butenolide **45** in PDB were varied (24-48 h) with similar results (TLC monitoring) so the 24 h incubation period was selected for further study. After ethyl acetate extraction of the crude reaction mixture and chromatographic separation (Scheme 15), four major metabolites, **101-104** (Scheme 16) were isolated.

Each of the isolated products were subjected to extensive spectroscopic analyses (see Experimental) in order to elucidate their structures. The starting material, butenolide **45**, shows characteristic aromatic proton signals in the NMR spectrum which are in good agreement with respect to chemical shifts and coupling patterns.

Scheme 15. Chromatographic Separation of Crude Ethyl Acetate Extract (Broth + Cell) of Biotransformation of **45** with *S. racemosum*.

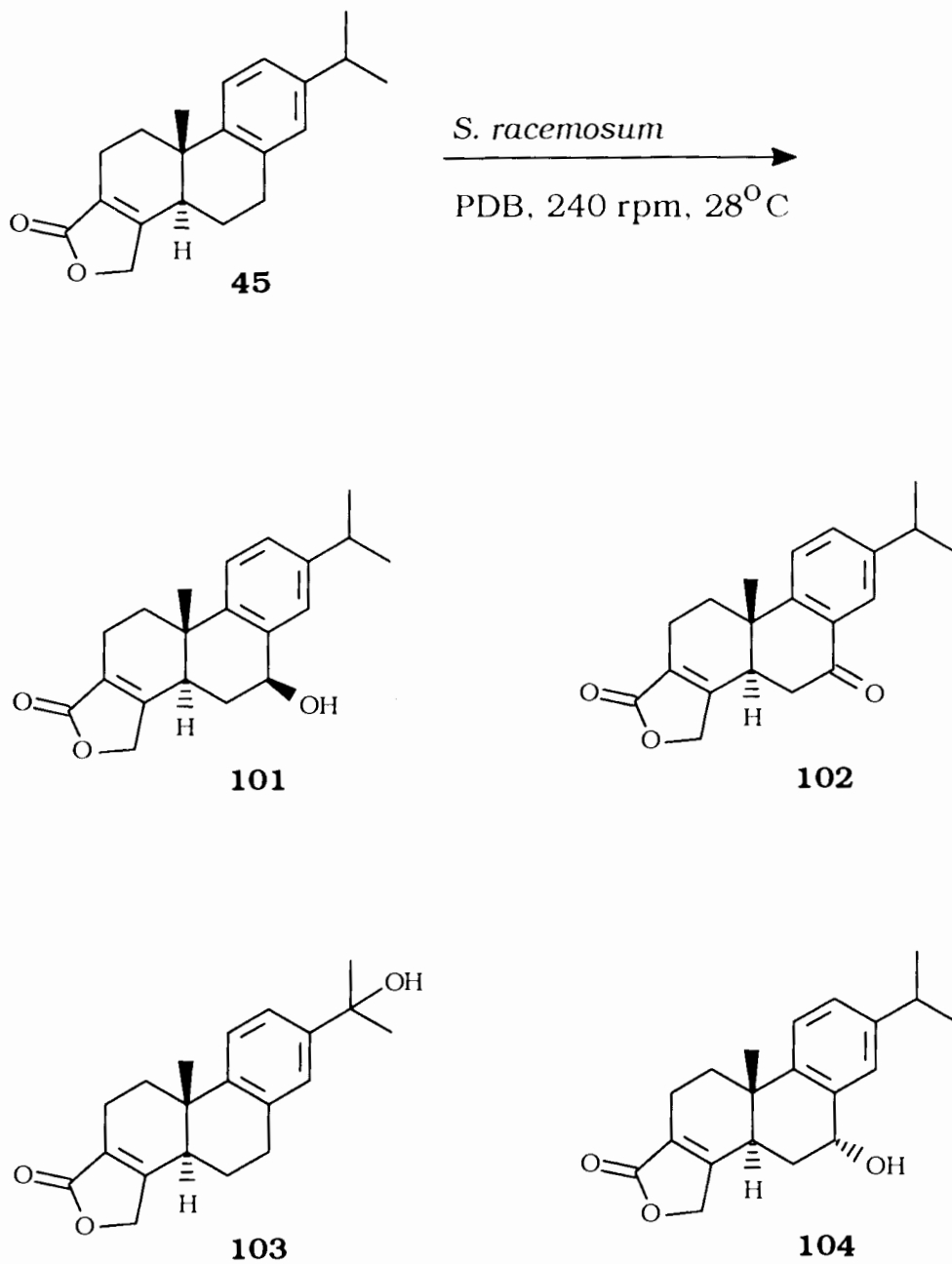


Since the metabolites represent introduction of substituents in ring B or the isopropyl side chain, the significant differences in their NMR spectra from those noted in **45** are in the aromatic region. The most pertinent data relating to this aspect are noted below.

The spectral data of the novel metabolites discussed below are presented in detail in the Experimental Section.

**7 $\beta$ -Hydroxybutenolide (101).** Substitution of OH at C-7 is supported by a change in the aromatic region: the C-14 signal in butenolide **45** ( $\delta$  6.99) was shifted downfield to  $\delta$  7.44. In addition, the two C-7 proton signals in butenolide **45** ( $\delta$  3.02) were now observed at  $\delta$  5.02 and with an intensity of only one proton.

Scheme 16. Biotransformation of Butenolide **45** with *S. racemosum*.



7 $\alpha$ -Hydroxybutenolide (**104**). This compound is present as an isomer of **101** with the characteristic C-7 proton signal at  $\delta$  4.95 as an unresolved multiplet. It showed an identical fragmentation pattern in the mass spectrum to that of **101**.

15-Hydroxybutenolide (**103**). This metabolite clearly shows the introduction of a hydroxyl function into the isopropyl side chain. The methyl group proton signals of butenolide **45** originally appearing as a six-proton doublet at  $\delta$  1.24 were shifted to  $\delta$  1.58 and appear as a six-proton singlet. In addition, the original butenolide C-15 proton multiplet ( $\delta$  2.86) was not present in the spectrum of the metabolite.

7-Ketobutenolide (**102**). The carbonyl group at C-7 has an influence on the C-14 aromatic proton signal in butenolide **45** ( $\delta$  6.99). The NMR spectrum of the 7-keto metabolite reveals a shift of this signal to  $\delta$  7.99. The C-7 protons at  $\delta$  3.02 have completely disappeared in the NMR spectrum of **102**.

### **Effect of Growth Media on Biotransformation of Butenolide 45**

To determine whether the composition of the growth medium influenced the pattern of metabolic products from butenolide **45**, *S. racemosum* was incubated with **45** in either YPD or SSBF medium. The metabolites produced by these media were identical in their TLC mobilities to the products observed with the PDB indicating that the composition of these media, at least, had no effect on the metabolism of butenolide **45** by *S. racemosum*.

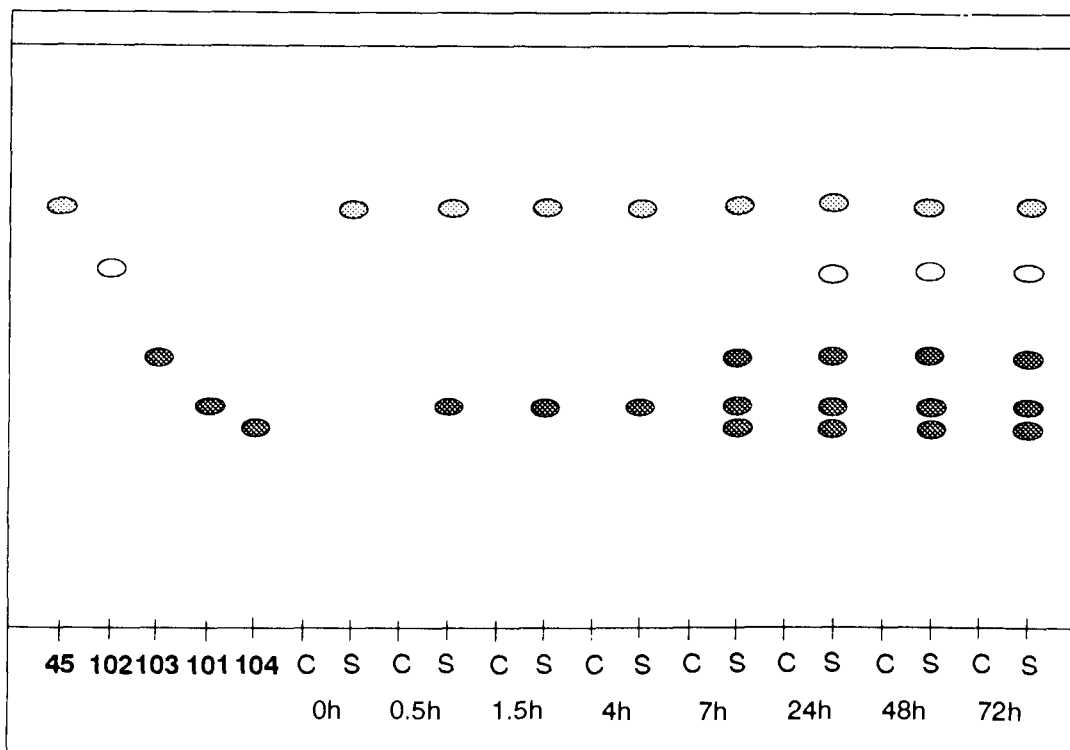


## **Time Course of Metabolism of the Butenolide 45 by *S. racemosum* Cultures**

Butenolide **45** was added to the *S. racemosum* culture after 48 h of incubation at 28° C, as noted above, and samples of the suspension were withdrawn at intervals (30 min, 90 min, 4 h, 7 h, 24 h, 48 h, 72 h). The metabolites were extracted with ethyl acetate, separated on TLC plates and comparisons (TLC) were then made with the authentic samples of **101-104** (Figure 1). Control cultures containing only the ethanol vehicle were processed in parallel. The 7 $\beta$ -hydroxybutenolide appeared after 30 min of incubation whereas the 7 $\alpha$ -hydroxybutenolide was not detectable until between 4 and 7 h suggesting that enzyme induction was required for the latter hydroxylation reactions. Similarly, the 15-hydroxy metabolite appeared at the same time as the 7 $\alpha$ -hydroxybutenolide, i.e., after a 4 h lag period. In contrast, the 7-ketobutenolide was not observed until 24 h of incubation which suggests that it may have been an oxidation product of the 7-hydroxybutenolide metabolites.

After 72 h of incubation, all of the metabolites noted above were detected in the cell supernatant (broth) and in washed cell suspensions. As fungi are capable of conjugation with glucuronide, sulfate, and glutathione (Cerniglia & Gibson 1974), we tested the possibility that some of the metabolites were present as conjugates. Control and butenolide-treated cell suspensions and filtered broth from 72-h incubations were acidified to pH 2 with HCl and left at 80° C overnight to cleave any conjugates which may have been formed.

Figure 1. TLC Analysis for the Time Course of Incubation of **45** with *S. racemosum*. (Schematic Presentation).



Legend:

- Butenolide **45**
- 15-Hydroxybutenolide (**103**)
- 7 $\alpha$ -Hydroxybutenolide (**104**)
- 7-Ketobutenolide (**102**)
- 7 $\beta$ -Hydroxybutenolide (**101**)
- S - sample; C - control

Thin-layer chromatograms of methylene chloride extracts of these solutions did not reveal any differences in the amounts of polar metabolites or in their  $R_f$  values when compared to the nonhydrolyzed broth or cell suspensions. Thus, the polar metabolites of *S. racemosum*

were not conjugated to any significant degree before excretion into the medium.

### **Effect of Cytochrome P-450 Inhibitors in Whole Cells on the Metabolism of Butenolide **45** to 7 $\beta$ -Hydroxy- and 15-Hydroxybutenolides**

To determine the possible role of fungal cytochrome P-450 monooxygenase enzymes in the hydroxylation of butenolide **45**, five different cytochrome P-450 inhibitors were added to 48-h old *S. racemosum* cultures 15 min prior to the addition of butenolide (see Experimental). After a further 24 h, the broth was extracted and the metabolites were separated by TLC as described in the Experimental Section. In the sample containing only butenolide and no inhibitors, 15-hydroxy- (**103**) and 7 $\alpha$ -hydroxybutenolide (**104**) are present (Table 4). Interestingly, the 7 $\beta$ -metabolite, present in the cell fractions after 30 min, was not detectable in the broth alone. All of the inhibitors prevented the appearance of the 15-hydroxy product. Carbon monoxide,  $\alpha$ -naphthoflavone and aminobenzothiazole also prevented the appearance of the 7 $\alpha$ -hydroxybutenolide metabolite. In contrast, the twoazole inhibitors, ketoconazole and miconazole, were not able to inhibit the 7 $\alpha$ -hydroxylation of butenolide **45** by *S. racemosum* (Table 4).

None of the agents had any effect on fungal growth in liquid medium except for carbon monoxide which reduced the growth of *S. racemosum* to 25% of the other control and treated cultures (Table 4). Butenolide **45** alone (0.1 mg/mL) had no effect on fungal growth when added after 48 h of incubation.

Table 4. The Effects of Cytochrome P-450 Inhibitors on the Oxidation of Butenolide **45** by *S. racemosum* to 7 $\alpha$ -Hydroxy- (**104**) and 15-Hydroxybutenolide (**103**)<sup>a</sup>

Sample <sup>b</sup>	% of control growth after 96 h	TLC-detectable metabolites extracted from broth	
		7 $\alpha$ -Hydroxy <b>104</b>	15-Hydroxy <b>103</b>
Control	100	-	-
Butenolide <b>45</b>	100	+	+
CO	25	-	-
CO + <b>45</b>	26	-	-
Keto	93	-	-
Keto + <b>45</b>	95	+	-
Mico	104	-	-
Mico + <b>45</b>	103	+	-
$\alpha$ -NF	109	-	-
$\alpha$ -NF + <b>45</b>	92	-	-
ABT	100	-	-
ABT + <b>45</b>	113	-	-

<sup>a</sup> Inhibitors were added to *S. racemosum* cultures after 48 h of growth. Butenolide **45** (0.1 mg/mL) was added 15 min later and the flasks were then incubated for an additional 24 h. Broth was extracted with ethyl acetate and the metabolites were separated and identified by TLC. The control mycelial wet weight after 96 h was 0.84 g.

<sup>b</sup> Abbreviations are: CO, solution bubbled for 2 min with sterile-filtered carbon monoxide prior to addition of **45** or ethanol addition; Keto, 20  $\mu$ M ketoconazole; Mico, 20  $\mu$ M miconazole;  $\alpha$ -NF, 50  $\mu$ M  $\alpha$ -naphthoflavone; ABT, 50  $\mu$ M aminobenzothiazole.

The 7 $\beta$ -hydroxylation was detected 6 h prior to the appearance of 7 $\alpha$ -hydroxybutenolide (30 min and 7 h post-butenolide addition, respectively) and was found in greater quantities after 24 h of biotransformation (7 mg of  $\beta$ -hydroxy- versus 3 mg of  $\alpha$ -hydroxybutenolide). As the C-7-OH function is fixed within the B ring,  $\beta$  to  $\alpha$  isomerization is only possible via the 7-keto intermediate followed by specific reduction to the 7 $\alpha$ -isomer. Alternatively, it is possible to consider direct hydroxylation to afford the  $\alpha$  isomer. Hydroxylated products were not detected prior to 30 min (7 $\beta$ -hydroxy) and 7 h (7 $\alpha$ -hydroxy and 15-hydroxy) after butenolide **45** addition to *S. racemosum* indicating that enzyme induction may have been required for the oxidation of **45**. Nevertheless, the evidence suggests that enzyme induction may have been necessary before oxidation occurred at C-15 and possibly also at C-7.

The differences in the regio- and stereoselectivity of the hydroxylation and in the time course of appearance of the 7-hydroxy- and 15-hydroxybutenolides both suggest that more than one enzyme was responsible for the hydroxylation reactions. Further evidence for this hypothesis came from the experiments using cytochrome P-450 inhibitors. Cytochrome P-450 enzymes catalyze a large number of oxidative reactions with a great diversity of substrate structures (Guengerich 1991). As in higher eukaryotes, fungal cytochrome P-450 enzymes have been shown to be important not only in sterol biosynthesis (lanosterol 14- $\alpha$ -demethylase) (Aoyama *et al.* 1984; Kalb *et al.* 1987) and xenobiotic oxidation (Cerniglia *et al.* 1978, Cerniglia & Gibson 1974) but also in the hydroxylation of long chain hydrocarbons and fatty acids (Duppel *et al.* 1973; Sanglard *et al.* 1989) and phytoalexin metabolism

(van Etten *et al.* 1982, 1989). Inhibitors of cytochrome P-450 can possess a selectivity for particular isozymes. In higher eukaryotes,  $\alpha$ -naphthoflavone inhibits the 3-methylcholanthrene or  $\beta$ -naphthoflavone-inducible form of P-450 (Huang *et al.* 1981). Ketoconazole and miconazole are specific inhibitors of the fungal cytochrome P-450 lanosterol-14 $\alpha$ -demethylase enzyme at nanomolar concentrations (van den Bossche *et al.* 1981) by coordination of the heme prosthetic group, but it can also inhibit other P-450 activities in enzymes such as mammalian lanosterol-14 $\alpha$ -demethylases and aminopyrine N-demethylase in concentrations of approximately 100  $\mu$ M (Willemsens *et al.* 1980). Inhibition of mammalian C<sub>17-20</sub> lyase has also been detected at lower concentrations (Santen *et al.* 1983). Aminobenzothiazole is less selective and alkylates the prosthetic heme group (Ortiz de Montellano & Mathews 1981). Finally, carbon monoxide is a competitive inhibitor of O<sub>2</sub> for the heme iron. All of the above inhibitors, regardless of mechanism, prevented the 15-hydroxylation of butenolide **45** and had no effect on fungal growth (with the exception of CO). In contrast, ketoconazole and miconazole did not inhibit 7 $\alpha$ -hydroxylation suggesting that separate enzymes are responsible for the 7- and 15-hydroxylations.

**Conclusion:** The zygomycete fungus, *S. racemosum*, is capable of biotransforming the butenolide **45** into several novel metabolites. The enzyme-catalyzed reactions involve hydroxylation at "activated" (benzylic) carbon sites. Aromatic hydroxylation was not observed. Overall yield of metabolites from the butenolide substrate **45** was approximately 10%. Thus further studies were undertaken to find strains with greater bioconversion activities.

The above study was recently published (Milanova & Moore 1993).

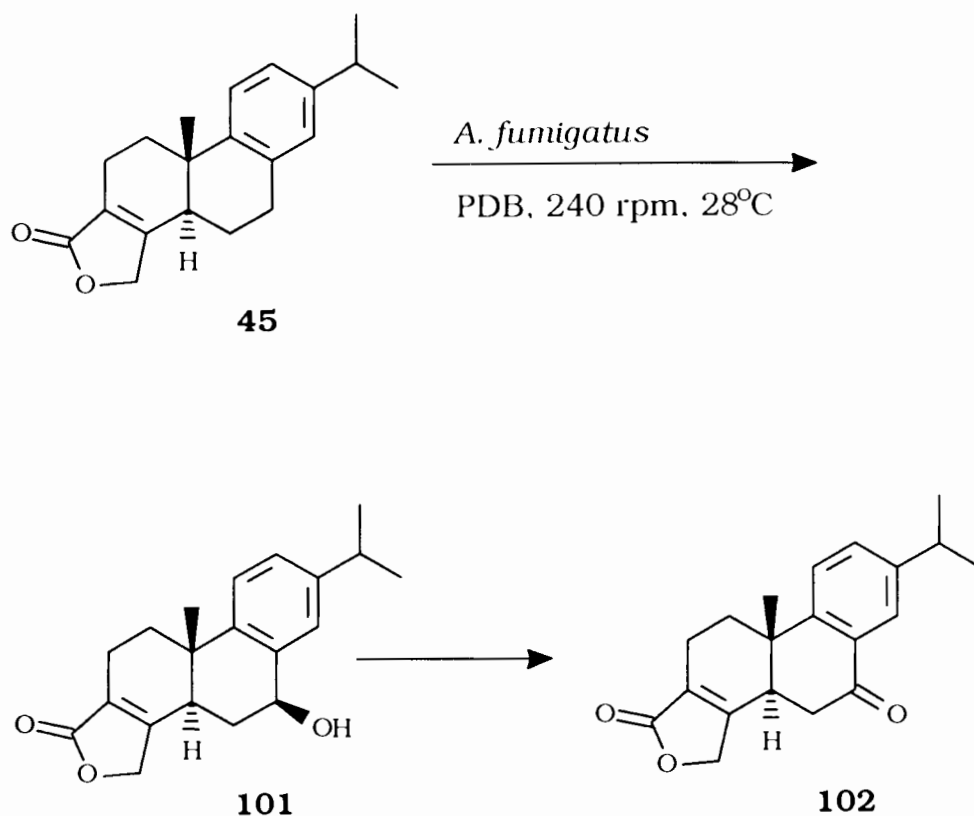
## **Biotransformation of Butenolide 45 with *Aspergillus fumigatus***

The next series of experiments which were undertaken with the butenolide **45** as substrate employed the fungus, *A. fumigatus*. It should be noted that the well characterized industrial strain of *A. niger* did not show any biotransformation activity. Thus, the ability to oxidize butenolide **45** was not uniform within a genus nor was it present in different strains of the same species.

The conditions of biotransformation were similar to those employed with *S. racemosum*. As in the latter experiments, cultures of *A. fumigatus* were stored on potato dextrose agar (PDA) slants. Spore suspensions were inoculated into PDB medium containing glucose (20 g) and grown for 48 h at 240 rpm on a rotary shaker.

Scheme 17 depicts the oxidation of **45** by *A. fumigatus*. Butenolide **45** (0.1 mg/mL) was added to 48-h old cultures of *A. fumigatus* (see Experimental) and incubation for a further 48 h resulted in the production of the 7 $\beta$ -hydroxybutenolide (**101**) and 7-ketobutenolide (**102**). This metabolism differed from that determined previously for *S. racemosum* which afforded the 7 $\beta$ -hydroxybutenolide (**101**), 7-ketobutenolide (**102**), and 7 $\alpha$ -hydroxybutenolide (**104**) compounds as well as oxidizing the isopropyl side chain to yield the 15-hydroxylated derivative (**103**).

Scheme 17. Biotransformation of Butenolide **45** with *Aspergillus fumigatus*.

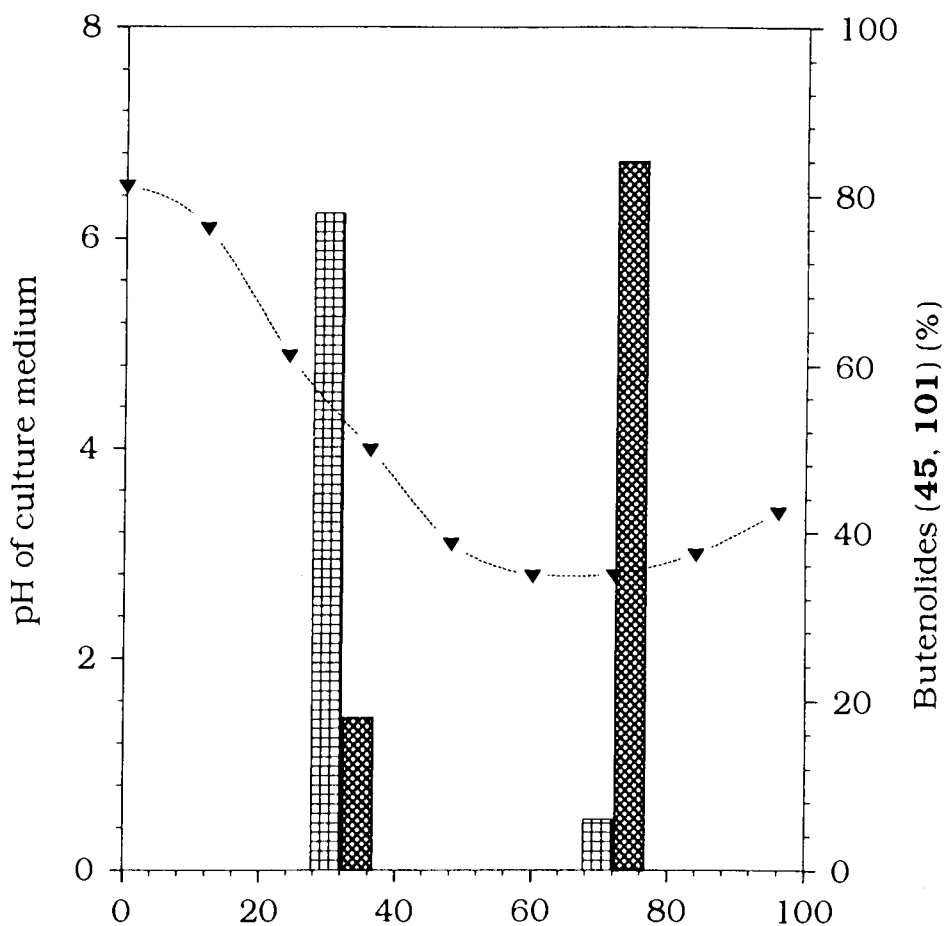


From preliminary experiments it was clear that in the addition of the substrate **45** to the growing culture of *A. fumigatus*, the best biotransformation was achieved when the pH was around 3.0 (60-70 h growth prior to addition of **45**, Figure 2). These conditions were employed in subsequent large scale experiments.

When butenolide **45** was added to *A. fumigatus* cultures during logarithmic phase (30 h), only 18% of the parent compound was oxidized after 48 h (Figure 2).



Figure 2. Influence of pH and Culture Age on the Biotransformation of Butenolide **45** with *Aspergillus fumigatus*.



Growth of culture (h) prior to substrate addition

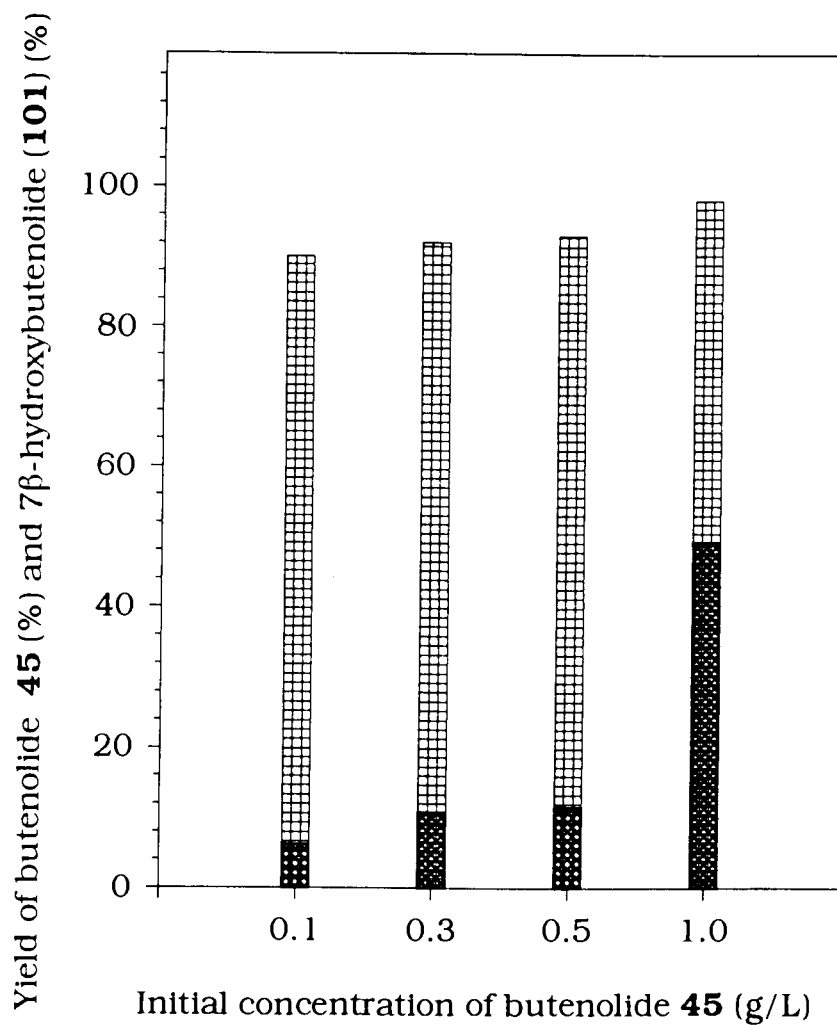
Legend:

Butenolide **45** (%)

7β-Hydroxybutenolide (**101**) (%)


pH of culture medium

Figure 3. Yield of 7 $\beta$ -Hydroxybutenolide (**101**) after 48 Hours Incubation Using a Different Initial Concentration of Butenolide **45**.



Legend:

Butenolide **45** (%) recovered after 48 hours 

7 $\beta$ -Hydroxybutenolide (**101**) (%) 

In contrast, over 80% of the butenolide was converted to 7 $\beta$ -hydroxybutenolide (**101**) in 48 h if the substrate was added during the stationary phase (70 h). It is probable that the greater conversion was due to the presence of a more active or a higher concentration of hydroxylase enzyme during stationary phase.

To determine the effect of substrate concentration on the biotransformation process, butenolide **45** was added to 48 h old cultures of *A. fumigatus* in concentrations of 0.1, 0.3, 0.5 and 1.0 g/L. The volume of the cultures used in each experiment was 1.0 L. The bioconversion of **45** resulted in a 84% yield of the major product 7 $\beta$ -hydroxybutenolide (**101**) after 48 h, when the concentration of the substrate was 0.1 g/L and 81% of **101** in case of 0.3 and 0.5 g/L. However, increasing the substrate concentration to 1.0 g/L resulted in only 49% yield of 7 $\beta$ -hydroxybutenolide (**101**) (Figure 3). Substrate saturation of the hydroxylase or substrate-induced cytotoxicity could account for the observed percentage decrease in bioconversion. However, the latter explanation is less likely as there was no apparent inhibition of *A. fumigatus* growth by the higher concentration of the butenolide. More likely, the solubility of **45** may have been the limiting step as the solubility of **45** in water was 0.015 g/100 g water.

### **Influence of Growth Media on Biotransformation of Butenolide 45**

The composition of the culture medium influenced the enzymatic activity of the fungus to metabolize butenolide **45**. As noted above, *A. fumigatus* oxidized **45** to the 7 $\beta$  derivative in PDB medium. In contrast, no metabolites were formed when this fungus was incubated with **45** in

SSBF medium even though the culture had shown excellent growth (see Experimental Section).

**Conclusion:** *A. fumigatus* grown in PDB medium was found to be an excellent system for introducing a hydroxyl group in ring B (C-7) in the substrate **45**. Since chemical and/or enzymatic oxidation of the C-7 hydroxy to the corresponding 7-keto analogue is readily available, this fungus similarly allows an entry into this series as well.

The above studies are part of a recent publication (Milanova *et al.* 1994).

Having achieved hydroxylation at the benzylic site in ring B, our attention turned to experiments with other microorganisms in the hope that functionalization of **45** could be obtained at other sites in rings B and/or C.

### **Biotransformation of Butenolide 45 with *Cunninghamella elegans***

As summarized in Chapter 1 *C. elegans* has been shown to generate regio- and stereoselective modifications to a variety of organic substrates. It was therefore of interest to evaluate its enzymatic activity and to compare data already available from the experiments noted above.

The fungus was stored on PDA medium. Spore suspensions were added to SSBF liquid medium (see Experimental) and grown on a rotary shaker at 240 rpm at 28° C.

Incubation of stationary phase cultures of *C. elegans* with substrate **45** for 20 h yielded 9 products (of which 7 were novel compounds) which were extracted from the broth and the mycelia, and separated using extensive silica gel chromatography followed by flash chromatography. Scheme 18 summarizes the chromatographic

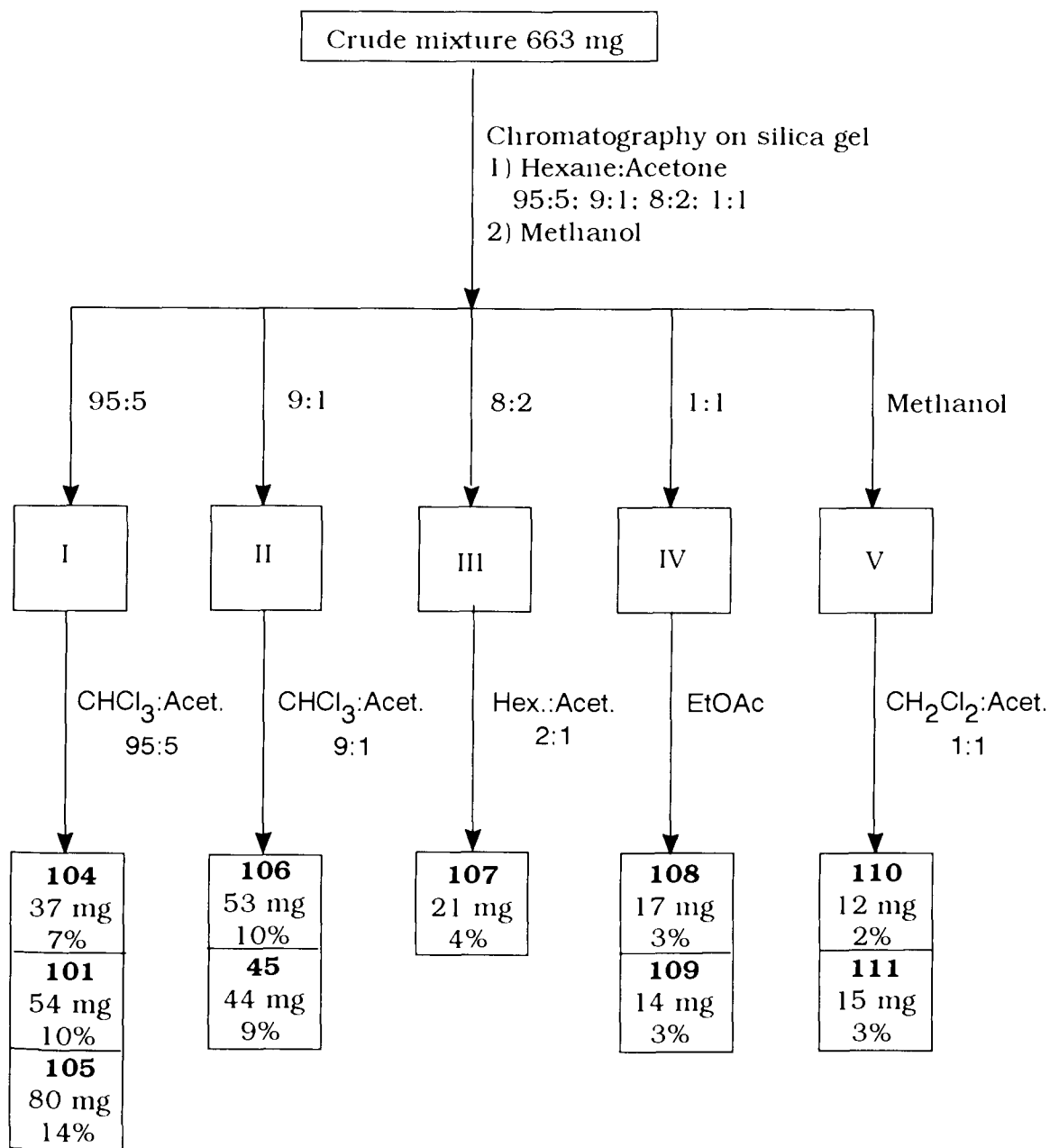
separation of the ethyl acetate extraction of the broth while Scheme 19 provides a similar outline for the separation of the crude cell extract. Scheme 20 summarizes the structures of the metabolites isolated.

Pertinent  $^1\text{H}$ -NMR and MS data for the butenolide **45** and for the novel metabolites **105-111** isolated from *C. elegans* are shown below. *C. echinulata* (ATCC #9244) also oxidized the butenolide **45** but afforded only one product, 7 $\beta$ -hydroxybutenolide (**101**). It should be noted that even though *Cunninghamella* sp. were able to oxidize polycyclic aromatic hydrocarbons (Cerniglia 1992), the fungal strains and used in this study did not possess the ability to attack the aromatic ring of **45**.

The two metabolites produced by *C. elegans* were identical to the 7 $\beta$ - and 7 $\alpha$ -hydroxybutenolides (**101** and **104**) obtained from biotransformation with *S. racemosum* as shown by TLC, NMR, and MS.

Metabolites **105** and **106** showed a molecular ion peak at  $m/z$  328 in the mass spectrum which was 32 mass units larger than the butenolide **45**. The  $^{13}\text{C}$  NMR spectrum of both products showed a tertiary hydroxyl group at C-5 (**105**:  $\delta$  69.2; **106**:  $\delta$  69.2) and the  $^1\text{H}$  NMR a secondary hydroxyl group at C-7 (**105**:  $\delta$  4.97, d,  $J = 5$  Hz and **106**:  $\delta$  5.15, dd,  $J = 8, 8$  Hz). Finally, from the coupling constants of each signal in the  $^1\text{H}$ -NMR spectrum, **105** was characterized as 5 $\alpha$ ,7 $\alpha$ -dihydroxybutenolide, and **106** as 5 $\alpha$ ,7 $\beta$ -dihydroxybutenolide. Compound **107** showed a molecular ion peak at  $m/z$  328 in the mass spectrum which was 32 mass units larger than the butenolide, **45**. The  $^1\text{H}$ -NMR spectrum of **107** indicated the existence of a tertiary hydroxyl group at C-5 (no proton signal due to C-5) and a primary hydroxyl group on C-16 ( $\delta$  3.72, d,  $J = 8$  Hz).

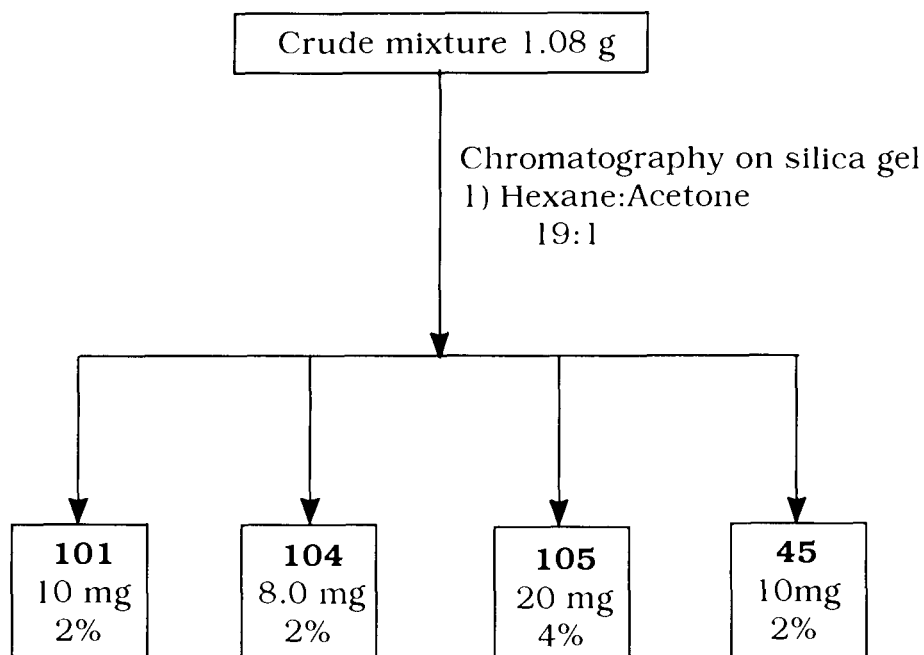
Scheme 18. Chromatographic Separation of Crude Ethyl Acetate Extract (Broth) of Biotransformation of **45** with *C. elegans*.



Legend:

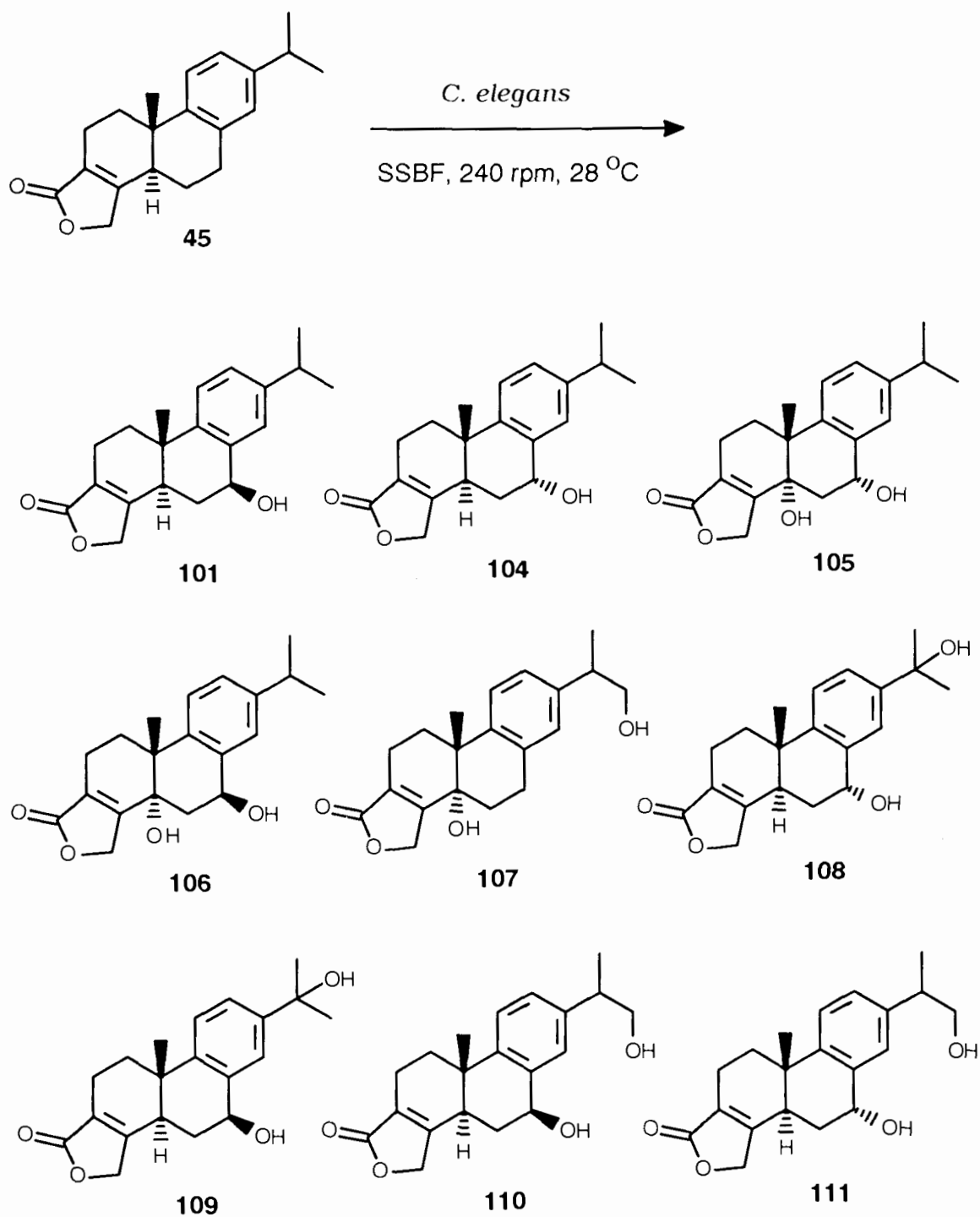
I, II, III, IV and V → Fractions subjected to further chromatographic separation

Scheme 19. Chromatographic Separation of Crude Ethyl Acetate Extract (Cells) of Biotransformation of **45** with *C. elegans*



Compounds **108** and **109** showed an MS molecular ion peak at  $m/z$  328 which was 32 mass units larger than the butenolide **45**. The  $^1\text{H-NMR}$  spectrum of both products showed the existence of a secondary hydroxyl group at C-7 (**108**:  $\delta$  4.95, dd,  $J = 5, 1$  Hz); (**109**:  $\delta$  5.03, dd,  $J = 8, 8$  Hz) and a tertiary hydroxyl group at C-15 (neither compound showed a proton signal due to C-15 and both had signals due to C-16 and C-17 protons as singlets: **108**:  $\delta$  1.60; **109**:  $\delta$  1.61). From determination of the coupling constants of each signal in the  $^1\text{H-NMR}$  spectrum, **108** was established as  $7\alpha,15$ -dihydroxybutenolide and **109** as  $7\beta,15$ -dihydroxybutenolide.

Scheme 20. Biotransformation of Butenolide **45** with *Cunninghamella elegans*.





Compounds **110** and **111** showed a molecular ion peak at  $m/z$  328 in the mass spectrum which was 32 mass units larger than the butenolide **45**. The  $^1\text{H-NMR}$  spectrum of both products showed the existence of a secondary hydroxyl group at C-7 (**110**:  $\delta$  5.00, dd,  $J = 8, 8$  Hz; **111**:  $\delta$  4.92, br s) and a primary hydroxyl group at C-16 (**110**:  $\delta$  3.72; **111**:  $\delta$  3.74, d,  $J = 8$  Hz). From the coupling constants of the relevant signals in the  $^1\text{H-NMR}$  spectrum, **110** was determined to be 7 $\beta$ ,16-dihydroxybutenolide and **111** as 7 $\alpha$ ,16-dihydroxybutenolide.

The pertinent data from the proton NMR spectra of the fungal metabolites are summarized in Table 5.

As was found with *S. racemosum*, *C. elegans* oxidized only ring B and not ring C. This fungus also oxidized, to some extent, the isopropyl side chain of butenolide **45**. In contrast, as noted in Chapter 1, Biellmann and coworkers have found that certain bacteria can hydroxylate the aromatic ring of a related diterpene structure, dehydroabiatic acid, which has a carboxylic acid group at C-4 on ring A. They showed that *Flavobacterium resinovorum*, *Pseudomonas* sp. and *Alcaligenes eutrophus* degraded dehydroabiatic acid by C-7 hydroxylation followed by aromatic hydroxylation and subsequent cleavage of ring B (Biellmann *et al.* 1973a, b). *F. resinovorum* (ATCC #12524) was tested in the present study for its ability to oxidize butenolide **45** and biotransformation was not observed with this organism (TLC monitoring).

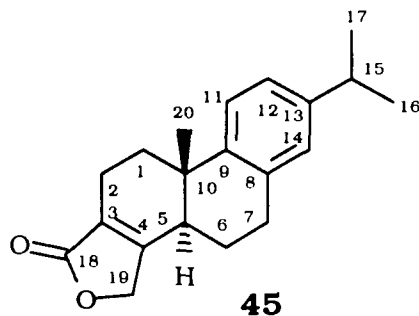


Table 5. Pertinent  $^1\text{H-NMR}$  Data of Butenolide Metabolites Produced by *C. elegans*<sup>a</sup>.

Compound No.	C5	C7	C14	C16 and C17
<b>45</b>	2.73 (m, 1H)	3.02 (m, 2H)	6.99 (brs, 1H)	1.24 (d, 6H)
<b>105</b>	-	4.97 (d, 1H)	7.36 (d, 1H)	1.28 (d, 6H)
<b>106</b>	-	5.15 (dd, 1H)	7.38 (d, 1H)	1.26 (d, 6H)
<b>107</b>	-	3.12 (m, 2H)	7.06 (d, 1H)	1.28 (d, 3H, C17)
	-	-	-	3.72 (d, 2H, C16)
<b>108</b>	3.20 (m, 1H)	4.92 (dd, 1H)	7.24 (d, 1H)	1.60 (s, 6H)
<b>109</b>	2.82 (m, 1H)	5.03 (dd, 1H)	7.71 (d, 1H)	1.61 (s, 6H)
<b>110</b>	2.80 (m, 1H)	5.00 (dd, 1H)	7.45 (d, 1H)	1.29 (d, 3H, C17)
	-	-	-	3.72 (d, 2H, C16)
<b>111</b>	3.19 (m, 1H)	4.92 (dd, 1H)	7.27 (d, 1H)	1.30 (d, 3H, C17)
	-	-	-	3.74 (d, 2H, C16)

<sup>a</sup>All chemical shift values are given in ppm ( $\delta$  scale, TMS at 0)

**Conclusion:** In contrast to *A. fumigatus* which provided essentially one exclusive product in 90% yield, *C. elegans* (ATCC#20230) produced a complex mixture of 9 products, of which 7 are novel compounds in yields varying from 2-14%. This fungus, in agreement with the broad substrate capability evident in the scientific literature, *C. elegans* contains a variety of enzymes capable of attack at different sites of the diterpene.

The above results are part of a recent publication (Milanova *et al.* 1994).

### **3.3 Biotransformation of 7 $\beta$ -Hydroxybutenolide (101) with Fungi**

In order to assess whether a ring B functionalized metabolite could serve as a substrate for further hydroxylation in ring C, one of the metabolites obtained in the above experiments, the 7 $\beta$ -hydroxybutenolide (**101**), was selected for further study. The compound **101** (0.1 mg/mL) was incubated with the fungal strains shown in Table 3, in PDB medium over the time period of 96-120 h. As in previous studies, TLC monitoring of the mixture was performed at 24 h intervals. Unfortunately substrate **101** was not biotransformed to any novel products and remained unattacked under any reaction conditions.

It should be noted that none of the other fungal metabolites were tested for further biotransformation.

### **3.4 Biotransformation of Isotriptophenolide (86) with *Cunninghamella echinulata***

The previous experiments with butenolide **45** indicated that the various fungal strains evaluated were incapable of introducing an oxygen functionality in the aromatic ring C under the conditions tested. Since one of the initial objectives was to generate diterpene analogues which possessed oxygen functions similar to those in triptolide (**2**) and triptidiolide (**3**), that is, in rings B and C, attention was turned to studies with "activated" ring C diterpene analogues. It was felt that a phenolic hydroxyl group in this ring (C-12) would render more facile enzymatic attack by the oxidative enzymes present in the fungal strains. For this

purpose, isotriptophenolide (**86**) was used as a substrate in another series of biotransformation studies.

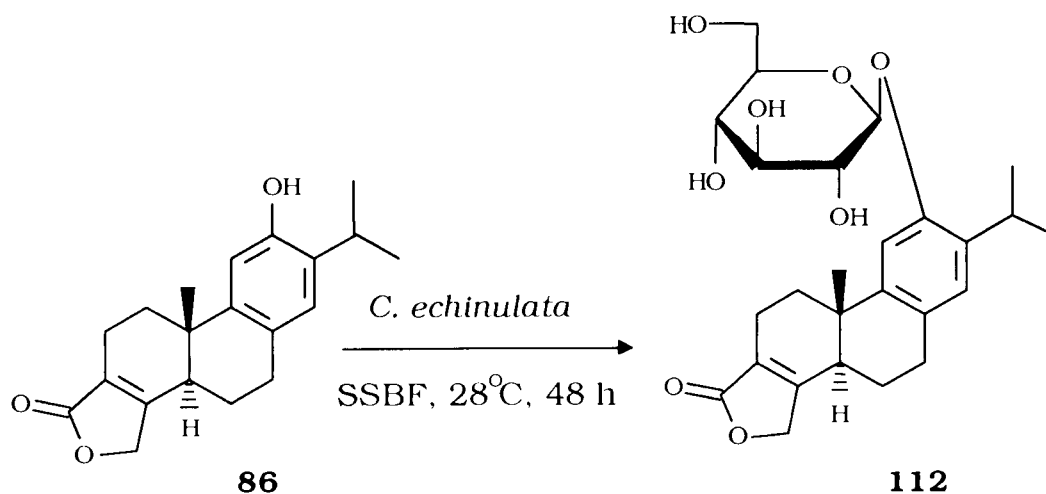
### **Preliminary Screening Experiments**

In order to evaluate the efficacy of various filamentous fungi and yeasts in biotransformation of isotriptophenolide (**86**), a series of small scale experiments was conducted. The overall procedures were identical to those presented earlier with substrate **45**. In brief, the substrate (0.1 mg/mL) was dissolved in ethanol and incubated with the microorganisms listed in Tables 2 and 3. TLC monitoring was again utilized to determine the extent, if any, of biotransformation of **86**. From these extensive experiments, none of the yeasts produced novel products. In contrast, two fungi, *Cunninghamella elegans* and *C. echinulata*, produced identical polar compounds on thin layer chromatoplates. Therefore, more detailed studies with *C. echinulata* were initiated.

### **Detailed Studies of Isotriptophenolide (86) Biotransformation by *C. echinulata***

Isotriptophenolide (**86**) (180 mg at a concentration of 0.1 mg/mL) was added to 48-h old cultures of *C. echinulata* grown on SSBF medium (see Experimental). After an incubation time of 48 h, the substrate was completely biotransformed to a novel more polar product. Scheme 21 depicts the overall result.

Scheme 21. Biotransformation of Isotriptophenolide (**86**) with *Cunninghamella echinulata*.



The structure of glucoside **112** was readily established from its characteristic spectroscopic data. Glucoside **112** showed the  $[(M.NH_4)^+]$  peak at  $m/z$  492 in the CI mass spectrum which was 180 mass units higher than substrate **86**. The molecular formula of **112** ( $C_{26}H_{34}O_8$ ) was established by the HR CIMS peak at 475.2337  $[(M.H)^+]$ . It showed UV maxima at 220, 276 nm and IR bands at 3486 (OH), 2632 (aromatic CH), and 1763 (C=O).

The  $^1H$ -NMR spectrum of **112** resembled that of isotriptophenolide (**86**) except for the additional signals for the glucose unit, which are in the expected range of  $\delta$  3.17 to 4.60. The characteristic anomeric proton of the sugar was seen as a doublet ( $J = 7$  Hz) at  $\delta$  4.93. The dihedral angle between the anomeric and the adjacent protons (the angle between H-1' and H-2' in the glucose unit) was  $150^\circ$ . It was determined by use of the Karplus curve and provides evidence in support of the  $\beta$ -anomeric

configuration for **112**. The signals corresponding to the hydroxyl groups in the sugar moiety were exchangeable with D<sub>2</sub>O.

**Conclusion:** Glucose conjugation was observed as the only biotransformation when isotriptophenolide (**86**) was incubated with *C. echinulata* and *C. elegans*. It is rather remarkable that the glucoside **112** was the exclusive product, in 80% yield, when, in earlier studies, these *Cunninghamella* species had performed a variety of hydroxylations with the butenolide **45**.

### **3.5 Biotransformation of Triptophenolide (12) with *Cunninghamella elegans***

Another synthetic substrate, triptophenolide (**12**), which is activated in ring C by the presence of a hydroxyl group at C-14 was selected for the next series of biotransformation experiments. As mentioned in Chapter I, **12** is also a natural product originally isolated from *T. wilfordii* plants. Sufficient quantities of **12** for the biotransformation studies were obtained via the synthetic route outlined in Chapter II. The synthetic triptophenolide (**12**) was shown to be identical, by spectroscopic analyses, with an authentic sample.

#### **Preliminary Screening Experiments**

As with the previous substrates butenolide **45** and isotriptophenolide (**86**), a series of small scale experiments were conducted with the various strains of yeasts and fungi presented in Tables 2 and 3. The media compositions and other parameters were identical to those described previously. Except for the *Cunninghamella* species, none of the other strains showed any biotransformation of

tryptophenolide (**12**). It was therefore decided to proceed directly with the fungal strain *C. elegans* since evidence from TLC monitoring provided the most encouraging results.

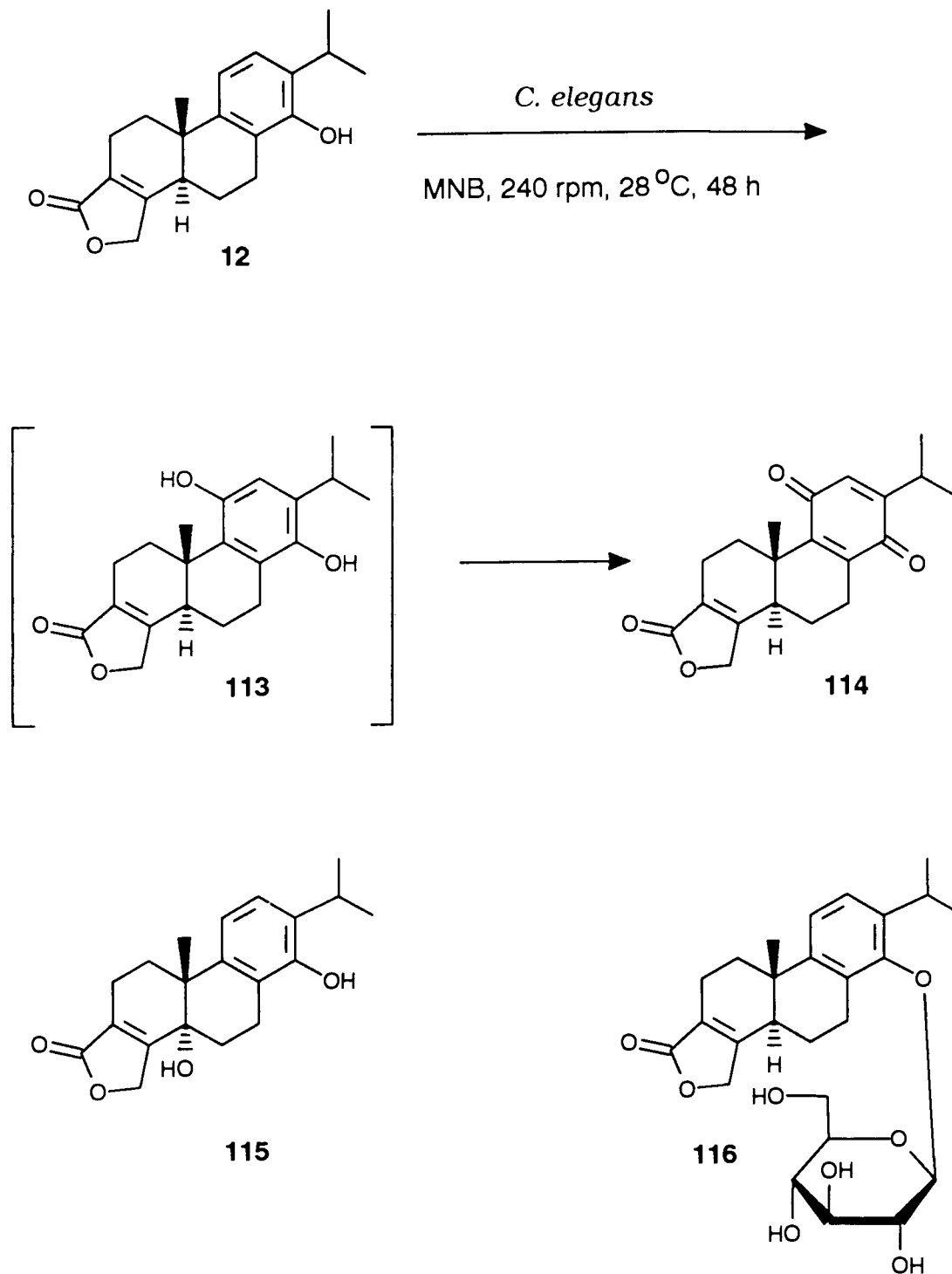
### **Detailed Studies with *C. elegans***

Incubation of stationary phase cultures of *C. elegans* grown in MNB medium (see Experimental) with tryptophenolide (**12**) for 48 h yielded 3 products which were extracted from the cell suspension and separated by flash chromatography on silica gel. Scheme 22 presents the structures of the tryptophenolide metabolites produced by *C. elegans*. Whereas the major route of metabolism of isotryptophenolide (**86**) was  $\beta$ -glucosyl conjugation, tryptophenolide (**12**) oxidation was primarily an aromatic hydroxylation (35%) yielding compound **113**. Only 5% of the starting material **12** was glucosylated to afford **116**. The diol **113** was not isolated from the extracts as it rapidly converted to the quinone **114**. The benzoquinone **114** is structurally related to the anti-inflammatory triptoquinones (see structures **26** and **27** in Chapter I) with the exception that it is a butenolide whereas the triptoquinones have a carboxylic acid group attached to ring A (Takaishi *et al.* 1992a, b; Shishido *et al.* 1993, 1994). The glucosyl conjugate **116** and the 5 $\alpha$ ,14-diol **115** are novel compounds.

The structures **114-116** were identified by <sup>1</sup>H-NMR and MS spectral data.

Compound **114** showed a molecular ion peak at  $m/z$  326 in the mass spectrum which was 14 mass units higher than **12**.

Scheme 22. Biotransformation of Triptophenolide (**12**) with *Cunninghamella elegans*.





The molecular formula  $C_{20}H_{22}O_4$  was determined by HR EIMS ( $m/z$  326.1523,  $M^+$ ). Compound **114** showed IR absorption at 2929 (aromatic CH), 1756, 1680 (C=O)  $cm^{-1}$  and a UV maximum at 261 nm due to the quinone chromophore. The  $^1H$  and  $^{13}C$ -NMR spectra of **114** showed the signals for the quinone unit at  $\delta$   $^1H$ : 6.40,  $\delta$   $^{13}C$ : 131.6, 153.4 and 187.1; isopropyl group ( $\delta$   $^1H$ : 1.10 and 3.00;  $\delta$   $^{13}C$ : 21.2, 21.2 and 26.4), a tertiary methyl ( $\delta$   $^1H$ : 1.14,  $\delta$   $^{13}C$ : 18.3), double bond ( $\delta$   $^{13}C$ : 125.4 and 161.3), five methylenes ( $\delta$   $^{13}C$ : 18.6, 24.7, 30.7, 30.8 and 70.1) and one quaternary carbon ( $\delta$   $^{13}C$ : 36.6). The structure of compound **114** was compared with an authentic sample obtained from synthesis by the UBC group. The quinone **114** was also generated as a minor oxidation product in the synthesis of racemic triptolide and triptonide (Lai *et al.* 1982).

Metabolite **115** showed a molecular ion peak at  $m/z$  328, which is 16 mass units higher than the parent compound **12**. Its molecular formula,  $C_{20}H_{24}O_4$ , was obtained from HR EIMS ( $m/z$  328.1675,  $M^+$ ). The IR spectrum of this compound has absorption bands for hydroxyl groups at 3607 and 3560  $cm^{-1}$  while the  $^1H$ -NMR displayed a spectrum similar to **12**. However, the absence of the H-5 proton in the spectrum and the presence of a new hydroxyl proton at  $\delta$  1.90, which was exchangeable with  $D_2O$ , suggested a C-5 hydroxy analogue. The H-19 protons were also shifted downfield from  $\delta$  4.77 to 4.90 and revealed a wider splitting thereby further confirming that the new hydroxyl group is at C-5. The C-20 methyl is located at  $\delta$  1.09 and the isopropyl methyls are found at  $\delta$  1.25 and 1.27. The signal of the C-20 angular methyl group was seen at higher field than the isopropyl methyl groups which suggested a *trans* junction of the A and B rings and therefore, the C-5

hydroxyl was  $\alpha$  oriented. The COSY spectrum showed that the H-19 protons are coupled with two H-2 protons at  $\delta$  2.39 (1 H, m) and 2.55 (1 H, br d,  $J = 16$  Hz) (homoallylic coupling). The H-7 protons are located between  $\delta$  2.80 and 3.02 (2 H, m), and showed cross peaks to one multiplet between  $\delta$  1.98 and 2.15 (2 H, m) and one proton at  $\delta$  2.23 (1 H, ddd,  $J = 9.9, 14$  Hz). This indicates that one H-6 proton is situated in the multiplet and the other is the one at  $\delta$  2.23. Irradiation of the C-20 methyl resulted in enhancement of the H-2 proton signal at  $\delta$  2.39, a signal at  $\delta$  2.31 (1H, dd,  $J = 6, 13$  Hz) and the H-6 proton signal at  $\delta$  2.23, thereby suggesting that these protons are  $\beta$ H-2,  $\beta$ H-1 and  $\beta$ H-6 respectively. Irradiation of the  $\beta$ H-1 proton increased signal intensities of the H-11 signal at  $\delta$  6.91 (1H, d,  $J = 8$  Hz) as expected, and one proton in the multiplet between  $\delta$  1.98 and 2.15, which indicated that the remaining proton in that multiplet is  $\alpha$ H-1. The above results were in agreement with the structure of **115**.

These studies were presented in a recent publication (Milanova *et al.* 1995, in press).

### **Biotransformation of Triptophenolide (12) with *Cunninghamella echinulata***

In order to compare the biotransformation of triptophenolide (**12**) with the related fungal strain, *C. echinulata*, several small scale experiments (TLC monitoring) were performed. The data obtained revealed that this microorganism produced metabolites with the same  $R_f$  values (TLC) as authentic **114-116** from *C. elegans*.

## **Biotransformation of Triptophenolide (12) with Immobilized Cells of *Cunninghamella elegans***

As noted earlier, *C. elegans* provided the first example in this study of aromatic hydroxylation and, in particular, the opportunity to obtain novel quinones of potential pharmaceutical interest. For this reason, it was of interest to determine whether this microorganism could be immobilized on a solid support in the hope that a stable biotransformation system could be developed. Kutney and co-workers (Kutney *et al.* 1988) published an extensive study in which the fungus *Mortierella isabellina* could be immobilized on polyurethane foam and retained bioconversion activity for up to 90 days. Consequently, experiments were devised to determine whether *C. elegans* could be immobilized in polyurethane foam and if so, how long the enzymatic activity could be maintained.

Orange reticulated polyurethane foam, (see Experimental Section), was washed in soapy water, rinsed initially in tap water, then 70% aqueous ethanol and finally in distilled water. This clean foam was cut into small cubes (1 cm<sup>3</sup>) and added to the MNB culture broth, prior to autoclaving. *C. elegans* cultures were then grown in the presence of cubes for a 48 h period. During this time, the mycelia was completely entrapped into the foam. The cubes were then aseptically resuspended in sterile citrate buffer (pH 4.4) and the substrate **12**, added at a concentration of 0.1 mg/mL, was incubated for a 48 h period. The biotransformation was monitored by TLC. After decanting the solution under aseptic conditions, extraction of the reaction mixture with ethyl acetate and TLC monitoring revealed some depletion of triptophenolide

(**12**) as was shown earlier with the suspension culture of *C. elegans*. The metabolites benzoquinone (**114**), 5 $\alpha$ ,14-dihydroxybutenolide (**115**) and 14-glucosyl triptophenolide (**116**) were obtained.

In order to establish whether the enzymatic activity of the immobilized system could be maintained over time, the same cubes with fungal mycelia were resuspended repeatedly in fresh citrate buffer, pH 4.4, substrate **12** was added, and incubated in each experiment for a further 48 h period.

Seven separate additions of triptophenolide (**12**) to freshly resuspended immobilized *C. elegans* were made intermittently over a period of more than one month and conversion of **12** to the metabolites **114** - **116** was observed in each case. The biotransformation was monitored by TLC. Further experiments were not conducted because the supply of substrate **12** was exhausted. Therefore it was not known how long the enzymatic activity could have been maintained over and above 30 days.

It is important to note that the microorganism appeared to be very tightly bound to the foam since there was no evidence of any release of mycelia from the foam during the month of repeated incubation and resuspension. Further, the only growth substance present in the flasks was citric acid-sodium citrate, therefore growth was assumed to be extremely low or absent.

**Conclusion:** The filamentous fungus *C. elegans* has the enzymes to hydroxylate the aromatic ring of triptophenolide (**12**). This substrate, with an "activated" ring C of the abietane skeleton allows introduction of a hydroxyl group in the *para* position relative to the initial phenolic group of **12**. The intermediate hydroquinone **113** is unstable and rapidly

undergoes further oxidation to the novel quinone **114** as a major product (35% yield).

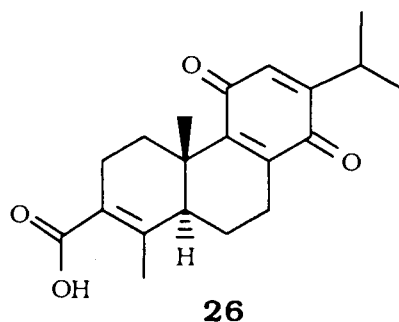
The fungus *C. elegans* was efficiently immobilized in polyurethane foam and possessed a constant level of enzymatic activity for oxidation of **12** to **114-116** over a period of at least one month. Further studies are required in order to further assess the stability of the immobilized system over longer periods.

In view of the potential activity of triptoquinone (**114**) as an interleukin-1 inhibitor (see below) and also as a potential intermediate for the synthesis of ring C epoxides similar to those of triptiolide (**3**), it was of interest to evaluate methods for improving the yield of quinone **114**. For this purpose, a factorial design experiment (Chapter IV) was selected.

### **3.6 Diterpene Quinones as Novel Interleukin-1 Inhibitors**

As the above studies were underway, two publications of direct relevance to the present studies appeared in the literature (Takaishi *et al.* 1992a, b, Shishido *et al.* 1993). These investigators had obtained an interesting quinone from a Japanese variety of *Tripterygium wilfordii* var. *regelii*, a related plant from which Chinese scientists had earlier isolated triptiolide (**3**) and triptolide (**2**). This natural product, which they called triptoquinone A (**26**), showed significant inhibitory activities for IL-1 $\alpha$  and IL-1 $\beta$  releases from lipopolysaccharide-stimulated human peripheral mononuclear cells. Interleukin-1 (IL-1) has various biological activities and is thought to be a biologically active substance necessary for the maintenance of homeostasis of the human body and it is an important factor in cell-mediated immunity (Kluger *et al.* 1985; Gilman *et al.* 1990).

It has been shown that if the controlling function of IL-1 production seems abnormal to give rise to accentuation of IL-1 production, various diseases can be promoted. For example, in rheumatoid arthritis, it has been reported that there is a strong relationship between the production of IL-1 by the synovium and the degree of inflammation of articular synovial membrane (Miyazaki *et al.* 1988). Therefore, agents which block IL-1 production are of interest in the development of pharmaceuticals for the treatment of rheumatoid arthritis and other inflammatory diseases.



Triptoquinone A (**26**) resembles the quinone **114** which was isolated in the bioconversion of triptophenolide (**12**) by *C. elegans*. The butenolide system in **114** is merely the ring closed form of the unsaturated acid function in the natural product **26**. Based on the results with **26** (Takaishi *et al.* 1992a), **114** appeared to be a good candidate for pharmacological screening for anti-inflammatory activity.

**CHAPTER IV -- OPTIMIZATION OF TRIPTOQUINONE**  
**(114) PRODUCTION BY FACTORIAL DESIGN**  
**EXPERIMENT**

The composition of the medium used in fermentation processes must provide all elements required for the synthesis of cell material. In addition, media must be designed to satisfy the objectives of the process by providing a favorable environment for growth and/or efficient product formation. Fermentation processes have several stages: initial development of inocula, satisfactory growth of inocula in shake flasks, and scale-up for product formation in shake flasks and/or bioreactors. Each stage has different objectives and therefore different medium requirements. In inoculum development and scale-up stages, the objective is usually to achieve high growth rates and to prepare sufficient quantities of viable biomass in a form which will allow efficient biotransformation. On the other hand, in stages involving product formation, it is important to generate the relevant enzymes within the growing culture for biotransformation of substrate to product.

An understanding of the growth and morphological complexity of the filamentous fungi is important for developing a consistent, scalable, and productive fungal fermentation process. Filamentous fungi are well known as producers of commercially-important products such as antibiotics, chemicals, and enzymes (Greasham 1986). Unlike many unicellular microbes, the fungi usually present special challenges during scaleup because of their various morphological forms. Filamentous fungi exhibit different structural forms throughout their life cycles. The basic vegetative structure of growth consists of a tubular filament known as a

hypha that originates from the germination of a single reproductive spore. As the hypha continues to grow, it frequently branches repeatedly to form a mass of hyphal filaments referred to as a mycelium. Under appropriate conditions, the vegetative mycelium gives rise to a reproductive mycelium that supports the production of reproductive spores. The type of sporulation as well as the morphology of the spores and spore bearing structures are key characteristics in fungus identification (Hawksworth 1977). Growth kinetics of filamentous fungi in submerged culture are quite similar to those of unicellular microorganisms that reproduce by binary fission. The growth rate may generally be defined as the increase of biomass with time. Fungal cells growing in shake flasks usually undergo four distinct growth phases: a lag phase, an active growth phase, a stationary (plateau) phase and a declining phase (Finkelstein & Ball 1991; Pelczar 1993; Tortora *et al.* 1989). The lag phase represents a period during which the fungal cells or spores adapt to a new environment. Adaptation includes formation of enzymes and intermediates to support resumption of growth. The length of this phase is dependent not only on the physiological state of the microorganism, but also on the morphology and level of the inoculum. For instance, spore inocula require a germination period which could cause extended lag phase. Minimization of the lag phase may be achieved by using 5 - 10% inoculum of actively growing, dispersed mycelia (Finkelstein & Ball 1991). Although spore inocula prolongate the lag phase it is recommended for use in optimization experiments. In order to achieve uniform quantities of mycelia in each experiment and allow for reproducibility of the results, an exact amount of spore suspension (known concentration) should be employed.



The active growth phase is divided in two parts: exponential and reduced growth. The exponential growth is characterized by a significant increase of cell mass. The rate of hyphal growth depends not only on the strain of fungus, but also on the environmental conditions. Usually the cultivation medium during this phase of growth contains an excess of required nutrients. A reduction in the specific growth rate occurs when the cells meet an unfavorable growth environment such as limitation of nutrients, development of an adverse pH value or accumulation of inhibitors. In some cases, a higher concentration of product may also serve as an inhibitor due to product toxicity to the cells. At stationary phase the cells have reached balance between hyphal mass increase and decrease so the biomass concentration remains constant. As more nutrients are depleted, cells lysis becomes greater than cell production and the culture enters the declining phase (Finkelstein & Ball 1991).

All living organisms require nutrients for growth, synthesis of their cellular constituents and energy-generating system. The most important elements necessary for the living cells are carbon, hydrogen, oxygen, nitrogen and phosphorus. A wide range of other elements and compounds is also required in much smaller amounts (Hawker & Linton 1979). In case of bacteria and fungi, 98% of the dry weight consists of the above mentioned elements as well as sulfur, potassium, and magnesium. These eight elements are usually called macro nutrients and their required concentration in the growth media is greater than  $10^{-4}$  mol/L (Dunn 1985).

Pirt has listed five criteria for optimal growth of microorganisms, namely, an energy source, nutrients to provide essential materials for growth, absence of inhibitors, a viable inoculum and suitable

environmental conditions (Pirt 1975). In all of these parameters, medium design governs the first three parameters.

The properties of the growth medium are considered to be important and optimization of the medium constituents is essential to achieve an efficient biotransformation process (high reaction rate, maximum yield of desired product and high substrate conversion). If the desired product is formed during active growth, the substrate is usually introduced with the inoculum or at the beginning of the growth phase. Where the product formation occurs after cell growth, i.e. during the stationary or plateau phase, the substrate is introduced when cell growth has ceased. However, in both cases, the medium must simultaneously provide sufficient biomass production as well as optimum product formation.

The optimal design of culture media is a relevant aspect to be considered in the development of fermentation processes. In the particular case of a biotransformation process (substrate as a foreign compound), the interaction between growth metabolism and product formation is critically influenced by growth limiting nutrient concentrations. Experimental design techniques are very useful tools for this purpose, as they can provide statistical models with a relatively small number of experiments. From these models, the relative influence of the various factors studied can be determined, and their optimal concentration for a given target (i.e., maximum growth, maximal metabolite production) calculated.

## 4.1 Experimental Design

An experimental design (plan of an experiment) is a matrix (table) of predetermined settings of the process variables (parameters) (Deming & Morgan 1987).

- (1) Each process variable (parameter of the experiment) is called an experimental **factor**.
- (2) Each combination of settings for the process variables (the values of all parameters for a single experiment) is called a **run** (a single experiment).
- (3) A **response variable** (result or yield of the experiment in general) is a measure of process performance.
- (4) Each value of the response variable (result from a single experiment) is called an **observation**.

In the discussion which follows, it will become clear that the specific experimental design used here will be illustrated with a table containing the value of each studied (varied) parameter in each single experiment. Experimental factors (parameters) varied were 1) the concentrations of media components, and 2) the duration of the experiment. The response variable was the yield of desired product. The specific yield of desired product was the observation in a single experiment.

Finally, statistical analysis provided estimates of how strongly each experimental factor affected process performance, in the present case, the yield of metabolite. These estimates revealed which factors were most important and how a change of their settings affected process performance (Raktol *et al.* 1981; Davies 1963).

## **Optimization Requirements of Biological Systems**

For most biological processes, the experiments involve the following considerations:

### (A) Complex combinations of parameters

Microbial systems are complex and the result in a biotransformation experiment depends on many parameters. Some of these parameters are difficult to control or they are not well studied. The employed method should provide an opportunity to obtain sufficient information about the influence of such parameters in order to maximize or minimize their effect (Mead *et al.* 1993).

### (B) Development of a mathematical model for the process

A theoretical model is represented by one or more mathematical equations, derived from the theory of the studied process, and presents a correlation between the parameters and the performance of the system (result of the experiment). A specific characteristic of these type models is that the mathematical relationship illustrates the effect of each parameter on the result of the process. In the case of complex and insufficiently studied systems, the use of quantitative theoretical models is not appropriate (Deming & Morgan 1987).

A mathematical model is an alternative to the theoretical model and does not require an understanding of the nature of the process. It is a system of one or more mathematical equations, which are derived from experimental information and predicts the result of an experiment (without performing the experiment). Polynomial models are the most commonly used to describe the interactions between the parameters and

their influence on the outcome of a process/experiment. Such models generally involve a sum of expressions such as  $Y = A_0 + A_1X_1 + A_{1,1}X_1^2$  ... etc. where  $A_0$ ,  $A_1$ ,  $A_{1,1}$ , etc. are constants and  $X_1$  is a factor (parameter) value.  $Y$  is the response variable, i.e. the experimental result obtained (Deming & Morgan 1987).

#### (C) Data which may include a high level of deviation

The average deviations of the experimental results obtained during repetitions of experiments under identical conditions is called noise. It is caused by:

(a) limitations on the accuracy of the measurements (values of the factors and the response);

(b) effect of parameters which cannot be controlled or measured during the course of the experiment.

The factorial design experiment, when combined with the necessary statistical methods can account for the variations caused by non-controllable factors and effects.

#### (D) Possible interactions among factors

Interactions are non-additive influences of the parameters on the result of the experiment. For example, the alteration of two single parameters, e.g. pH, pO<sub>2</sub>, may have a minimal effect on the outcome when changed one at the time, while a simultaneous alteration of two parameters may result in a non-additive increase/decrease in the overall result (Manly 1992).

## **Strategies for Optimization**

There are four methods of experimental design and data analysis available for process optimization.

The first method is "one-variable-at-a-time". This traditional strategy is employed to investigate one factor while keeping all other factors at a constant value, and subsequently to select another factor for the next set of experiments. However, this one-factor-at-a-time strategy has been shown to be inefficient and lacks the ability to detect interactions among factors. This single-dimensional search is time-consuming, especially for a large number of variables, and frequently does not guarantee determination of optimal conditions.

Increased efficiency can be gained by studying several factors simultaneously using a "matrix" experimental strategy. This method lays out a matrix of all combinations of interest with respect to the variables being investigated. In these cases, all of the combinations in the matrix are investigated until the solution is found. The matrix method has the advantage to detect the interactions among factors but it usually requires a very large number of experiments.

The third method is sequential simplex optimization. The idea of the method is that once a small number of experiments are done then each single result of a subsequent experiment can be used to determine mathematically the direction of improvement, as well as the conditions for the next experiment.

The fourth method involves the application of factorial design. This strategy uses a series of smaller carefully-designed experiments and allows one to obtain detailed quantitative information for the effect of

each factor as well as for their interactions. This full factorial search would examine every possible combination of the variables at appropriate levels. This latter method was selected for the present study.

### **Advantages of the Factorial Design**

The most important advantages of this method are as follows:

- (1) no limitations on the choice or the nature of different variables,
- (2) no assumptions need to be made about the relationship between the variables (no theoretical model or sufficient theoretical knowledge about the process required),
- (3) is readily adapted for simultaneous investigation of many variables.

A factorial experiment is one in which chosen levels of a given factor are combined with chosen levels of every other factor in the experiment.

The factorial design used for an optimization experiment usually includes two to five levels of each factor. The number of levels and the number of runs (experiments) depends on the number of factors and on the specific type of design (Deming & Morgan 1987; Raktol *et al.* 1981; Manly 1992). Because of the complex interactions among the fermentation parameters, optimization of the critical parameters may be enhanced by employing multifactorial design experimentation.

Although, the use of factorial design has attractive features, the literature citations on application of this method are rather limited. Only two publications of direct relevance to the present study have been recently published. Factorial design was been used to optimize the medium composition in batch cultures of *Streptomyces lividans* TK 21

producing a hybrid antibiotic (Sarra *et al.* 1993). The composition of the liquid medium employed has been optimized by a central composite experimental design. The results have shown maximum yield of the antibiotic production within the range of studied parameters (Sara *et al.* 1993).

Another study using factorial design was carried out in the production of xanthan gum by Garcia-Ochoa and coworkers. Four variables were studied: nitrogen, phosphorus, magnesium and sulfur contents. A two-level factorial design with four central points has been applied to the four factors studied. An optimized medium has been proposed for xanthan production (Garcia-Ochoa *et al.* 1992).

The factorial design method is described in more detail in the following sections of this Chapter as well as in the Appendix.

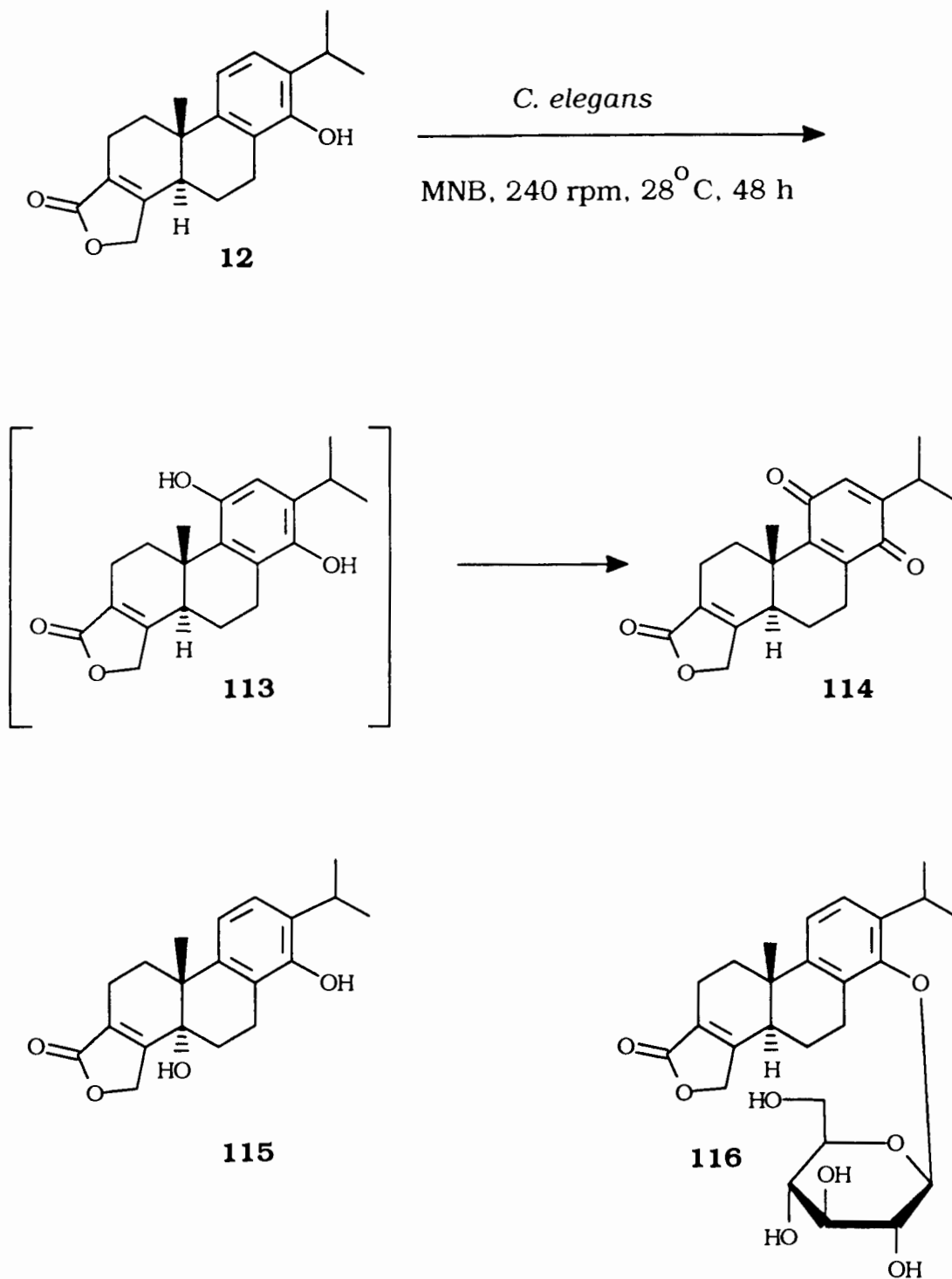
#### **4.2 First Optimization of the Biotransformation of Triptophenolide (12) with *C. elegans***

All of the experiments described below, were designed to optimize the biotransformation of triptophenolide (**12**) to triptoquinone (**114**), 5 $\alpha$ ,14-dihydroxybutenolide (**115**) and 14-glucosyl triptophenolide (**116**) by the filamentous fungus *C. elegans* (Scheme 22).

The original biotransformation experiment was conducted in MNB medium containing (g/L): glucose (10 g/), nutrient broth (8 g/), and malt extract (20 g). The substrate **12** (0.1 mg/mL) was incubated for 48 h at 28 $^{\circ}$  C on a rotary shaker at 240 rpm. Three products were formed: triptoquinone (**114**), 5 $\alpha$ ,14-dihydroxybutenolide (**115**), and 14-glucosyl-triptophenolide (**116**).



Scheme 22. Biotransformation of Triptophenolide (**12**) with *Cunninghamella elegans*.



The yields of the products obtained under the above conditions were: **114** (35%), **115** (12%), and **116** (5%) (Chapter III, Section 3.6).

### **Factors and Levels for Optimization**

In view of the above, it was essential to optimize the growth conditions to achieve a yield of the desired triptoquinone (**114**) higher than 35%. The initial optimization parameter to be studied was the medium composition and its influence on the rate and selectivity of the biochemical conversion of the substrate **12**.

The optimization procedure required the development of a mathematical model which could be used to predict the yield of **114** as a function of the medium composition and the biotransformation time. This mathematical model provided a prediction of the "best" settings of the above-mentioned parameters.

For optimization four growth factors were chosen: glucose, nutrient broth, malt extract concentrations, and the time of biotransformation with the hope of increasing the yield of desired quinone **114** and simultaneously decreasing or eliminating the appearance of the other metabolites. The medium composition used in the initial experiment was adjusted slightly and placed in the middle of the factor ranges as shown in Table 6. Since the middle levels represent an equal increment to the high and low levels respectively, this adjustment was essential in order to eliminate very low concentrations at the low levels of the varied factors. For example, the middle value of 8.4 g/L for nutrient broth represents an incremental increase of 7.6 g/L for the high value (16.0 g/L) and a corresponding incremental decrease of 7.6 g/L for the low value (0.8 g/L).

The relationships between the standardized and actual settings are shown in Table 6. Factorial design was made with a wide range of the parameters and the probability to screen a larger number of factor combinations in order to establish a maximum yield of **114**.

### **Matrix of the First Set of Experiments**

The experiment was designed according to the method described by Mead and Deming & Morgan (Mead *et al.* 1993, Deming & Morgan 1987). This type of design when combined with a polynomial model provides an opportunity to evaluate all relevant effects of the process.

The design used for the first optimization experiment is given in Table 7 (Haaland 1989). The specific conditions (actual levels) for these experiments are summarized in Table 7. These conditions are derived from the standardized levels in Tables 6 and 7. For example, in run #1, a standard level of +1 for the four factors shown in Table 7 represents a time of 72 h, 20 g/L glucose, 16 g/L nutrient broth and 40 g/L malt extract, the latter values being derived from the high (level 1) factor shown in Table 6. In similar fashion, the conditions in run #4 which have the standard levels of +1, +1, -1, and -1 respectively for the four factors studied (Table 7) provide the values of 72 h (time), 20 g/L (glucose), 0.8 g/L (nutrient broth) and 2 g/L (malt extract) (Table 6).

The first set of experiments consisted of 25 runs given by the matrix of the factorial design. The experiments were conducted in 15 different medium compositions derived from the plan.

Table 6. Factor Settings for the First Set of Experiments.

Standardized levels		Actual levels			
		Factors			
		Time	Glucose	Nutrient Broth	Malt Extract
High	1	72 h	20.0 g/L	16.0 g/L	40.0 g/L
Middle	0	36 h	10.5 g/L	8.4 g/L	21.0 g/L
Low	-1	0 h	1.0 g/L	0.8 g/L	2.0 g/L

As it is illustrated in Table 7 some of the runs have been performed in the same medium composition in order to satisfy the requirements of the selected experimental design. For instance, run #1 and #9 were performed both in medium composition 1, as only the value of the time factor changed.

Table 7. First Factorial Design Experiment Showing Selected Factors (Parameters) and Their Levels.

Run	Standardized levels				Actual levels				Medium composition
	Time	Glucose	Nutrient broth	Malt Extract	Time h	Glucose g/L	Nutrient broth g/L	Malt Extract g/L	
1	+1	+1	+1	+1	72	20	16	40	1
2	+1	+1	+1	-1	72	20	16	2	2
3	+1	+1	-1	+1	72	20	0.8	40	3
4	+1	+1	-1	-1	72	20	0.8	2	4
5	+1	-1	+1	+1	72	1	16	40	5
6	+1	-1	+1	-1	72	1	16	2	6
7	+1	-1	-1	+1	72	1	0.8	40	7
8	+1	-1	-1	-1	72	1	0.8	2	8
9	-1	+1	+1	+1	0	20	16	40	1
10	-1	+1	+1	-1	0	20	16	2	2
11	-1	+1	-1	+1	0	20	0.8	40	3
12	-1	+1	-1	-1	0	20	0.8	2	4
13	-1	-1	+1	+1	0	1	16	40	5
14	-1	-1	+1	-1	0	1	16	2	6
15	-1	-1	-1	+1	0	1	0.8	40	7
16	-1	-1	-1	-1	0	1	0.8	2	8
17	+1	0	0	0	72	10.5	8.4	21	9
18	-1	0	0	0	0	10.5	8.4	21	9
19	0	+1	0	0	36	20	8.4	21	10
20	0	-1	0	0	36	1	8.4	21	11
21	0	0	+1	0	36	10.5	16	21	12
22	0	0	-1	0	36	10.5	0.8	21	13
23	0	0	0	+1	36	10.5	8.4	40	14
24	0	0	0	-1	36	10.5	8.4	2	15
25	0	0	0	0	36	10.5	8.4	21	9

## Mathematical Model for Optimization

A full second-order polynomial model (Deming & Morgan 1987) was used to evaluate the yield of the product as a function of the medium composition and the biotransformation time.

$$Y = a_0 + a_1x_1 + a_2x_2 + a_3x_3 + a_4x_4 + a_{1,2}x_1x_2 + a_{1,3}x_1x_3 + a_{1,4}x_1x_4 + a_{2,3}x_2x_3 + a_{2,4}x_2x_4 + a_{3,4}x_3x_4 + a_{1,1}x_1^2 + a_{2,2}x_2^2 + a_{3,3}x_3^2 + a_{4,4}x_4^2 \quad (1)$$

where

Y = yield of product (%)

$a_0, a_1, a_2 \dots$  = coefficients determined from the results of the experiment

variable parameters:

$x_1$  = time (h);

$x_2$  = glucose (g/L);

$x_3$  = nutrient broth (g/L);

$x_4$  = malt extract (g/L)

The linear terms of the type  $a_1x_1$  portray the linear relationship between the factor (x) and the yield (response variable, Y). The two factor interaction terms, for example,  $a_{1,2}x_1x_2$  show yield variation when two factors are simultaneously varied. The terms of the type  $a_{1,1}x_1^2$  give the non-linear relationship between each factor and the yields. These terms allow one to find minimum or maximum values of the response variables within the studied range.

It was essential to include factor interaction and quadratic terms as an addition to the linear expression in order to achieve a high precision of the result.

### **Influence of Medium Composition on Metabolite Production by *C. elegans***

Three sets of experiments were conducted in the above medium variations (Table 7) which were run at different time to determine the reproducibility of the process.

The actual media preparation is described in the Experimental section. Each flask was inoculated with 0.5 mL of spore suspension of *C. elegans* ( $2 \times 10^8$  spores/mL) to obtain a final spore concentration of  $2 \times 10^6$  spores/mL. The cultures were grown at 28°C on a rotary shaker at 220 rpm for 48 h prior to the addition of the substrate triptophenolide (**12**). The substrate triptophenolide (**12**) was added as a 0.2% ethanolic solution to the cultures in a concentration of 0.1 mg/mL and incubated for further 72 h.

All of the experiments were run in presence of controls which were inoculated and grown at the above described conditions without addition of substrate.

Aliquots were withdrawn in intervals of 12-24 h and analyzed by HPLC to determine the product formation and substrate depletion. The metabolites were separated using a reverse phase column C<sub>18</sub> (100 x 8 mm, 5 µm, Waters) and a mobile phase as follows: H<sub>2</sub>O (55.3%), MeOH (29.7%), MeCN (15%), containing AcOH (0.1%) at a flow rate of 1.5 ml/min. (isocratic conditions).

## **Standard Curves**

The concentrations of the substrate (**12**) and the biotransformation products triptoquinone (**114**), 5 $\alpha$ ,14-dihydroxybutenolide (**115**), and 14-glucosyl-triptophenolide (**116**) were determined by UV detection of the absorption at 254 nm ( $A_{254}$ ). Standard curves of the pure synthetic substrate (**12**) and metabolites isolated from previous biotransformation experiments (Chapter III) and purified by column chromatography (see Experimental) are shown in Figures 4-7. Linear equations were used to evaluate the concentrations accurately. A linear relationship between the  $A_{254}$  and the concentration was obtained for all compounds. The equations shown in the legend of Figures 4-7 are derived as shown in the Appendix.

The HPLC profile of the substrate **12** and the products obtained from the biotransformation process with *C. elegans* is shown in Figure 8.

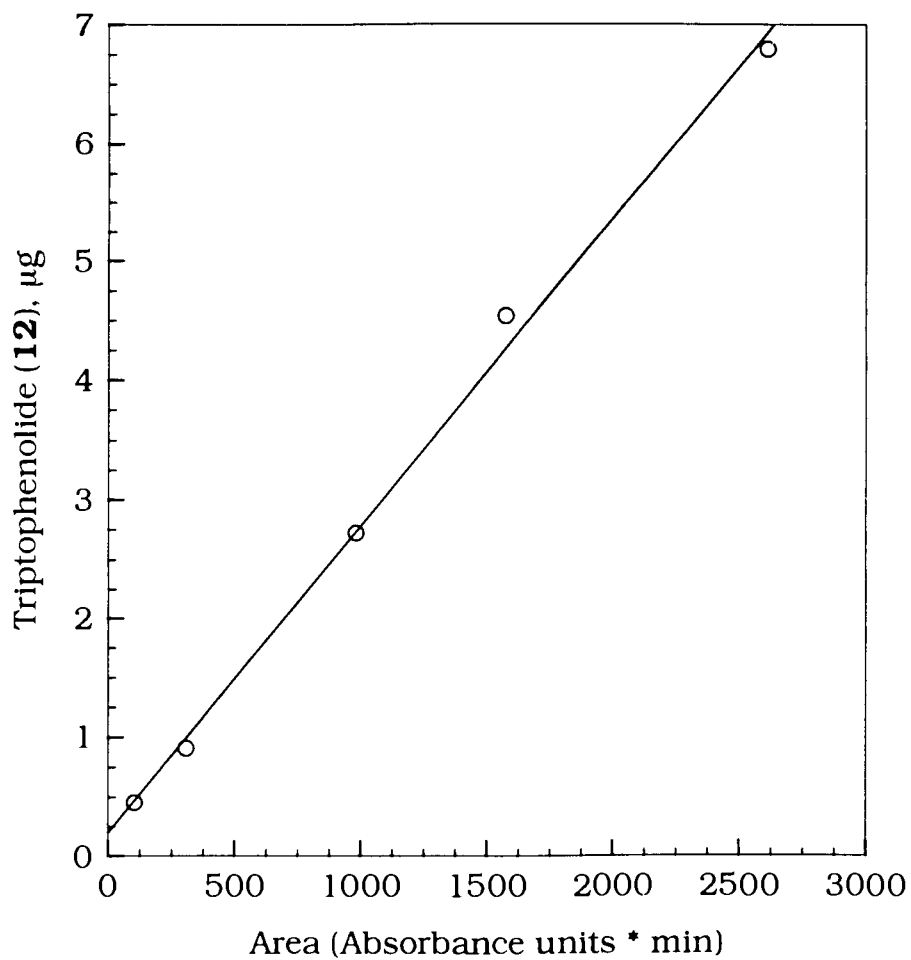
## **Time Course Experiments Relating to Metabolite Production - First Set of Experiments**

It was appropriate to evaluate medium composition and optimum biotransformation time in order to improve the yields of desired metabolites.

As shown in Table 7, experiments were conducted with 15 different medium variations in order to derive information relating to maximum consumption of substrate and higher yield of biotransformation products.



Figure 4. Standard Curve for Triptophenolide (**12**).

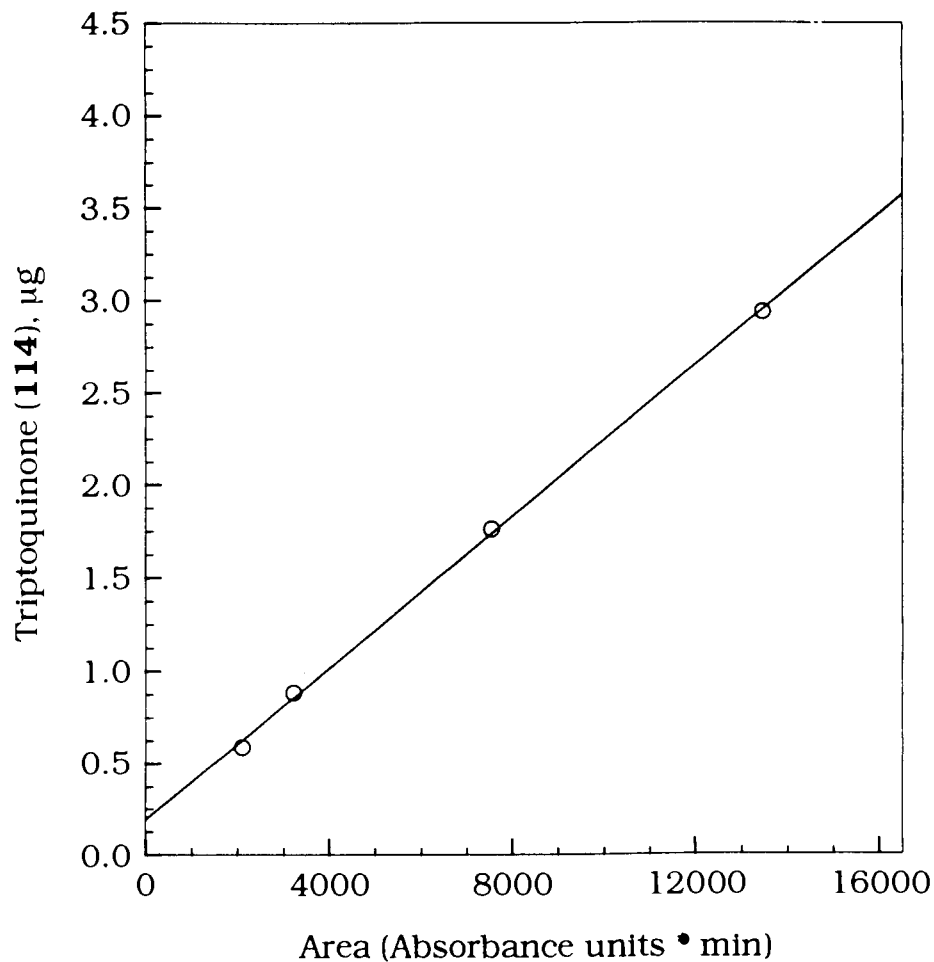


Legend:

$$\text{Triptophenolide (12), } \mu\text{g} = 0.199 + 0.00258 \cdot \text{Area}$$

Retention time = 36.6 min.

Figure 5. Standard Curve for Triptoquinone (**114**).

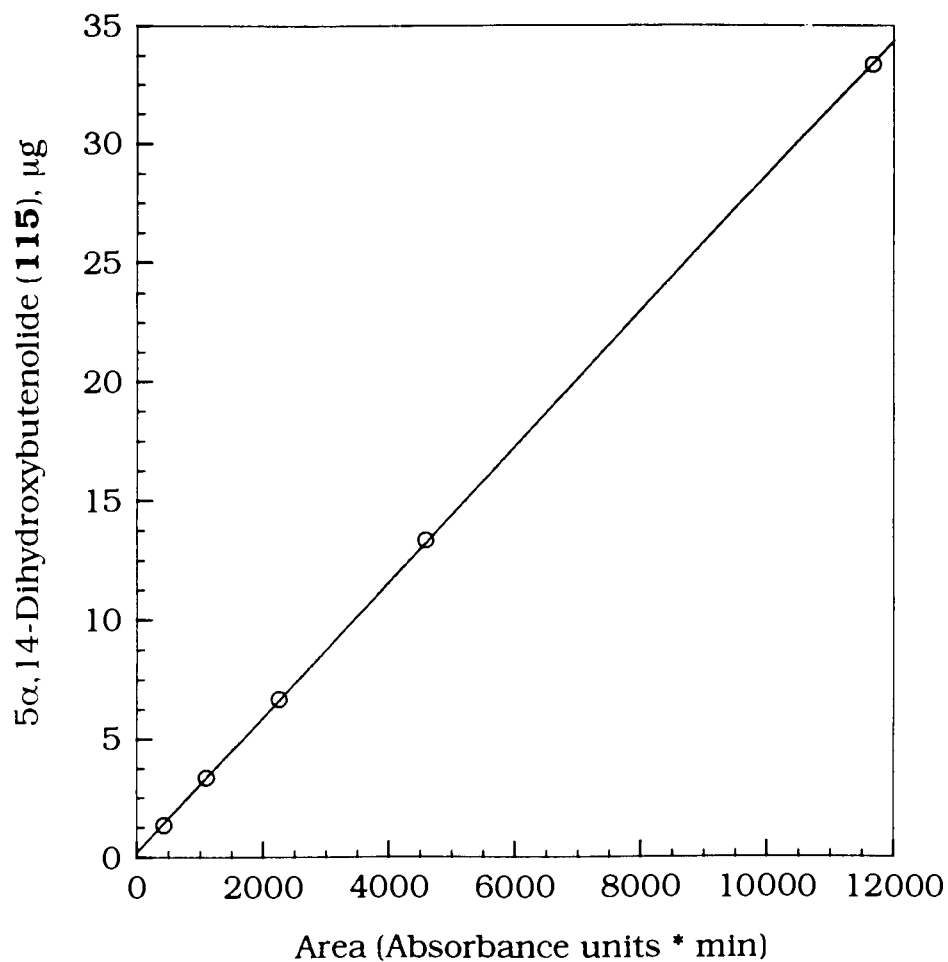


Legend:

$$\text{Triptoquinone (114), } \mu\text{g} = 0.194 + 0.000205 \cdot \text{Area}$$

Retention time = 40.3 min.

Figure 6. Standard Curve for 5 $\alpha$ ,14-Dihydroxybutenolide (**115**).



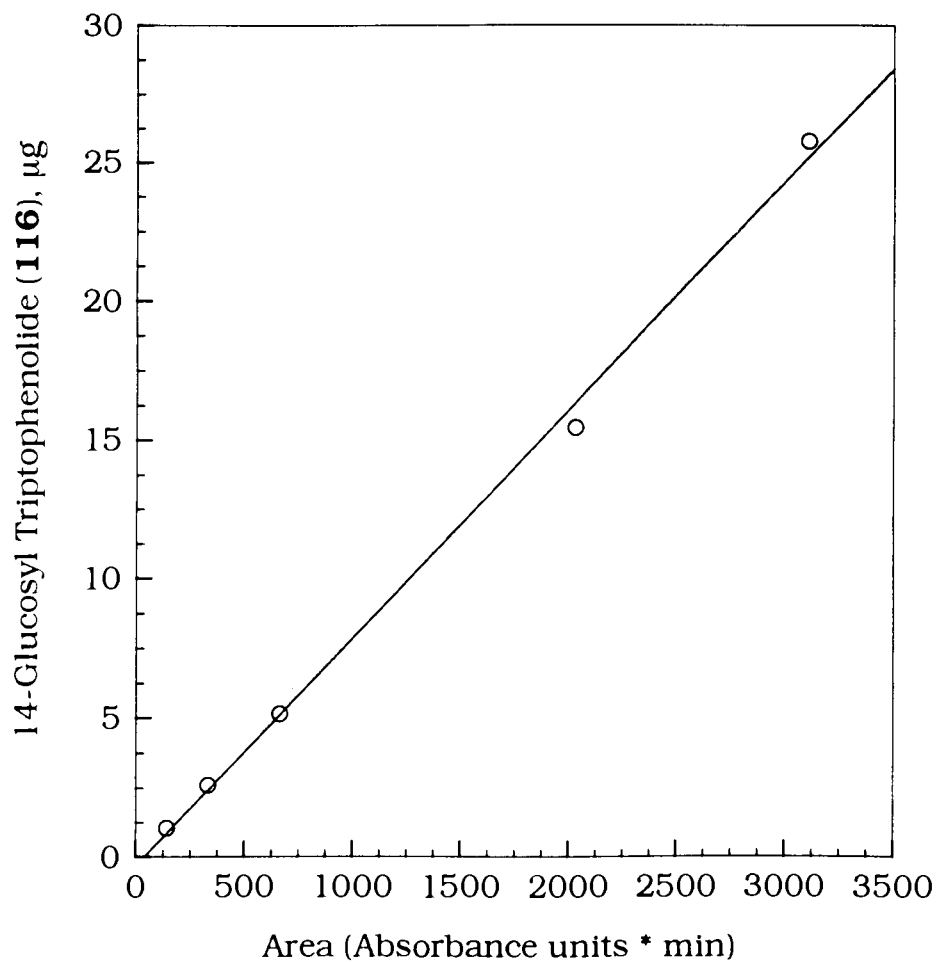
Legend:

5 $\alpha$ ,14-Dihydroxybutenolide (**115**),  $\mu\text{g}$  =

$$+= 0.206 + 0.00285 \cdot \text{Area}$$

Retention time = 16.7 min.

Figure 7. Standard Curve for 14-Glucosyl Tryptophenolide (**116**).

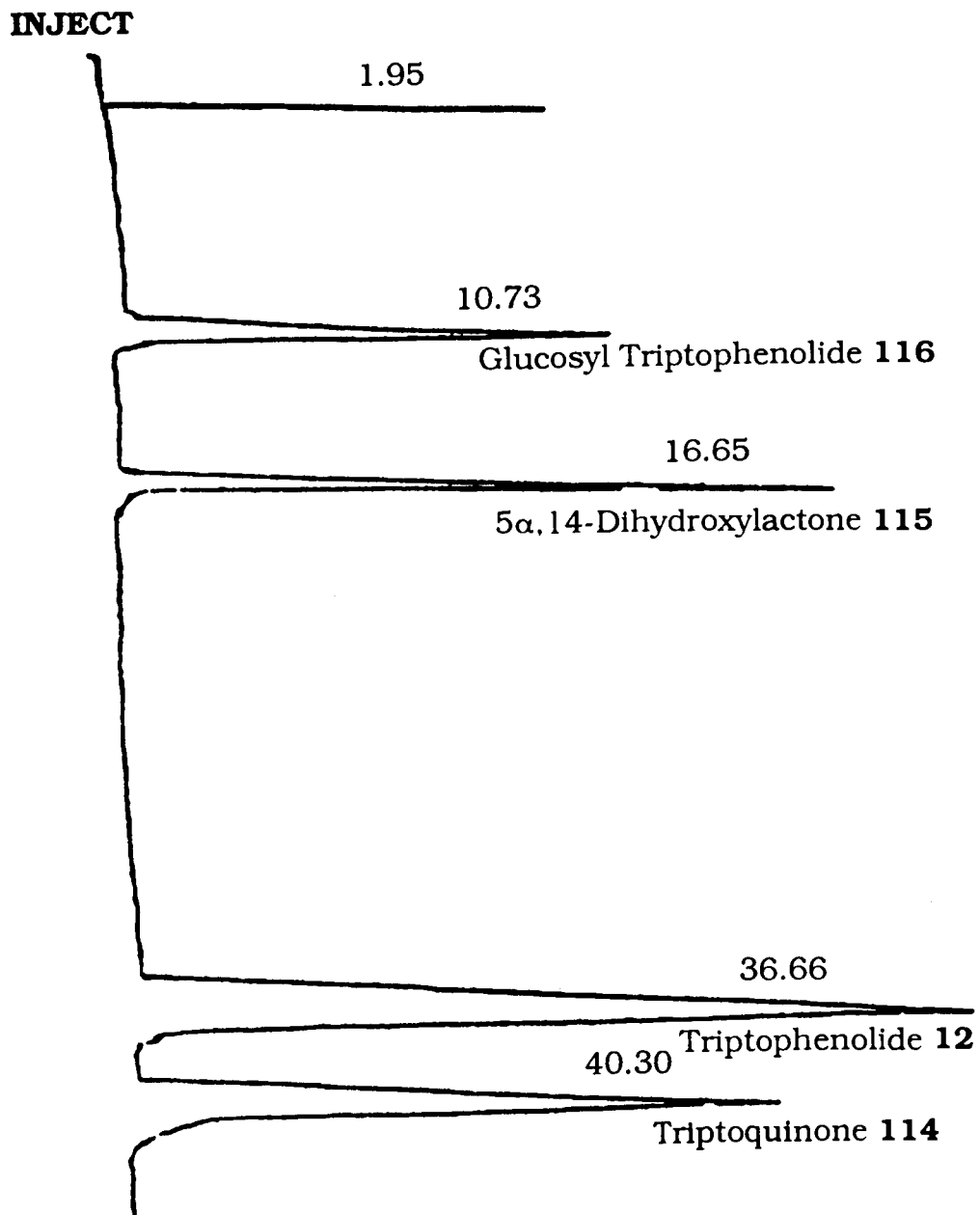


Legend:

$$\text{14-Glucosyl Tryptophenolide (116), } \mu\text{g} = -0.319 + 0.00821 \cdot \text{Area}$$

Retention time = 10.7 min.

Figure 8. HPLC Profile of the Substrate **12** and Products from the Biotransformation with *C. elegans*.



The time course of the substrate conversion was monitored by HPLC analysis at the above-mentioned conditions. In order to evaluate the rate of the bioconversion with time, the analyses were performed regularly every 24 h.

Three parallel experiments utilizing 15 different media (Table 7) were conducted at different times and the average of the metabolite concentrations were determined. The standard deviations for the concentrations of the four compounds were:

$$\sigma^2 = 0.82 \text{ for triptophenolide (12)}$$

$$\sigma^2 = 0.12 \text{ for triptoquinone (114)}$$

$$\sigma^2 = 0.016 \text{ for } 5\alpha,14\text{-dihydroxybutenolide (115)}$$

$$\sigma^2 = 0.062 \text{ for 14-glucosyl triptophenolide (116)}$$

The results of these experiments are summarized in Figures 9 - 23. The results have shown a complex relationship between component variations, product formation, and biotransformation time, suggesting that the hydroxylase enzyme synthesized by *C. elegans* depended strongly on the medium composition.

The rate of triptoquinone (**114**) production during the first 24 h was higher in medium compositions 1, 3, 5 and 7 (Table 7) which contained high levels (40 g/L) of malt extract, whereas medium compositions 2, 4, 6 and 8, with low levels (2.0 g/L) of malt extract, showed lower rates of the formation of **114**. Therefore, the high concentration of malt extract used in the present optimization experiments enhanced the formation of the target product, triptoquinone (**114**).

The experiments also revealed that the yield of 14-glucosyl triptophenolide (**116**) was unaffected by the concentration of glucose in

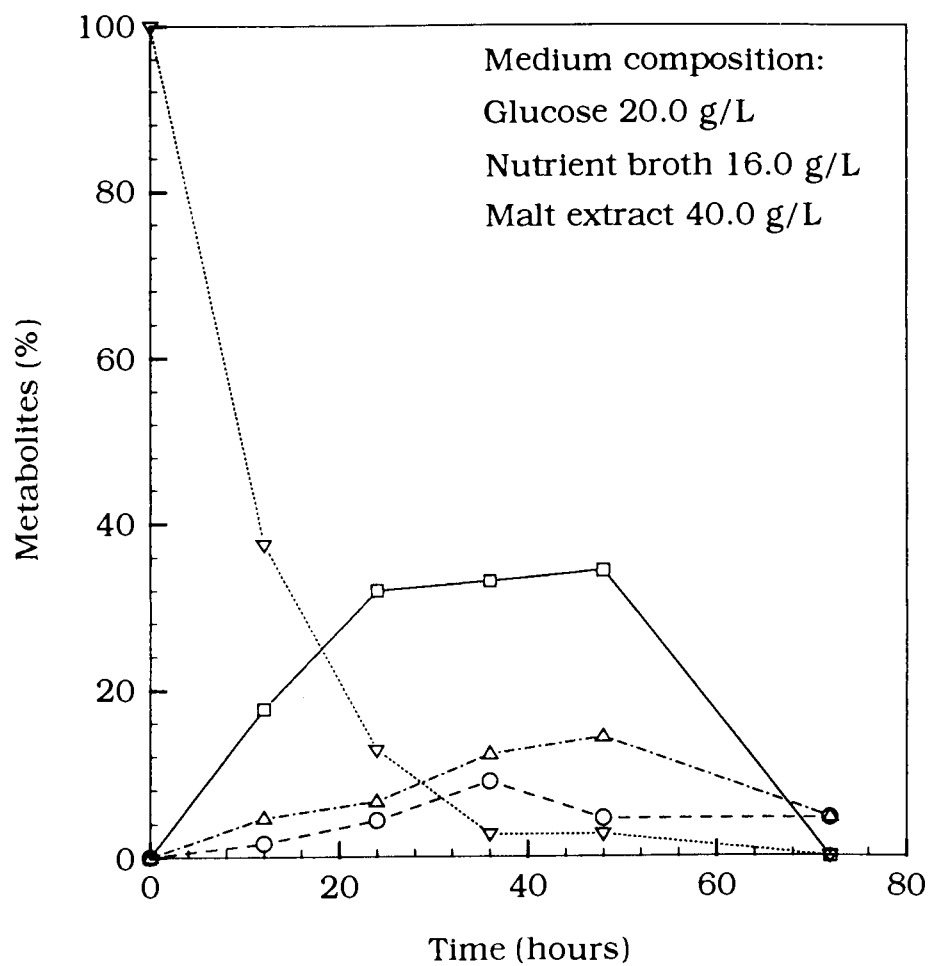
the medium suggesting that within the levels examined in this study (1.0 to 20.0 g/L), glucose conjugation was not related to glucose availability.

The highest yield of **116** was obtained with a low level of nutrient broth and a high level of malt extract (in medium compositions 3 and 7) and this is illustrated in Figures 10 and 14. When either nutrient broth and malt extract were present in low levels, the production of **116** was suppressed. However, in this case a two-factor interaction took place (nutrient broth and malt extract) which apparently exerted a synergistic effect in terms of product formation.

In contrast to the results with the formation of **114** and **116**, neither malt extract nor nutrient broth nor their combinations had a significant influence on the production of **115**.

A mathematical model (Equations 2-5) obtained from the results of the first factorial design experiment (Table 7) was used to summarize all the factor effects and interactions on the yield of the metabolites (see Appendix).

Figure 9. Time Course of Biotransformation of Triptophenolide (**12**) to **114**, **115** and **116** in Medium Composition 1.

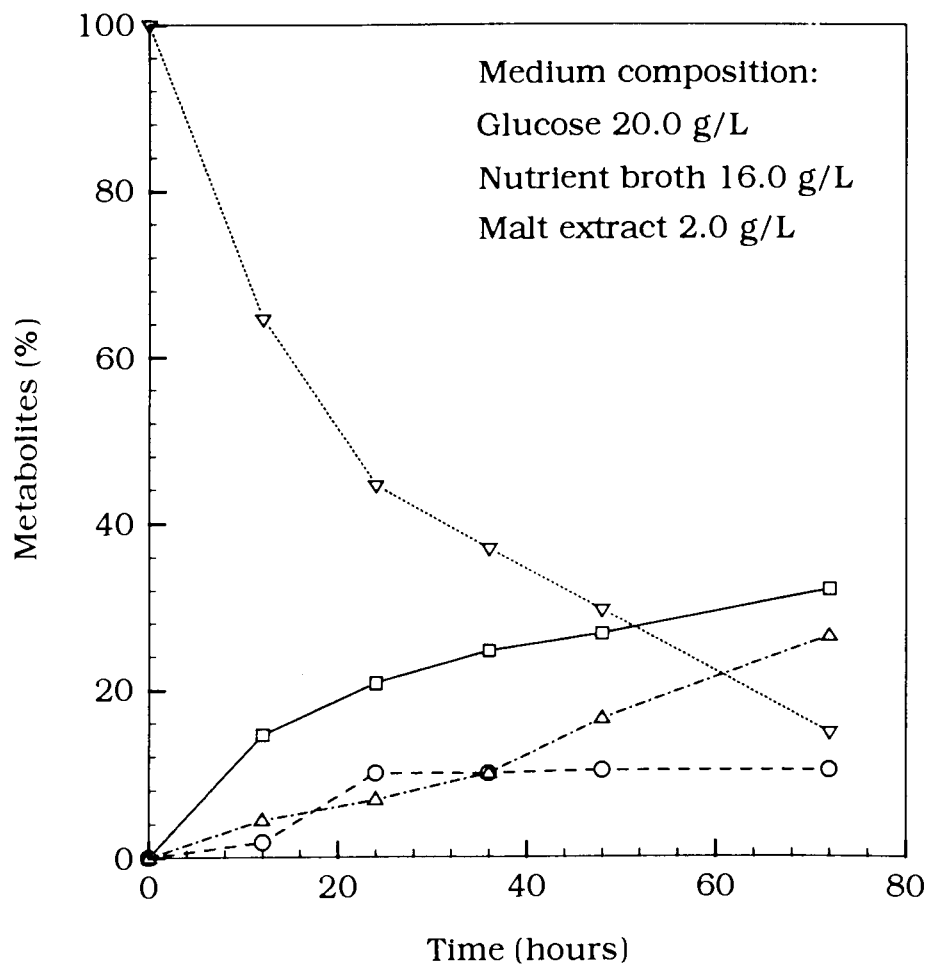


Legend:

- Triptophenolide (**12**)    ···▽···
- Triptoquinone (**114**)    —□—
- 5 $\alpha$ ,14-Dihydroxybutenolide (**115**)    -○-
- 14-Glucosyl Triptophenolide (**116**)    ---△---



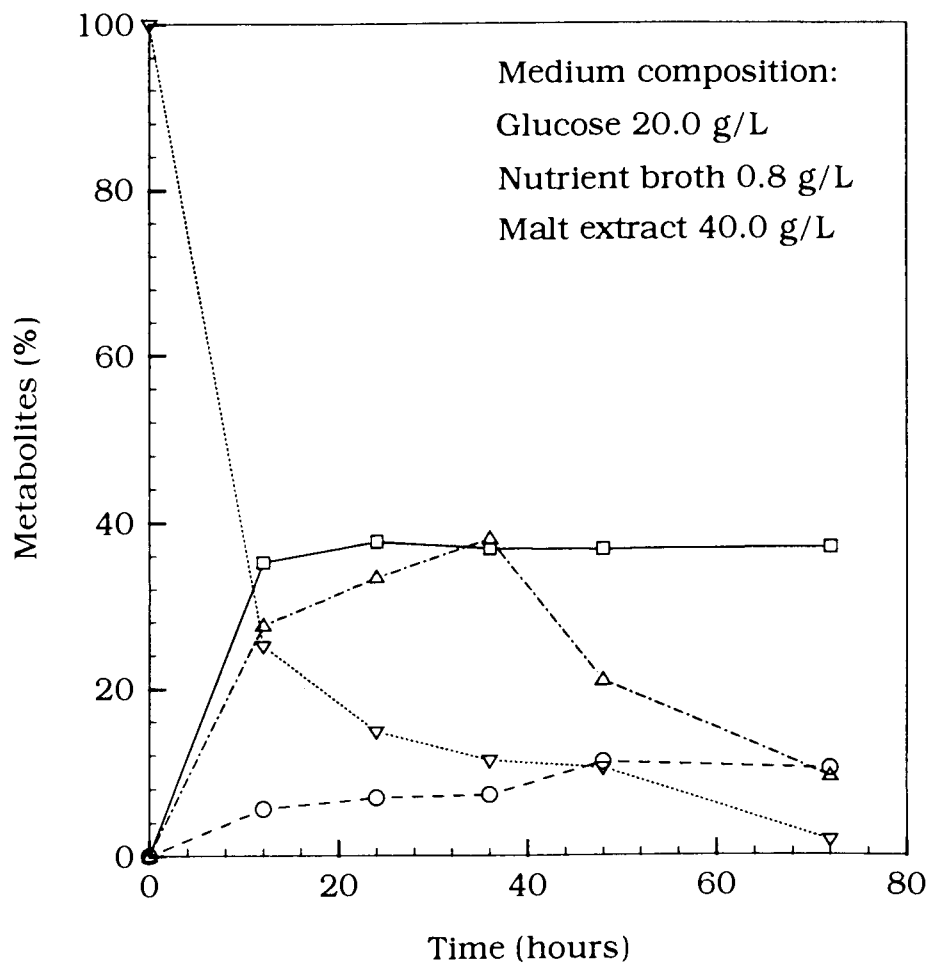
Figure 10. Time Course of Biotransformation of Tryptophenolide (**12**) to **114**, **115** and **116** in Medium Composition 2.



Legend:

- Tryptophenolide (**12**)    ▽
- Triptoquinone (**114**)    □
- 5α,14-Dihydroxybutenolide (**115**)    ○
- 14-Glucosyl Tryptophenolide (**116**)    △

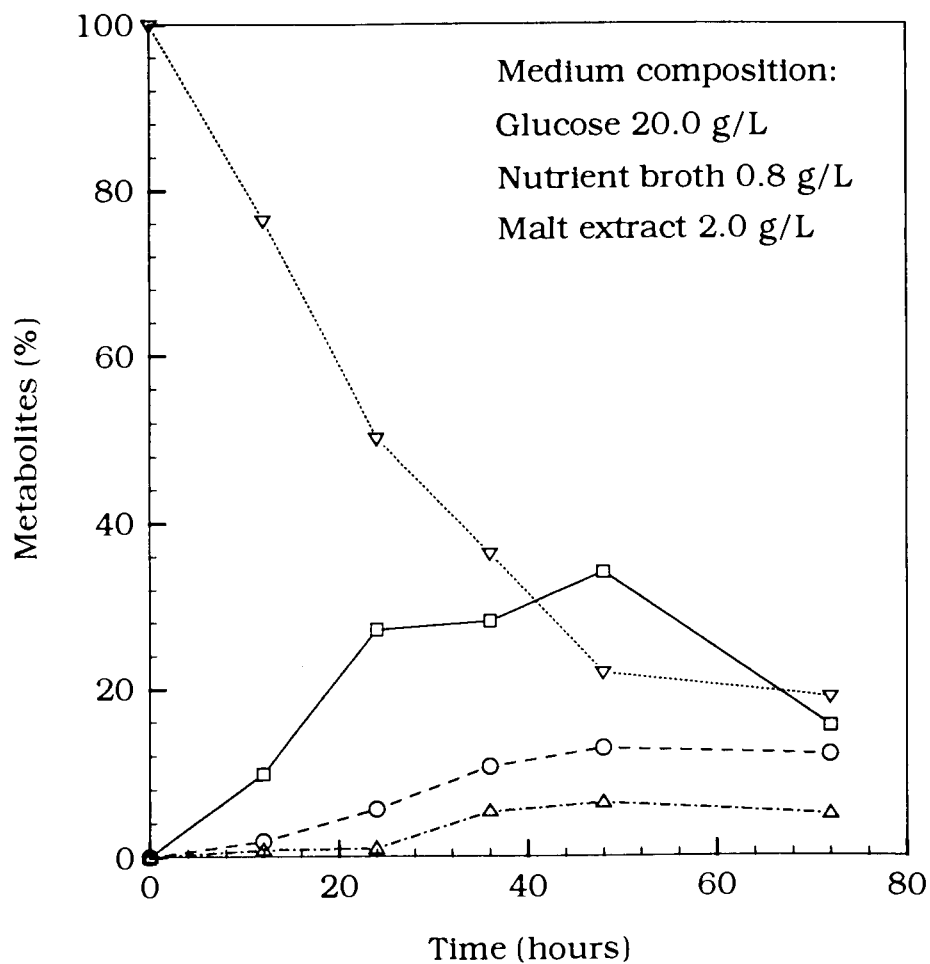
Figure 11. Time Course of Biotransformation of Triptophenolide (**12**) to **114**, **115** and **116** in Medium Composition 3.



Legend:

- Triptophenolide (**12**)     $\nabla$
- Triptophenone (**114**)     $\square$
- 5 $\alpha$ ,14-Dihydroxybutenolide (**115**)     $\circ$
- 14-Glucosyl Triptophenolide (**116**)     $\triangle$

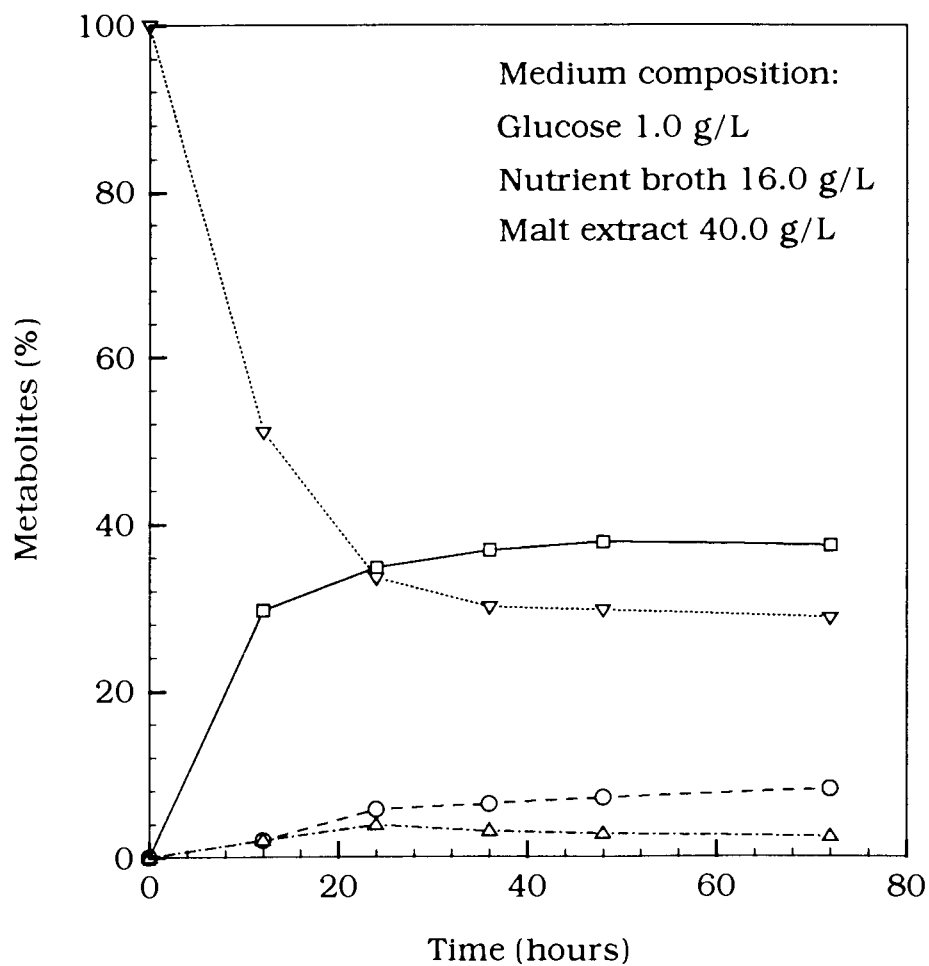
Figure 12. Time Course of Biotransformation of Triptophenolide (**12**) to **114**, **115** and **116** in Medium Composition 4.



Legend:

- Triptophenolide (**12**)     $\nabla$ .....
- Triptiquinone (**114**)     $\square$ —
- 5 $\alpha$ ,14-Dihydroxybutenolide (**115**)    -  $\circ$  - -
- 14-Glucosyl Triptophenolide (**116**)    - -  $\Delta$  - -

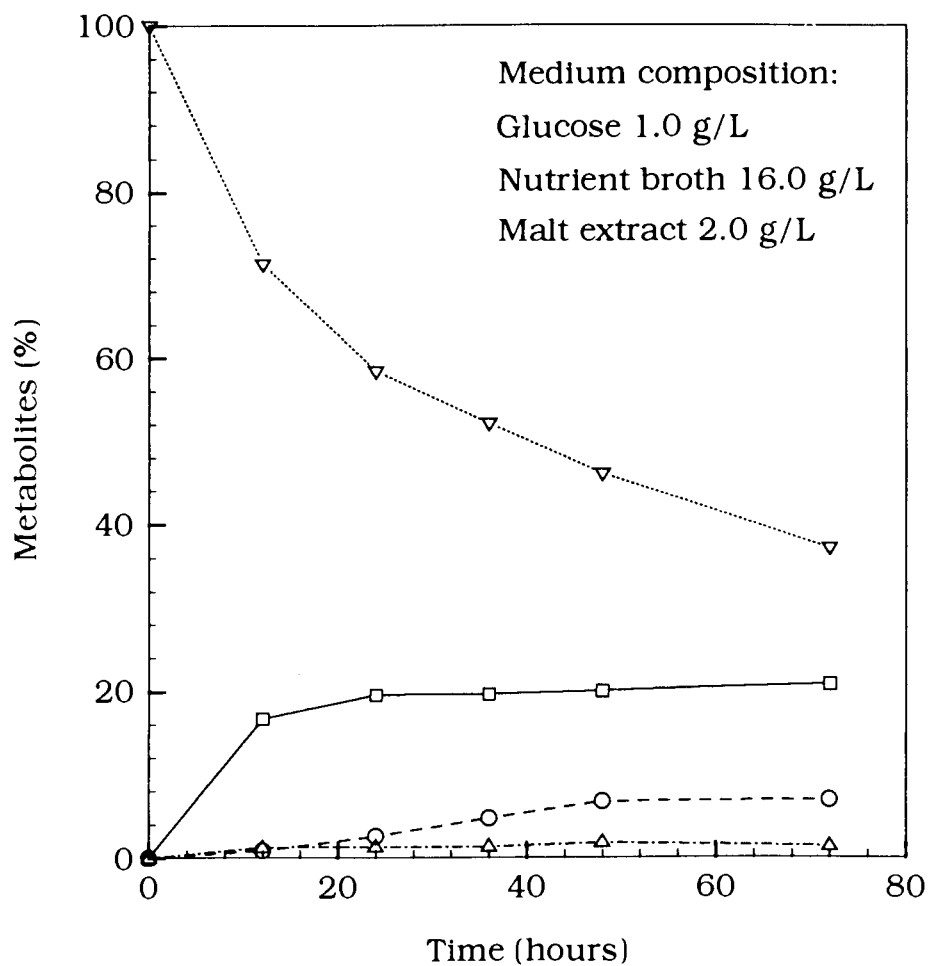
Figure 13. Time Course of Biotransformation of Triptophenolide (**12**) to **114**, **115** and **116** in Medium Composition 5.



Legend:

- Triptophenolide (**12**)    ···▽···
- Triptoquinone (**114**)    -□-
- 5 $\alpha$ ,14-Dihydroxybutenolide (**115**)    -○-
- 14-Glucosyl Triptophenolide (**116**)    ···△···

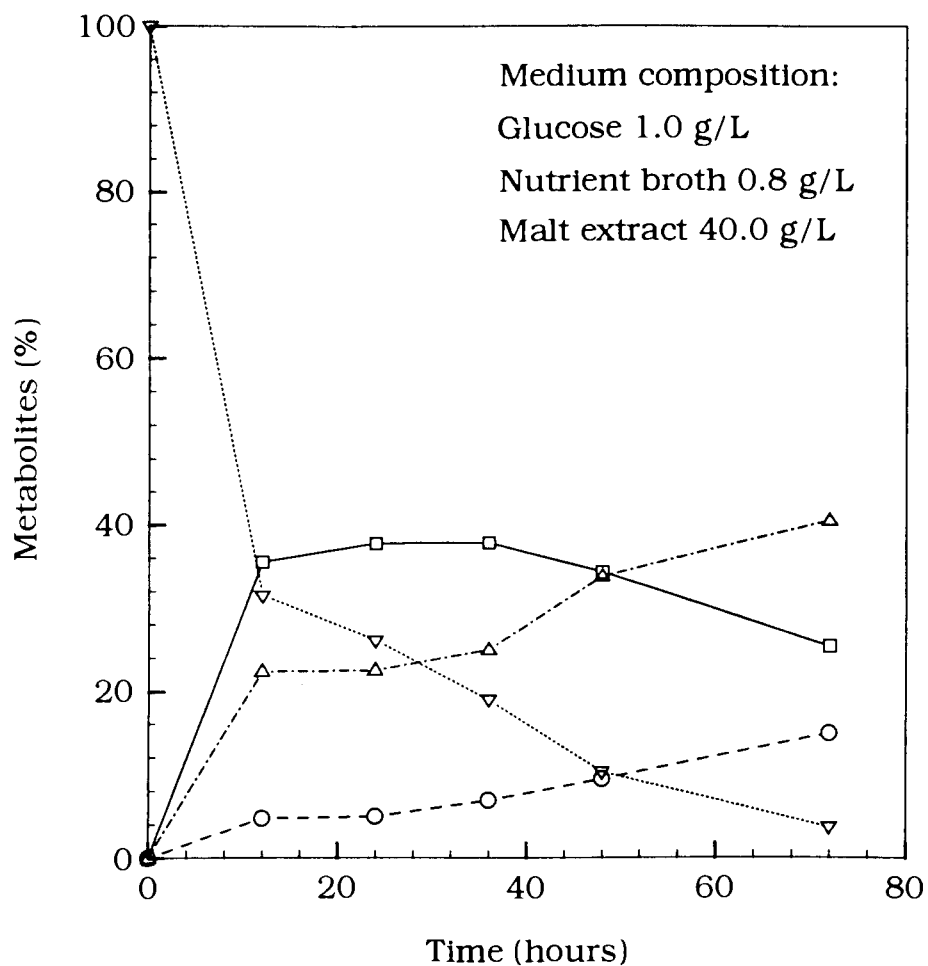
Figure 14. Time Course of Biotransformation of Triptophenolide (**12**) to **114**, **115** and **116** in Medium Composition 6.



Legend:

- Triptophenolide (**12**)     $\nabla$
- Triptoquinone (**114**)     $\square$
- 5 $\alpha$ ,14-Dihydroxybutenolide (**115**)     $\circ$
- 14-Glucosyl Triptophenolide (**116**)     $\triangle$

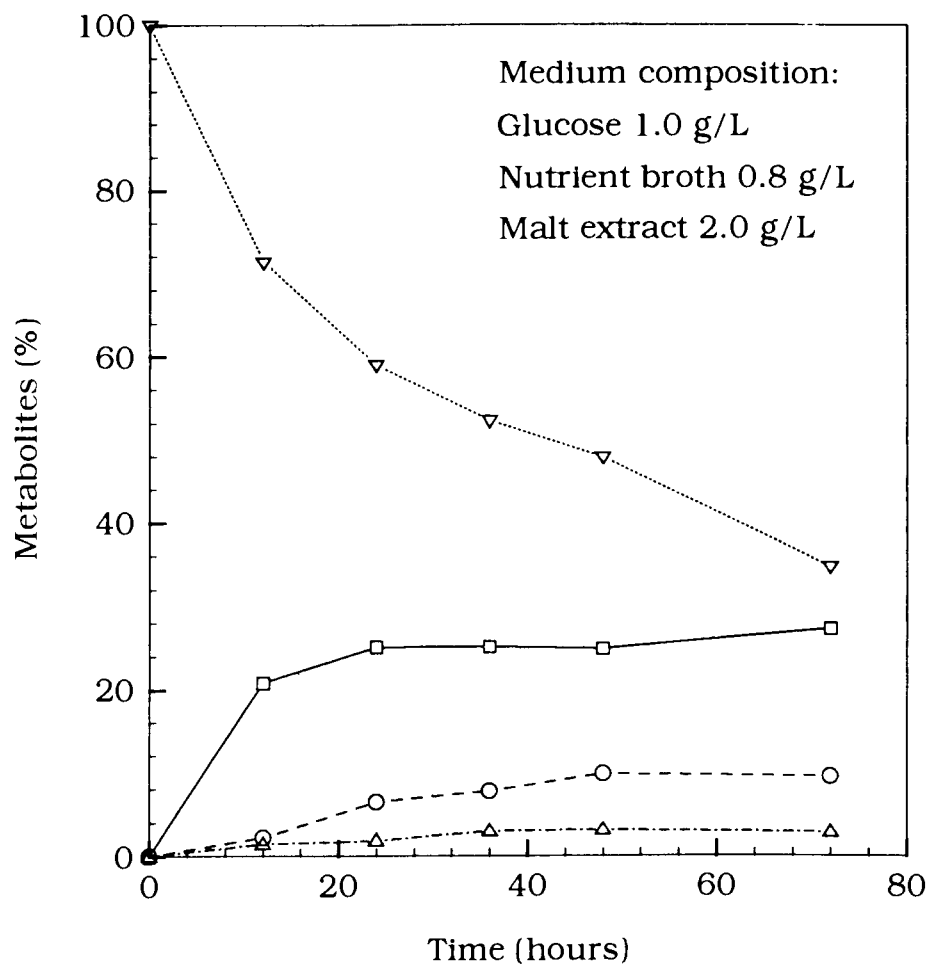
Figure 15. Time Course of Biotransformation of Triptophenolide (**12**) to **114**, **115** and **116** in Medium Composition 7.



Legend:

- Triptophenolide (**12**)    ···▽···
- Triptoquinone (**114**)    —□—
- 5α,14-Dihydroxybutenolide (**115**)    -○-
- 14-Glucosyl Triptophenolide (**116**)    ---△---

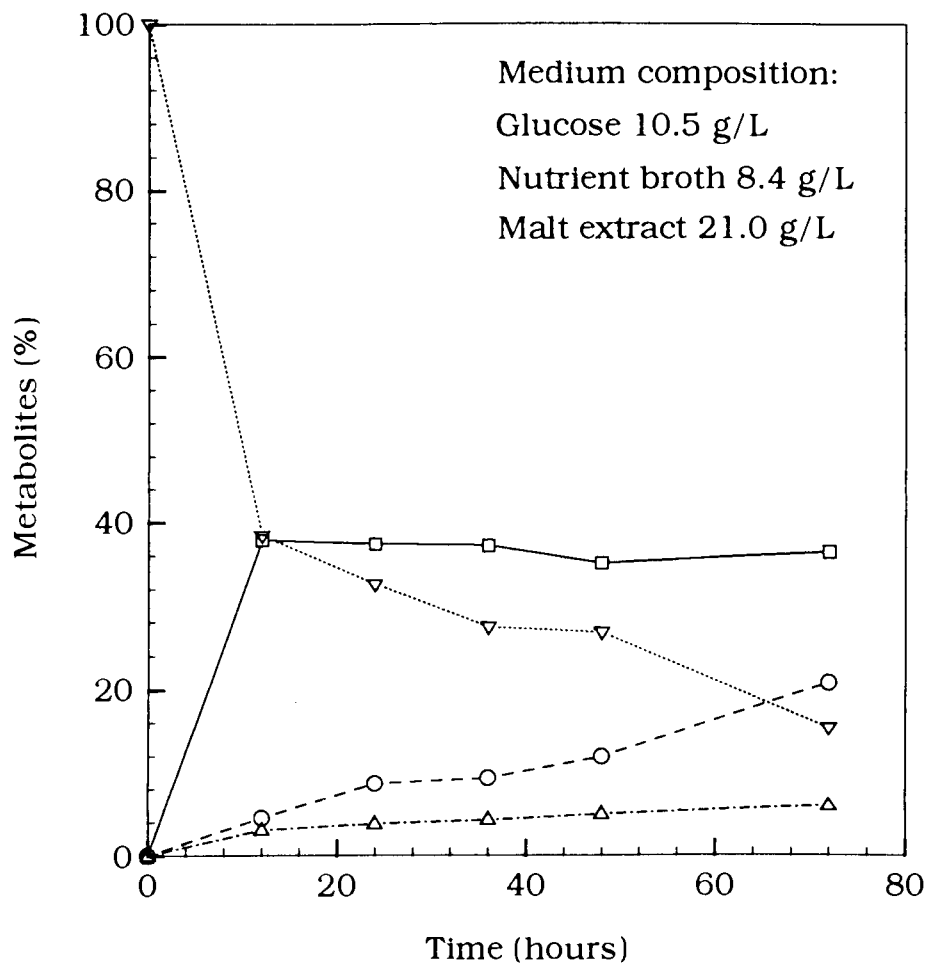
Figure 16. Time Course of Biotransformation of Triptophenolide (**12**) to **114**, **115** and **116** in Medium Composition 8.



Legend:

- Triptophenolide (**12**)     $\nabla$
- Triptoquinone (**114**)     $\square$
- 5 $\alpha$ ,14-Dihydroxybutenolide (**115**)     $\circ$
- 14-Glucosyl Triptophenolide (**116**)     $\triangle$

Figure 17. Time Course of Biotransformation of Triptophenolide (**12**) to **114**, **115** and **116** in Medium Composition 9.

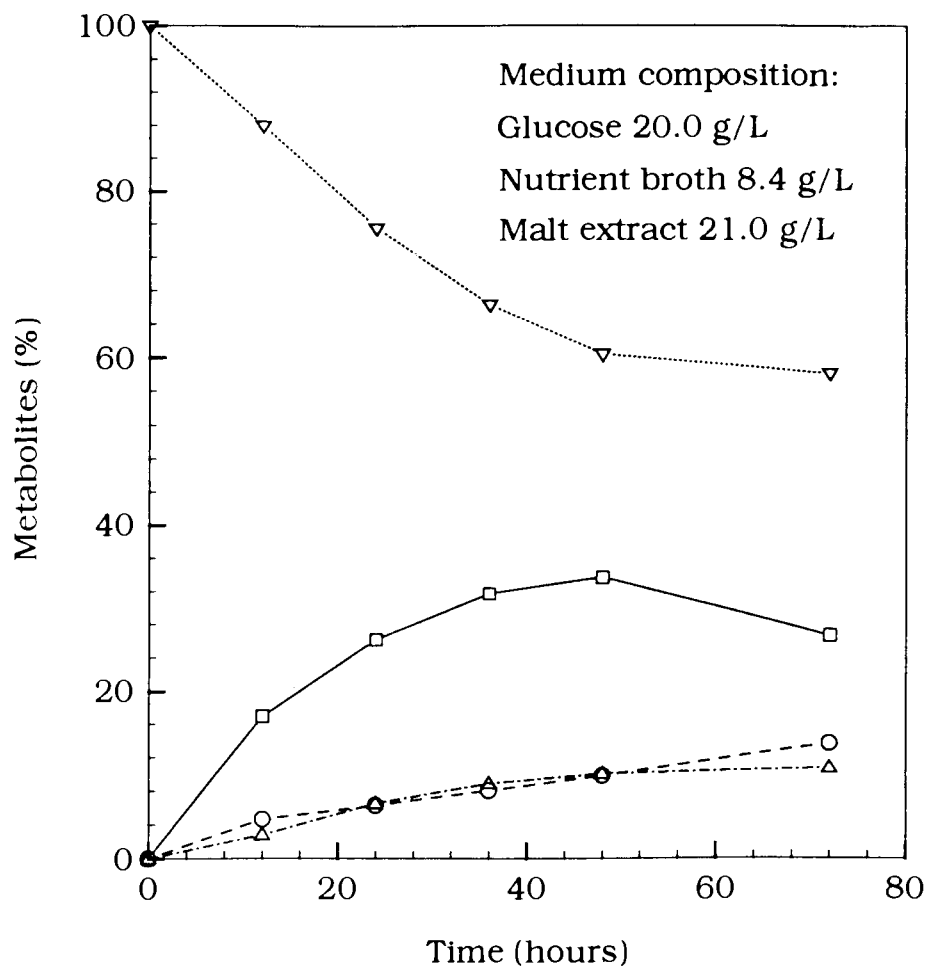


Legend:

- Triptophenolide (**12**)    ···▽···
- Triptoquinone (**114**)    -□-
- 5 $\alpha$ ,14-Dihydroxybutenolide (**115**)    -○-
- 14-Glucosyl Triptophenolide (**116**)    ···△···



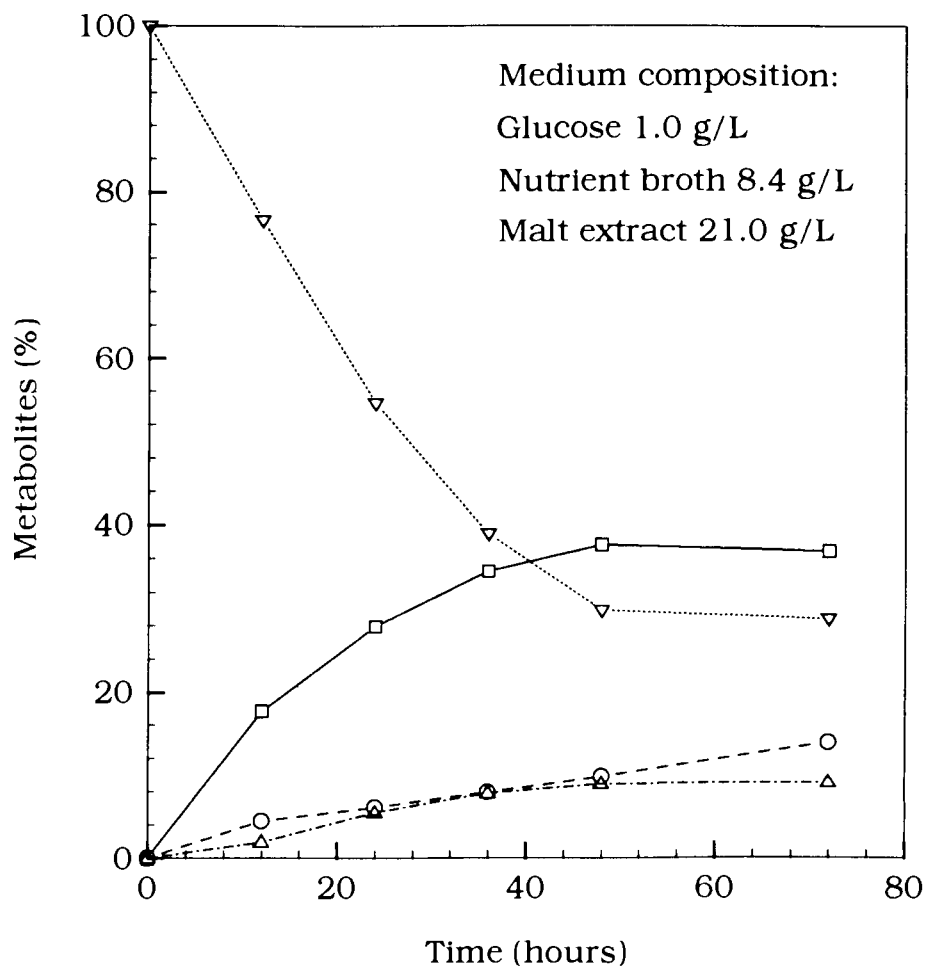
Figure 18. Time Course of Biotransformation of Triptophenolide (**12**) to **114**, **115** and **116** in Medium Composition 10.



Legend:

- Triptophenolide (**12**)    ···▽···
- Triptoquinone (**114**)    —□—
- 5 $\alpha$ ,14-Dihydroxybutenolide (**115**)    -○-
- 14-Glucosyl Triptophenolide (**116**)    ---△---

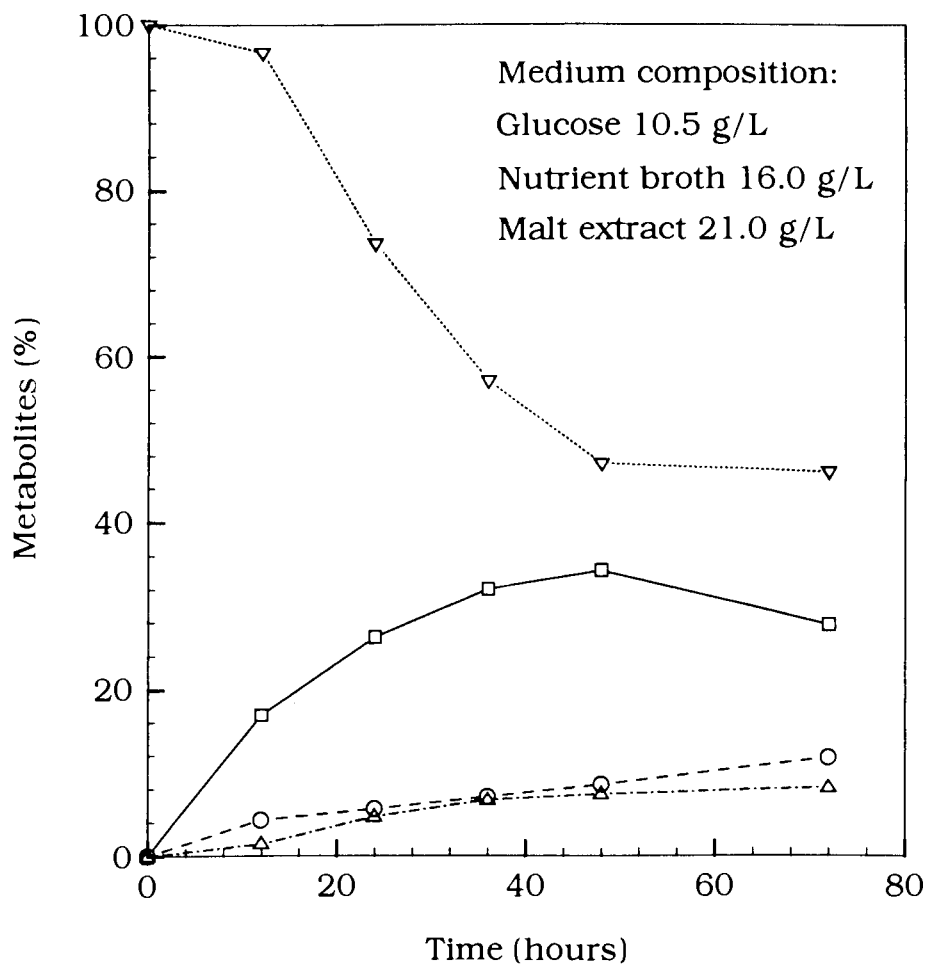
Figure 19. Time Course of Biotransformation of Triptophenolide (**12**) to **114**, **115** and **116** in Medium Composition 11.



Legend:

- Triptophenolide (**12**)    ···▽···
- Triptoquinone (**114**)    —□—
- 5 $\alpha$ ,14-Dihydroxybutenolide (**115**)    -○-
- 14-Glucosyl Triptophenolide (**116**)    ---△---

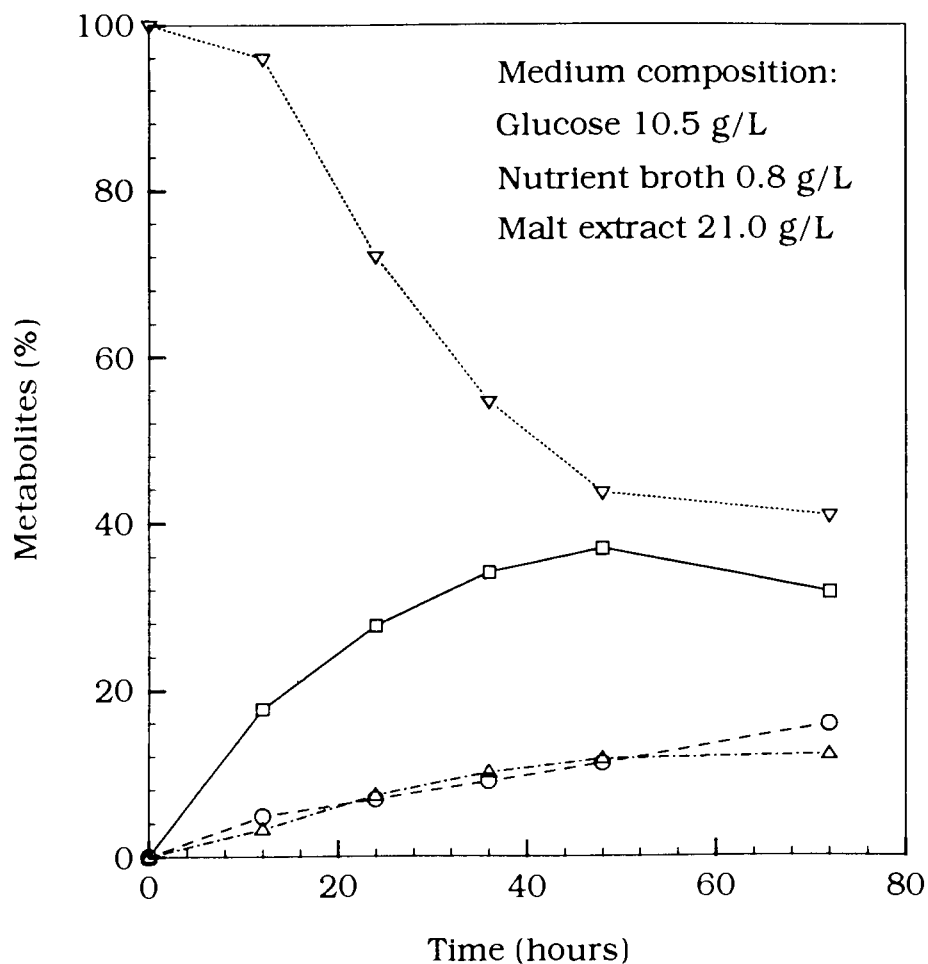
Figure 20. Time Course of Biotransformation of Triptophenolide (**12**) to **114**, **115** and **116** in Medium Composition 12.



Legend:

- Triptophenolide (**12**)     $\nabla$  (dotted line)
- Triptoquinone (**114**)     $\square$  (solid line)
- 5 $\alpha$ ,14-Dihydroxybutenolide (**115**)     $\circ$  (dashed line)
- 14-Glucosyl Triptophenolide (**116**)     $\triangle$  (dash-dot line)

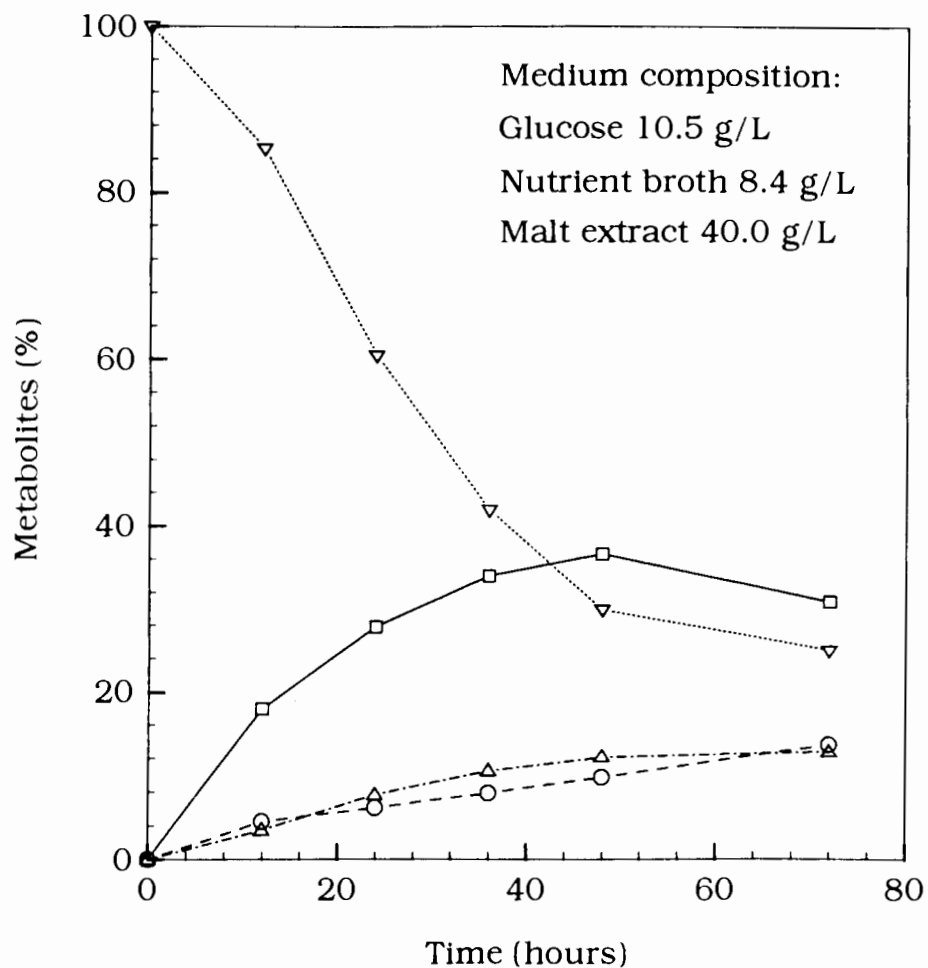
Figure 21. Time Course of Biotransformation of Triptophenolide (**12**) to **114**, **115** and **116** in Medium Composition 13.



Legend:

- Triptophenolide (**12**)     $\nabla$
- Triptoquinone (**114**)     $\square$
- 5 $\alpha$ ,14-Dihydroxybutenolide (**115**)     $\circ$
- 14-Glucosyl Triptophenolide (**116**)     $\triangle$

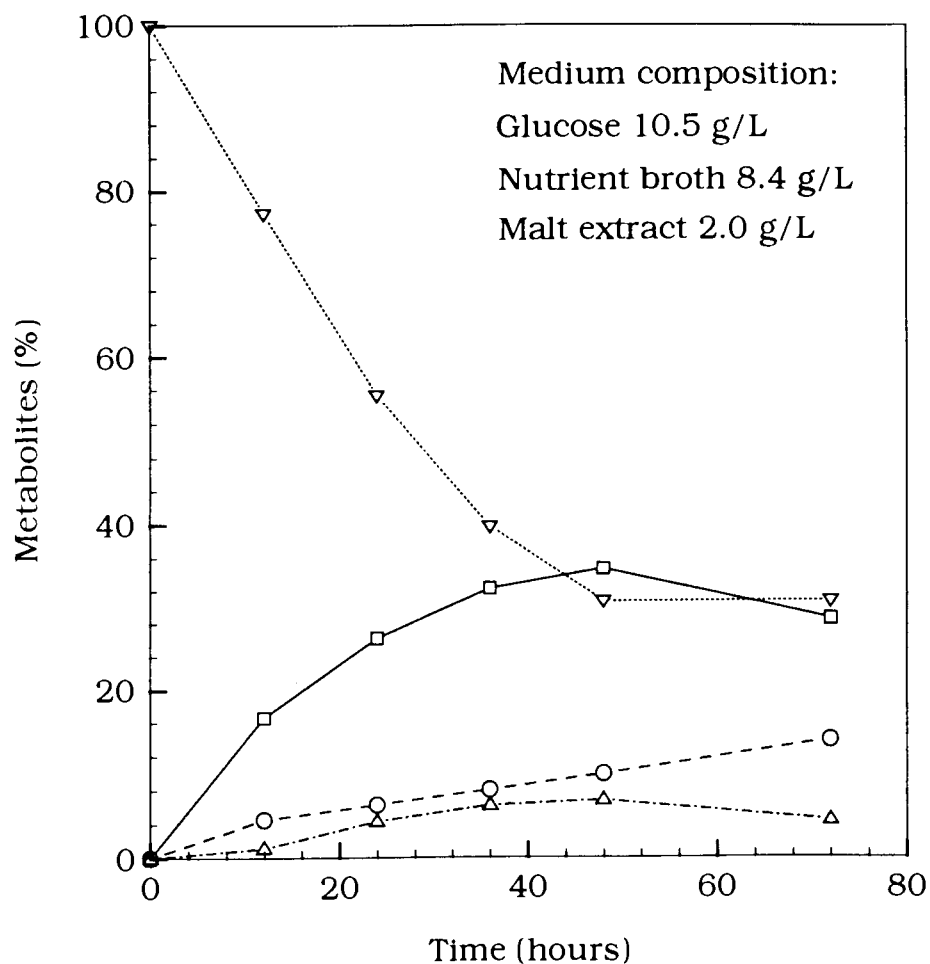
Figure 22. Time Course of Biotransformation of Triptophenolide (**12**) to **114**, **115** and **116** in Medium Composition 14.



Legend:

- Triptophenolide (**12**)     $\nabla$  (dotted line)
- Triptoquinone (**114**)     $\square$  (solid line)
- 5 $\alpha$ ,14-Dihydroxybutenolide (**115**)     $\circ$  (dashed line)
- 14-Glucosyl Triptophenolide (**116**)     $\triangle$  (dash-dot line)

Figure 23. Time Course of Biotransformation of Triptophenolide (**12**) to **114**, **115** and **116** in Medium Composition 15.



Legend:

- Triptophenolide (**12**)    ···▽···
- Triptoquinone (**114**)    —□—
- 5 $\alpha$ ,14-Dihydroxybutenolide (**115**)    -○-
- 14-Glucosyl Triptophenolide (**116**)    ---△---

$$\begin{aligned}
Y_1 = & 99.7 - 2.52*X_1 + 0.195*X_2 + 0.0619*X_3 - 0.148*X_4 - 0.0125*X_1*X_2 \\
& + 0.00494*X_1*X_3 - 0.00649*X_1*X_4 - 0.0287*X_2*X_3 + \\
& 0.0107*X_3*X_4 + 0.0222*X_1^2
\end{aligned} \tag{2}$$

$$\begin{aligned}
Y_2 = & - 10.1 + 1.34*X_1 + 0.950*X_2 + 1.24*X_3 + 0.543*X_4 - \\
& 0.00482*X_1*X_2 - 0.00337*X_1*X_3 - 0.0224*X_2*X_3 - \\
& 0.00870*X_2*X_4 - 0.0151*X_3*X_4 - 0.0126*X_1^2 - 0.0265*X_2^2 - \\
& 0.0414*X_3^2 - 0.00662*X_4^2
\end{aligned} \tag{3}$$

$$\begin{aligned}
Y_3 = & - 3.54 + 0.164*X_1 + 0.511*X_2 + 0.596*X_3 + 0.285*X_4 - \\
& 0.00380*X_1*X_3 - 0.00488*X_2*X_4 - 0.00352*X_3*X_4 - \\
& 0.000250*X_1^2 - 0.0195*X_2^2 - 0.0304*X_3^2 - 0.00487*X_4^2
\end{aligned} \tag{4}$$

$$\begin{aligned}
Y_4 = & - 4.66 + 0.450*X_1 - 0.257*X_2 - 0.390*X_3 + 0.310*X_4 - \\
& 0.00454*X_1*X_2 + 0.00222*X_1*X_4 + 0.0461*X_2*X_3 - 0.0203*X_2*X_4 \\
& - 0.0283*X_3*X_4 - 0.00432*X_1^2 + 0.0167*X_2^2 + 0.0261*X_3^2 + \\
& 0.00417*X_4^2
\end{aligned} \tag{5}$$

where:

$Y_1$  = Recovered Triptophenolide (**12**), (%)

$Y_2$  = Triptoquinone (**114**), (%)

$Y_3$  = 5 $\alpha$ , 14-Dihydroxytriptophenolide (**115**), (%)

$Y_4$  = 14-Glucosyl Triptophenolide (**116**), (%)

$X_1$  = Time (h)

$X_2$  = Glucose (g/L)

$X_3$  = Nutrient broth (g/L)

$X_4$  = Malt extract (g/L)

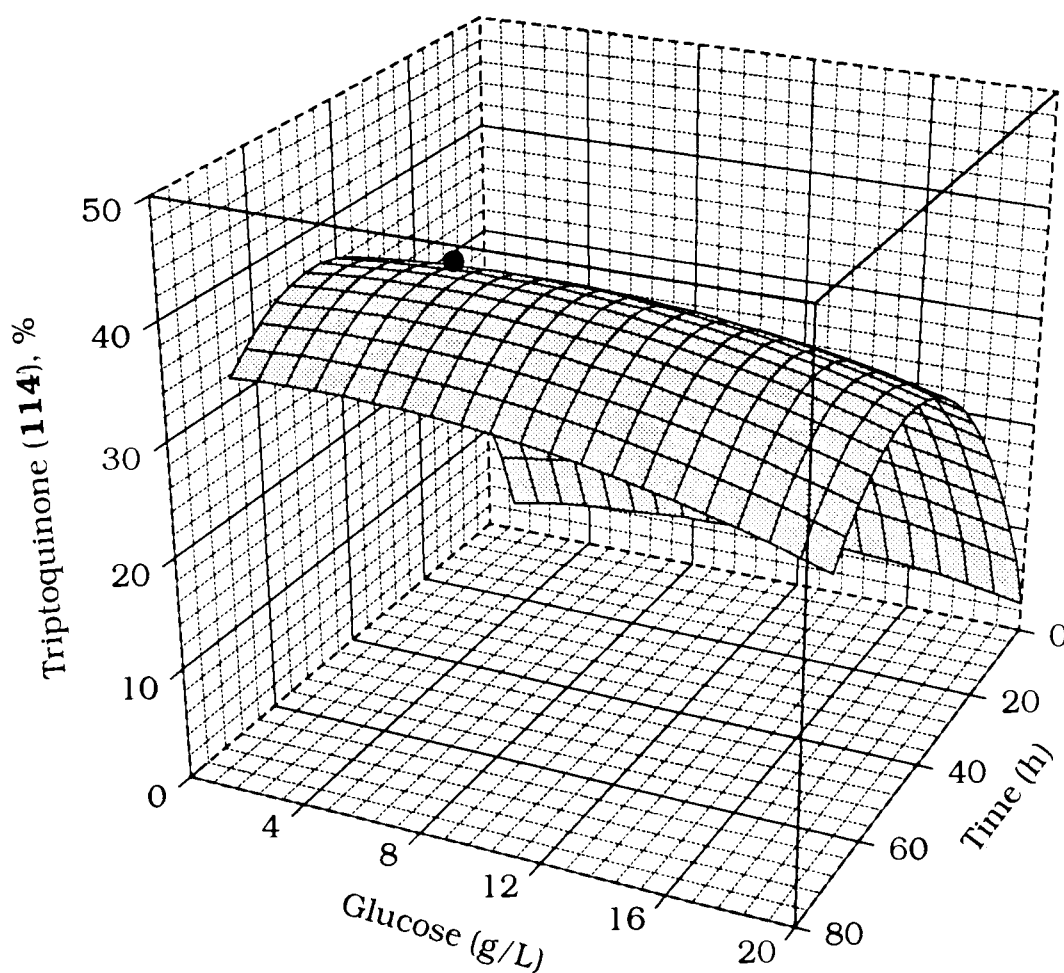
The equations (2-5) were used to predict the maximum yields of the metabolites and recovered substrate at different values of the studied factors. The results for the target product **114** are obtained by equation (3) and are illustrated in Figures 24 and 25. Figure 24 shows the influence of glucose concentration within the studied range (1.0 - 20.0 g/L) and biotransformation time (0 - 72 h) at optimum values of nutrient broth (5.59 g/L) and malt extract (31.3 g/L) on the yield of triptoquinone (**114**). In this case, the glucose concentration within the studied range has no significant influence on the yield of the product.

In contrast, biotransformation time was critical with maximum product formation occurring after approx. 50 h of incubation (Figure 24). When biotransformation time and glucose concentration were held at optimum values (51.5 h and 5.75 g/L respectively), the influence of variable nutrient broth and malt extract on triptoquinone (**114**) production were evaluated by Equation 3 (Figure 25). Under optimum conditions, a 41% yield of triptoquinone (**114**) was obtained (Figures 24 and 25).

The maximum yields of the various metabolites obtained from the above-described experiments at specific concentrations of the nutrients are presented in Table 8.



Figure 24. Influence of the Glucose Concentration and Biotransformation Time on the Yield of Triptoquinone (**114**) at the Optimum Values of the Other Factors (Nutrient Broth and Malt Extract Concentrations).



Legend:

Biotransformation time = 0 to 72 hours

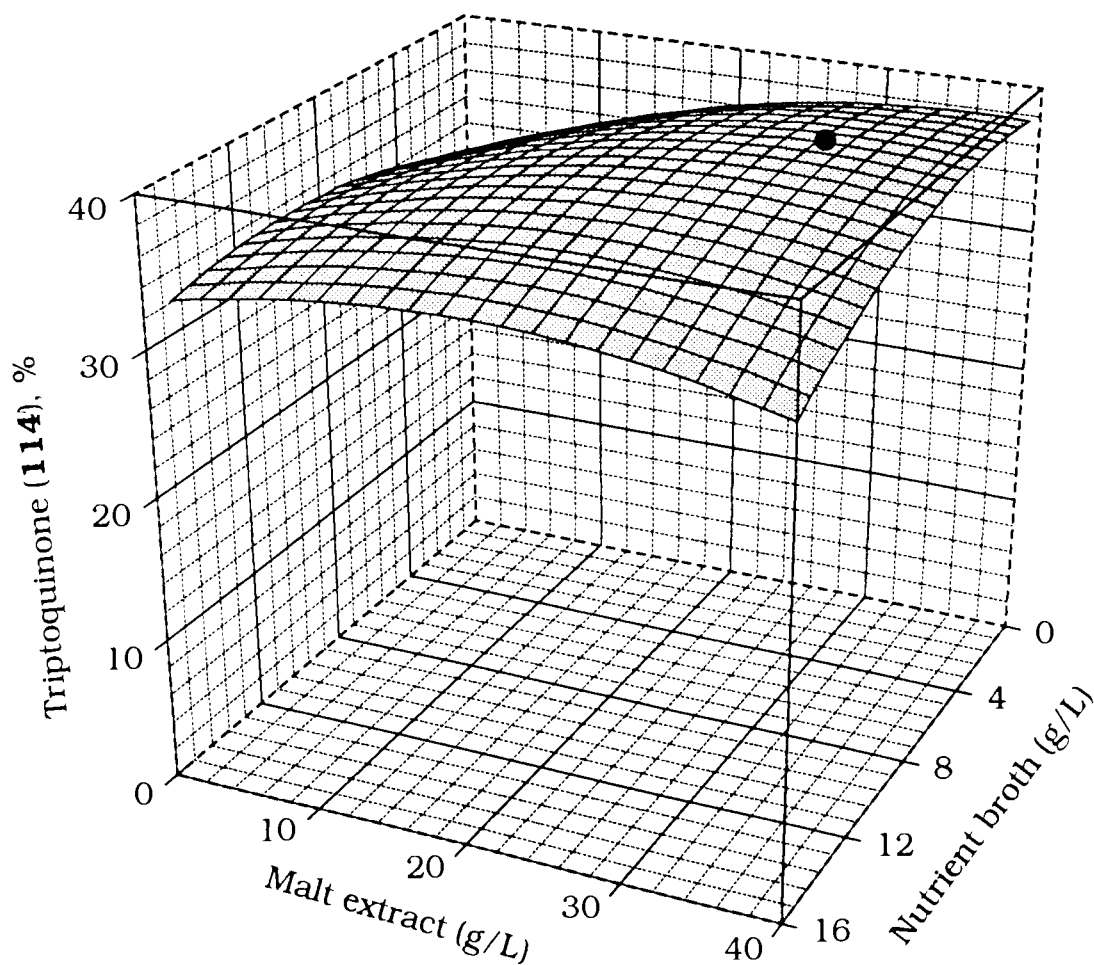
Glucose = 1 to 20 g/L

Nutrient broth = 5.59 g/L

Malt extract = 31.3 g/L

Maximum yield of triptoquinone (**114**) ●

Figure 25. Influence of the Nutrient Broth and Malt Extract Concentrations on the Yield of Triptoquinone (**114**) at the Optimum Values of the Other Factors (Glucose Concentration and Biotransformation Time).



Legend:

Biotransformation time = 51.5 hours

Glucose = 5.75 g/L

Nutrient broth = 0.8 to 16.0 g/L

Malt extract = 2.0 to 40.0 g/L

Maximum yield of triptoquinone (**114**) ●

Table 8. Summary of Optimum Conditions and Yields of Metabolites.

Compound #	Maximum yield	Time (h)	Glucose (g/L)	Nutrient broth (g/L)	Malt extract (g/L)
<b>12</b>	100.0	0.0	10.5	16.0	21.0
<b>114</b>	40.9	51.5	5.75	5.59	31.3
<b>115</b>	13.8	72.0	10.5	12.7	21.0
<b>116</b>	19.4	44.4	20.0	16.0	2.0

**12** - Triptophenolide

**114** - Triptoquinone

**115** - 5 $\alpha$ ,14-Dihydroxytriptophenolide

**116** - 14-Glucosyl Triptophenolide

### **Effect of Medium Composition on Biomass Production**

In order to derive information as to whether medium composition had an effect on biomass production and pH, a set of 3 x 15 Erlenmeyer flasks were inoculated with an equal amount of inoculum, as indicated earlier (see Section 4.2, Chapter IV), with spore suspension of *C. elegans*. Different medium compositions used for this experiment are shown in Table 9. The cultures were grown for 120 h at 28°C and 220 rpm on a rotary shaker.

Table 9. Experiments with Different Medium Composition.

Medium composition	Glucose	Nutrient broth	Malt Extract
1	20.0	16.0	40.0
2	20.0	16.0	2.0
3	20.0	0.8	40.0
4	20.0	0.8	2.0
5	1.0	16.0	40.0
6	1.0	16.0	2.0
7	1.0	0.8	40.0
8	1.0	0.8	2.0
9*	10.5	8.4	21.0
10	20.0	8.4	21.0
11	1.0	8.4	21.0
12	10.5	16.0	21.0
13	10.5	0.8	21.0
14	10.5	8.4	40.0
15	10.5	8.4	2.0

\* Composition in the middle of the range studied.

The pH variations recorded during growth and the yields of biomass at the end of the experiment are given in Table 10.

From the data obtained, it was apparent that variations in the composition of the growth medium caused dramatic changes in pH and biomass formation. As expected, pH declined during fungal growth and increased at the end of the process. This situation was observed in every case except in medium composition 1. The highest yield of biomass was obtained in medium composition 2 where malt extract was at minimum concentration while glucose and nutrient broth were maximal.

The yield of fresh and dried biomass, derived from the 15 medium compositions was determined using the following procedure. After 120 h the mycelia from each flask were separated from the broth (spent medium) by filtration in vacuo. Fresh weight was determined by a gravimetric method and then it was dried at 120°C until a constant weight was reached.

The fresh and dry biomass values obtained in different medium compositions are presented in Figure 26 and Table 10. In the case of composition 1 where all components were in high concentration, the yield of biomass was reduced by one half compared to medium composition 2 with minimum malt extract. Minimum nutrient broth gave minimum growth in all cases thus nutrient broth was essential for high biomass production.

The two other components of the medium, glucose and malt extract, had variable effects. The results indicated that when one factor was present in high concentration sufficient yield of biomass was obtained when the second variable was low.

Table 10. Changes in pH During Growth of *C. elegans* and Final Biomass Yields.

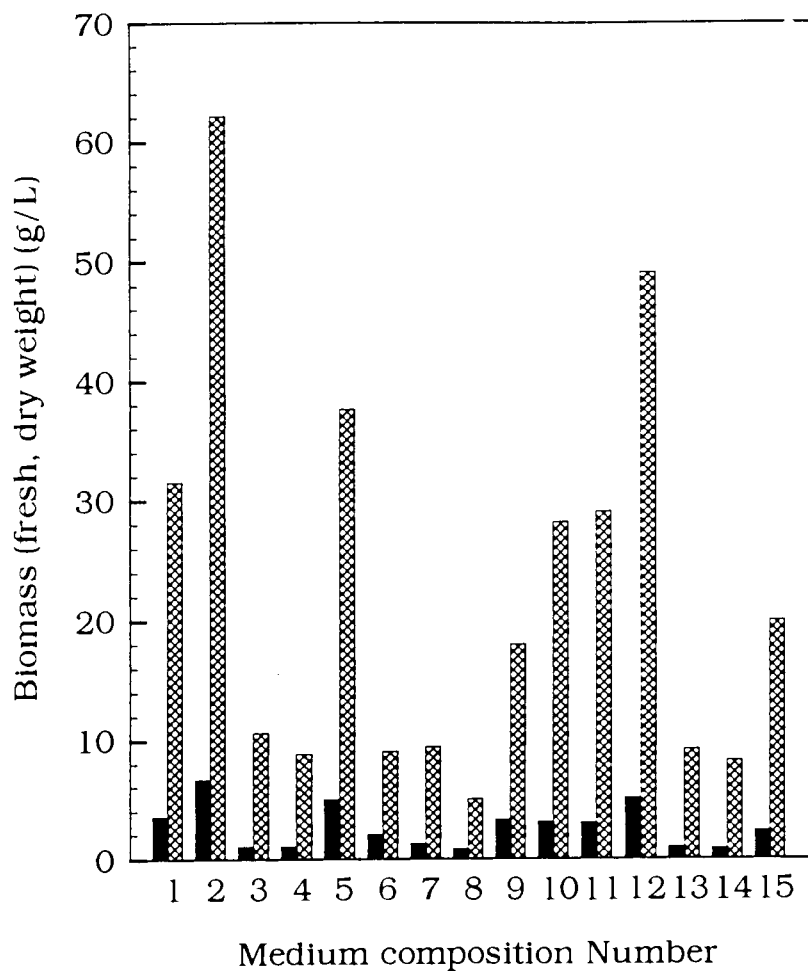
Medium composition	pH			Biomass F.W. (g/L)	Biomass D.W. (g/L)	Quality of the suspension
	33 h	48 h	120 h			
1	5.0	4.75	4.00	31.51	3.54	Coarse
2	5.5	4.75	7.50	62.08	6.68	Medium
3	6.0	4.60	6.00	10.61	1.08	Medium
4	6.5	4.00	6.00	8.84	1.06	Coarse
5	5.5	5.05	6.80	37.62	5.01	Rough
6	7.5	7.95	8.00	9.06	2.05	Medium
7	5.7	4.50	6.00	9.46	1.24	Medium
8	6.5	4.70	7.00	5.03	0.86	Fine
9*	4.8	4.35	6.50	17.97	3.28	Medium/Fine
10	5.5	4.75	4.50	28.16	3.06	Coarse
11	6.0	5.25	6.80	29.02	3.01	Medium
12	6.0	4.50	6.20	49.06	5.05	Medium
13	6.7	4.30	6.00	9.16	0.92	Medium
14	6.5	4.20	6.00	8.17	0.83	Fine
15	5.8	4.35	6.20	19.92	2.28	Coarse

\* Experiment in the middle of the ranges studied.


F.W. = Fresh weight


D.W. = Dry weight

Figure 26. Yield of Biomass (Fresh and Dry Weight) in Different Media.



Legend:

Biomass (fresh weight) 

Biomass (dry weight) 

By statistical analysis (see Appendix), the following equations (6, 7) were obtained which predict the yield of the biomass in any medium combinations within the studied range (Table 7).

$$Y_f = 20.5 + 6.48*X_2 + 13.3*X_3 + 5.24*X_2*X_3 - 7.72*X_2*X_4 - 1.03*X_3*X_4 + 1.269*X_2^2 \quad (6)$$

$$Y_d = 2.89 + 0.400*X_2 + 1.63*X_3 + 0.390*X_2*X_3 - 0.808*X_2*X_4 - 0.182*X_2^2 \quad (7)$$

where:

$Y_f$  = yield of biomass after 144 hours (fresh weight), (g/L)

$Y_d$  = yield of biomass after 144 hours (dry weight), (g/L)

$X_2$  = Glucose (g/L)

$X_3$  = Nutrient broth (g/L)

$X_4$  = Malt extract (g/L)

The standard deviations of the yield of biomass were:

$\sigma^2 = 0.14$  for fresh biomass

$\sigma^2 = 0.0023$  for dry biomass

The calculated and experimental values for the maximum yield of biomass were:

Yield of biomass (F.W. g/L)

55.0 g/L (calculated)

62.1 g/L (actual)

Yield of biomass (D.W. g/L)



5.96 g/L (calculated)

6.68 g/L (actual).

Both maxima (fresh and dry weight) were at levels of the factors glucose 20.0 g/L, nutrient broth 16.0 g/L, and malt extract 2.0 g/L (see Table 8).

The above results have shown that maximum biomass production does not correspond to maximum yield of triptoquinone (**114**). Therefore, optimization of **114** production by medium variations was more appropriate than by biomass maximization.

In spite of studies discussed above, the yield of the desired product **114** was still unsatisfactory. Further optimization in a narrow range of factor variations (medium components and biotransformation time) was undertaken to increase the yield of triptoquinone (**114**).

#### **4.3 Second Optimization of the Biotransformation of Triptophenolide (12) with *C. elegans***

The first factorial design experiment discussed in Section 4.2 was performed using a very broad range of each of the studied parameters (Table 6).

From these results it was concluded that the factor variations evaluated could either improve or diminish the yields of the metabolites during the different biotransformation times (Table 8). As the main goal was to maximize the yield of **114**, another set of experiments was then conducted using a narrower range of the parameters within the experimentally determined optimal range.

## Matrix of the Second Set of Experiments

For these experiments, the same growth factors (glucose, nutrient broth, and malt extract concentrations and the biotransformation time) were evaluated in order to specifically increase the yield of triptoquinone (**114**). The optimum medium composition and the biotransformation time were placed in the middle of the factor ranges as indicated in Table 11. The high and low values of the factors were selected to give a narrow range and these were adjusted to be equidistant from the middle of the range.

The relationship between the standardized and actual settings is shown in Table 11.

This set of experiments was designed according to the method described by Haaland and Mead (Haaland 1989, Mead *et al.* 1993). The design used for the optimization experiment is shown in Table 12.

Incubations of triptophenolide (**12**), performed in the above medium variations and using 3 x 15 flasks, each containing an equal amount of *C. elegans* inoculum ( $2.5 \times 10^6$  spores/ml) and with the substrate concentration of 0.1 mg/ml, were conducted. Parallel experiments were also carried out in a total of 15 flasks as controls (without the substrate present). The samples for analysis were taken at the specific biotransformation times (48, 54, 60 h) shown in Table 12. As before, the biotransformation process was monitored by HPLC for product formation.

Three parallel experiments (Table 12) were conducted at different times. The average of the product concentrations were determined and the standard deviation for triptoquinone (**114**) was  $\sigma^2 = 0.059$

Table 11. Factor Settings for the Second Set of Experiments.

Standardized levels		Actual levels			
		Factors			
		Time	Glucose	Nutrient Broth	Malt Extract
High	1	60 h	8.0 g/L	8.0 g/L	35.0 g/L
Middle	0	54 h	5.5 g/L	6.0 g/L	30.0 g/L
Low	-1	48 h	3.0 g/L	4.0 g/L	25.0 g/L

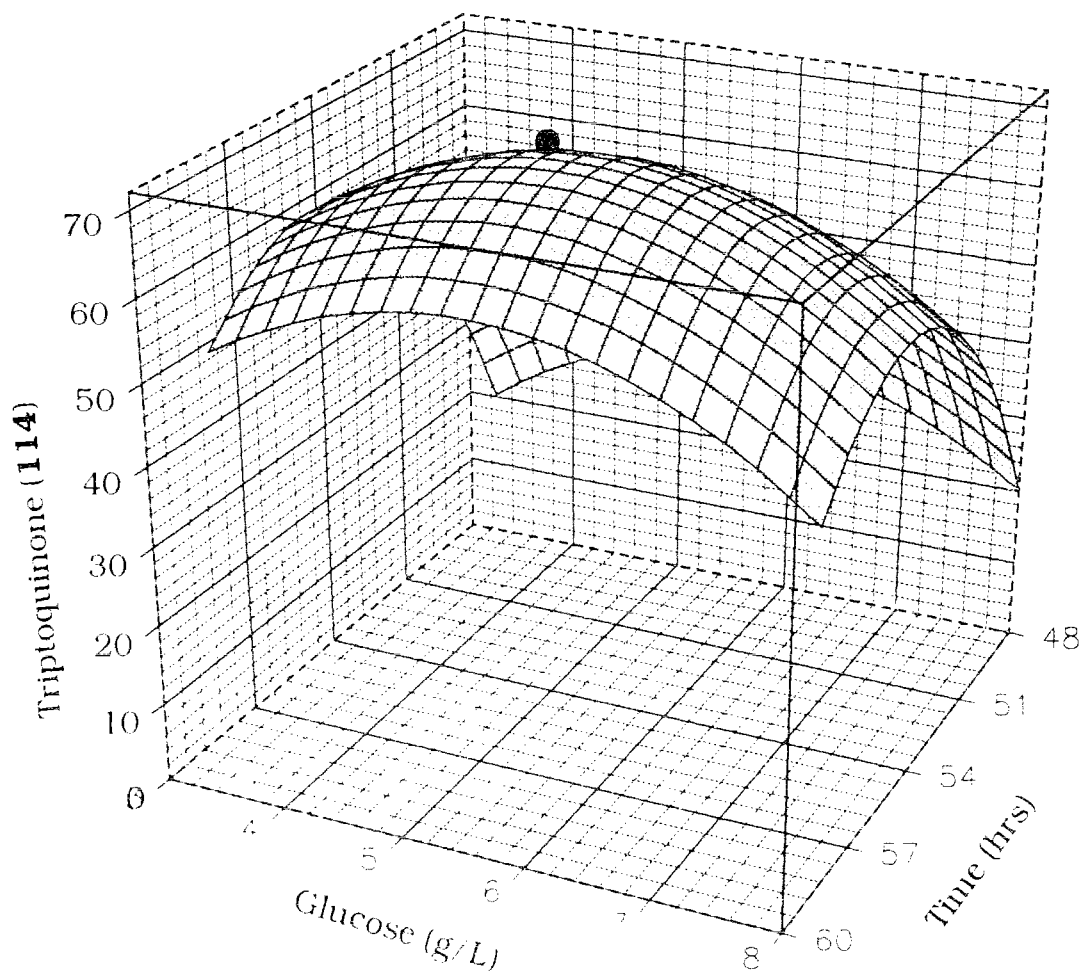
### Results from the Second Set of Experiments

The experimental data were analyzed and the detailed derivation of the result (equation 8) is shown in the Appendix.

$$\begin{aligned}
 Y_2 = & - 830.8 + 34.7*x_1 - 1.86*x_2 - 6.90*x_3 - 2.23*x_4 - 0.00504*x_1*x_2 - \\
 & 0.00351*x_1*x_3 + 0.000404*x_1*x_4 - 0.0234*x_2*x_3 - 0.00909*x_2*x_4 - \\
 & 0.0158*x_3*x_4 - 0.320*x_1^2 + 0.204*x_2^2 + 0.638*x_3^2 + 0.0381*x_4^2
 \end{aligned}$$

(8)

Figure 27. Influence of the Glucose Concentration and the Biotransformation Time on the Yield of Triptoquinone (114) at the Optimum Values of the Other Factors (Nutrient Broth and Malt Extract).



Legend:

Biotransformation time = 48.0 to 60.0 hours

Glucose = 3.0 to 8.0 g/L

Nutrient broth = 5.32 g/L

Malt extract = 32.7 g/L

Maximum yield of triptoquinone (114) ●

Table 12. Second Factorial Design Experiment Showing Selected Factors (Parameters) and Their Levels.

Run	Standardized levels				Actual levels				Medium composition
	Time	Glucose	Nutrient broth	Malt Extract	Time h	Glucose g/L	Nutrient broth g/L	Malt Extract g/L	
1	+1	+1	+1	+1	60	8.0	8.0	35	1
2	+1	+1	+1	-1	60	8.0	8.0	25	2
3	+1	+1	-1	+1	60	8.0	4.0	35	3
4	+1	+1	-1	-1	60	8.0	4.0	25	4
5	+1	-1	+1	+1	60	3.0	8.0	35	5
6	+1	-1	+1	-1	60	3.0	8.0	25	6
7	+1	-1	-1	+1	60	3.0	4.0	35	7
8	+1	-1	-1	-1	60	3.0	4.0	25	8
9	-1	+1	+1	+1	48	8.0	8.0	35	1
10	-1	+1	+1	-1	48	8.0	8.0	25	2
11	-1	+1	-1	+1	48	8.0	4.0	35	3
12	-1	+1	-1	-1	48	8.0	4.0	25	4
13	-1	-1	+1	+1	48	3.0	8.0	35	5
14	-1	-1	+1	-1	48	3.0	8.0	25	6
15	-1	-1	-1	+1	48	3.0	4.0	35	7
16	-1	-1	-1	-1	48	3.0	4.0	25	8
17	+1	0	0	0	60	5.5	6.0	30	9
18	-1	0	0	0	48	5.5	6.0	30	9
19	0	+1	0	0	54	8.0	6.0	30	10
20	0	-1	0	0	54	3.0	6.0	30	11
21	0	0	+1	0	54	5.5	8.0	30	12
22	0	0	-1	0	54	5.5	4.0	30	13
23	0	0	0	+1	54	5.5	6.0	35	14
24	0	0	0	-1	54	5.5	6.0	25	15
25	0	0	0	0	54	5.5	6.0	30	9

The influence of the glucose concentration within the studied range (3.0 - 8.0 g/L) and the biotransformation time (48 - 60 h) when nutrient broth and malt extract concentrations were held at their optimum values (5.32 g/L and 32.7 g/L respectively) on the yield of triptoquinone (**114**) is illustrated in Figure 27. With the second set of experiments it was confirmed that the glucose concentration and the biotransformation time were important factors for optimization of the yield of **114**.

This further optimization predicted the maximum yield (71.3%) of the desired product **114**. The maximum production of **114** could therefore be achieved by using the following medium composition (g/L) and biotransformation time:

- (i) glucose - 4.35 g
- (ii) nutrient broth - 5.32 g
- (iii) malt extract - 32.7 g
- (iv) biotransformation time - 54 h

#### **4.4 A Verification Experiment**

The final step was to verify that the predicted settings for optimal yield would result in an experimental yield close to the calculated value. Therefore the biotransformation of triptophenolide (**12**) was performed under the conditions indicated above. The experimental yield using the predicted optimal parameters was 70%. This result was very close to the yield interpolated from the data shown in Figure 27, that is, 71%. Thus from an initial yield of triptoquinone (**114**) of 35%, the first optimization increased the yield to 41% and the second to 70%.

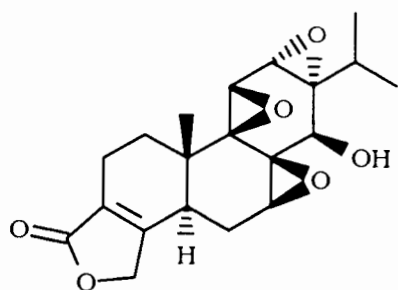
## 4.5 Conclusion

It was demonstrated that by utilization of factorial design experiment significant increase in the yield of a specific biotransformation product can be achieved. Here a modification of the individual parameters doubled the yield of triptoquinone (**114**) from 35% to 70%. It is interesting to note that the yield of 71% predicted from the factorial design has been confirmed by the actual experiment (70%).

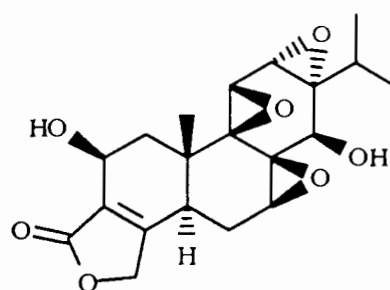
## CHAPTER V -- PHARMACOLOGICAL DATA ON ANTI-NEOPLASTIC ACTIVITY OF *T. WILFORDII* CONGENERS

A number of abietane diterpenes and their analogues (Figure 28), were submitted to the Arizona Cancer Institute, Tempe, Arizona, U.S.A., for evaluation as potential anti-neoplastic agents. The compounds, 12- $\beta$ -glucosyl isotriptophenolide (**112**), triptoquinone (**114**), triptophenolide (**12**) and butenolide **45** were obtained from these studies (Chapter II, III).

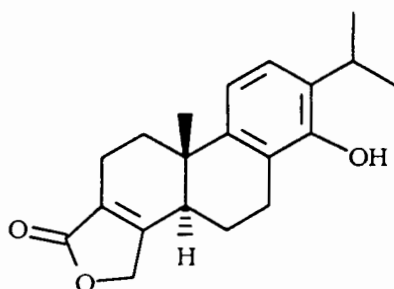
Figure 28. Compounds Tested for Potential Anti-neoplastic Activity.



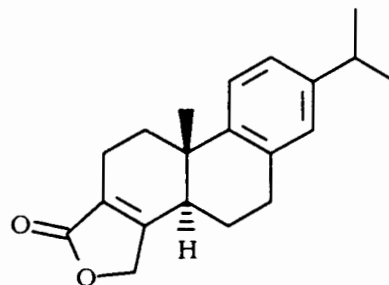
Triptolide (**2**)



Triptdiolide (**3**)



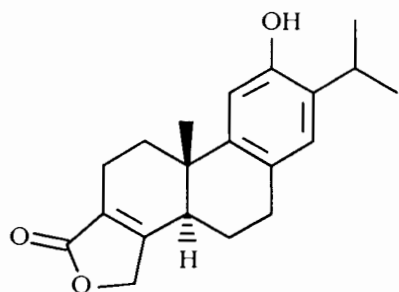
Triptophenolide (**12**)



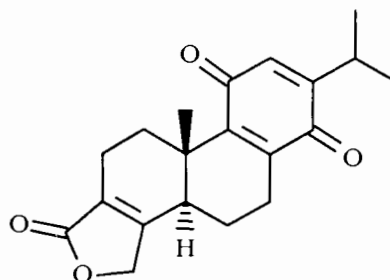
Butenolide **45**



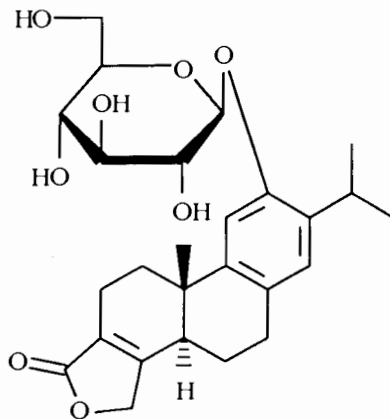
Figure 28. (Continued).



Isotriptophenolide (**86**)



Triptoquinone (**114**)



12-β-Glucosyl isotriptophenolide (**112**)

Triptolide (**2**) and triptiolide (**3**) were isolated from *T. wilfordii* cell cultures and isotriptophenolide (**86**) was prepared by synthesis (Group of Prof. Kutney, Dept. of Chemistry, UBC).

Evaluation of anti-neoplastic activity was performed in six human cancer cell lines. These cell lines have been selected from a larger number of lines available at the National Cancer Institute, National Institutes of Health, Bethesda, Maryland, USA. Selection was based on

their success in predicting potential anti-neoplastic efficacy of novel compounds.

The results obtained in the Murine P-388 lymphocytic leukaemia model are summarized in Table 13. The most potent compounds inhibiting the growth of murine lymphocytic leukaemia cells *in vitro* are triptolide (**2**) and triptidiolide (**3**).

Table 13. Evaluation of Compounds in the Murine P388 Lymphocytic Leukaemia System.

Compound	ED <sub>50</sub> (µg/mL)
Triptolide ( <b>2</b> )	< 0.01
Triptidiolide ( <b>3</b> )	0.0040
Triptophenolide ( <b>12</b> )	4.4
Butenolide ( <b>45</b> )	7.5
Isotriptophenolide ( <b>86</b> )	3.6
Glucosyl ITP ( <b>112</b> )	>10
Triptoquinone ( <b>114</b> )	2.4

Legend: P388 system grown in culture (specific culture conditions are not available).

ED<sub>50</sub> concentration of compound required to kill 50% of cells, µg/mL.

The remaining compounds, except for 12-glucosyl isotriptophenolide (**112**), are significantly active with ED<sub>50</sub> values less than 10 micrograms per mL. The glucosyl derivative **112** was actually less active than the parent compound (**86**).

The pharmacological data obtained from the evaluation of isolated diterpenes and their analogues in human cancer cell lines grown *in vitro* are shown in Table 14.

GI<sub>50</sub> values represent the concentration of a compound required for 50% growth inhibition. TGI (total growth inhibition) values give the concentration of compound required for 100% growth inhibition and LC<sub>50</sub> (50% cell kill) values give the concentration of compound required to kill 50% of all cells. All concentrations are in µg/mL culture. It is clear that significant activity is found in several of the compounds, particularly the triepoxides, triptolide (**2**) and triptodiolide (**3**), which are highly potent. The compounds **2** and **3** have revealed significant activity in human cancer cell lines grown *in vitro* as shown in Table 14. It should be noted that earlier studies by Kupchan and coworkers (Kupchan *et al.* 1972) had shown that **2** and **3** possessed cytotoxic activity *in vivo* against L-1210 and P-388 leukaemias in mice. Triptophenolide (**12**), butenolide **45**, isotriptophenolide (**46**) and quinone **114** have exhibited lower potency. Compound **112** with the glucosyl moiety has no inhibitory effect on these cell lines. It should be noted that butenolide **45**, which lacks hydroxyl or epoxide functionality in rings B and/or C is more potent than the ring C hydroxylated triptophenolide (**12**) and isotriptophenolide (**86**).

Table 14. Evaluation of Compounds for Activity in Human Cancer Cell

Lines *in vitro*.

GI <sub>50</sub> (50% growth inhibition; $\mu\text{g/mL}$ )						
Compound #	Ovarian <sup>a</sup> OVCAR-3 <sup>b</sup>	CNS <sup>a</sup> SF-295 <sup>b</sup>	Renal <sup>a</sup> A498 <sup>b</sup>	Lung-NSC <sup>a</sup> NCI-H460 <sup>b</sup>	Colon <sup>a</sup> KM20L2 <sup>b</sup>	Melanoma <sup>a</sup> SK-MEL-5 <sup>b</sup>
<b>2</b>	0.0013	0.0064	0.0040	<0.0010	0.00086	0.0014
<b>3</b>	0.0023	0.013	0.017	<0.0010	0.0013	0.0023
<b>12</b>	>10	7.1	3.9	3.4	2.6	3.9
<b>45</b>	4.5	3.7	3.5	2.5	1.7	3.1
<b>86</b>	5.6	7.3	5.1	3.5	4.3	3.3
<b>112</b>	>10	>10	>10	>10	>10	>10
<b>114</b>	3.7	>10	>10	7.9	5.3	3.8

TGI (total growth inhibition, $\mu\text{g/mL}$ )						
Compound #	Ovarian <sup>a</sup> OVCAR-3 <sup>b</sup>	CNS <sup>a</sup> SF-295 <sup>b</sup>	Renal <sup>a</sup> A498 <sup>b</sup>	Lung-NSC <sup>a</sup> NCI-H460 <sup>b</sup>	Colon <sup>a</sup> KM20L2 <sup>b</sup>	Melanoma <sup>a</sup> SK-MEL-5 <sup>b</sup>
<b>2</b>	0.65	>10	0.045	0.0019	2.8	0.011
<b>3</b>	0.0055	>10	0.069	0.0031	>10	0.025
<b>12</b>	>10	>10	>10	>10	>10	>10
<b>45</b>	>10	>10	>10	6.4	4.7	>10
<b>86</b>	>10	>10	>10	>10	>10	>10
<b>112</b>	>10	>10	>10	>10	>10	>10
<b>114</b>	>10	>10	>10	>10	>10	>10

LC <sub>50</sub> (50% cells killed, $\mu\text{g/mL}$ )						
Compound #	Ovarian <sup>a</sup> OVCAR-3 <sup>b</sup>	CNS <sup>a</sup> SF-295 <sup>b</sup>	Renal <sup>a</sup> A498 <sup>b</sup>	Lung-NSC <sup>a</sup> NCI-H460 <sup>b</sup>	Colon <sup>a</sup> KM20L2 <sup>b</sup>	Melanoma <sup>a</sup> SK-MEL-5 <sup>b</sup>
<b>2, 3, 12,</b> <b>45, 86,</b> <b>112, 114</b>	>10	>10	>10	>10	>10	>10

<sup>a</sup>Cell type

<sup>b</sup>Cell line

**Conclusion:** Triptolide (**2**) and triptdiolide (**3**), were potent growth inhibitors both in the P388 lymphocyte leukaemia system, as well as in the six human cancer cell lines grown *in vitro*. It is clear that the presence of epoxide functionality in ring B and/or C provided a significant increase in the antitumour activity when compared to the remaining compounds. Nevertheless, also the other compounds exhibited some activity against the selected tumour lines in micromolar quantities. Further pharmacological evaluation is necessary to determine the therapeutic index of these diterpene analogues in the inhibition of human tumours.

In addition, pharmacological screening of these agents for their ability to inhibit cell-mediated immune responses both *in vitro* and *in vivo* would indicate their use as immunosuppressive agents.

## CHAPTER VI -- SUMMARY AND OVERVIEW

Previous studies had shown that selected abietane diterpenes exhibited a considerable potential as a novel family of pharmacologically active compounds. Due to a lack of adequate quantities of such compounds possessing sufficient structural diversity, a basic understanding of structure - activity relationship was severely limited.

The objectives of the present study were directed toward the development of suitable diterpene analogues which, when subjected to pharmacological screening, could provide additional information concerning the above. The strategy involved an interdisciplinary program combining synthetic chemistry with microbiological methods, so as to provide the target molecules via efficient and versatile routes.

Selected diterpene analogues, butenolide **45**, isotriptophenolide (**86**) and triptophenolide (**12**) which were prepared via chemical synthesis were hydroxylated and/or glucosylated to novel products by specific filamentous fungi: *Syncephalastrum racemosum* (UBC#60), *Aspergillus fumigatus* (ATCC#13073), *Cunninghamella echinulata* (ATCC#9244) and *C. elegans* (ATCC#20230).

The substrate **45** was obtained from readily available dehydroabietic acid (**42**) in gram quantities by the present author and the synthetic sequences are outlined in Chapter II. Although this route has been already established by previous workers, large scale preparation of this compound helped to improve significantly the key steps of the synthetic pathway. The parent compounds isotriptophenolide (**86**) and triptophenolide (**12**) were also obtained via

synthesis from the intermediate butenolide **45** in sufficient quantities for the biotransformation experiments.

Butenolide **45**, which possesses the abietane skeleton but without functionality in ring C, was incubated with a series of yeasts and fungi in the hope of achieving biotransformations to novel products with oxygen functionality in the B and/or C rings.

The results showed that yeast strains were unable to biotransform the synthetic analogue **45** even though many experiments with a variety of media were conducted. Although the filamentous fungi selected for these biotransformations had shown, in previous published studies, an ability to hydroxylate aromatic compounds, no evidence of such hydroxylation was observed with **45**. In general, butenolide **45** was attacked mainly at the "activated" (benzylic) site in ring B to afford 7-hydroxy and 7-keto analogues as major metabolites and, to a lesser extent, hydroxylation in the isopropyl side chain. In order to assess the extent of biotransformation of **45** by the fungus *S. racemosum*, large scale experiments were conducted. The crude mixtures obtained from these experiments were subjected to chromatographic separations and the products were identified by spectroscopic analysis. Parallel experiments were run in order to determine the time course of metabolite(s) formation and the influence of inhibitors on the biotransformation process. These studies indicated that different hydroxylases mediated the 7 $\beta$ - and 15-hydroxylations.

The results of this study have been recently published (Milanova & Moore 1993).

The next series of experiments which were undertaken with the butenolide **45** as a substrate employed the fungi: *A. fumigatus* and *C.*

*elegans*. Exclusive hydroxylations in ring B, and to some extent in the isopropyl side chain, of **45** were observed. In contrast, *A. fumigatus* provided essentially one major product (7 $\beta$ -hydroxybutenolide, **101**) in 90% yield while *C. elegans* produced a complex mixture of 9 products, of which 7 were novel compounds, in yields varying from 2 to 14%. Although this complex mixture created difficulties in the steps of the purification, all the products were isolated and characterized. Studies on the influence of pH, culture age and substrate concentration were performed.

These results were subject of a recent publication (Milanova *et al.* 1994).

Since the selected fungi were incapable of oxidizing the aromatic ring of **45**, studies with the synthetic analogues **86** and **12** were undertaken. These ring C "activated" analogues, isotriptophenolide (**86**), which possessed a C12-hydroxyl function and the isomeric C14-hydroxyl compound, triptophenolide (**12**), afforded different types of enzyme - catalyzed bioconversions.

The fungus *C. echinulata*, as well as *C. elegans*, biotransformed isotriptophenolide (**86**) to afford the C12  $\beta$ -glucosyl analogue **112** in 80% yield without evidence of aromatic ring hydroxylation. In contrast, *C. elegans* oxidized the C14-hydroxy isomer, triptophenolide (**12**), at the reactive C11 position of the aromatic ring to provide the 11,14-quinone **114** as a major metabolite. Glucosylation at C14 was also observed and the 14- $\beta$ -glucosyl triptophenolide (**116**) was obtained as a minor product. The metabolite, 5 $\alpha$ ,14-dihydroxytriptophenolide (**115**) with a hydroxyl group at the junction of the A and B rings of the triptophenolide skeleton was also obtained as a minor product.



The results from these biotransformations were presented in a recent publication (Milanova *et al.* 1995, in press).

Some experiments were performed with cells immobilized in polyurethane foam. Although the results were only monitored by TLC, the biotransformation experiments with entrapped mycelia repeatedly confirmed the ability of this fungus to convert the substrate **12** to quinone **114**, 5 $\alpha$ ,14-dihydroxytryptophenolide (**115**) and 14- $\beta$ -glucosyl tryptophenolide (**116**). Enzymatic activity responsible for this bioconversion remained apparently stable for over 30 days.

Since the quinone **114** represented the only example of aromatic ring oxidation in the biotransformation of tryptophenolide (**12**) by the fungus *C. elegans*, it was essential to optimize the composition of the growth medium of *C. elegans* and evaluate the biotransformation time in order to maximize the yield of this important product. The excretion of this compound into the broth of the culture provided an excellent opportunity for optimization experiments. Initial studies allowed isolation of the 11,14-quinone **114** in 35% yield but subsequent optimization of fermentation conditions via a factorial design experiment provided this compound in 70% yield.

The quinone **114** is an attractive intermediate as a potentially active compound since a closely related structure, triptoquinone A (**26**), was shown to inhibit the production of interleukin IL-1 (Takaishi *et al.* 1992a, b; Shishido *et al.* 1993). Furthermore, **114** could also serve as a substrate for enzyme - catalyzed and/or chemical epoxidations to afford a series of novel diterpene epoxides structurally related to the active diterpene triepoxides, triptolide (**2**) and triptiolide (**3**). Such novel analogues may possess interesting pharmacological activities.

Finally, several of the compounds obtained in this study were screened for antineoplastic activity. The pharmacological data have shown that the highly oxygenated triptolide (**2**) and triptidiolide (**3**) systems possessed cytotoxic activity in the P388 lymphocytic leukaemia as well as in six human cancer cell lines grown *in vitro*. Although, epoxide functionality in rings B and/or C is preferred for enhancing cytotoxicity, some of the other diterpene analogues did exhibit activity, although to a much lesser extent, against the selected tumour lines. For example, butenolide **45** which lacks hydroxyl or epoxide functionality in rings B and/or C, is a better cell growth inhibitor than triptophenolide (**12**) and isotriptophenolide (**86**). It is worthy to note that compound **112**, with a C12- $\beta$ -glucosyl moiety, has no inhibitory effect in the cultures evaluated.

Further pharmacological studies are required in order to assess these diterpene analogues for their potential as immunosuppressive agents.

## CHAPTER VII - EXPERIMENTAL PROCEDURES

### 7.1 Synthesis of Diterpene Analogues

#### 7.1.1 General Experimental Procedures

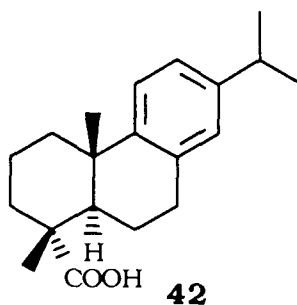
All experiments involving moisture-sensitive reagents were carried out under a pressure of nitrogen or argon gas. Solvents were reagent grade except that technical grade ether, methylene chloride, and ethyl acetate were used for extractions in most instances. Anhydrous magnesium or sodium sulphate were used to dry organic solutions prior to solvent removal.

Tetrahydrofuran, ether, benzene, methylene chloride and toluene were freshly distilled from sodium and benzophenone ketal under argon prior to use if strictly anhydrous solvents were required; otherwise, reagent grade was used. Column chromatography was carried out using Merck silica gel 60, 230-400 mesh, while analytical chromatography was performed using Merck pre-coated silica gel 60 F<sub>254</sub> TLC plates. All solvents for column chromatography were reagent grade and received no additional purification or drying prior to use. Synthetic samples were visualized on analytical TLC plates by UV and by spraying with a 5% solution of ammonium molybdate in 10% sulphuric acid, followed by heating at 125° C until blue spots developed. In some instances, a 5% solution of anisaldehyde in isopropanol was used for spraying, followed by heating at 125° C for approximately 10 min. <sup>1</sup>H-NMR spectra were run in CDCl<sub>3</sub> at 400 MHz using a Bruker WH 400 spectrometer. Tetramethylsilane was used as the internal standard and all peaks were

recorded in ppm ( $\delta$ ) relative to TMS ( $\delta$  0.00 ppm). The  $^{13}\text{C}$ -NMR spectra were recorded on Bruker AE-20 or Varian XL-300 spectrometers and the chemical shifts were reported on the delta ( $\delta$ ) scale in ppm relative to TMS.

Low resolution mass spectra (MS) were recorded using Kratos MS 50 and MS 80 mass spectrometers. High resolution mass spectra (HRMS) were run on a Kratos MS 50 mass spectrometer. The IR spectra were recorded on a Perkin Elmer 710B infrared spectrophotometer in  $\text{CHCl}_3$  (using NaCl cells of 0.1 mm path length) or as a thin film (using NaCl plates). The UV were recorded on a Unicam SP800 spectrometer using quartz cells of 1 cm path length. Melting points were determined using a Kofler block melting point apparatus and are uncorrected.

### 7.1.2 Purification of Dehydroabietic Acid (42)



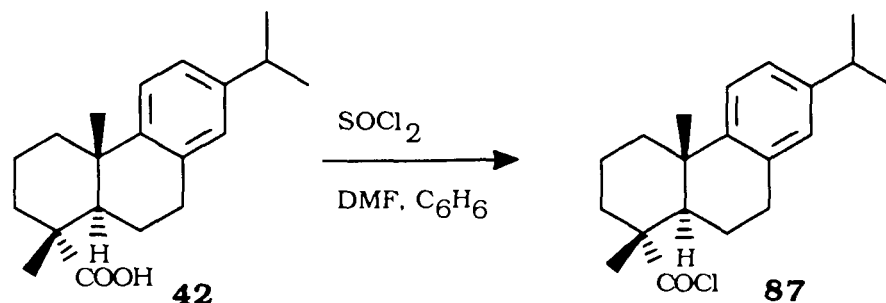
Technical grade dehydroabietic acid (DHA) (Pfaltz and Bauer, Inc. 534.7 g) was dissolved in warm ethanol (840 mL) in a 6.0 L capacity liquid-liquid extractor. Ethanolamine (84 mL) and water (840 mL) were added while stirring, and the resulting mixture extracted continuously with petroleum ether for 20 h, while being kept at 55-60 $^{\circ}$  C. The resulting aqueous solution, thus freed of neutral material (organic phase)

by separatory funnel, was heated at 65° C for 15-20 min to drive out any dissolved petroleum ether. The aqueous solution was left to cool down at room temperature for 10-15 min. Cooling this solution to 0-5° C overnight, resulted in a semi-solid mass, which was broken up manually. Filtration provided the ethanolamine salt of dehydroabietic acid, which was stirred with 50% aqueous ethanol (330 mL) at 4° C and vacuum filtered. The moist salt was dissolved in hot ethanol (750 mL), acetic acid (84 mL) was added, and water (400 mL) was gradually added to the boiling solution until the cloud point was reached. The hot solution was filtered, and cooled to room temperature. The crystallized acid was isolated by filtration, rinsed with 50% aqueous ethanol (170 mL), and air-dried to provide 155.9 g of dehydroabietic acid (**42**), 89% pure by GC analysis with mp of 160-162° C.

### 7.1.3 Synthesis of 18-Norabieta-4(19),8,11,13-tetraene (**91**) (Exo-olefin)

Note: In this synthesis, the intermediates **87**, **117**, **88**, **89** and **90** were not purified but converted directly in sequence to exo-olefin **91**. The latter was then vigorously purified and characterized.

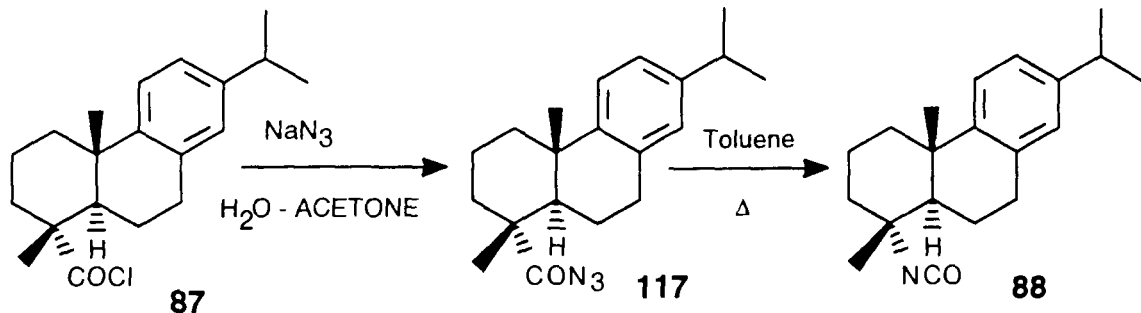
#### Acid Chloride **87**



Dehydroabietic acid (DHA) ( $C_{20}H_{28}O_2$ ) (**42**) (70.0 g, 0.233 mol) was dissolved in dry benzene (545 mL). Thionyl chloride (97%, 20.3 mL, 0.280 mol, 1.2 eq) was added to the reaction mixture. Dry dimethyl formamide (0.78 mL) was added dropwise and the solution was stirred for 1 h at room temperature.

After this time, the mixture was warmed to 68-74 $^{\circ}$  C and this range of temperature was maintained for 30 min. The solution was refluxed for 15 min, then cooled to room temperature and rotary evaporated *in vacuo* to dryness. The crude acid chloride **87** (79.27 g) was obtained as a dark thick oil [IR (neat)  $\nu_{max}$ : 1786  $cm^{-1}$ ].

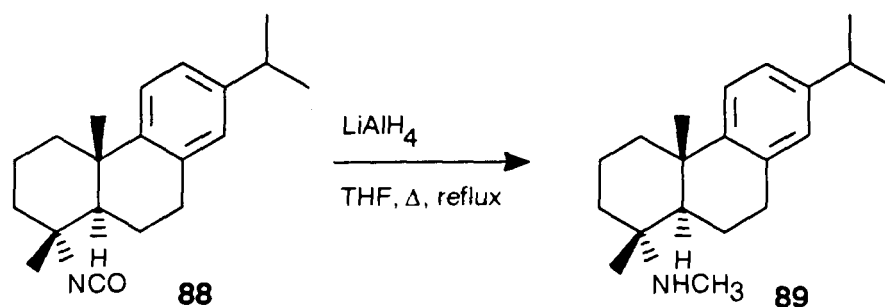
### Isocyanate **88**



The crude acid chloride **87** (79.27 g, 0.249 mol) was dissolved in reagent grade acetone (487 mL). The solution was cooled to -5-0 $^{\circ}$  C in a methanol-ice bath. Sodium azide (19.39 g, 0.298 mol, 1.2 eq) was dissolved in water (65 mL) and was added dropwise to the reaction mixture with vigorous stirring. After the addition, the mixture was stirred for 5-10 min at -5-0 $^{\circ}$  C. Toluene (162 mL) was added at room temperature, and the organic layer decanted, dried over anhydrous

sodium sulphate and the remaining acetone was removed by rotary evaporation to a volume of 190 mL. The solution of acyl azide **117** [IR  $\nu_{\text{max}}$  toluene: 2120 (azide), 1695 (carbonyl)  $\text{cm}^{-1}$ ] was brought to 490 mL with additional toluene and was heated slowly to reflux. During this time, the condenser was equipped with a trap of calcium chloride. After refluxing for 1 h, with continual IR monitoring of samples of the reaction mixture, the process was stopped. The solvent was then removed *in vacuo*. The crude isocyanate **88** (73.27 g) was obtained as a dark thick oil [IR (neat)  $\nu_{\text{max}}$ : 2250  $\text{cm}^{-1}$ ].

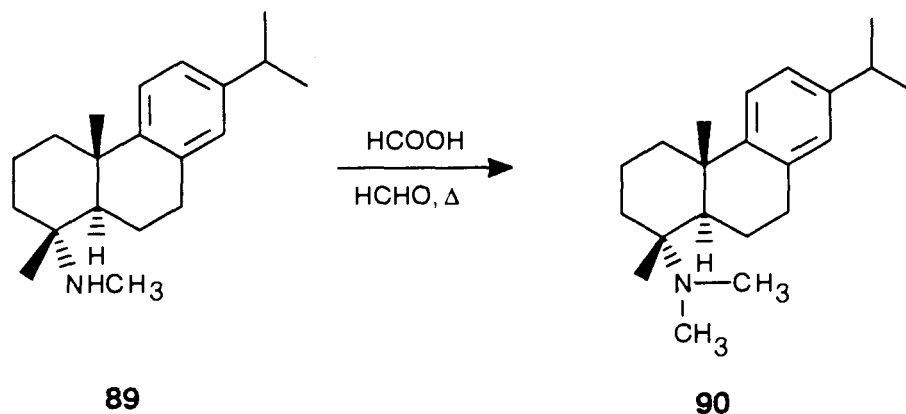
### Monomethylamine **89**



Lithium aluminum hydride (LiAlH<sub>4</sub>) (11.22 g, 0.296 mol, 1.2 eq) was dissolved in anhydrous tetrahydrofuran (THF) (570 mL) under a light stream of argon. The solution was then cooled to -5.0° C in a methanol-ice bath. The crude isocyanate **88** (73.28 g, 0.246 mol, 1.0 eq) was dissolved in anhydrous THF (325 mL) and was transferred into a dry addition funnel by using argon pressure. It was added dropwise to the suspension of LiAlH<sub>4</sub> for 30 min at -5.0° C. The ice-methanol bath was removed and the stirred reaction mixture was allowed to reach room temperature and was kept for 1 h. The reaction mixture was then heated

to 66° C and was refluxed with stirring under argon for 22 h. After this time, passage of argon was stopped and the mixture was cooled to room temperature. Successive dropwise additions of reagent grade acetone (16 mL), water (11 mL), 15% aqueous sodium hydroxide (11 mL), and more water (32 mL) produced a thick white suspension which was filtered through a porous glass funnel (packed with Celite-545) and triturated with hot THF (325 mL). The combined organic solutions were rotary evaporated to dryness. The residue was dissolved in diethyl ether (325 mL), dried over anhydrous sodium sulphate and evaporated *in vacuo* to form the crude monomethyl amine **89** (63.97 g) as a thick yellow syrup [IR (neat)  $\nu_{\text{max}}$ : 3300  $\text{cm}^{-1}$ ].

### Dimethylamine 90

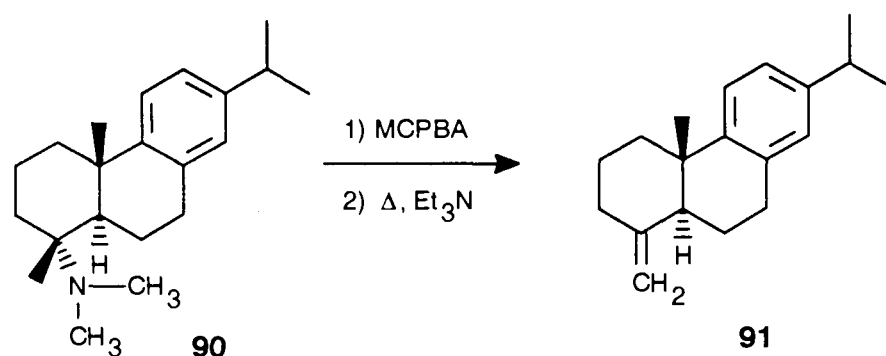


The crude monomethyl amine **89** (63.97 g, 0.224 mol) was dissolved in reagent grade formic acid (172 mL) under a light stream of argon. Aqueous formaldehyde (37%, 86 mL) was added dropwise to the reaction mixture. (The reaction is slightly exothermic.) The solution was then heated to 115-120° C, gently refluxed for 3 h, cooled to room temperature, and the solvents were removed *in vacuo* at 70° C. The



resulting tarry mass was dissolved in anhydrous diethyl ether (527 mL) and a solution of NaOH (4 N) was added dropwise to complete dissolution. The organic layer was separated, dried over anhydrous magnesium sulphate, filtered, and evaporated to dryness. The crude dimethylamine **90** (60.92 g) was obtained as a golden syrup.

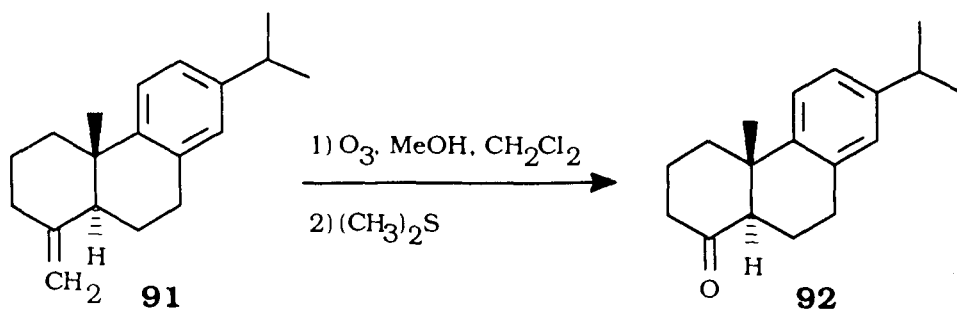
### Exo-olefin **91**



The crude dimethylamine **90** (60.92 g, 0.203 mol) was dissolved in reagent grade chloroform (1220 mL). The solution was cooled to -40° C in a dry-ice acetone-acetonitrile bath and reagent grade *m*-chloroperbenzoic acid (MCPBA) (60%, 72.65 g, 0.305 mol, 1.5 eq) was added by portions over a 20 min period. After the addition had been completed, the mixture was stirred for 30 min at -40° C. Triethylamine (12.2 mL) was added dropwise and the mixture was warmed to room temperature and then refluxed at 61° C for 1 h. The reaction was examined by thin layer chromatography (TLC) (silica gel 60 F<sub>254</sub>, mobile phase: hexanes). Compound **91** had an R<sub>f</sub> value of 0.39. The reaction mixture was cooled to room temperature and the solvent removed *in vacuo*. The residue was taken up in diethyl ether (800 mL), washed with 10% sulfuric acid (800 mL), 10% potassium carbonate (2 x 800 mL) and

brine (800 mL). The organic layer was dried over anhydrous magnesium sulphate, filtered, and rotary evaporated to afford crude *exo*-olefin (49.73 g). The crude residue was dissolved in hexanes (5 mL) and was purified by column chromatography on silica gel 60 (230-400 mesh) (600 g) eluting with hexanes, followed by hexanes:EtOAc (96:4). Pure *exo*-olefin **91** (30.96 g, 60%) was obtained as a colourless oil. IR (neat)  $\nu_{\text{max}}$ ; 3050, 2925, 1650  $\text{cm}^{-1}$ ;  $^1\text{H}$  NMR ( $\text{CDCl}_3$ )  $\delta$ : 1.01 (3H, s,  $\text{CH}_3$ -20), 1.20 (6H, d,  $J = 6$  Hz,  $\text{CH}_3$ -16 and 17), 1.51-2.92 (m, aliphatic H), 4.60 (1H, d,  $J = 2$  Hz, H-4), 4.85 (1H, d,  $J = 2$  Hz, H-4), 6.90 (1H, brs, H-14), 7.01 (1H, brd, H-12), 7.20 (1H, d, H-11); MS [ $m/z$ ]: 254 ( $\text{M}^+$ ) (base peak), 239, 211, 196; HRMS calcd. for  $\text{C}_{19}\text{H}_{26}$ : 254.2034; Found: 254.2030.

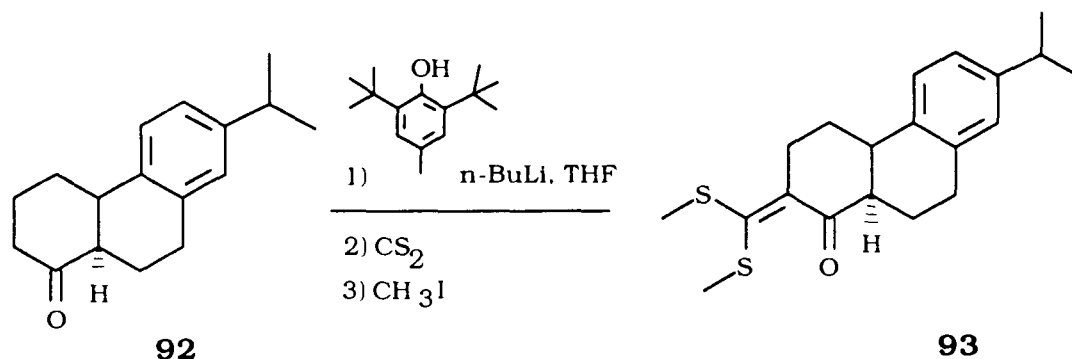
#### 7.1.4 Synthesis of 18,19-Dinorabieta-8,11,13-trien-4-one (**92**) (Ketone)



Pure *exo*-olefin **91** (30.96 g, 0.122 mol) was dissolved in methanol-methylene chloride (5:1, 1205 mL) and was divided into 3 portions of 468 mL in each flask. The solutions were cooled to  $-78^\circ\text{C}$  in a dry ice-acetone bath. Ozone was passed into the stirred solutions at  $-78^\circ\text{C}$  until they turned a pale blue colour (1 h per flask at 2.2 psi of oxygen, 90 volts, and flow of 0.015 L/min). The reaction was monitored every 15

min by TLC (silica gel 60 F<sub>254</sub>, mobile phase: hexane:EtOAc 9:1). Ketone **92** had an R<sub>f</sub> value of 0.11. The reaction mixtures were stirred for a further 30 min at -70° C without the ozone stream. Dimethyl sulphide (3.7 mL, 0.050 mol) was added to each flask and the reaction mixtures were stirred at room temperature for 20 h. Analytical TLC (mobile phase: hexanes:EtOAc, 9:1) showed that all the reactions were identical, and they were combined at this point, and the solvent removed *in vacuo*. The residue was dissolved in hexanes:diethyl ether 2:1 (1072 mL) and washed with water (3 x 128 mL) and brine (128 mL). The aqueous layer was extracted with diethyl ether (202 mL) and the combined organic layers were dried over anhydrous magnesium sulphate, filtered, and rotary evaporated to afford the crude ketene (31.28 g) as a light yellow oil. The crude oil was separated by flash column chromatography on silica gel 60 (230-400 mesh) using hexanes:EtOAc, 9:1. Pure ketone **92** (25.81 g, 82%) was obtained as a colourless oil which crystallized at room temperature to a snow white powder. mp 40-42° C; IR  $\nu_{\max}$  (CHCl<sub>3</sub>): 2950, 1710 cm<sup>-1</sup>; <sup>1</sup>H NMR (CDCl<sub>3</sub>)  $\delta$ : 1.05 (3H, s, CH<sub>3</sub>-20), 1.25 (6H, d, CH<sub>3</sub>-16 and 17), 1.76-2.95 (m, aliphatic), 6.95 (1H, brs, H-14), 7.04 (1H, brd, H-12), 7.20 (1H, d, H-11); MS [m/z]: 256 (M<sup>+</sup>) base peak, 241; HRMS calcd. for C<sub>18</sub>H<sub>24</sub>O: 256.1827; Found: 256.1826.

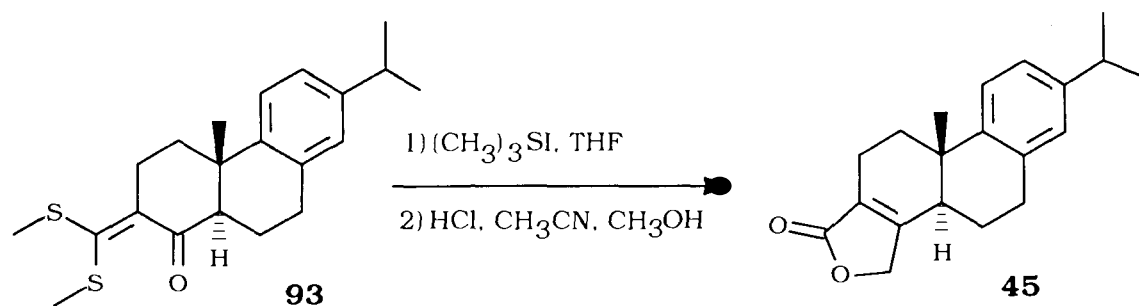
### 7.1.5 Synthesis of 3-Dimethylthiomethylene-18,19-dinorabieta-8,11,13-trien-4-one (**93**) (Ketene Thioketal)



Solution of *n*-butyl lithium (*n*-BuLi) (1.6 M in hexanes, 165 mL, 0.264 mol) was added dropwise to a stirred solution of 4-methyl-2,6-di-*t*-butylphenol (58.1 g, 0.264 mol, 2.6 eq) in anhydrous THF (1370 mL) at 0-5° C under argon. Carbon disulphide (58.8 mL, 0.872 mol) was added, and the resulting red solution was allowed to warm to room temperature. A solution of the ketone **92** (25.81 g, 0.101 mol) in dry THF (200 mL) was added dropwise to the reaction mixture. The flask containing the ketone solution was washed with anhydrous THF (73 mL) and was also added to the reaction flask. Stirring was continued at room temperature for 48 h. Completion of the reaction was examined by TLC (mobile phase: hexanes:EtOAc, 9:1, developed with anisaldehyde spray reagent). The ketene thioketal **93** had an *R<sub>f</sub>* value of 0.27. Methyl iodide (35.4 mL, 0.568 mol, 5.6 eq) was then added dropwise and the reaction mixture was stirred at room temperature for a further 20 h. During this time, the reaction flask was wrapped in aluminum foil to minimize photo-oxidation. The solvent was evaporated and the residue dissolved in

diethyl ether (2000 mL), washed with water (3 x 1000 mL) and brine (1000 mL) and the organic layer was dried over anhydrous magnesium sulphate, filtered, and concentrated *in vacuo*. The crude red oil of the ketene thioketal **93** (109.32 g) was purified by flash column chromatography (9 cm diameter), using silica gel 60 (230-400 mesh) (800 g) and hexanes as an eluent to recover the phenol, followed by hexanes:EtOAc (9:1) to yield pure ketene thioketal **93** as a light orange oil which rapidly solidified into a crystal-like mass upon cooling (34.52 g, 95%). mp 68-70° C; IR  $\nu_{\text{max}}$  (CHCl<sub>3</sub>): 2956, 1714, 1680 cm<sup>-1</sup>; <sup>1</sup>H NMR (CDCl<sub>3</sub>)  $\delta$ : 1.10 (3H, s, CH<sub>3</sub>-20), 1.21 (6H, d, CH<sub>3</sub>-16 and 17), 1.76-3.40 (m, aliphatic, H), 2.38 (3H, s, CH<sub>3</sub>-S), 2.40 (3H, s, CH<sub>3</sub>-S), 6.95 (1H, brs, H-14), 7.02 (1H, brd, H-12), 7.20 (1H, d, H-11); MS [m/z]: 360 (M<sup>+</sup>), 345, 313, 256, 253, 241, 220, 213, 141; HRMS calcd. for C<sub>21</sub>H<sub>28</sub>OS<sub>2</sub>: 360.1583; Found: 360.1583.

### 7.1.6 Synthesis of 19-Hydroxy-18 (4->3) abeo-abieta-3,8,11,12-tetraen-18-oic acid Lactone (**45**) (Butenolide)



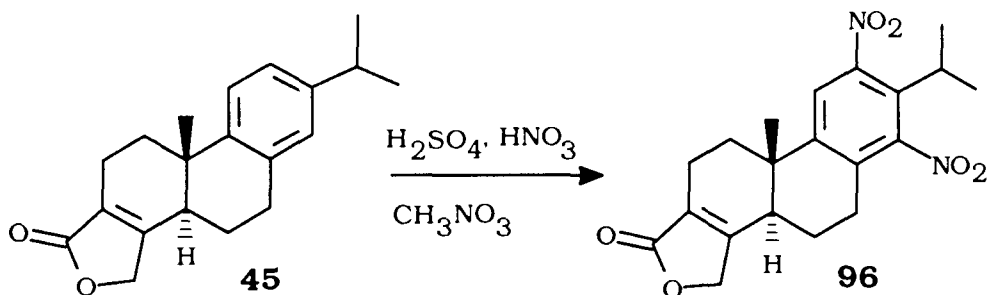
Solution of n-butyl lithium (1.6M in hexanes, 77.8 mL, 0.124 mol, 1.3 eq) was added dropwise to a stirred suspension of trimethylsulphonium iodide (29.30 g, 0.144 mol, 1.5 eq) in dry THF (600

mL) at  $-60^{\circ}\text{C}$  under argon. The reaction mixture was allowed to warm to  $-10^{\circ}\text{C}$  and stirred at this temperature for 30 min. The reaction mixture was cooled to  $-60^{\circ}\text{C}$ . The ketene thioketal **93** (34.52 g, 0.096 mol) was dissolved in dry THF (180 mL) and under argon pressure the solution was transferred into an addition funnel. It was then added dropwise to the reaction mixture at  $-60^{\circ}\text{C}$  and under an argon stream. The flask that contained the ketene thioketal was washed with anhydrous THF (10 mL) and added to the reaction flask. Some precipitation was noted at this time. The colour of the reaction mixture had now changed from yellow-green to yellow-brown. The mixture was stirred at  $-60^{\circ}\text{C}$  for 30 min, and then allowed to reach room temperature (in approximately 1 h). It was noted that the mixture became very dense in the temperature range of  $-10$ – $5^{\circ}\text{C}$ . After stirring at room temperature for 2 h, TLC monitoring (mobile phase: hexanes:EtOAc, 9:1) showed no remaining starting material. The TLC plates were developed with anisaldehyde spray reagent and sulphuric acid. The solvent was evaporated and the residue was dissolved in diethyl ether (188 mL) and again evaporated to dryness. The residue was dissolved in diethyl ether (2.4 L) and washed with water (2 x 315 mL). Removal of the solvent *in vacuo* left a residue which was dissolved in acetonitrile (221 mL) and methanol (611 mL), and the solution was cooled in an ice-bath to  $-5$ – $5^{\circ}\text{C}$ . Concentrated HCl (75 mL) was added while stirring and the cooling bath was removed immediately after the addition. The reaction mixture was stirred at room temperature for 40 h, and the methanol and acetonitrile were evaporated. The residual suspension was extracted with diethyl ether (2.4 L) and the organic solution was washed with saturated sodium bicarbonate (3 x 315 mL) and water (80 mL). The water phase was extracted with ethyl

acetate (2 x 500 mL). The organic layers were combined, dried over magnesium sulphate, filtered, and rotary evaporated to afford an orange-brown residue of crude lactone (**45**) (24.35 g). The purification of lactone **45** was done by crystallization with hexanes:EtOAc (1:1), and by column chromatography, using silica gel 60 (230-400 mesh) and hexane:EtOAc, 4:1 as eluent. Pure lactone **45** (14.33 g, 51% overall from **93** and 20% overall yield), from the starting dehydroabietic acid (**42**) was obtained as a clear oil which slowly solidified to give a white solid powder. mp 97-99° C; IR  $\nu_{\text{max}}$  (CHCl<sub>3</sub>): 2959, 1757, 1678 cm<sup>-1</sup>; UV  $\lambda_{\text{max}}$  (MeOH) (log  $\epsilon$ ): 221 (4.00) nm; <sup>1</sup>H NMR (CDCl<sub>3</sub>)  $\delta$ : 1.05 (3, s, CH<sub>3</sub>-20), 1.30 (6H, d, CH<sub>3</sub>-16 and 17), 1.75-2.60 (m, aliphatic), 2.70 (1H, m, H-5), 2.86 (1H, septet, H-15), 3.05 (2H, m, H-7), 4.82 (2H, m, H-19), 6.98 (1H, brs, H-14), 7.05 (1H, brd, H-12), 7.28 (1H, d, H-11); MS [m/z]: 296 (M<sup>+</sup>) (base peak), 281; HRMS calcd. for C<sub>20</sub>H<sub>24</sub>O<sub>2</sub>: 296.1776; Found: 296.1775.

### 7.1.7 Synthesis of Triptophenolide (**12**) from Lactone **45**

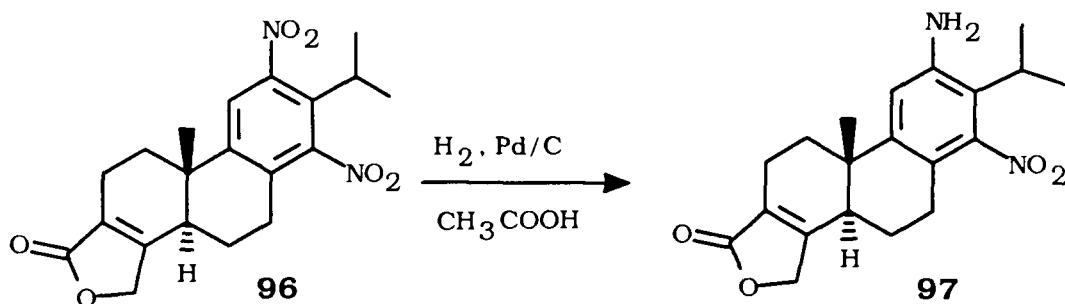
#### Synthesis of 19-Hydroxy-12,14-dinitro-18 (4->3) *abeo*-abieta-3,8,11,13-tetraen-18-oic Acid Lactone (**96**)



Concentrated  $\text{H}_2\text{SO}_4$  (30.6 mL) was mixed with concentrated (fuming)  $\text{HNO}_3$  (22 mL) at  $0^\circ\text{C}$ . The mixture was stirred for 10 min at  $-5-0^\circ\text{C}$ , using an ice-water bath. A solution of lactone **45** (6.0 g, 0.020 mol) in anhydrous nitromethane (24 mL) was added dropwise over a period of 17 min while stirring at  $-5-0^\circ\text{C}$ , followed by addition of the flask washings (nitromethane, 5 mL). The resulting light orange mixture was stirred at the bath temperature for 1.5 h, then poured into a beaker of crushed ice (180 mL). The reaction flask was washed with EtOAc (2 x 30 mL) and the washings were also added to the beaker. After all the ice had melted, the suspension was extracted with EtOAc (3 x 180 mL), and then the combined organic layers were washed with saturated  $\text{NaHCO}_3$  (2 x 120 mL), brine (120 mL), and dried over anhydrous magnesium sulphate and filtered. Removal of the solvent *in vacuo* gave a crude product (9.25 g). The crude mixture was purified by flash column chromatography (silica gel 60, 230-400 mesh) with hexanes:EtOAc (7:3) as an eluent. The purification was monitored by TLC (mobile phase: hexanes:EtOAc, 7:3). Pure **96** (6.98 g, 90% yield) was obtained as a pale yellow powder with  $R_f$  value of 0.25 on TLC. mp  $110-112^\circ\text{C}$ ; UV  $\lambda_{\text{max}}$  (MeOH) ( $\log \epsilon$ ): 214 (4.42) nm;  $^1\text{H NMR}$  ( $\text{CDCl}_3$ )  $\delta$ : 1.05 (3H, s,  $\text{CH}_3$ -20), 1.30 (6H, d,  $\text{CH}_3$ -16 and 17), 1.71-2.55 (m, aliphatic), 2.70 (1H, brd,  $J = 13$  Hz, H-5), 2.89 (2H, m, H-7), 3.01 (1H, septet,  $J = 7$  Hz, H-15), 4.72 (2H, m, H-19), 7.62 (1H, s, H-11); MS [ $m/z$ ]: 386 ( $\text{M}^+$ ), 369 (base peak), 356, 327, 309, 296, 280, 109; HRMS calcd. for  $\text{C}_{20}\text{H}_{22}\text{N}_2\text{O}_6$ : 386.1478; Found: 386.1476.



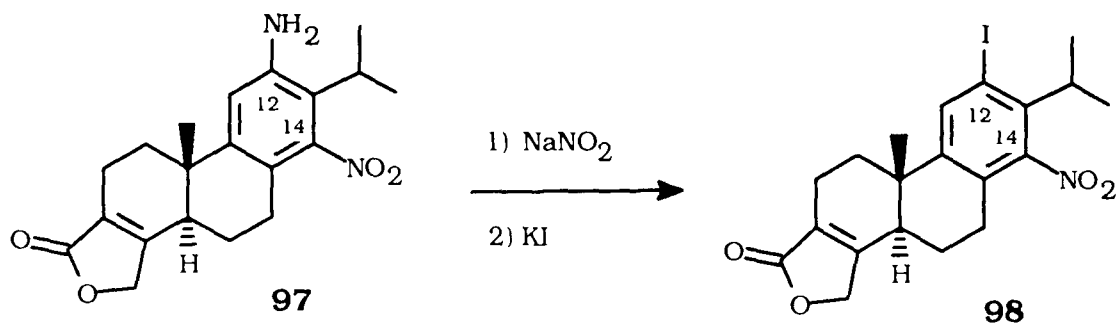
**Synthesis of 12-Amino-19-hydroxy-14-nitro-18 (4->3) abeo-abieta-3,8,11,13-tetraen-18-oic Acid Lactone (97)**



Into a solution of **96** (6.98 g, 0.018 mol) in glacial acetic acid (91 mL) was placed 10% Pd/C (0.325 g) and the mixture was stirred under hydrogen (atmospheric pressure) for 22 h at room temperature. The reaction was examined by TLC (mobile phase: hexane:EtOAc (1:1)) (product  $R_f$  value of 0.24). Ethyl acetate (79 mL) was added to dissolve the yellow solid product and the catalyst was removed by filtration through Celite 545. The Celite was washed thoroughly with EtOAc (250 mL) and the combined filtrate was concentrated *in vacuo*. The crude product (7.60 g) was recrystallized in EtOAc to afford **97** as yellow crystals (3.75 g). The remaining mother liquor was chromatographed on a column using silica gel (230-400 mesh) and hexane:EtOAc (6:4) to give a second crop of **97** (2.45 g), bringing the total amount to 5.6 g (87% yield). Pure **97** was obtained as yellow needles. mp 226-228° C; UV  $\lambda_{\text{max}}$  (MeOH) (log  $\epsilon$ ): 210, 296 nm; IR  $\nu_{\text{max}}$  ( $\text{CHCl}_3$ ): 3500, 3400, 2975, 1750, 1670, 1620, 1520, 1360  $\text{cm}^{-1}$ .  $^1\text{H}$  NMR ( $\text{CDCl}_3$ )  $\delta$ : 1.02 (3H, s,  $\text{CH}_3$ -20), 1.35 (6H, d,  $\text{CH}_3$ -16, and 17), 1.62-2.56 (m, aliphatic), 2.59-2.78 (3H, m, H-5 and H-7), 2.82 (1H, septet,  $J = 7$  Hz, H-15), 3.82 (2H,

brs, -NH<sub>2</sub>), 4.80 (2H, m, H-19), 6.72 (1H, s, H-11); MS [m/z]: 356 (M<sup>+</sup>) 339, 323, 311, 294, 280; HRMS calcd. for C<sub>20</sub>H<sub>24</sub>N<sub>2</sub>O<sub>4</sub>: 356.1736; Found: 356.1738.

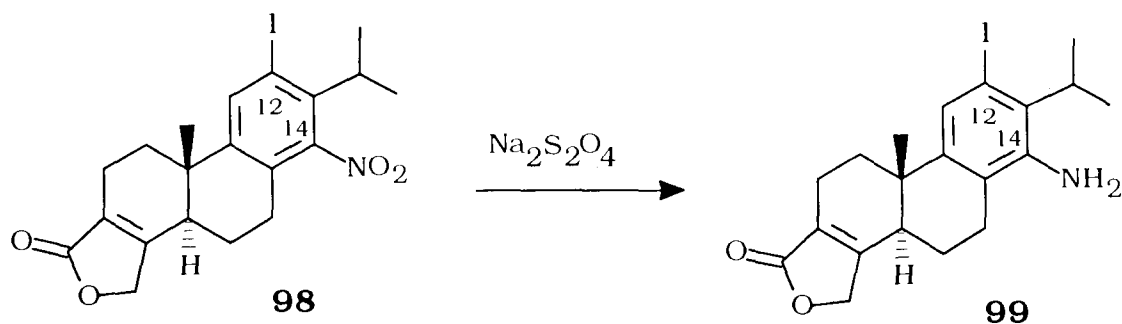
**Synthesis of 14,19-Dihydroxy-12-iodo-18 (4->3) abeo-abieta-3,8,11,13-tetraen-18-oic Acid Lactone (98)**



Into a mixture of trifluoroacetic acid (TFA) (37 mL) and cold acetic acid (AcOH) (37 mL), **97** (5.6 g, 0.016 mol) was added followed by dropwise addition of water (37 mL). The clear solution was cooled to -5-0° C (ice-water-acetone bath) and NaNO<sub>2</sub> (1.73 g, 0.020 mol, 1.2 eq) was added portionwise over 15 min. The reaction mixture was stirred at the bath temperature (-5-0° C) for 30 min, and then a solution of KI (5.62 g, 0.034 mol, 2.0 eq) in water (12 mL) was added dropwise over 10 min. The resulting dark brown suspension was stirred for a further 15 min until gas evolution ceased. A solution of Na<sub>2</sub>SO<sub>3</sub> (1.34 g, 0.011 mol, 0.63 eq) in water (62 mL) was added dropwise to the reaction mixture. The ice bath was removed and the stirring was continued for 30 min at room temperature. Water (974 mL) was added to the suspension and the mixture extracted with ethyl acetate (3 x 649 mL). The combined organic layers were washed with saturated NaHCO<sub>3</sub> (2 x 487 mL), brine (487

mL), dried over anhydrous sodium sulphate, filtered, and rotary evaporated to give crude **98** (8.86 g) as a red-purple oil. The purification of **98** was performed by column chromatography (5 cm diameter, h=30 cm) on silica gel 60 (230-400 mesh) with eluent hexanes:EtOAc (4:1). TLC monitoring (mobile phase: hexanes:EtOAc (6:4) showed a pure product **98** with  $R_f$  value of 0.43, yield (5.2 g, 69%) obtained as colourless prisms. mp 182-184<sup>o</sup> C; UV  $\lambda_{max}$  (MeOH) (log  $\epsilon$ ): 214 nm; IR  $\nu_{max}$  (CHCl<sub>3</sub>): 2980, 1760, 1540, 1370 cm<sup>-1</sup>; <sup>1</sup>H NMR (CDCl<sub>3</sub>)  $\delta$ : 1.02 (3H, s, CH<sub>3</sub>-20), 1.30 (6H, brs, CH<sub>3</sub>-16 and 17), 1.66-2.55 (m, aliphatic), 2.62 (1H, brd, J = 13 Hz, H-5), 2.78 (2H, m, H-7), 3.30 (1H, brs, H-15), 4.78 (2H, m, H-19), 7.98 (1, s, H-11); MS [m/z]: 467 (M<sup>+</sup>), 450, 434, 409, 323, 308, 128, 109; HRMS calcd. for C<sub>20</sub>H<sub>22</sub>INO<sub>4</sub>: 467.0596; Found: 467.0592.

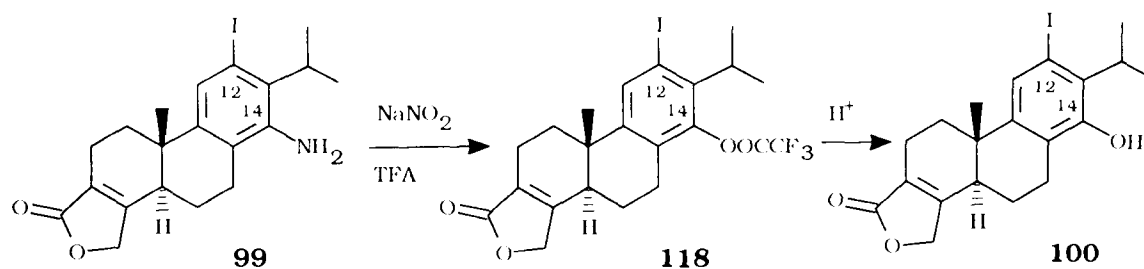
**Synthesis of 14-Amino-19-hydroxy-12-iodo-18 (4->3) abeo-abieta-3,8,11,13-tetraen-18-oic Acid Lactone (99)**



A suspension of **98** (5.2 g, 0.011 mol) in ethanol (136 mL) was heated to reflux until all starting material had dissolved, followed by dropwise addition of a solution of sodium dithionate ( $\text{Na}_2\text{S}_2\text{O}_4$ ) (23.07 g,

0.132 mol) in water (68 mL). The reaction mixture was stirred for 30 min under reflux. Completion of the reaction was monitored by TLC (mobile phase: hexanes:EtOAc (6:4)), and the product **99** showed a  $R_f$  value of 0.20. The mixture was then cooled to room temperature. The solvent was removed *in vacuo* and the residue was dissolved in EtOAc (975 mL) and washed with brine (975 mL). A small amount of water was added to dissolve some remaining inorganic salts. The organic layer was separated and the aqueous layer was extracted with EtOAc (3 x 487 mL) and the combined EtOAc extract was dried over anhydrous sodium sulphate, filtered, and concentrated *in vacuo*. The crude product (4.55 g) was purified by column chromatography with CH<sub>2</sub>Cl<sub>2</sub>:EtOAc, 90:5) and TLC monitoring (mobile phase: hexanes:EtOAc, 6:4) to afford pure **99** as a colourless crystalline solid (4.02 g, 83%). mp 216-218°C; UV  $\lambda_{max}$  (MeOH) (log  $\epsilon$ ): 220, 294 nm; IR  $\nu_{max}$  (CHCl<sub>3</sub>) cm<sup>-1</sup>: 3525, 3426, 3020, 2977, 1743, 1680, 1622, 1050 cm<sup>-1</sup>; <sup>1</sup>H NMR (CDCl<sub>3</sub>)  $\delta$ : 1.02 (3H, s, CH<sub>3</sub>-20), 1.33 (6H, d, CH<sub>3</sub>-16 and 17), 1.62-2.80 (m, aliphatic), 2.60 (1H, septet,  $J = 7$  Hz, H-15), 4.77 (2H, m, H-19), 7.30 (1H, brs, H-11); MS [m/z]: 437 (M<sup>+</sup>), 421, 312, 296; HRMS calcd. for C<sub>20</sub>H<sub>24</sub>O<sub>2</sub>Ni: 437.0855; Found: 437.0852.

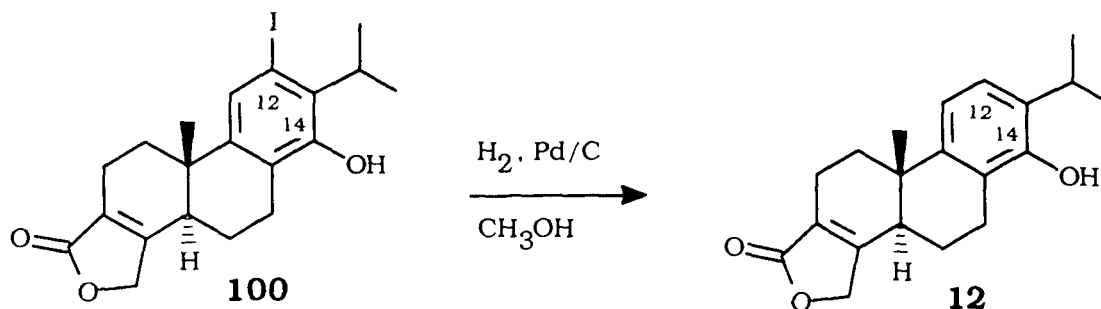
**Synthesis of 14,19-Dihydroxy-12-iodo-18 (4->3) *abeo*-abieta-3,8,11,13-tetraen-18-oic Acid Lactone (100)**



To a stirred solution of **99** (4.02 g, 0.009 mol) in reagent grade trifluoroacetic acid (TFA) (65 mL) at  $-12$ - $10^\circ\text{C}$  (ice-acetone-water bath), analytical reagent  $\text{NaNO}_2$  (1.3 g, 0.018 mol) was added portionwise over 10 min. The mixture turned brown and gas evolution was noted. The reaction mixture was stirred at the bath temperature for 35 min and a solution of analytical reagent  $\text{Na}_2\text{SO}_3$  (0.578 g, 0.004 mol) in water (8.0 mL) was added dropwise. The ice bath was removed and the mixture was stirred for 30 min at room temperature. Water (31 mL) was added and stirring was continued overnight. The reaction was examined by TLC (mobile phase: hexane:EtOAc, 1:1). The reaction mixture was then diluted with water (1180 mL) and extracted with EtOAc (3 x 835 mL). The combined EtOAc extract was washed with saturated  $\text{NaHCO}_3$  solution (594 mL), brine (594 mL), and dried over anhydrous sodium sulphate. Removal of the solvent gave the crude intermediate **118** (8.35 g) which was then dissolved in MeOH (139 mL) followed by dropwise addition of concentrated HCl (21 mL) while stirring at  $-10$ - $0^\circ\text{C}$ . The

reaction mixture was stirred overnight at room temperature and some product precipitated. The reaction was monitored by TLC (mobile phase: hexane:EtOAc, 1:1) and the desired product **100** showed  $R_f$  value of 0.42. The solvent was removed *in vacuo* and the residue was dissolved in EtOAc (285 mL). The organic layer was washed with water (2 x 650 mL), brine (650 mL) and the water phase was extracted with EtOAc (2 x 400 mL). The combined EtOAc extracts were dried over anhydrous sodium sulphate and rotary evaporated to give the crude product (3.88 g). Purification of the crude mixture was done by column chromatography using hexanes:EtOAc (6:4 and 1:1) as eluting solvents. The pure **100** (3.05 g, 77%) was obtained as a white crystalline solid. mp 217-219° C; UV  $\lambda_{max}$  (MeOH) (log  $\epsilon$ ): 220, 280 nm; IR  $\nu_{max}$  (CHCl<sub>3</sub>): 3650, 3040, 2960, 1780, 1680, 1600, 1240, 1020 cm<sup>-1</sup>. <sup>1</sup>H NMR (CDCl<sub>3</sub>)  $\delta$ : 1.01 (3H, s, CH<sub>3</sub>20), 1.34 (6H, d, CH<sub>3</sub>-16 and 17), 1.64-2.50 (m, aliphatic), 2.59-2.81 (3H, m, H-5, H-7), 3.40 (1H, septet, J = 7 Hz, H-15), 4.75 (2H, m, H-19), 4.85 (1H, s, C14-OH, D<sub>2</sub>O exchangeable), 7.42 (1H, s, H-11). MS  $m/z$ : 438 (M<sup>+</sup>, base peak), 423, 312, 296, 275, 197, 165, 147, 128. HRMS calculated for C<sub>20</sub>H<sub>23</sub>O<sub>3</sub>I: 438.0692; Found: 438.0694.

**Synthesis of 14,19-Dihydroxy-18 (4->3) abeo-abietic-3,8,11,13-tetraen-18-oic Acid Lactone (12) (Tryptophenolide)**



Into a solution of **100** (3.05 g, 0.006 mol) in MeOH (226 mL) were placed 10% Pd/C (0.296 g) and K<sub>2</sub>CO<sub>3</sub> (0.444 g, 0.0032 mol). The mixture was stirred under H<sub>2</sub> (1 atm) for 15 h at room temperature. The reaction was monitored by TLC (mobile phase: hexane:EtOAc, 7:3 and 1:1). After the reaction was completed, the mixture was filtered through a sintered glass funnel and the filtrate was concentrated *in vacuo*. The residue was then resuspended in 5% NaH<sub>2</sub>PO<sub>4</sub> (250 mL) and extracted with EtOAc (3 x 250 mL). The combined organic layers were washed with brine (250 mL) and dried over anhydrous sodium sulphate. Removal of the solvent afforded a crude product (2.37 g), which was purified by column chromatography, using silica gel 60 (230-400 mesh) and petroleum ether:EtOAc, 6:4 and 1:1 as eluting solvent. Pure **12** was obtained as colourless prisms (1.77 g, 94%). The overall yield of **12** was 30% from the starting compound **45**. mp. 228-230° C; UV λ<sub>max</sub> (MeOH) (log ε): 278, 226, 204 nm; IR ν<sub>max</sub> (CHCl<sub>3</sub>): 3620, 3020, 2964, 1743, 1421, 1217, 1070, 1021 cm<sup>-1</sup>; <sup>1</sup>H NMR (CDCl<sub>3</sub>) δ: 1.02 (3H, s, CH<sub>3</sub>-20), 1.25, 1.26 (3H each, d, J = 7 Hz, CH<sub>3</sub>-16 and 17), 1.65 (1H, m, H-1α), 1.91 (1H, m, H-6β), 2.0 (1H, m, H-6α), 2.36 (1H, m, H-2β), 2.42-2.54 (2H, m, H-1β and H-2α), 2.68 (1H, brd, J = 13 Hz, H-5), 2.74-2.95 (2H, m, H-7), 3.1 (1H, septet, J = 7 Hz, H-15), 4.75 (1H, brs, C14-OH, D<sub>2</sub>O exchangeable), 4.79 (2H, m, H-19), 6.92 (1H, d, J = 8 Hz, H-11), 7.02 (1H, d, J = 8, H-12); <sup>13</sup>C NMR (CDCl<sub>3</sub>) δ: 18.1, 19.6, 22.4, 22.7, 26.8, 32.5, 40.8, 70.5, 116.2, 123.3, 130.9, 142.0, 150.3, 161.5, 172.1; MS [m/z]: 312 (M<sup>+</sup>), 297 (base peak), 281, 269, 255, 237, 165, 149, 134; HRMS calcd. for C<sub>20</sub>H<sub>24</sub>O<sub>3</sub>: 312.1725; Found: 312.1723.

## 7.2 Biotransformation Studies

### 7.2.1 General Experimental Procedures

Media preparations were made by the use of commercial medium components (Difco Laboratories). The pH was measured on the Fisher Scientific Accumet<sup>®</sup> 925 pH/ion meter and media were adjusted with 0.1 or 1.0 M NaOH and 0.1 or 1.0 M HCl. The cultures were grown on a portable Model G2 New Brunswick Scientific rotary shaker.

Samples and controls were visualized by UV on analytical thin-layer chromatography (TLC) plates, using Merck pre-coated silica gel 60 F254, and by spraying with a 10% solution of ammonium molybdate in 10% sulphuric acid, followed by heating at 125° C until blue spots developed. Column chromatography was carried out using Merck silica gel 60, 230-400 A mesh, and Sigma silica gel type H, 10-40 µm. Some purifications were performed on preparative TLC plates pre-coated with silica gel 60 F<sub>254</sub>. Solvents for extractions were technical grade. All solvents for column chromatography were reagent grade and received no additional purification or drying prior to use. Most of the purifications were carried out under a pressure of nitrogen or argon gas. Radial chromatography was performed using a Chromatotron Model 8924 with 1 mm silica gel 60 plates (PF 254) which contained gypsum. Anhydrous magnesium sulphate or sodium sulphate were used to dry the organic solutions.

<sup>1</sup>H NMR spectra were run in CDCl<sub>3</sub> or acetone-d<sub>6</sub> at 400 MHz using Bruker WH-400 and AE-200 spectrometers. Tetramethylsilane was used as the internal standard and all peaks were recorded in ppm (δ)



relative to TMS ( $\delta$  0.00 ppm). Assignments were given and are based on a combination of chemical shift, coupling constant, decoupling, COSY, and NOE difference data. The  $^{13}\text{C}$  NMR spectra were recorded on Varian XL-300 spectrometers and the chemical shifts are reported in ppm relative to TMS. Low and high resolution mass spectra were run using the Kratos MS-50 mass spectrometer. Chemical ionization mass spectra were recorded on a Delsi Nermag R10-10C mass spectrometer using isobutane as the carrier gas.

The IR spectra were recorded on Perkin-Elmer 710, 710B and 1710 spectrometers in  $\text{CHCl}_3$  or acetone solution (using NaCl cells of 0.1 mm path length) or as a thin film (using NaCl plates). The UV spectra were recorded on a Unicam SP800 spectrometer using quartz cells of 1 cm path length.

Melting points were determined using a Kofler block melting point apparatus and are uncorrected. Optical rotations were recorded on a Perkin-Elmer 141 automatic polarimeter in chloroform solution using a quartz cell of 10 cm path length with the concentration (in g/100 mL) given in parentheses.

Elemental analyses were determined by Mr. P. Borda, UBC, Microanalytical Facility.

High pressure liquid chromatography was performed using a Waters  $\text{C}_{18}$  "Radial Pak" liquid chromatography cartridge 8 x 100 mm, a Waters 440 Absorbance Detector set at 280 and 254 nm, and a mobile phase of  $\text{H}_2\text{O}$  (55.3%), MeOH (29.7%), MeCN (15%), containing AcOH (0.1%) at a flow rate of 1.5 mL/min (isocratic conditions).

## **7.2.2 Experimental Procedure for Biotransformation of Butenolide 45 by *Syncephalastrum racemosum***

### **Fungal Material**

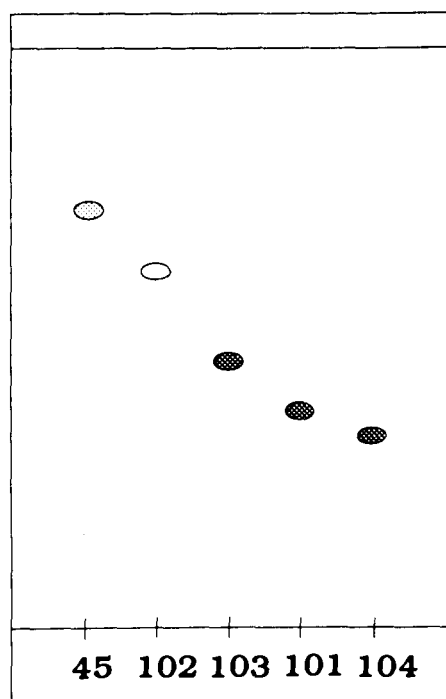
After a preliminary screening of several fungal strains, the zygomycete *Syncephalastrum racemosum* (UBC #60) was found to oxidize the parent compound, butenolide **45**.

### **Growth Conditions**

Cultures were maintained on potato-dextrose agar medium and spore suspensions of  $1 \times 10^6$  spores/mL were used to inoculate the main cultures of the following medium Potato Dextrose Broth (PDB): freshly prepared potato extract (23%), yeast extract (0.5%), glucose (2%), pH 6.5. This primary culture was used to inoculate a secondary culture (10%, v/v). Cultures were incubated on a rotary shaker at 240 rpm at 28° C. The ratio of cell suspension volume to flask volume was always 1:5. Butenolide **45** was added as an ethanolic solution to a final concentration of 0.1 mg/mL. Ethanol was added to control flasks; the volume of ethanol in either control or flasks containing substrate **45** never exceeded 1% of the total volume of the suspension.

## Isolation and Purification of Metabolites

Figure 29. Thin Layer Chromatogram of the Metabolites Isolated from Biotransformation of **45** by *S. racemosum* (Schematic Presentation).



Legend:

Butenolide **45**

7-Ketobutenolide (**102**)

15-Hydroxybutenolide (**103**)

7 $\beta$ -Hydroxybutenolide (**101**)

7 $\alpha$ -Hydroxybutenolide (**104**)

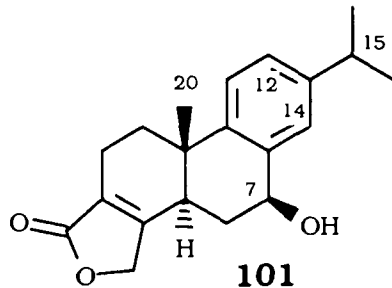
Butenolide **45** (300 mg, 1.012 mmol) was dissolved in 10 mL of ethanol and added to PDB medium (3.0 L) containing 48 h growing culture of *S. racemosum* which had been inoculated from spore

suspension. After 24 h incubation time, the cell suspension (broth + cells) was extracted with ethyl acetate (3 x 1 L). The combined extracts were dried over anhydrous sodium sulphate. The organic layer was concentrated *in vacuo* to yield a crude extract (483 mg). The compounds present in the crude mixture were initially separated on a silica gel 60 column by eluting with a gradient of hexane-ethyl acetate (95:5 to 50:50, v/v). The column fractions were then further purified on silica gel 60 F<sub>254</sub> preparative TLC plates. The following compounds were obtained: **101** (7.0 mg, 2%), **102** (10 mg, 3%), **103** (6.0 mg, 2%), **104** (5.0 mg, 2%). Overall conversion of butenolide **45** to products was 10%. The products from this separation were examined by thin layer chromatography (silica gel 60 F<sub>254</sub>, mobile phase: hexane:EtOAc, 3:7); **45** had an R<sub>f</sub> value of 0.73, **101** had a value of 0.38, **102** had a value of 0.63, **103** had a value of 0.46 and **104** had a value of 0.33 (Figure 29).

### **Identification of Metabolites**

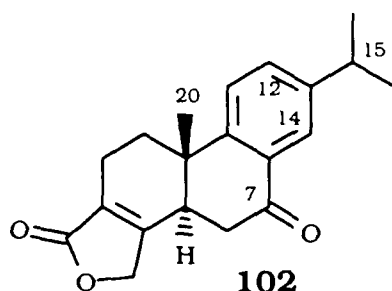
Each of the isolated products was subjected to spectroscopic analyses in order to elucidate its structure. The physical properties of the metabolites from the biotransformation of **45** by *S. racemosum* are as follows:

**7 $\beta$ ,19-Dihydroxy-18 (4->3) *abeo*-abieta-3,8,11,13-tetraen-18- oic Acid  
Lactone (101) (7 $\beta$ -Hydroxybutenolide)**



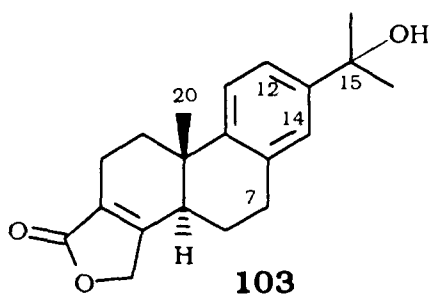
**101** was obtained as white powder (hexanes:acetone), mp 63-67° C;  $[\alpha]^{19.3}_D + 76.0^\circ$  ( $c = 1.00$ ,  $\text{CHCl}_3$ ); IR  $\nu_{\text{max}}$  ( $\text{CHCl}_3$ ): 3470, 2960, 1740  $\text{cm}^{-1}$ ; UV  $\lambda_{\text{max}}$  ( $\log \epsilon$ ) (MeOH): 216 (4.31) nm;  $^1\text{H}$  NMR ( $\text{CDCl}_3$ )  $\delta$ : 1.12 (3H, s,  $\text{CH}_3$ -20), 1.17 (6H, d,  $J = 8$  Hz,  $\text{CH}_3$  - 16 and 17), 1.70 (1H, m,  $\text{H}_A$  - 1), 1.94 (1H, ddd,  $J = 12, 12, 8$  Hz,  $\text{H}_B$  - 6), 2.34 (1H, ddd,  $J = 12, 8, 2$  Hz,  $\text{H}_B$  - 6), 2.38 (1H, m,  $\text{H}_A$  - 2), 2.50 (1H, m,  $\text{H}_B$  - 1), 2.53 (1H, m,  $\text{H}_B$  - 2), 2.81 (1H, brd,  $J = 12$  Hz, H - 5), 2.92 (1H, m, H - 15), 4.77 (1H, brd,  $J = 16$  Hz,  $\text{H}_A$  - 19), 4.84 (1H, brd,  $J = 16$  Hz,  $\text{H}_B$  - 19), 5.02 (1H, dd,  $J = 8, 8$  Hz,  $\alpha\text{H}$  - 7), 7.18 (1H, dd,  $J = 8, 2$  Hz, H - 12), 7.28 (1H, d,  $J = 8$  Hz, H - 11), 7.44 (1H, d,  $J = 2$  Hz, H - 14);  $^{13}\text{C}$  NMR ( $\text{CDCl}_3$ )  $\delta$ : 32.7 (C-1), 18.1 (C-2), 125.8 (C-3), 162.1 (C-4), 36.8 (C-5), 30.7 (C-6), 69.3 (C-7), 137.4 (C-8), 147.5 (C-9), 40.8 (C-10), 126.3 (C-11), 124.3 (C-12), 142.4 (C-13), 126.1 (C-14), 33.7 (C-15), 24.0 (C-16), 23.8 (C-17), 174.0 (C-18), 70.4 (C-19), 23.0 (C-20); MS [ $m/z$ ]: 312 ( $\text{M}^+$ ), 294, 279, 237 (base peak). HRMS calcd. for  $\text{C}_{20}\text{H}_{24}\text{O}_3$ : 312.1726; found: 312.1717.

**19-Hydroxy-7-oxo-18 (4->3) abeo-abieta-3,8,11,13-tetraen-18-oic Acid Lactone (102) (7-Ketobutenolide)**



**102** was obtained as light yellow plate-like crystals (hexanes:acetone). IR  $\nu_{\max}$  (CDCl<sub>3</sub>): 2950, 1710 cm<sup>-1</sup>. <sup>1</sup>H NMR (CDCl<sub>3</sub>)  $\delta$ : 1.17 (3H, s, CH<sub>3</sub> - 20), 1.27 (6H, d,  $J$  = 8 Hz, CH<sub>3</sub> - 16 and 17), 1.8-2.80 (m, aliphatic H), 2.99 (1H, septet, H - 15), 4.78 (2H, m, H - 19), 7.42 (1H, d,  $J$  = 8 Hz, H - 11), 7.58 (1H, dd,  $J$  = 8, 2 Hz, H - 12), 7.97 (1H, d,  $J$  = 2 Hz, H - 14); MS [ $m/z$ ]: 310 (M<sup>+</sup>), 295 (base peak), 291, 273, 237. HRMS calcd. for C<sub>20</sub>H<sub>22</sub>O<sub>3</sub>: 310.1569; found: 310.1560.

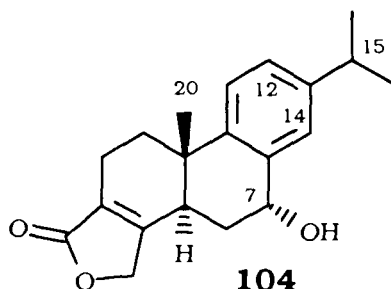
**15,19-Dihydroxy-18 (4->3) abeo-abieta-3,8,11,13-tetraen-18-oic Acid Lactone (103) (15-Hydroxybutenolide)**



**103** was obtained as a white powder (hexanes:EtOAc). IR  $\nu_{\max}$  (CHCl<sub>3</sub>): 3610, 2950 cm<sup>-1</sup>. <sup>1</sup>H NMR (CDCl<sub>3</sub>)  $\delta$ : 1.06 (3H, s, CH<sub>3</sub> - 20),

1.58 (6H, d,  $J = 8$  Hz, CH<sub>3</sub>-16 and 17), 1.60-2.65 (m, aliphatic H), 3.05 (2H, m, H - 7), 4.78 (1H, brd,  $J = 16$  Hz, H<sub>A</sub> - 19), 4.88 (1H, brd,  $J = 16$  Hz, H<sub>B</sub> - 19), 7.20 (1H, d,  $J = 2$  Hz, H - 14), 7.32 (1H, d,  $J = 8$  Hz, H - 11), 7.40 (1H, dd,  $J = 8, 2$  Hz, H - 12); MS [ $m/z$ ]: 312 (M<sup>+</sup>), 294, 279 (base peak). HRMS calcd. for C<sub>20</sub>H<sub>27</sub>O<sub>3</sub>: 312.1725; Found: 312.1727.

**7 $\alpha$ ,19-Dihydroxy-18 (4->3) abeo-abieta-3,8,11,13-tetraen-18-olc Acid Lactone (104) (7 $\alpha$ -Hydroxybutenolide)**



**104** was obtained as white powder (hexanes-acetone), mp 132-136°;  $[\alpha]^{19.3}_D + 24.8^\circ$  ( $c = 1.00$ , CHCl<sub>3</sub>); IR  $\nu_{\max}$  (CHCl<sub>3</sub>): 3485, 2965, 1740 cm<sup>-1</sup>; UV  $\lambda_{\max}$  (MeOH) ( $\log \epsilon$ ): 216.7 (4.37) nm; <sup>1</sup>H NMR (CDCl<sub>3</sub>)  $\delta$ : 1.00 (3H, s, CH<sub>3</sub> - 20), 1.28 (6H, d,  $J = 8$  Hz, CH<sub>3</sub> - 16 and 17), 1.77 (1H, m, H<sub>A</sub> - 1), 2.01 (1H, ddd,  $J = 12, 1, 1$  Hz, H<sub>A</sub> - 6), 2.17 (1H, ddd,  $J = 12, 12, 5$  Hz, H<sub>B</sub> - 6), 2.40 (1H, m, H<sub>A</sub> - 2), 2.51 (1H, m, H<sub>B</sub> - 1), 2.54 (1H, m, H<sub>B</sub> - 2), 2.91 (1H, m, H - 15), 3.20 (1H, brd,  $J = 12$  Hz, H<sub>A</sub> - 5), 4.76 (1H, brd,  $J = 16$  Hz, H<sub>A</sub> - 19), 4.89 (1H, brd,  $J = 16$  Hz, H<sub>B</sub> - 19), 4.92 (1H, dd,  $J = 5, 1$  Hz,  $\beta$ H - 7), 7.21 (1H, dd,  $J = 8, 2$  Hz, H - 12), 7.24 (1H, d,  $J = 2$  Hz, H - 14), 7.32 (1H, d,  $J = 8$  Hz, H - 11); <sup>13</sup>C NMR (CDCl<sub>3</sub>)  $\delta$ : 32.5 (C-1), 18.2 (C-2), 125.4 (C-3), 163.2 (C-4), 36.7 (C-5), 29.4 (C-6), 67.2 (C-7), 136.2 (C-8), 147.6 (C-9), 36.6 (C-10), 126.9 (C-11), 124.6 (C-12), 142.4 (C-13), 128.3 (C-14), 33.6 (C-15), 24.0 (C-16), 13.8 (C-17), 174.1

(C-18), 70.5 (C-19), 22.1 (C-20); MS [ $m/z$ ]: 312 ( $M^+$ ), 294, 279, 237 (base peak); HRMS calcd. for  $C_{20}H_{24}O_3$ : 312.1726; Found: 312.1566. Anal. calcd. for  $C_{20}H_{24}O_3$ : C 76.89; H 7.74; Found: C 76.66; H. 7.69.

### **Effect of Cytochrome P-450 Inhibitors on Hydroxylation of 45**

The effect of inhibiting cytochrome P-450 activity on the metabolism of butenolide 45 by *S. racemosum* was studied by incubating cultures of *S. racemosum* in PD broth for 48 h after which the inhibitors were added. After a further 15 min incubation period, **45** (0.1 mg/mL) was added. The inhibitors studied were ketoconazole (20  $\mu$ M), miconazole (20  $\mu$ M),  $\alpha$ -naphthoflavone (50  $\mu$ M), aminobenzothiazole (50  $\mu$ M), and carbon monoxide. Chemical inhibitors were added dissolved in ethanol, and sterile-filtered CO was bubbled into the cell suspensions for 2 min prior to the addition of butenolide 45. Control flasks received only the inhibitor and the ethanol vehicle. After 24 h, the broth was checked for contamination by microscope and sampled, and the extracted compounds were separated by TLC (hexanes:EtOAc, 3:7). Metabolites were detected as described above. In addition, to establish whether the inhibitors had any effect on the growth of *S. racemosum*, the wet weights of the mycelia were assessed visually after 24 h and the mycelial weights were measured after 96 h.



### **7.2.3 Experimental Procedures for Biotransformation of Butenolide 45 by *Aspergillus fumigatus* and *Cunninghamella elegans***

#### **Fungal Material**

The following strains were able to oxidize **45**: *Aspergillus fumigatus* Fresenius (ATCC #13073) and *Cunninghamella elegans* var. *chibaensis* Kuwabara et Hoshino (ATCC #20230).

#### **Growth Conditions**

Fungi were stored on potato dextrose agar slants under sterile mineral oil. Erlenmeyer flasks were inoculated with a spore suspension prepared from these slants to a final spore concentration of  $2.5 \times 10^6$  spores/ml. The ratio of flask volume to medium volume was 5:1. *A. fumigatus* spores were inoculated into PDB medium (1.0 L) containing glucose (2%) and grown for 48 h at 28°, 240 rpm on a rotary shaker. *C. elegans* spores were inoculated into SSBF medium (3.0 L) containing glucose (2%) and the cells were grown at 28° C, 240 rpm for 72 h. Butenolide **45** was dissolved in ethanol (final volumes of ethanol were not more than 2% of the total medium volume) and added to the culture and further incubated for various periods which are noted on the figures. The composition of the media used for filamentous fungi were: PDB; glucose (2%), freshly-prepared potato extract (23%), yeast extract (0.5%), pH 6.5, and SSBF; glucose (2%), soya bean flour containing 1% fat (0.5%), NaCl (0.5%),  $\text{KH}_2\text{PO}_4$  (0.5%), yeast extract (0.5%), pH 7.0. The ethyl acetate extracts of cell suspensions or separate broth and mycelia fractions were

analyzed for metabolites of compound **45** by thin layer chromatography (mobile phase: EtOAc:hexane 7:3).

### **Isolation and Purification of Metabolites**

#### i) Conversion of **45** by *A. fumigatus*

Butenolide **45** (100 mg, 2.961 mmol) was dissolved in 5 mL of ethanol and added to PDB medium (1.0 L) containing 48 h growing culture of *A. fumigatus* which had been inoculated from spore suspension. The compound **45** was incubated for 48 h and the biotransformation was examined by TLC (mobile phase: EtOAc:hexane 7:3); **102** had an  $R_f$  value 0.23 and **103** had a value of 0.47. After 48 h of biotransformation of **45**, the suspension was extracted with ethyl acetate (3x500 mL), the organic layer was then dried over magnesium sulphate, and evaporated *in vacuo* to afford the crude extract (187 mg). The crude residue was separated by column chromatography on silica gel (230-400 mesh) and an eluting solvent of hexane:EtOAc, 4:1. The mixture was resolved into two products: **102** (72 mg, 72%), and **103** (3 mg, 3%), respectively. Unreacted compound **45** (5 mg, 5%) was also recovered. Overall recovery was 80%. The spectroscopic data (NMR and MS) of the metabolites were identical to those of the authentic compounds, obtained from *S. racemosum*.

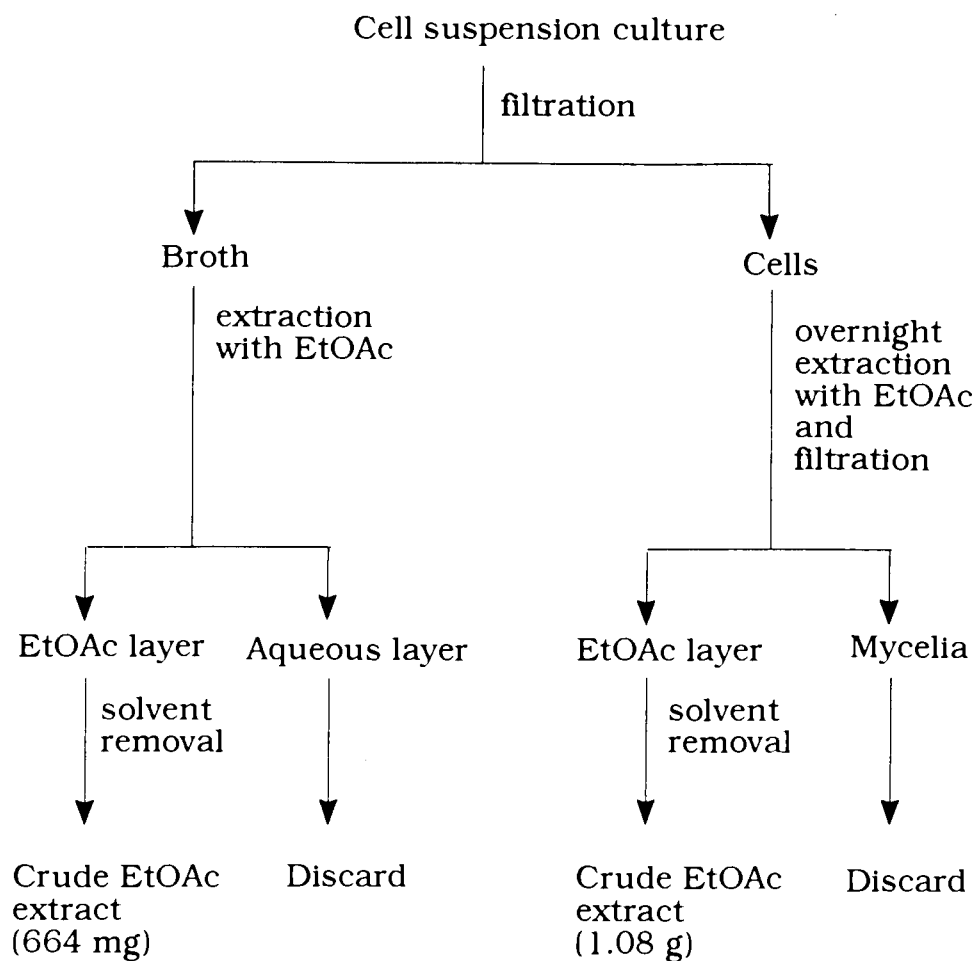
#### ii) Conversion of **45** by *C. elegans*

Butenolide **45** (500 mg, 0.592 mmol) was dissolved in 45.0 mL of ethanol and added directly to 3.0 L of SSBF medium containing 72-h culture of *C. elegans* (0.17 mg/mL) which had been inoculated from a spore suspension. The culture was further incubated for 20 h at 240 rpm

and 28° C. After this period, the cell suspension was filtered through Miracloth in a Buchner funnel to afford broth and cells (Scheme 23). The broth was extracted with ethyl acetate (3 x 1.5 L). The combined extracts were washed with water (750 mL) and then with sat. NaCl (750 mL) and then dried over anhydrous magnesium sulphate. This material was concentrated under vacuum to yield a crude broth extract (664 mg). The crude extract was chromatographed over silica gel with hexane:acetone (95:5, 9:1, 8:2, 1:1) followed by methanol which afforded 6 fractions (Fr. 1 and Fr. 2 were obtained with hexane:acetone 95:5, Fr. 3 was obtained with 9:1, Fr. 4 was obtained with 8:2, Fr. 5 was obtained with 1:1, and Fr. 6 was obtained with methanol). Fractions 1-6 were further chromatographed as follows: Fr. 1 (CHCl<sub>3</sub>:Acetone, 95:5) yielded compounds **45**, **101**, **104** and **105**, Fr. 2 (CHCl<sub>3</sub>:Acetone, 9:1) yielded compound **106**, Fr. 3 (Hex:Acetone, 2:1) yielded compound **107**, Fr. 4 (EtOAc) yielded compounds **108** and **109** and Fr. 5 (CH<sub>2</sub>Cl<sub>2</sub>:Acetone, 1:1) yielded compounds **110** and **111**. After the evaporation of solvent, the percent yields were determined by weighing the vacuum-dried, pure compounds, the mole percent of starting material was then calculated: **45** (44 mg, 9%), **101** (54 mg, 10%), **104** (37 mg, 7%), **105** (80 mg, 14%), **106** (53 mg, 10%), **107** (21 mg, 4%), **108** (17 mg, 3%), **109** (14 mg, 3%), **110** (12 mg, 2%) and **111** (15 mg, 3%). The total recovery from the extract of the broth was therefore 65 %.

To separate the metabolites contained in the fungal biomass from this incubation, 2 L of ethyl acetate was added to the combined cell material and the resulting suspension was allowed to extract overnight at 4°C

Scheme 23. Extraction Procedure for *C. elegans* Suspension Culture.

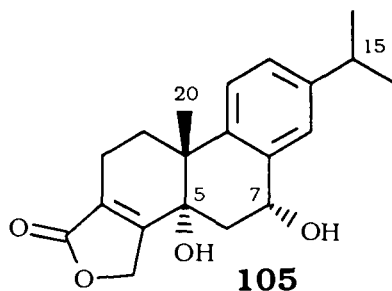


The cell suspension was filtered through Miracloth and the filtrate washed with water (500 mL) and then NaCl (500 mL) and dried over anhydrous magnesium sulphate. Concentration of the extract *in vacuo* resulted in a crude mixture (1.08 g) which was chromatographed over silica gel using hexane: acetone 19:1. Yields of compounds: **45** (10 mg, 2%), **101** (10 mg, 2%), **104** (8 mg, 2%) and **105** (20 mg, 4%), respectively. The recovery from the extract of the cell material was 10 %. The overall recovery from the broth and cell material was 75%.

## Identification of Metabolites

Spectroscopic analyses were performed for each product and the structure was assigned. The physical properties of the metabolites from the biotransformation of **45** by *C. elegans* are as follows:

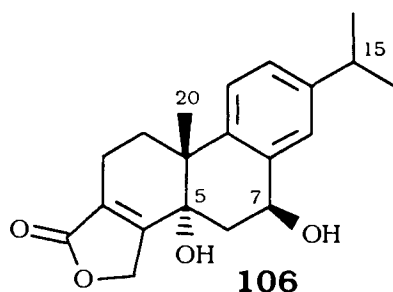
### **5 $\alpha$ ,7 $\alpha$ ,19-Trihydroxy-18 (4->3) abeo-abieta-3,8,11,13-tetraen-18-oic Acid Lactone (105) (5 $\alpha$ ,7 $\alpha$ -Dihydroxybutenolide)**



**105** was obtained as colourless prisms (hexane - acetone 9:1), mp 156-158°;  $[\alpha]^{19.3}_D - 89.3^\circ$  ( $c = 0.44$ ,  $\text{CHCl}_3$ ); IR  $\nu_{\text{max}}$  ( $\text{CHCl}_3$ ): 3434, 2934, 1724  $\text{cm}^{-1}$ ; UV  $\lambda_{\text{max}}$  (MeOH) ( $\log \epsilon$ ): 214 (4.36) nm;  $^1\text{H}$  NMR ( $\text{CDCl}_3$ )  $\delta$ : 1.07 (3H, s,  $\text{CH}_3$ -20), 1.28 (6H, d,  $J = 8$  Hz,  $\text{CH}_3$  - 16 and 17), 2.20 (1H, m,  $\text{H}_A$  - 1), 2.25 (1H, d,  $J = 13$  Hz,  $\text{H}_A$  - 6), 2.38 (1H, m,  $\text{H}_B$  - 1), 2.43 (1H, m,  $\text{H}_A$  - 2), 2.52 (1H, dd,  $J = 13, 8$  Hz,  $\text{H}_B$  - 6), 2.58 (1H, m,  $\text{H}_B$  - 2), 2.93 (1H, m, H - 15), 4.82 (1H, brd,  $J = 16$  Hz,  $\text{H}_A$  - 19), 4.97 (1H, d,  $J = 5$  Hz,  $\beta\text{H}$  - 7), 5.07 (1H, dt,  $J = 16, 2$  Hz,  $\text{H}_B$  - 19), 7.22 (1H, dd,  $J = 8, 1$  Hz, H - 12), 7.31 (1H, d,  $J = 8$  Hz, H - 11), 7.36 (1H, d,  $J = 1$  Hz, H - 14);  $^{13}\text{C}$  NMR ( $\text{CDCl}_3$ )  $\delta$ : 34.0 (C-1), 18.0 (C-2), 126.97 (C-3), 161.1 (C-4), 69.2 (C-5), 26.1 (C-6), 67.0 (C-7), 135.9 (C-8), 147.4 (C-9), 41.7 (C-10), 128.4 (C-11 or C-14), 124.6 (C-12), 139.3 (C-13), 127.01 (C-14 or C-11), 33.6 (C-15), 24.0 (C-16), 23.8 (C-17), 174.1 (C-18), 70.5 (C-

19), 27.1 (C-20); MS [ $m/z$ ]: 328 ( $M^+$ ), 310, 189 (base peak); HRMS calcd. for  $C_{20}H_{24}O_4$ : 328.1675; Found: 328.1682. Anal. calcd. for  $C_{20}H_{24}O_4$ : C 73.14, H 7.37; Found C 73.06, H 7.40.

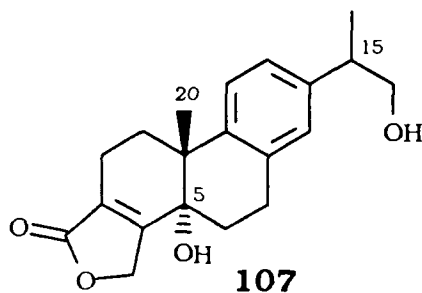
**5 $\alpha$ ,7 $\beta$ ,19-Trihydroxy-18 (4->3) abeo-abieta-3,8,11,13-tetraen-18-oic Acid Lactone (106) (5 $\alpha$ ,7 $\beta$ -Dihydroxybutenolide)**



**106** was obtained as colourless plates (hexanes - acetone 5:1), mp 198-203°;  $[\alpha]^{19.3}_D - 13.9^\circ$  ( $c = 1.00$ ,  $CHCl_3$ ); IR  $\nu_{max}$  ( $CHCl_3$ ): 3430, 2930, 1720  $cm^{-1}$ ; UV  $\lambda_{max}$  (MeOH) ( $\log \epsilon$ ): 214 (4.31) nm;  $^1H$  NMR ( $CDCl_3$ )  $\delta$ : 1.22 (3H, s,  $CH_3$  - 20), 1.26 (6H, d,  $J = 8$  Hz,  $CH_3$  - 16 and 17), 2.04 (1H, m,  $H_A$  - 1), 2.19 (1H, dd,  $J = 13, 8$  Hz,  $H_A$  - 6), 2.35 (1H, m,  $H_B$  - 1), 2.55 (1H, m,  $H_A$  - 2), 2.52 (1H, dd,  $J = 13, 10$  Hz,  $H_B$  - 6), 2.41 (1H, m,  $H_B$  - 2), 2.90 (1H, m, H - 15), 4.80 (1H, ddd,  $J = 16, 4, 2$  Hz,  $H_A$  - 19), 5.15 (1H, dd,  $J = 8, 8$  Hz,  $\alpha H$  - 7), 5.00 (1H, dt,  $J = 16, 3$  Hz,  $H_B$  - 19), 7.18 (1H, dd,  $J = 8, 1$  Hz, H - 12), 7.24 (1H, d,  $J = 8$  Hz, H - 11), 7.38 (1H, d,  $J = 1$  Hz, H - 14);  $^{13}C$  NMR ( $CDCl_3$ )  $\delta$  36.4 (C-1), 17.9 (C-2), 126.6 (C-3), 161.3 (C-4), 69.2 (C-5), 26.1 (C-6), 66.7 (C-7), 136.9 (C-8), 147.6 (C-9), 41.4 (C-10), 127.0 (C-11 or C-14), 124.5 (C-12), 139.6 (C-13), 126.8 (C-14 or C-11), 33.7 (C-15), 24.0 (C-16), 23.8 (C-17), 173.9 (C-18), 72.0 (C-19), 27.4 (C-20); MS [ $m/z$ ]: 328 ( $M^+$ ), 310, 43 (base peak);

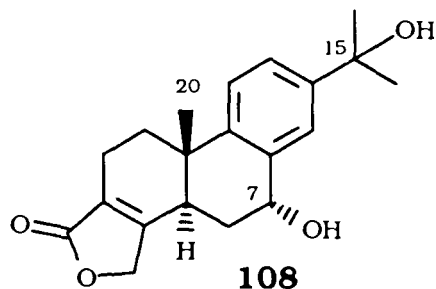
HRMS calcd. for C<sub>20</sub>H<sub>24</sub>O<sub>4</sub>: 328.1675; Found: 328.1670. *Anal.* calcd. for C<sub>20</sub>H<sub>24</sub>O<sub>4</sub>: C, 73.14; H 7.37; Found C, 72.98; H 7.42

**5 $\alpha$ ,16,19-Trihydroxy-18 (4 $\rightarrow$ 3) abeo-abieta-3,8,11,13-tetraen-18-oic Acid Lactone (107) (5 $\alpha$ ,16-Dihydroxybutenolide)**



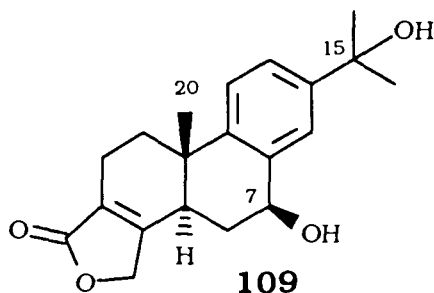
**107** was obtained as a white powder (hexane-acetone 5:1), mp 72-75°;  $[\alpha]^{19.3}_D -37.9^\circ$  ( $c = 1.00$ , CHCl<sub>3</sub>); IR  $\nu_{max}$  (CHCl<sub>3</sub>): 3430, 2950, 1750 cm<sup>-1</sup>; UV  $\lambda_{max}$  (MeOH) (log  $\epsilon$ ): 215 (4.31) nm; <sup>1</sup>H NMR (CDCl<sub>3</sub>)  $\delta$ : 1.13 (3H, s, CH<sub>3</sub> - 20), 1.28 (3H, d,  $J = 8$  Hz, CH<sub>3</sub> - 17), 2.03 (1H, ddd,  $J = 14, 8, 3$  Hz, H<sub>A</sub> - 6), 2.13 (1H, m, H<sub>A</sub> - 1), 2.25 (1H, ddd,  $J = 14, 8, 8$  Hz, H<sub>B</sub> - 6), 2.35 (1H, m, H<sub>B</sub> - 1), 2.43 (1H, m, H<sub>A</sub> - 2), 2.60 (1H, m, H<sub>B</sub> - 2), 2.92 (1H, m, H - 15), 3.12 (2H, m,  $\beta$ H - 7), 3.72 (2H, d,  $J = 8$  Hz, CH<sub>2</sub> - 16), 4.83 (1H, ddd,  $J = 16, 4, 2$  Hz, H<sub>A</sub> - 19), 5.02 (1H, ddd,  $J = 16, 2, 2$  Hz, H<sub>B</sub> - 19), 7.06 (1H, d,  $J = 2$  Hz, H - 14), 7.11 (1H, dd,  $J = 8, 2$ , Hz, H - 12), 7.30 (1H, d,  $J = 8$  Hz, H - 11); MS [ $m/z$ ]: 328 (M<sup>+</sup>), 310, 297, 280 (base peak), 251; HRMS calcd. for C<sub>20</sub>H<sub>24</sub>O<sub>4</sub>: 328.1675; Found: 328.1675. *Anal.* calcd. for C<sub>20</sub>H<sub>24</sub>O<sub>4</sub>: C 73.14, H 7.37; Found C 73.00, H 7.50

**7 $\alpha$ ,15,19-Trihydroxy-18 (4->3) abeo-abieta-3,8,11,13-tetraen-18-oic  
Acid Lactone (108) (7 $\alpha$ ,15-Dihydroxybutenolide)**



**108** was obtained as white powder (hexanes - acetone 5:1), mp 193-195°;  $[\alpha]^{19.3}_D +24.9^\circ$  ( $c = 1.00$ ,  $\text{CHCl}_3$ ); IR  $\nu_{\text{max}}$  ( $\text{CHCl}_3$ ): 3460, 2990, 1750  $\text{cm}^{-1}$ ; UV  $\lambda_{\text{max}}$  (MeOH) ( $\log e$ ): 216 (4.35) nm;  $^1\text{H}$  NMR ( $\text{CDCl}_3$ )  $\delta$ : 1.00 (3H, s,  $\text{CH}_3$  - 20), 1.60 (6H, s,  $\text{CH}_3$  - 16 and 17), 1.77 (1H, m,  $\text{H}_A$  - 1), 2.19 (2H, m,  $\text{H}_A$  - 6), 2.42 (1H, ddd,  $J = 12, 12, 5$  Hz,  $\text{H}_B$  - 6), 2.51 (1H, m,  $\text{H}_B$  - 1), 2.54 (1H, m,  $\text{H}_B$  - 2), 3.20 (1H, brd,  $J = 12$  Hz, H - 6), 4.78 (1H, brd,  $J = 16$  Hz,  $\text{H}_A$  - 19), 4.88 (1H, brd,  $J = 16$  Hz,  $\text{H}_B$  - 19), 4.92 (1H, dd,  $J = 5, 1$  Hz,  $\beta\text{H}$  - 7), 7.24 (1H, d,  $J = 2$  Hz, H - 14), 7.32 (1H, d,  $J = 8$  Hz, H - 11), 7.39 (1H, dd,  $J = 8, 2$  Hz, H - 12); MS [ $m/z$ ]: 328 ( $\text{M}^+$ ), 313, 310, 295, 292, 277 (base peak); HRMS calcd. for  $\text{C}_{20}\text{H}_{24}\text{O}_4$ : 328.1675; Found 328.1667.

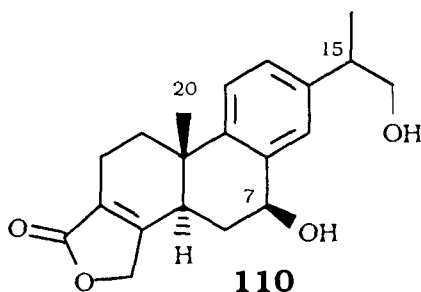
**7 $\beta$ ,15,19-Trihydroxy-18 (4->3) abeo-abieta-3,8,11,13-tetraen-18-oic  
Acid Lactone (109) (7 $\beta$ ,15-Dihydroxybutenolide)**





**109** was obtained as white powder (hexanes - acetone 5:1), mp 92-95°;  $[\alpha]^{19.3}_D +41.1^\circ$  ( $c = 1.00$ ,  $\text{CHCl}_3$ ); IR  $\nu_{\text{max}}$  ( $\text{CHCl}_3$ ): 3450, 2950, 1740  $\text{cm}^{-1}$ ; UV  $\lambda_{\text{max}}$  (MeOH) ( $\log \epsilon$ ): 216 (4.39) nm;  $^1\text{H}$  NMR ( $\text{CDCl}_3$ )  $\delta$ : 1.12 (3H, s,  $\text{CH}_3$  - 20), 1.61 (6H, s,  $\text{CH}_3$  - 16 and 17), 1.70 (1H, m,  $\text{H}_A$  - 1), 1.95 (1H, ddd,  $J = 12, 12, 8$  Hz,  $\text{H}_A$  - 6), 2.35 (1H, ddd,  $J = 12, 8, 2$  Hz,  $\text{H}_B$  - 6), 2.39 (1H, m,  $\text{H}_A$  - 2), 2.51 (1H, m,  $\text{H}_B$  - 1), 2.53 (1H, m,  $\text{H}_B$  - 2), 2.82 (1H, brd,  $J = 12$  Hz,  $\text{H}_B$  - 19), 5.03 (1H, dd,  $J = 8, 8$  Hz,  $\alpha\text{H}$  - 7), 7.32 (1H, d,  $J = 8$  Hz, H - 11), 7.42 (1H, dd,  $J = 8, 2$  Hz, H - 12), 7.71 (1H,  $J = 2$  Hz, H - 14); MS [ $m/z$ ]: 328 ( $\text{M}^+$ ), 313, 310, 295, 292, 277 (base peak); HRMS calcd. for  $\text{C}_{20}\text{H}_{24}\text{O}_4$ ; 328.1675; Found: 328.1669.

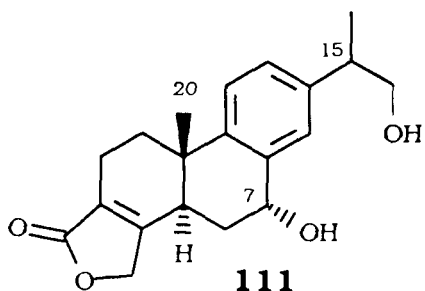
**7 $\beta$ ,16,19-Trihydroxy-18 (4->3) abeo-abieta-3,8,11,13-tetraen-18-oic Acid Lactone (110) (7 $\beta$ ,16-Dihydroxybutenolide)**



**110** was obtained as a white powder (hexanes - acetone 5:1), mp 93-95°;  $[\alpha]^{19.3}_D +63.8^\circ$  ( $c = 1.00$ ,  $\text{CHCl}_3$ ); IR  $\nu_{\text{max}}$  ( $\text{CHCl}_3$ ): 3445, 2945, 1745  $\text{cm}^{-1}$ ; UV  $\lambda_{\text{max}}$  (MeOH) ( $\log \epsilon$ ): 216 (4.34) nm;  $^1\text{H}$  NMR ( $\text{CDCl}_3$ )  $\delta$ : 1.12 (3H, s,  $\text{CH}_3$  - 20), 1.29 (3H, d,  $J = 8$  Hz,  $\text{CH}_3$  - 17), 1.70 (1H, m,  $\text{H}_A$  - 1), 1.94 (1H, ddd,  $J = 13, 13, 4$  Hz,  $\text{H}_A$  - 6), 2.32 (1H, ddd,  $J = 13, 8, 2$  Hz,  $\text{H}_B$  - 6), 2.40 (1H, m,  $\text{H}_A$  - 2), 2.50 (1H, m,  $\text{H}_B$  - 1), 2.52 (1H, m,  $\text{H}_B$  - 2), 2.98 (1H, m, H - 15), 2.80 (1H, brd,  $J = 13$  Hz, H - 5), 3.72 (2H, d,  $J =$

8 Hz, CH<sub>2</sub> - 16), 4.75 (1H, brd, *J* = 16 Hz, H<sub>A</sub> - 19), 4.84 (1H, brd, *J* = 16 Hz, H<sub>B</sub> - 19), 5.00 (1H, dd, *J* = 8, 8 Hz, αH - 7), 7.18 (1H, dd, *J* = 8, 2 Hz, H - 12), 7.31 (1H, d, *J* = 8 Hz, H - 11), 7.45 (1H, d, *J* = 2 Hz, H - 11); MS [*m/z*]: 328 (M<sup>+</sup>), 310, 297 (base peak); HRMS calcd. for C<sub>20</sub>H<sub>24</sub>O<sub>4</sub>, 328.1675; Found 328.1675.

**7α,16,19-Trihydroxy-18 (4->3) abeo-abieta-3,8,11,13-tetraen-18-oic Acid Lactone (111) (7α,16-Dihydroxybutenolide)**



**111** was obtained as a white powder (hexanes - acetone 5:1) mp 83-85°; [ $\alpha$ ]<sup>19.3</sup><sub>D</sub> +42.1° (*c* = 1.00, CHCl<sub>3</sub>); IR  $\nu_{\max}$  (CHCl<sub>3</sub>): 3440, 2950, 1740 cm<sup>-1</sup>; UV  $\lambda_{\max}$  (MeOH) (log  $\epsilon$ ): 217 (4.52) nm; <sup>1</sup>H NMR (CDCl<sub>3</sub>)  $\delta$ : 1.00 (3H, s, CH<sub>3</sub> - 20), 1.30 (3H, d, *J* = 8 Hz, CH<sub>3</sub> - 17), 1.74 (1H, m, H<sub>A</sub> - 1), 2.01 (1H, d, *J* = 13 Hz, H<sub>A</sub> - 6), 2.17 (1H, ddd, *J* = 13, 13 4 Hz, H<sub>B</sub> - 6), 2.41 (1H, m, H<sub>A</sub> - 2), 2.52 (1H, m, H<sub>B</sub> - 1), 2.55 (1H, m, H<sub>B</sub> - 2), 2.96 (1H, m, H - 15), 3.19 (1H, brd, *J* = 13 Hz, H - 5), 3.74 (2H, d, *J* = 8 Hz, H<sub>2</sub> - 16), 4.75 (1H, brd, *J* = 16 Hz, H<sub>A</sub> - 19), 4.89 (1H, brd, *J* = 16 Hz, H<sub>B</sub> - 19), 4.92 (1H, br. s, βH - 7), 7.21 (1H, dd, *J* = 8, 2 Hz, H - 12), 7.27 (1H, d, *J* = 2 Hz, H - 14), 7.37 (1H, d, *J* = 8 Hz, H - 11); MS [*m/z*]: 328 (M<sup>+</sup>), 310, 297 (base peak); HRMS calcd. for C<sub>20</sub>H<sub>24</sub>O<sub>4</sub>: 328.1675; Found: 328.1676.

## **7.2.4 Experimental Procedures for Biotransformation of Isotriptophenolide (86) by *Cunninghamella echinulata* and Triptophenolide (12) by *Cunninghamella elegans***

### **Fungal Material**

The following strains were able to oxidize and glucosylate **86** and **12**: *Cunninghamella echinulata* (ATCC#9244) and *Cunninghamella elegans* var. *chibaensis* Kuwabara et Hoshino (ATCC#20230).

### **Growth Conditions**

Fungi were stored on potato dextrose agar slants under sterile mineral oil. Erlenmeyer flasks were inoculated with 1 ml of spore suspension ( $2 \times 10^8$  spores/ml) prepared from 7 slants in distilled water to obtain a final spore concentration of  $2.5 \times 10^6$  spores/ml. The ratio of flask volume to medium volume was 5:1. *C. echinulata* spores were inoculated into SSBF medium (1.8 L) (see below) containing glucose (2%) and the culture was grown for 48 h at 28° C, 240 rpm on a rotary shaker. *C. elegans* spores were inoculated into MNB medium (2.0 L) (see below) containing glucose (1%) and the culture grown under the same conditions as for *C. echinulata*. Compounds **86** or **12** were dissolved in EtOH (final volumes of EtOH were not more than 2% of the total medium volume) and added to the culture and further incubated for another 48 hours. The composition of the media used for filamentous fungi were: SSBF: glucose (2%), soya bean flour containing 1% fat (0.5%), NaCl (0.5%),  $\text{KH}_2\text{PO}_4$  (0.5%), yeast extract (0.5%), pH 7.0; MNB: glucose (1%), malt extract (2%), nutrient broth (0.8%), pH 6.2. The ethyl acetate

extracts of cell suspensions of separate broth and mycelia fractions were analyzed for metabolites of compounds **86** and **12** by TLC and the individual products purified as described below.

### **Isolation and Purification of Metabolites**

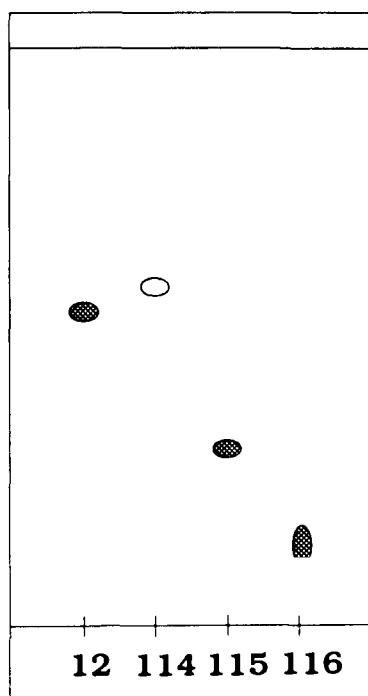
#### i) Conversion of **86** by *C. echinulata*

After 48 hours of biotransformation of isotriptophenolide (**86**) (180 mg, 579  $\mu$ mol) in SSBF medium (1.8 L), the broth and mycelia were separated by filtration through Miracloth, extracted separately with ethyl acetate (3x500 mL), the extracts were then combined and dried over  $\text{Na}_2\text{SO}_4$  and evaporated under vacuum. The crude residue (356 mg) was dissolved in  $\text{CHCl}_3$ :MeOH (95:5) and chromatographed on Silica gel 60 (230-400 mesh). The product **112** from this separation was examined by TLC (mobile phase:  $\text{CHCl}_3$ :MeOH, 4:1). **112** had an  $R_f$  value of 0.44. The above column fraction was further purified by radial chromatography using  $\text{CHCl}_3$ : MeOH (9:1). The yield of **112** from 180 mg of starting material **86** was 145 mg (80%) and 17 mg (9%) of unreacted compound **86** was also recovered. Overall recovery was 89%.

#### ii) Conversion of **12** by *C. elegans*

Triptophenolide (**12**) (200 mg, 641  $\mu$ mol) was dissolved in ethanol (20 mL) and added directly to MNB medium (2.0 L) containing 48-h growing culture of *C. elegans* with pH 4.2. (0.1 mg/ml) which had been inoculated from a spore suspension. The culture was further incubated for 48 h at 240 rpm and 28°C. After this period, the cell suspension was filtered through Miracloth in a Buchner funnel and the filtrate and mycelia were extracted separately with ethyl acetate (3 x 1.0 L). The combined extracts were dried over anhydrous sodium sulphate.

Figure 30. Thin Layer Chromatogram of the Metabolites Isolated from Biotransformation of **12** by *C. elegans* (Schematic Presentation).



Legend:

Triptophenolide (**12**)

Triptoquinone (**114**)

5 $\alpha$ ,14-Dihydroxybutenolide (**115**)

14- $\beta$ -Glucosyl Triptophenolide (**116**)

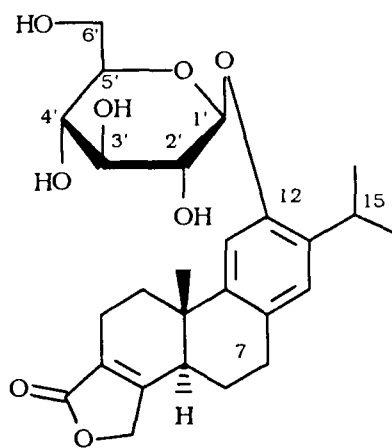
This material was concentrated under vacuum to yield a crude extract (229 mg). The latter extract was chromatographed on silica gel with hexane: ethyl acetate (4:1) followed by chloroform:methanol (95:5) to afford 2 fractions. Fr. 1 (hexanes : ethyl acetate 4:1) yielded compounds **114** and **115**. Final purification was performed by radial chromatography with hexane:EtOAc 4:1. Fr. 2 (CHCl<sub>3</sub>:MeOH 95:5)

yielded compound **116**. The products from this separation were examined by TLC (mobile phase: ethyl acetate:hexane, 3:2). The  $R_f$  values were as follows: **12** - 0.56, **114** - 0.60, **115** - 0.31 and **116** - 0.15 (Figure 30). The following yields were obtained: **12** (54 mg, 27 %), **114** (73 mg, 35 %), **115** (26 mg, 12 %), **116** (14 mg, 5 %). The total recovery from the broth and cells was 79 %.

### Identification of Metabolites

The physical properties of the metabolites obtained from the biotransformation of **86** and **12** by *C. echinulata* and *C. elegans* are as follows:

#### **12- $\beta$ -Glucosyl-19-hydroxy-18 (4->3) abeo-abietic-3,8,11,13-tetraen-18-oic Acid Lactone (112) (12- $\beta$ -Glucosyl Isotriptophenolide)**

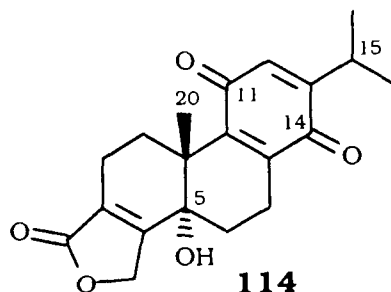


**112**

12- $\beta$ -Glucosyl isotriptophenolide (**112**) was obtained as colorless plate-like crystals ( $\text{CHCl}_3/\text{MeOH}$ ): mp 138 - 139 $^\circ$ ; UV  $\lambda_{\text{max}}$  (MeOH) (log  $\epsilon$ ): 220 (4.25), 276 (0.88) nm; IR  $\nu_{\text{max}}$ : ( $\text{CH}_3\text{COCH}_3$ ) 3486, 2632, 1763, 1702, 1424, 1369, 1233, 1048  $\text{cm}^{-1}$ ;  $^1\text{H}$  NMR ( $\text{CD}_3\text{COCD}_3$ , 400 MHz)  $\delta$ :

1.02 (3H, s, CH<sub>3</sub>-20), 1.18 (6H, d,  $J = 7$  Hz, CH<sub>3</sub>-16 and 17), 1.69 (1H, ddd,  $J = 7, 12, 12$  Hz, H<sub>A</sub>-1), 1.85 - 1.98 (2H, m, H-6), 2.26-2.40 (1H, m,  $\beta$ H-2), 2.55 (1H, dd,  $J = 7, 7$  Hz,  $\alpha$ H-2), 2.58 - 2.63 (1H, m, H<sub>B</sub>-1), 2.71 (1H, brd,  $J = 11$  Hz, H-5), 2.87 - 2.94 (2H, m, H-7), 3.42 (1H, septet,  $J = 7$  Hz, H-15), 3.48-3.50 (2H, m, H-6'), 3.52 (1H, m, H-2'), 3.59 (1H, dd,  $J = 3, 11$  Hz, H-5'), 3.68 (1H, dd,  $J = 6, 14$  Hz, H-3'), 3.89 (1H, s, D<sub>2</sub>O+, OH-6'), 3.90 (1H, dd,  $J = 6, 11$  Hz H-4'), 4.19 (1H, s, D<sub>2</sub>O+, OH-2'), 4.27 (1H, s, D<sub>2</sub>O+, OH-3'), 4.42 (1H, s, D<sub>2</sub>O+, OH-4'), 4.85 (2H, m, H-19), 4.93 (1H, d,  $J = 7$  Hz, H-1'), 6.94 (1H, s, H-14), 7.18 (1H, s, H-11); <sup>13</sup>C NMR (CDCl<sub>3</sub>, 75 MHz)  $\delta$ : 18.9, 20.7, 22.4, 23.2, 23.4, 26.8, 28.5, 33.2, 37.2, 42.3, 62.8, 71.0, 71.6, 74.8, 77.7, 78.3, 102.7, 112.4, 124.8, 127.5, 129.0, 136.24, 144.6, 154.1, 164.4, 174.2; CIMS [ $m/z$ ]: 492 ([M.NH<sub>4</sub>]<sup>+</sup>), 475 ([M.H]<sup>+</sup>), 459 (base peak), 330, 313, 297, 282, 254, 224, 198, 180, 162; CIHRMS calcd. for C<sub>26</sub>H<sub>35</sub>O<sub>8</sub>: ([M.H]<sup>+</sup>): 475.2332; Found: 475.2337.

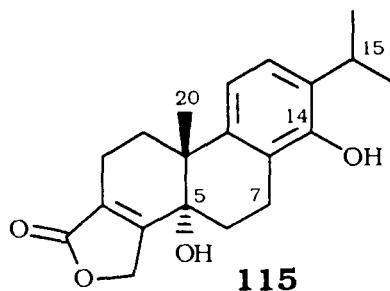
**19-Hydroxy-11,14-dioxo-18 (4->3) abeo-abieta-3,8,12-trien-18-oic Acid Lactone (114) (Triptoquinone)**



Triptoquinone (**114**) was obtained as yellow crystals (hexanes:EtOAc): mp 55-58°;  $[\alpha]_D^{20} +121.6^\circ$  ( $c = 1.00$ , CHCl<sub>3</sub>); UV  $\lambda_{max}$  (MeOH) ( $\log \epsilon$ ): 348 (0.09), 261 (2.06), 227 (3.01), 199 (2.45) nm; IR  $\nu_{max}$ :

(CHCl<sub>3</sub>) 2929, 1756, 1680, 1649, 755 cm<sup>-1</sup>; <sup>1</sup>H NMR (CDCl<sub>3</sub>, 400 MHz) δ: 1.10 (6H, d, *J* = 7 Hz, CH<sub>3</sub>-16 and 17), 1.14 (3H, s, CH<sub>3</sub>-20), 1.47 (1H, m, H<sub>A</sub>-1), 1.69 (1H, m, H<sub>A</sub>-6), 1.87 (1H, m, H<sub>B</sub>-6), 2.39 (2H, m, H-2), 2.48 (1H, ddd, *J* = 4, 8, 12 Hz, H<sub>A</sub>-7), 2.60 (1H, br d, *J* = 10 Hz, H-5), 2.78 (1H, dd, *J* = 8, 12 Hz, H<sub>B</sub>-7), 3.00 (1H, septet, *J* = 7, 1 Hz, H-15), 3.10 (1H, m, H<sub>B</sub>-1), 4.72 (1H, brd, *J* = 16 Hz, H<sub>A</sub>-19), 4.81 (1H, br d, *J* = 16 Hz, H<sub>B</sub>-19), 6.40 (1H, s, H-12); <sup>13</sup>C NMR (CDCl<sub>3</sub>, 75 MHz) δ: 18.3, 18.6, 21.2, 21.2, 24.7, 26.4, 30.7, 30.8, 36.6, 42.3, 70.1, 125.4, 131.6, 142.5, 147.6, 153.4, 161.3, 173.7, 187.1, 187.4; MS [*m/z*]: 326 (M<sup>+</sup>) (base peak), 311, 298, 283, 267, 253, 239; HRMS calcd. for C<sub>20</sub>H<sub>22</sub>O<sub>4</sub>: 326.1518; Found: 326.1523.

**5 $\alpha$ ,14,19-Trihydroxy-18 (4 $\rightarrow$ 3) abeo-abieta-3,8,11,13-tetraen-18-oic Acid Lactone (115) (5 $\alpha$ ,14-Dihydroxybutenolide)**

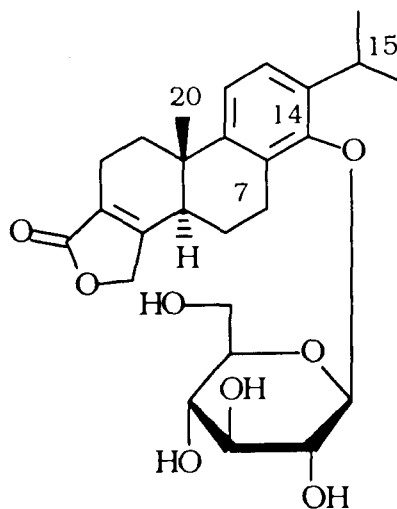


5 $\alpha$ ,14-Dihydroxybutenolide (**115**) was obtained as fine colorless prisms (hexane/acetone): mp 190-191°; [ $\alpha$ ]<sub>D</sub><sup>20</sup> -58.8° (*c* = 0.32, CH<sub>3</sub>OH); UV  $\lambda$ <sub>max</sub> (MeOH) (log  $\epsilon$ ): 223 (3.86), 282 (3.55) nm; IR  $\nu$ <sub>max</sub>: (CHCl<sub>3</sub>) 3607, 3560, 3020, 2973, 1756, 1430, 1240, 1180 cm<sup>-1</sup>; <sup>1</sup>H NMR (CDCl<sub>3</sub>, 400 MHz) δ: 1.09 (3H, s, CH<sub>3</sub>-20), 1.25, 1.27 (3H each, both d, *J* = 7 Hz, CH<sub>3</sub>-16 and 17), 1.90 (1H, s, D<sub>2</sub>O<sup>+</sup>, OH-5), 1.98-2.15 (2H, m,  $\alpha$ H-1 and



$\alpha$ H-6), 2.23 (1H, ddd,  $J = 9, 9, 14$  Hz,  $\beta$ H-6), 2.31 (1H, dd,  $J = 6, 13$  Hz,  $\beta$ H-1), 2.39 (1H, m,  $\beta$ H-2), 2.55 (1H, br d,  $J = 16$  Hz,  $\alpha$ H-2), 2.80-3.02 (2H, m, H-7), 3.08 (1H, septet,  $J = 7$  Hz, H-15), 4.80 (1H, s, OH-14), 4.90 (2H, br d, AB<sub>q</sub>, Dn = 0.19 ppm,  $J = 17$  Hz, H-19), 6.91 (1H, d,  $J = 8$  Hz, H-11), 7.08 (1H, d,  $J = 8$  Hz, H-12); <sup>13</sup>C NMR (CDCl<sub>3</sub>, 75 MHz)  $\delta$ : 18.0, 18.3, 22.5, 22.6, 25.4, 26.2, 26.3, 26.9, 41.3, 69.2 (C - 19), 69.8 (C - 5), 117.1, 119.7, 124.1, 127.1, 131.4, 140.4, 150.7, 160.9, 173.8; MS [ $m/z$ ]: 328 (M<sup>+</sup>), 310, 295, 267, 253 (base peak), 165, 147; HRMS calcd. for C<sub>20</sub>H<sub>24</sub>O<sub>4</sub>: 328.1674; Found: 328.1675.

**14- $\beta$ -glucosyl-19-hydroxy-18 (4->3) *abeo*-abieta-3,8,11,13-tetraen-18-oic-acid Lactone (116) (14- $\beta$ -Glucosyl Triptophenolide)**



**116**

14- $\beta$ -Glucosyl triptophenolide (**116**) was obtained as colorless fine crystals (CHCl<sub>3</sub>/CH<sub>3</sub>OH): mp 139-141°; UV  $\lambda_{\text{max}}$  (CH<sub>3</sub>OH) (log  $\epsilon$ ): 195 (0.58), 217 (2.66), 270 (0.89) nm; IR  $\nu_{\text{max}}$ : (CH<sub>3</sub>COCH<sub>3</sub>) 3608, 3005, 1713, 1422, 1364, 1223, 1093, 904 cm<sup>-1</sup>; <sup>1</sup>H NMR (CD<sub>3</sub>COCD<sub>3</sub>, 400 MHz)  $\delta$ : 1.02 (3H, s, CH<sub>3</sub>-20), 1.13 (3H, d,  $J = 7$  Hz, CH<sub>3</sub>-16), 1.17 (3H, d,

$J = 7$  Hz, CH<sub>3</sub>-17), 1.68 (1H, ddd,  $J = 7, 12, 12$  Hz, H<sub>A</sub>-1), 1.86 (2H, m, H-6), 2.35 (1H, m, βH-2), 2.35 (1H, dd,  $J = 6, 12$  Hz, H<sub>B</sub>-1), 2.56 (1H, dd,  $J = 6, 7$  Hz, αH-2), 2.67 (1H, dd,  $J = 2, 14$  Hz, H-5), 3.03-3.11 (1H, dd,  $J = 7, 17$  Hz, H<sub>A</sub>-7), 3.17-3.21 (2H, m, H-4' and H-6'), 3.22-3.32 (1H, dd,  $J = 9, 17$  Hz, H<sub>B</sub>-7), 3.43-3.57 (3H, m, H-2', H-3' and H-6'), 3.62-3.68 (1H, m, H-5'), 3.65 (1H, s, D<sub>2</sub>O+, OH-6'), 3.66 (1H, septet,  $J = 5$  Hz, H-15), 4.17 (1H, s, D<sub>2</sub>O+, OH-2'), 4.26 (1H, s, D<sub>2</sub>O+, OH-3'), 4.60 (1H, s, D<sub>2</sub>O+, OH-4'), 4.71 (1H, d,  $J = 7$  Hz, H-1'), 4.85 (2H, m, H-19), 7.13 (1H, d,  $J = 8$  Hz, H-12), 7.21 (1H, d,  $J = 8$  Hz, H-11); <sup>13</sup>C NMR (CDCl<sub>3</sub>, 75 MHz) δ: 18.8, 20.3, 22.1, 24.0, 24.1, 26.0, 29.8, 33.5, 37.1, 41.8, 62.9, 71.0, 71.6, 75.6, 77.4, 78.1, 105.8, 110.6, 121.5, 124.5, 129.3, 140.6, 145.1, 153.0, 164.4, 172.5; CIMS [ $m/z$ ]: 492 ([M.NH<sub>4</sub>]<sup>+</sup>), 475 ([M.H]<sup>+</sup>), 330 (base peak), 313, 297, 197, 180; CIHRMS calcd. for C<sub>26</sub>H<sub>35</sub>O<sub>8</sub> ([M.H]<sup>+</sup>): 475.2332; Found: 475.2339.

### **7.2.5 Experimental Procedure for Immobilization of *C. elegans* in Polyurethane Foam**

#### **Growth Conditions**

Orange reticulated polyurethane foam was obtained from UBC (Scotfoam Corp., Eddystone, Pa., USA). The average pore size was 790 μm in diameter. Before use, the foam was washed in soapy water, rinsed (in tap water, then 70% ethanol, then distilled water) and cut into 1 cm<sup>3</sup> cubes. Usually, four cubes were added in culture medium (50 mL) prior to autoclaving. The culture medium used in this case was MNB, containing (g/L) as follows: glucose (10 g), malt extract (20 g), and nutrient broth (8 g), pH 6.2. The flasks containing medium and foam

were inoculated with spore suspension of  $2 \times 10^6$  spores/mL of *C. elegans* and were grown for 48 h at 28° C and 220 rpm on a rotary shaker. After 48 h, the foam-immobilized mycelia were aseptically washed and resuspended in sterile citrate buffer (0.05M, 50 mL, pH 4.4). The substrate **12** (5 mg) was dissolved in ethanol (1.0 mL) and added to the flask containing the immobilized mycelia (0.1 mg/mL).

### **Metabolite Formation**

The biotransformation of triptophenolide **12** was monitored by TLC (mobile phase: hexanes:EtOAc, 6:4). After 48 h incubation time, the broth was removed by decanting and extracted with ethyl acetate (2 x 25 mL). TLC investigation of the extract revealed the presence of metabolites **114**, **115**, and **116**.

In order to establish whether enzymatic activity was maintained, the cubes were washed with citrate buffer under aseptic conditions and again resuspended in fresh citrate buffer (50 mL). A new addition of **12** (5 mg) dissolved in ethanol (1 mL) was made and the above incubation (48 h) was repeated. Isolation of metabolites and TLC investigation revealed the same spectrum of metabolites **114-116**. This process was repeated seven times and it was clear that enzymatic activity remained throughout the study.

In conclusion, the foam-entrapped mycelia were not affected by washing and shaking and, furthermore, maintained enzymatic activity for more than 30 days. Due to unavailability of substrate **12**, further experiments were not performed so it was not possible to determine how long the enzymatic activity could have been maintained within the immobilized system.

## **7.2.6 Experimental Procedure for Optimization of Triptoquinone**

### **(114) Production by Factorial Design Experiment**

#### **Basic Experiment**

The experiment which varied the different factors (low and high levels, Table 6) was described in Chapter 4. The incubation time, and concentrations of glucose, nutrient broth and malt extract which were used in this experiment are shown as the "middle" levels in Table 6. These levels allowed the metabolite, triptoquinone (**114**), to be produced in 35% yield. The studies described below summarize the factor variations which eventually afforded **114** in 70% yield.

#### **Media Preparation**

Utilizing the MNB medium, 15 different medium compositions were prepared, in which the components were varied according to the variations shown in Table 7. Stock solution of glucose (10 g), Difco nutrient broth (10 g), and Difco malt extract (25 g) were dissolved in distilled water and made up to 100 mL, 100 mL and 250 mL respectively. The actual medium preparations for the first factorial design experiment consisted of 15 media which are listed in Table 15.

Table 15. Medium Preparation for the First Factorial Design Experiment.

Medium composition #	Concentration in the medium			Volume of stock solution			Added water up to 20 mL
	Glucose (g/L)	Nutrient broth (g/L)	Malt extract (g/L)	Glucose (mL)	Nutrient broth (mL)	Malt extract (mL)	
1	20.0	16.0	40.0	4.00	3.20	8.00	4.80
2	20.0	16.0	2.0	4.00	3.20	0.40	12.40
3	20.0	0.8	40.0	4.00	0.16	8.00	7.84
4	20.0	0.8	2.0	4.00	0.16	0.40	15.44
5	1.0	16.0	40.0	0.20	3.20	8.00	8.60
6	1.0	16.0	2.0	0.20	3.20	0.40	16.20
7	1.0	0.8	40.0	0.20	0.16	8.00	11.54
8	1.0	0.8	2.0	0.20	0.16	0.40	19.24
9	10.5	8.4	21.0	2.10	1.68	4.20	12.02
10	20.0	8.4	21.0	4.00	1.68	4.20	10.12
11	1.0	8.4	21.0	0.20	1.68	4.20	13.92
12	10.5	16.0	21.0	2.10	3.20	4.20	10.50
13	10.5	0.8	21.0	2.10	0.16	4.20	13.54
14	10.5	8.4	40.0	2.10	1.68	8.00	8.22
15	10.5	8.4	2.0	2.10	1.68	0.40	15.82

Each medium was prepared by mixing the appropriate volume of the stock solutions and distilled water up to 20 mL in total and the pH was adjusted with 0.1 M NaOH or 0.1 M HCl to 6.2 prior to autoclaving. Four flasks of each medium compositions were prepared (one as control, and three as samples). Erlenmeyer flasks with the medium variations were inoculated with 0.5 mL of spore suspension ( $2 \times 10^8$  spores/mL) prepared from 9 slants in distilled water to obtain a final spore suspension of  $2.5 \times 10^6$  spores/mL. The cultures were grown for 48 h prior to addition of the substrate **12**. The substrate was added as 0.2% ethanolic solution to the cultures to obtain a concentration of 0.1 mg/mL and incubated for a further 72 h.

The medium variations for the second factorial design experiment were chosen to represent conditions close to the expected optimum (evaluated from the mathematical model) of triptoquinone (**114**) production based on the result of the first factorial design experiment. The different concentrations of MNB medium for the second experiment are shown in Table 12. These media were prepared according to the procedure for the first factorial design experiment and are presented in Table 16.

### **HPLC Analyses**

Aliquots were taken in intervals of 12 h and analyzed by HPLC to determine the substrate depletion and product formation.

Table 16. Medium Preparation for the Second Factorial Design Experiment.

Medium composition #	Concentration in the medium			Volume of stock solution			Added water up to 20 mL
	Glucose (g/L)	Nutrient broth (g/L)	Malt extract (g/L)	Glucose (mL)	Nutrient broth (mL)	Malt extract (mL)	
1	8.0	8.0	35.0	1.60	1.60	7.00	9.80
2	8.0	8.0	25.0	1.60	1.60	5.00	11.80
3	8.0	4.0	35.0	1.60	0.80	7.00	10.60
4	8.0	4.0	25.0	1.60	0.80	5.00	12.60
5	3.0	8.0	35.0	0.60	1.60	7.00	10.80
6	3.0	8.0	25.0	0.60	1.60	5.00	12.80
7	3.0	4.0	35.0	0.60	0.80	7.00	11.60
8	3.0	4.0	25.0	0.60	0.80	5.00	13.60
9	5.5	6.0	30.0	1.10	1.20	6.00	11.70
10	8.0	6.0	30.0	1.60	1.20	6.00	11.20
11	3.0	6.0	30.0	0.60	1.20	6.00	12.20
12	5.5	8.0	30.0	1.10	1.60	6.00	11.30
13	5.5	4.0	30.0	1.10	0.80	6.00	12.10
14	5.5	6.0	35.0	1.10	1.20	7.00	10.70
15	5.5	6.0	25.0	1.10	1.20	5.00	12.70

## Materials

A Resolve C<sub>18</sub>, 5 μm Waters reverse phase column (100 x 8 mm) equipped with Waters Resolve C<sub>18</sub> Guard-Pak pre-column was used in all separations. An isocratic gradient at a flow rate of 1.5 mL/min for the mobile phase: H<sub>2</sub>O (55.3%), MeOH (29.7%) and MeCN (15%) containing AcOH (0.1%) was used. The total analytical run for each sample was 45 min. HPLC grade methanol and acetonitrile, distilled water and reagent grade acetic acid were used. All solvents were filtered through a 0.45 μm HVLP Millipore membrane, except the water for which a 0.45 μm HA Millipore membrane was used.

## Standard Compounds

Triptophenolide (**12**) was prepared from chemical synthesis (see Chapter VII). The products **114**, **115** and **116** were obtained from biotransformation experiments by *C. elegans* (see Chapter III), isolated and purified, using column chromatography on silica gel. The solutions of standards (**12**, **114**, **115** and **116**) were prepared in a mixture of CH<sub>3</sub>OH:MeCN:H<sub>2</sub>O (29.7%:15%:55.3%) to give a 80 μg/mL concentration of each compound. For the standard curves illustrated in Chapter IV, 5-150 μL volumes of these solutions were injected.

## Sample Preparation for HPLC Analyses

Periodically (every 12 h), an aliquot of broth (1.0 mL) was withdrawn from the control (without starting material), as well as from the sample (starting material present). The aliquots were mixed well with



methanol (1.0 mL) and then filtered through a 0.45  $\mu\text{m}$  HVLP Millipore membrane from which a 50  $\mu\text{L}$  volume was analyzed by HPLC.

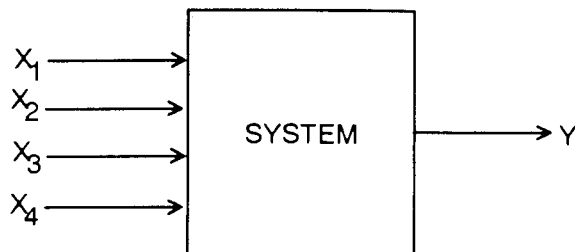
## APPENDIX. FACTORIAL DESIGN

The application of factorial design in the present study is discussed below. Details on this method are provided in a number of books (Quenouille 1953; Davies 1956; Raktoc *et al.* 1981; Petersen 1985; Deming & Morgan 1987).

Each process variable (parameter of the experiment) is called a factor.

A response variable (result or yield of the experiment in general) is a measure of process performance and depends on a number of factors (Figure 31).

Figure 31. Four-Factor, Single-Response System.



where:  $X_1$ ,  $X_2$ ,  $X_3$ ,  $X_4$  - factors

$X_1$  - time of biotransformation

$X_2$  - glucose concentration

$X_3$  - nutrient broth concentration

$X_4$  - malt extract concentration

$Y$  - yield

Each value of the response variable (result from a single experiment) is called an observation.

A response surface is the graph of a system response plotted against one or more of the system factors. It is assumed that all other controllable factors are held constant, each at a specified level, otherwise, the four-factor response surface might appear to change shape or to be excessively noisy. A response surface shows a system response, Y plotted against the system factors,  $X_1, X_2, X_3, X_4$ . If there is no uncertainty associated with the response, and if the response is known for all values of the factors, then the response surface might be described by some mathematical model M that relates the response Y to the factors  $X_1, X_2, X_3, X_4$ :

$$Y = M (X_1, X_2, X_3, X_4) \quad (8)$$

for example

$$Y_2 = - 10.1 + 1.34*X_1 + 0.950*X_2 + 1.24*X_3 + 0.543*X_4 - 0.00482*X_1*X_2 - 0.00337*X_1*X_3 - 0.0224*X_2*X_3 - 0.00870*X_2*X_4 - 0.0151*X_3*X_4 - 0.0126*X_1^2 - 0.0265*X_2^2 - 0.0414*X_3^2 - 0.00662*X_4^2 \quad (3)$$

Such a relationship (and corresponding response surface) might accurately represent yield Y as a function of conditions: biotransformation time and medium composition. If an adequate model is established it could be used to predict the outcome of an experiment at variable conditions. An adequate model is a model which describes the

already obtained experimental results with calculation error less than the experimental error.

It should be noted that there are theoretical and experimental models. A theoretical model is one which can be established on the basis of theoretical knowledge without performing experiments. An experimental model requires experimental information in order to be completed. Since there is insufficient theoretical information for quantification of the studied process of biotransformation of triptophenolide (**12**) by *C. elegans* (Chapter IV), an experimental model was used.

### A.1 Polynomial Models

Polynomial models are most commonly used to describe the interactions between the parameters and their influence on the outcome of a process/experiment. Such models generally involve a sum of expressions (Deming & Morgan 1987). The most common polynomial models are of linear, incomplete second, full second order.

a) A linear model is comprised of linear expressions  $a_i X_i$  and a constant  $a_0$ :

$$Y_{\text{calc}} = a_0 + a_1 X_1 + a_2 X_2 + a_3 X_3 + a_4 X_4 \quad (9)$$

b) Incomplete second order model contains a linear model plus expressions  $a_{i,j} X_i X_j$  where (i) is not equal to (j):

$$Y_{\text{calc}} = a_0 + a_1 X_1 + a_2 X_2 + a_3 X_3 + a_4 X_4 + a_{1,2} X_1 X_2 + a_{1,3} X_1 X_3 + a_{1,4} X_1 X_4 + a_{2,3} X_2 X_3 + a_{2,4} X_2 X_4 + a_{3,4} X_3 X_4 \quad (10)$$

c) Full second order model includes all possible second order expressions,  $a_{i,j}X_iX_j$ :

$$Y_{\text{calc}} = a_0 + a_1X_1 + a_2X_2 + a_3X_3 + a_4X_4 + a_{1,2}X_1X_2 + a_{1,3}X_1X_3 + a_{1,4}X_1X_4 + a_{2,3}X_2X_3 + a_{2,4}X_2X_4 + a_{3,4}X_3X_4 + a_{1,1}X_1^2 + a_{2,2}X_2^2 + a_{3,3}X_3^2 + a_{4,4}X_4^2 \quad (11)$$

where

$a_0, a_1, a_{1,1}$ , etc. are coefficients of the model (constants)

$X_1$  is a factor (parameter) value

$Y_{\text{calc}}$  is the calculated (predicted value) for the response variable.

(i), (j) are varied factor numbers (from 1 to 4 in case of four factors).

The full second order model can be used to calculate values of the response variable (i.e. to predict a result of one experiment) by choosing the conditions ( $X_1, X_2, X_3$  and  $X_4$ ). However, before an experimental model is used it is necessary to evaluate the coefficients of the model ( $a_0, a_1, a_{1,1}$ ).

## **A.2 Evaluation of the Coefficients in the Mathematical Model**

The coefficients  $a_0, a_1, a_{1,1}$ , etc. in the model should provide the best approximation of the experimental results when they are used in the mathematical model, that is the least difference between experimental and calculated values:

$$(Y_{\text{exp}} - Y_{\text{calc}}) \Rightarrow \text{minimum} \quad (12)$$

where

$Y_{\text{exp}}$  is an experimentally determined value.

After substitution of  $Y_{\text{calc}}$  with a full second order expression:

$$Y_{\text{calc}} = a_0 + a_1X_1 + a_2X_2 + a_3X_3 + a_4X_4 + a_{1,2}X_1X_2 + a_{1,3}X_1X_3 + a_{1,4}X_1X_4 + a_{2,3}X_2X_3 + a_{2,4}X_2X_4 + a_{3,4}X_3X_4 + a_{1,1}X_1^2 + a_{2,2}X_2^2 + a_{3,3}X_3^2 + a_{4,4}X_4^2 \quad (1)$$

will be obtained

$$(Y_{\text{exp}} - a_0 + a_1X_1 + a_2X_2 + a_3X_3 + a_4X_4 + a_{1,2}X_1X_2 + a_{1,3}X_1X_3 + a_{1,4}X_1X_4 + a_{2,3}X_2X_3 + a_{2,4}X_2X_4 + a_{3,4}X_3X_4 + a_{1,1}X_1^2 + a_{2,2}X_2^2 + a_{3,3}X_3^2 + a_{4,4}X_4^2) \Rightarrow \text{minimum} \quad (13)$$

The best values of the coefficients ( $a_0$ ,  $a_1$ ,  $a_2$  etc) are determined by the least squares method (minimum sum of the difference between each experimental and calculated value taken as its square):

$$\Sigma(Y_{\text{exp}} - a_0 + a_1X_1 + a_2X_2 + a_3X_3 + a_4X_4 + a_{1,2}X_1X_2 + a_{1,3}X_1X_3 + a_{1,4}X_1X_4 + a_{2,3}X_2X_3 + a_{2,4}X_2X_4 + a_{3,4}X_3X_4 + a_{1,1}X_1^2 + a_{2,2}X_2^2 + a_{3,3}X_3^2 + a_{4,4}X_4^2)^2 \Rightarrow \text{minimum} \quad (14)$$

where  $\Sigma$  is the sum for all experimental results used to determine the coefficients of the model. Solving this equation for each parameter will give the following system of equations:

$$\begin{aligned}
\Sigma d(Y_{\text{exp}} - Y_{\text{calc}})^2 / da_0 &= 0 \\
\Sigma d(Y_{\text{exp}} - Y_{\text{calc}})^2 / da_1 &= 0 \\
\Sigma d(Y_{\text{exp}} - Y_{\text{calc}})^2 / da_2 &= 0 \\
\Sigma d(Y_{\text{exp}} - Y_{\text{calc}})^2 / da_3 &= 0 \\
\Sigma d(Y_{\text{exp}} - Y_{\text{calc}})^2 / da_4 &= 0 \\
\Sigma d(Y_{\text{exp}} - Y_{\text{calc}})^2 / da_{1,2} &= 0 \\
\Sigma d(Y_{\text{exp}} - Y_{\text{calc}})^2 / da_{1,3} &= 0 \\
\Sigma d(Y_{\text{exp}} - Y_{\text{calc}})^2 / da_{1,4} &= 0 \\
\Sigma d(Y_{\text{exp}} - Y_{\text{calc}})^2 / da_{2,3} &= 0 \\
\Sigma d(Y_{\text{exp}} - Y_{\text{calc}})^2 / da_{2,4} &= 0 \\
\Sigma d(Y_{\text{exp}} - Y_{\text{calc}})^2 / da_{3,4} &= 0 \\
\Sigma d(Y_{\text{exp}} - Y_{\text{calc}})^2 / da_{1,1} &= 0 \\
\Sigma d(Y_{\text{exp}} - Y_{\text{calc}})^2 / da_{2,2} &= 0 \\
\Sigma d(Y_{\text{exp}} - Y_{\text{calc}})^2 / da_{3,3} &= 0 \\
\Sigma d(Y_{\text{exp}} - Y_{\text{calc}})^2 / da_{4,4} &= 0
\end{aligned}
\tag{15-29}$$

It should be noted, that:

the sum of the quadratic differences will only add up while if a sum of the differences is used then a negative and a positive difference would cancel;

the optimum of the function (best coefficients  $a_{i,j}$  could be determined when the function is differentiated with respect to each coefficient).

After substitution of  $Y_{\text{calc}}$  with the expression from Equation 1:





$$\Sigma d(Y_{\text{exp}} - a_0 + a_1X_1 + a_2X_2 + a_3X_3 + a_4X_4 + a_{1,2}X_1X_2 + a_{1,3}X_1X_3 + a_{1,4}X_1X_4 + a_{2,3}X_2X_3 + a_{2,4}X_2X_4 + a_{3,4}X_3X_4 + a_{1,1}X_1^2 + a_{2,2}X_2^2 + a_{3,3}X_3^2 + a_{4,4}X_4^2)^2 / da_{2,4} = 0$$

$$\Sigma d(Y_{\text{exp}} - a_0 + a_1X_1 + a_2X_2 + a_3X_3 + a_4X_4 + a_{1,2}X_1X_2 + a_{1,3}X_1X_3 + a_{1,4}X_1X_4 + a_{2,3}X_2X_3 + a_{2,4}X_2X_4 + a_{3,4}X_3X_4 + a_{1,1}X_1^2 + a_{2,2}X_2^2 + a_{3,3}X_3^2 + a_{4,4}X_4^2)^2 / da_{3,4} = 0$$

$$\Sigma d(Y_{\text{exp}} - a_0 + a_1X_1 + a_2X_2 + a_3X_3 + a_4X_4 + a_{1,2}X_1X_2 + a_{1,3}X_1X_3 + a_{1,4}X_1X_4 + a_{2,3}X_2X_3 + a_{2,4}X_2X_4 + a_{3,4}X_3X_4 + a_{1,1}X_1^2 + a_{2,2}X_2^2 + a_{3,3}X_3^2 + a_{4,4}X_4^2)^2 / da_{1,1} = 0$$

$$\Sigma d(Y_{\text{exp}} - a_0 + a_1X_1 + a_2X_2 + a_3X_3 + a_4X_4 + a_{1,2}X_1X_2 + a_{1,3}X_1X_3 + a_{1,4}X_1X_4 + a_{2,3}X_2X_3 + a_{2,4}X_2X_4 + a_{3,4}X_3X_4 + a_{1,1}X_1^2 + a_{2,2}X_2^2 + a_{3,3}X_3^2 + a_{4,4}X_4^2)^2 / da_{2,2} = 0$$

$$\Sigma d(Y_{\text{exp}} - a_0 + a_1X_1 + a_2X_2 + a_3X_3 + a_4X_4 + a_{1,2}X_1X_2 + a_{1,3}X_1X_3 + a_{1,4}X_1X_4 + a_{2,3}X_2X_3 + a_{2,4}X_2X_4 + a_{3,4}X_3X_4 + a_{1,1}X_1^2 + a_{2,2}X_2^2 + a_{3,3}X_3^2 + a_{4,4}X_4^2)^2 / da_{3,3} = 0$$

$$\Sigma d(Y_{\text{exp}} - a_0 + a_1X_1 + a_2X_2 + a_3X_3 + a_4X_4 + a_{1,2}X_1X_2 + a_{1,3}X_1X_3 + a_{1,4}X_1X_4 + a_{2,3}X_2X_3 + a_{2,4}X_2X_4 + a_{3,4}X_3X_4 + a_{1,1}X_1^2 + a_{2,2}X_2^2 + a_{3,3}X_3^2 + a_{4,4}X_4^2)^2 / da_{4,4} = 0 \quad (30-44)$$

which can be differentiated to:

$$\Sigma Y = na_0 + a_1\Sigma X_1 + a_2\Sigma X_2 + a_3\Sigma X_3 + a_4\Sigma X_4 + a_{1,2}\Sigma X_1X_2 + a_{1,3}\Sigma X_1X_3 + a_{1,4}\Sigma X_1X_4 + a_{2,3}\Sigma X_2X_3 + a_{2,4}\Sigma X_2X_4 + a_{3,4}\Sigma X_3X_4 + a_{1,1}\Sigma X_1^2 + a_{2,2}\Sigma X_2^2 + a_{3,3}\Sigma X_3^2 + a_{4,4}\Sigma X_4^2$$

$$\Sigma X_1Y = a_0\Sigma X_1 + a_1\Sigma X_1^2 + a_2\Sigma X_1X_2 + a_3\Sigma X_1X_3 + a_4\Sigma X_1X_4 + a_{1,2}\Sigma X_1^2X_2 + a_{1,3}\Sigma X_1^2X_3 + a_{1,4}\Sigma X_1^2X_4 + a_{2,3}\Sigma X_1X_2X_3 + a_{2,4}\Sigma X_1X_2X_4 + a_{3,4}\Sigma X_1X_3X_4 + a_{1,1}\Sigma X_1^3 + a_{2,2}\Sigma X_1X_2^2 + a_{3,3}\Sigma X_1X_3^2 + a_{4,4}\Sigma X_1X_4^2$$

$$\begin{aligned}
\Sigma X_2 Y &= a_0 \Sigma X_2 + a_1 \Sigma X_1 X_2 + a_2 \Sigma X_2^2 + a_3 \Sigma X_2 X_3 + a_4 \Sigma X_2 X_4 + a_{1,2} \Sigma X_1 X_2^2 + \\
& a_{1,3} \Sigma X_1 X_2 X_3 + a_{1,4} \Sigma X_1 X_2 X_4 + a_{2,3} \Sigma X_2^2 X_3 + a_{2,4} \Sigma X_2^2 X_4 + \\
& a_{3,4} \Sigma X_2 X_3 X_4 + a_{1,1} \Sigma X_1^2 X_2 + a_{2,2} \Sigma X_2^3 + a_{3,3} \Sigma X_2 X_3^2 + a_{4,4} \Sigma X_2 X_4^2 \\
\Sigma X_3 Y &= a_0 \Sigma X_3 + a_1 \Sigma X_1 X_3 + a_2 \Sigma X_2 X_3 + a_3 \Sigma X_3^2 + a_4 \Sigma X_3 X_4 + a_{1,2} \Sigma X_1 X_2 X_3 + \\
& a_{1,3} \Sigma X_1 X_3^2 + a_{1,4} \Sigma X_1 X_3 X_4 + a_{2,3} \Sigma X_2 X_3^2 + a_{2,4} \Sigma X_2 X_3 X_4 + \\
& a_{3,4} \Sigma X_3^2 X_4 + a_{1,1} \Sigma X_1^2 X_3 + a_{2,2} \Sigma X_2^2 X_3 + a_{3,3} \Sigma X_3^3 + a_{4,4} \Sigma X_3 X_4^2 \\
\Sigma X_4 Y &= a_0 \Sigma X_4 + a_1 \Sigma X_1 X_4 + a_2 \Sigma X_2 X_4 + a_3 \Sigma X_3 X_4 + a_4 \Sigma X_4^2 + a_{1,2} \Sigma X_1 X_2 X_4 + \\
& a_{1,3} \Sigma X_1 X_3 X_4 + a_{1,4} \Sigma X_1 X_4^2 + a_{2,3} \Sigma X_2 X_3 X_4 + a_{2,4} \Sigma X_2 X_4^2 + \\
& a_{3,4} \Sigma X_3 X_4^2 + a_{1,1} \Sigma X_1^2 X_4 + a_{2,2} \Sigma X_2^2 X_4 + a_{3,3} \Sigma X_3^2 X_4 + a_{4,4} \Sigma X_4^3 \\
\Sigma X_1 X_2 Y &= a_0 \Sigma X_1 X_2 + a_1 \Sigma X_1^2 X_2 + a_2 \Sigma X_1 X_2^2 + a_3 \Sigma X_1 X_2 X_3 + a_4 \Sigma X_1 X_2 X_4 + \\
& a_{1,2} \Sigma X_1^2 X_2^2 + a_{1,3} \Sigma X_1^2 X_2 X_3 + a_{1,4} \Sigma X_1^2 X_2 X_4 + a_{2,3} \Sigma X_1 X_2^2 X_3 + \\
& a_{2,4} \Sigma X_1 X_2^2 X_4 + a_{3,4} \Sigma X_1 X_2 X_3 X_4 + a_{1,1} \Sigma X_1^3 X_2 + a_{2,2} \Sigma X_1 X_2^3 + \\
& a_{3,3} \Sigma X_1 X_2 X_3^2 + a_{4,4} \Sigma X_1 X_2 X_4^2 \\
\Sigma X_1 X_3 Y &= a_0 \Sigma X_1 X_3 + a_1 \Sigma X_1^2 X_3 + a_2 \Sigma X_1 X_2 X_3 + a_3 \Sigma X_1 X_3^2 + a_4 \Sigma X_1 X_3 X_4 + \\
& a_{1,2} \Sigma X_1^2 X_2 X_3 + a_{1,3} \Sigma X_1^2 X_3^2 + a_{1,4} \Sigma X_1^2 X_3 X_4 + a_{2,3} \Sigma X_1 X_2 X_3^2 + \\
& a_{2,4} \Sigma X_1 X_2 X_3 X_4 + a_{3,4} \Sigma X_1 X_3^2 X_4 + a_{1,1} \Sigma X_1^3 X_3 + a_{2,2} \Sigma X_2^3 X_3 + \\
& a_{3,3} \Sigma X_1 X_3^3 + a_{4,4} \Sigma X_1 X_3 X_4^2 \\
\Sigma X_1 X_4 Y &= a_0 \Sigma X_1 X_4 + a_1 \Sigma X_1^2 X_4 + a_2 \Sigma X_1 X_2 X_4 + a_3 \Sigma X_1 X_3 X_4 + a_4 \Sigma X_1 X_4^2 + \\
& a_{1,2} \Sigma X_1^2 X_2 X_4 + a_{1,3} \Sigma X_1^2 X_3 X_4 + a_{1,4} \Sigma X_1^2 X_4^2 + a_{2,3} \Sigma X_1 X_2 X_3 X_4 + \\
& a_{2,4} \Sigma X_1 X_2 X_4^2 + a_{3,4} \Sigma X_1 X_3 X_4^2 + a_{1,1} \Sigma X_1^3 X_4 + a_{2,2} \Sigma X_1 X_2^2 X_4 + \\
& a_{3,3} \Sigma X_1 X_3^2 X_4 + a_{4,4} \Sigma X_1 X_4^3 \\
\Sigma X_2 X_3 Y &= a_0 \Sigma X_2 X_3 + a_1 \Sigma X_1 X_2 X_3 + a_2 \Sigma X_2^2 X_3 + a_3 \Sigma X_2 X_3^2 + a_4 \Sigma X_2 X_3 X_4 + \\
& a_{1,2} \Sigma X_1 X_2^2 X_3 + a_{1,3} \Sigma X_1 X_2 X_3^2 + a_{1,4} \Sigma X_1 X_2 X_3 X_4 + a_{2,3} \Sigma X_2^2 X_3^2 + \\
& a_{2,4} \Sigma X_2^2 X_3 X_4 + a_{3,4} \Sigma X_2 X_3^2 X_4 + a_{1,1} \Sigma X_1^2 X_2 X_3 + a_{2,2} \Sigma X_2^3 X_3 + \\
& a_{3,3} \Sigma X_2 X_3^3 + a_{4,4} \Sigma X_2 X_3 X_4^2 \\
\Sigma X_2 X_4 Y &= a_0 \Sigma X_2 X_4 + a_1 \Sigma X_1 X_2 X_4 + a_2 \Sigma X_2^2 X_4 + a_3 \Sigma X_2 X_3 X_4 + a_4 \Sigma X_2 X_4^2 + \\
& a_{1,2} \Sigma X_1 X_2^2 X_4 + a_{1,3} \Sigma X_1 X_2 X_3 X_4 + a_{1,4} \Sigma X_1 X_2 X_4^2 + a_{2,3} \Sigma X_2^2 X_3 X_4 +
\end{aligned}$$

$$\begin{aligned}
& a_{2,4}\Sigma X_2^2 X_4^2 + a_{3,4}\Sigma X_2 X_3^2 X_4 + a_{1,1}\Sigma X_1^2 X_2 X_4 + a_{2,2}\Sigma X_2^3 X_4 + \\
& a_{3,3}\Sigma X_2 X_3^2 X_4 + a_{4,4}\Sigma X_2 X_4^3 \\
\Sigma X_3 X_4 Y = & a_0 \Sigma X_3 X_4 + a_1 \Sigma X_1 X_3 X_4 + a_2 \Sigma X_2 X_3 X_4 + a_3 \Sigma X_3^2 X_4 + a_4 \Sigma X_3 X_4^2 + \\
& a_{1,2} \Sigma X_1 X_2 X_3 X_4 + a_{1,3} \Sigma X_1 X_3^2 X_4 + a_{1,4} \Sigma X_1 X_3 X_4^2 + a_{2,3} \Sigma X_2 X_3^2 X_4 + \\
& a_{2,4} \Sigma X_2 X_3 X_4^2 + a_{3,4} \Sigma X_3^2 X_4^2 + a_{1,1} \Sigma X_1^2 X_3 X_4 + a_{2,2} \Sigma X_2^2 X_3 X_4 + \\
& a_{3,3} \Sigma X_3^3 X_4 + a_{4,4} \Sigma X_3 X_4^3 \\
\Sigma X_1^2 Y = & a_0 \Sigma X_1^2 + a_1 \Sigma X_1^3 + a_2 \Sigma X_1^2 X_2 + a_3 \Sigma X_1^2 X_3 + a_4 \Sigma X_1^2 X_4 + \\
& a_{1,2} \Sigma X_1^3 X_2 + a_{1,3} \Sigma X_1^3 X_3 + a_{1,4} \Sigma X_1^3 X_4 + a_{2,3} \Sigma X_1^2 X_2 X_3 + \\
& a_{2,4} \Sigma X_1^2 X_2 X_4 + a_{3,4} \Sigma X_1^2 X_3 X_4 + a_{1,1} \Sigma X_1^4 + a_{2,2} \Sigma X_1^2 X_2^2 + \\
& a_{3,3} \Sigma X_1^2 X_3^2 + a_{4,4} \Sigma X_1^2 X_4^2 \\
\Sigma X_2^2 Y = & a_0 \Sigma X_2^2 + a_1 \Sigma X_1 X_2^2 + a_2 \Sigma X_2^3 + a_3 \Sigma X_2^2 X_3 + a_4 \Sigma X_2^2 X_4 + \\
& a_{1,2} \Sigma X_1 X_2^3 + a_{1,3} \Sigma X_1 X_2^2 X_3 + a_{1,4} \Sigma X_1 X_2^2 X_4 + a_{2,3} \Sigma X_2^3 X_3 + \\
& a_{2,4} \Sigma X_2^3 X_4 + a_{3,4} \Sigma X_2^2 X_3 X_4 + a_{1,1} \Sigma X_1^2 X_2^2 + a_{2,2} \Sigma X_2^4 + a_{3,3} \Sigma X_2^2 X_3^2 \\
& + a_{4,4} \Sigma X_2^2 X_4^2 \\
\Sigma X_3^2 Y = & a_0 \Sigma X_3^2 + a_1 \Sigma X_1 X_3^2 + a_2 \Sigma X_2 X_3^2 + a_3 \Sigma X_3^3 + a_4 \Sigma X_3^2 X_4 + \\
& a_{1,2} \Sigma X_1 X_2 X_3^2 + a_{1,3} \Sigma X_1 X_3^3 + a_{1,4} \Sigma X_1 X_3^2 X_4 + a_{2,3} \Sigma X_2 X_3^3 + \\
& a_{2,4} \Sigma X_2 X_3^2 X_4 + a_{3,4} \Sigma X_3^3 X_4 + a_{1,1} \Sigma X_1^2 X_3^2 + a_{2,2} \Sigma X_2^2 X_3^2 + a_{3,3} \Sigma X_3^4 \\
& + a_{4,4} \Sigma X_3^2 X_4^2 \\
\Sigma X_4^2 Y = & a_0 \Sigma X_4^2 + a_1 \Sigma X_1 X_4^2 + a_2 \Sigma X_2 X_4^2 + a_3 \Sigma X_3 X_4^2 + a_4 \Sigma X_4^3 + \\
& a_{1,2} \Sigma X_1 X_2 X_4^2 + a_{1,3} \Sigma X_1 X_3 X_4^2 + a_{1,4} \Sigma X_1 X_4^3 + a_{2,3} \Sigma X_2 X_3 X_4^2 + \\
& a_{2,4} \Sigma X_2 X_4^3 + a_{3,4} \Sigma X_3 X_4^3 + a_{1,1} \Sigma X_1^2 X_4^2 + a_{2,2} \Sigma X_2^2 X_4^2 + \\
& a_{3,3} \Sigma X_3^2 X_4^2 + a_{4,4} \Sigma X_4^4
\end{aligned} \tag{45-59}$$

Table 17. Factorial Design Showing the Factors (Parameters) and Their Levels.

Run	X <sub>1</sub>	X <sub>2</sub>	X <sub>3</sub>	X <sub>4</sub>	Y <sub>exp</sub>
1	+1	+1	+1	+1	Y <sub>1</sub>
2	+1	+1	+1	-1	Y <sub>2</sub>
3	+1	+1	-1	+1	Y <sub>3</sub>
4	+1	+1	-1	-1	Y <sub>4</sub>
5	+1	-1	+1	+1	Y <sub>5</sub>
6	+1	-1	+1	-1	Y <sub>6</sub>
7	+1	-1	-1	+1	Y <sub>7</sub>
8	+1	-1	-1	-1	Y <sub>8</sub>
9	-1	+1	+1	+1	Y <sub>9</sub>
10	-1	+1	+1	-1	Y <sub>10</sub>
11	-1	+1	-1	+1	Y <sub>11</sub>
12	-1	+1	-1	-1	Y <sub>12</sub>
13	-1	-1	+1	+1	Y <sub>13</sub>
14	-1	-1	+1	-1	Y <sub>14</sub>
15	-1	-1	-1	+1	Y <sub>15</sub>
16	-1	-1	-1	-1	Y <sub>16</sub>
17	+1	0	0	0	Y <sub>17</sub>
18	-1	0	0	0	Y <sub>18</sub>
19	0	+1	0	0	Y <sub>19</sub>
20	0	-1	0	0	Y <sub>20</sub>
21	0	0	+1	0	Y <sub>21</sub>
22	0	0	-1	0	Y <sub>22</sub>
23	0	0	0	+1	Y <sub>23</sub>
24	0	0	0	-1	Y <sub>24</sub>
25	0	0	0	0	Y <sub>25</sub>

where: X<sub>1</sub>, X<sub>2</sub>, X<sub>3</sub>, X<sub>4</sub> - factors (time of biotransformation, medium compositions)

Y - response variable (yield)

For the factorial design applied in the present study the values of some expressions (Equations 60-71) could be determined prior to the experiment using the values of the factors (Table 17). This table contains the standardized values of the factors for the factorial design used in Chapter IV (Tables 7, 12). The values of the rest of the sums could be calculated using experimental results.

$$n = 25 \quad (60)$$

$$\Sigma X_1 = \Sigma X_2 = \Sigma X_3 = \Sigma X_4 = 0 \quad (61)$$

$$\Sigma X_1 X_2 = \Sigma X_1 X_3 = \Sigma X_1 X_4 = \Sigma X_2 X_3 = \Sigma X_2 X_4 = \Sigma X_3 X_4 = 0 \quad (62)$$

$$\Sigma X_1^2 = \Sigma X_2^2 = \Sigma X_3^2 = \Sigma X_4^2 = 18 \quad (63)$$

$$\begin{aligned} \Sigma X_1^2 X_2 = \Sigma X_1^2 X_3 = \Sigma X_1^2 X_4 = \Sigma X_2^2 X_3 = \Sigma X_2^2 X_4 = \Sigma X_3^2 X_4 = \Sigma X_1 X_2^2 = \\ \Sigma X_1 X_3^2 = \Sigma X_1 X_4^2 = \Sigma X_2 X_3^2 = \Sigma X_2 X_4^2 = \Sigma X_3 X_4^2 = 0 \end{aligned} \quad (64)$$

$$\Sigma X_1^2 X_2^2 = \Sigma X_1^2 X_3^2 = \Sigma X_1^2 X_4^2 = \Sigma X_2^2 X_3^2 = \Sigma X_2^2 X_4^2 = \Sigma X_3^2 X_4^2 = 16 \quad (65)$$

$$\Sigma X_1 X_2 X_3 = \Sigma X_1 X_2 X_4 = \Sigma X_1 X_3 X_4 = \Sigma X_2 X_3 X_4 = 0 \quad (66)$$

$$\begin{aligned} \Sigma X_1^2 X_2 X_3 = \Sigma X_1^2 X_2 X_4 = \Sigma X_1 X_2^2 X_3 = \Sigma X_1 X_2^2 X_4 = \Sigma X_1 X_2 X_3^2 = \Sigma X_1 X_2 X_4^2 \\ = \Sigma X_1^2 X_3 X_4 = \Sigma X_1 X_3^2 X_4 = \Sigma X_1 X_3 X_4^2 = \Sigma X_2^2 X_3 X_4 = \Sigma X_2 X_3^2 X_4 = \\ \Sigma X_2 X_3 X_4^2 = 0 \end{aligned} \quad (67)$$

$$\Sigma X_1^3 = \Sigma X_2^3 = \Sigma X_3^3 = \Sigma X_4^3 = 0 \quad (68)$$

$$\begin{aligned} \Sigma X_1^3 X_2 = \Sigma X_1 X_2^3 = \Sigma X_1^3 X_3 = \Sigma X_2^3 X_3 = \Sigma X_1 X_3^3 = \Sigma X_1^3 X_4 = \Sigma X_1 X_4^3 = \\ \Sigma X_2^3 X_4 = \Sigma X_2 X_4^3 = \Sigma X_3^3 X_4 = \Sigma X_3 X_4^3 = 0 \end{aligned} \quad (69)$$

$$X_1 X_2 X_3 X_4 = 0 \quad (70)$$

$$\Sigma X_1^4 = \Sigma X_2^4 = \Sigma X_3^4 = \Sigma X_4^4 = 18 \quad (71)$$

Substitution of Equations (60-71) in Equations (45-59) will give:

$$\begin{aligned}
\Sigma Y &= 25a_0 + 0a_1 + 0a_2 + 0a_3 + 0a_4 + 0a_{1,2} + 0a_{1,3} + 0a_{1,4} + 0a_{2,3} + 0a_{2,4} \\
&\quad + 0a_{3,4} + 18a_{1,1} + 18a_{2,2} + 18a_{3,3} + 18a_{4,4} \\
\Sigma X_1 Y &= 0a_0 + 18a_1 + 0a_2 + 0a_3 + 0a_4 + 0a_{1,2} + 0a_{1,3} + 0a_{1,4} + 0a_{2,3} + \\
&\quad 0a_{2,4} + 0a_{3,4} + 0a_{1,1} + 0a_{2,2} + 0a_{3,3} + 0a_{4,4} \\
\Sigma X_2 Y &= 0a_0 + 0a_1 + 18a_2 + 0a_3 + 0a_4 + 0a_{1,2} + 0a_{1,3} + 0a_{1,4} + 0a_{2,3} + \\
&\quad 0a_{2,4} + 0a_{3,4} + 0a_{1,1} + 0a_{2,2} + 0a_{3,3} + 0a_{4,4} \\
\Sigma X_3 Y &= 0a_0 + 0a_1 + 0a_2 + 18a_3 + 0a_4 + 0a_{1,2} + 0a_{1,3} + 0a_{1,4} + 0a_{2,3} + \\
&\quad 0a_{2,4} + 0a_{3,4} + 0a_{1,1} + 0a_{2,2} + 0a_{3,3} + 0a_{4,4} \\
\Sigma X_4 Y &= 0a_0 + 0a_1 + 0a_2 + 0a_3 + 18a_4 + 0a_{1,2} + 0a_{1,3} + 0a_{1,4} + 0a_{2,3} + \\
&\quad 0a_{2,4} + 0a_{3,4} + 0a_{1,1} + 0a_{2,2} + 0a_{3,3} + 0a_{4,4} \\
\Sigma X_1 X_2 Y &= 0a_0 + 0a_1 + 0a_2 + 0a_3 + 0a_4 + 16a_{1,2} + 0a_{1,3} + 0a_{1,4} + 0a_{2,3} + \\
&\quad 0a_{2,4} + 0a_{3,4} + 0a_{1,1} + 0a_{2,2} + 0a_{3,3} + 0a_{4,4} \\
\Sigma X_1 X_3 Y &= 0a_0 + 0a_1 + 0a_2 + 0a_3 + 0a_4 + 0a_{1,2} + 16a_{1,3} + 0a_{1,4} + 0a_{2,3} + \\
&\quad 0a_{2,4} + 0a_{3,4} + 0a_{1,1} + 0a_{2,2} + 0a_{3,3} + 0a_{4,4} \\
\Sigma X_1 X_4 Y &= 0a_0 + 0a_1 + 0a_2 + 0a_3 + 0a_4 + 0a_{1,2} + 0a_{1,3} + 16a_{1,4} + 0a_{2,3} + \\
&\quad 0a_{2,4} + 0a_{3,4} + 0a_{1,1} + 0a_{2,2} + 0a_{3,3} + 0a_{4,4} \\
\Sigma X_2 X_3 Y &= 0a_0 + 0a_1 + 0a_2 + 0a_3 + 0a_4 + 0a_{1,2} + 0a_{1,3} + 0a_{1,4} + 16a_{2,3} + \\
&\quad 0a_{2,4} + 0a_{3,4} + 0a_{1,1} + 0a_{2,2} + 0a_{3,3} + 0a_{4,4} \\
\Sigma X_2 X_4 Y &= 0a_0 + 0a_1 + 0a_2 + 0a_3 + 0a_4 + 0a_{1,2} + 0a_{1,3} + 0a_{1,4} + 0a_{2,3} + \\
&\quad 16a_{2,4} + 0a_{3,4} + 0a_{1,1} + 0a_{2,2} + 0a_{3,3} + 0a_{4,4} \\
\Sigma X_3 X_4 Y &= 0a_0 + 0a_1 + 0a_2 + 0a_3 + 0a_4 + 0a_{1,2} + 0a_{1,3} + 0a_{1,4} + 0a_{2,3} + \\
&\quad 0a_{2,4} + 16a_{3,4} + 0a_{1,1} + 0a_{2,2} + 0a_{3,3} + 0a_{4,4} \\
\Sigma X_1^2 Y &= 18a_0 + 0a_1 + 0a_2 + 0a_3 + 0a_4 + 0a_{1,2} + 0a_{1,3} + 0a_{1,4} + 0a_{2,3} + \\
&\quad 0a_{2,4} + 0a_{3,4} + 18a_{1,1} + 16a_{2,2} + 16a_{3,3} + 16a_{4,4} \\
\Sigma X_2^2 Y &= 18a_0 + 0a_1 + 0a_2 + 0a_3 + 0a_4 + 0a_{1,2} + 0a_{1,3} + 0a_{1,4} + 0a_{2,3} + \\
&\quad 0a_{2,4} + 0a_{3,4} + 16a_{1,1} + 18a_{2,2} + 16a_{3,3} + 16a_{4,4}
\end{aligned}$$

$$\begin{aligned}\Sigma X_3^2 Y &= 18a_0 + 0a_1 + 0a_2 + 0a_3 + 0a_4 + 0a_{1,2} + 0a_{1,3} + 0a_{1,4} + 0a_{2,3} + \\ &0a_{2,4} + 0a_{3,4} + 16a_{1,1} + 16a_{2,2} + 18a_{3,3} + 16a_{4,4} \\ \Sigma X_4^2 Y &= 18a_0 + 0a_1 + 0a_2 + 0a_3 + 0a_4 + 0a_{1,2} + 0a_{1,3} + 0a_{1,4} + 0a_{2,3} + \\ &0a_{2,4} + 0a_{3,4} + 16a_{1,1} + 16a_{2,2} + 16a_{3,3} + 18a_{4,4}\end{aligned}$$

(72-86)

Simplifying equations (72-86) will give the following system (Eq. 87-101):

$$\begin{aligned}\Sigma Y &= 25a_0 + 18a_{1,1} + 18a_{2,2} + 18a_{3,3} + 18a_{4,4} \\ \Sigma X_1 Y &= 18a_1 \\ \Sigma X_2 Y &= 18a_2 \\ \Sigma X_3 Y &= 18a_3 \\ \Sigma X_4 Y &= 18a_4 \\ \Sigma X_1 X_2 Y &= 16a_{1,2} \\ \Sigma X_1 X_3 Y &= 16a_{1,3} \\ \Sigma X_1 X_4 Y &= 16a_{1,4} \\ \Sigma X_2 X_3 Y &= 16a_{2,3} \\ \Sigma X_2 X_4 Y &= 16a_{2,4} \\ \Sigma X_3 X_4 Y &= 16a_{3,4} \\ \Sigma X_1^2 Y &= 18a_0 + 18a_{1,1} + 16a_{2,2} + 16a_{3,3} + 16a_{4,4} \\ \Sigma X_2^2 Y &= 18a_0 + 16a_{1,1} + 18a_{2,2} + 16a_{3,3} + 16a_{4,4} \\ \Sigma X_3^2 Y &= 18a_0 + 16a_{1,1} + 16a_{2,2} + 18a_{3,3} + 16a_{4,4} \\ \Sigma X_4^2 Y &= 18a_0 + 16a_{1,1} + 16a_{2,2} + 16a_{3,3} + 18a_{4,4}\end{aligned}$$

(87-101)

The following calculations were then made to solve the system equations:

$$\Sigma Y = 25a_0 + 18a_{1,1} + 18a_{2,2} + 18a_{3,3} + 18a_{4,4} \quad (87)$$

$$\Sigma X_1^2 Y = 18a_0 + 18a_{1,1} + 16a_{2,2} + 16a_{3,3} + 16a_{4,4} \quad (98)$$

$$\Sigma X_2^2 Y = 18a_0 + 16a_{1,1} + 18a_{2,2} + 16a_{3,3} + 16a_{4,4} \quad (99)$$

$$\Sigma X_3^2 Y = 18a_0 + 16a_{1,1} + 16a_{2,2} + 18a_{3,3} + 16a_{4,4} \quad (100)$$

$$\Sigma X_4^2 Y = 18a_0 + 16a_{1,1} + 16a_{2,2} + 16a_{3,3} + 18a_{4,4} \quad (101)$$

$$\Sigma X_4^2 Y = 18a_0 + 16a_{1,1} + 16a_{2,2} + 16a_{3,3} + 18a_{4,4} \quad (101)$$

$$\Sigma Y - (25/18)\Sigma X_4^2 Y = (18-18)a_0 + (18-25*16/18)a_{1,1} + (18-25*16/18)a_{2,2} + (18-25*16/18)a_{3,3} + (18-25)a_{4,4} \quad (102)$$

$$\Sigma X_1^2 Y - \Sigma X_4^2 Y = 0a_0 + 2a_{1,1} + 0a_{2,2} + 0a_{3,3} - 2a_{4,4} \quad (103)$$

$$\Sigma X_2^2 Y - \Sigma X_4^2 Y = 0a_0 + 0a_{1,1} + 2a_{2,2} + 0a_{3,3} - 2a_{4,4} \quad (104)$$

$$\Sigma X_3^2 Y - \Sigma X_4^2 Y = 0a_0 + 0a_{1,1} + 0a_{2,2} + 2a_{3,3} - 2a_{4,4} \quad (105)$$

$$\Sigma X_4^2 Y = 18a_0 + 16a_{1,1} + 16a_{2,2} + 16a_{3,3} + 18a_{4,4} \quad (101)$$

$$18\Sigma Y - 25\Sigma X_4^2 Y = 0a_0 - 76a_{1,1} - 76a_{2,2} - 76a_{3,3} - 126a_{4,4} \quad (106)$$

$$\Sigma X_1^2 Y - \Sigma X_4^2 Y = 0a_0 + 2a_{1,1} + 0a_{2,2} + 0a_{3,3} - 2a_{4,4} \quad (103)$$

$$\Sigma X_2^2 Y - \Sigma X_4^2 Y = 0a_0 + 0a_{1,1} + 2a_{2,2} + 0a_{3,3} - 2a_{4,4} \quad (104)$$

$$\Sigma X_3^2 Y - \Sigma X_4^2 Y = 0a_0 + 0a_{1,1} + 0a_{2,2} + 2a_{3,3} - 2a_{4,4} \quad (105)$$

$$\Sigma X_4^2 Y = 18a_0 + 16a_{1,1} + 16a_{2,2} + 16a_{3,3} + 18a_{4,4} \quad (101)$$

$$18\Sigma Y - 25\Sigma X_4^2 Y + 38(\Sigma X_1^2 Y - \Sigma X_4^2 Y + \Sigma X_2^2 Y - \Sigma X_4^2 Y + \Sigma X_3^2 Y - \Sigma X_4^2 Y) = 0a_0 + 0a_{1,1} + 0a_{2,2} + 0a_{3,3} - 354a_{4,4} \quad (106)$$

$$\Sigma X_1^2 Y - \Sigma X_4^2 Y = 0a_0 + 2a_{1,1} + 0a_{2,2} + 0a_{3,3} - 2a_{4,4} \quad (103)$$

$$\Sigma X_2^2 Y - \Sigma X_4^2 Y = 0a_0 + 0a_{1,1} + 2a_{2,2} + 0a_{3,3} - 2a_{4,4} \quad (104)$$

$$\Sigma X_3^2 Y - \Sigma X_4^2 Y = 0a_0 + 0a_{1,1} + 0a_{2,2} + 2a_{3,3} - 2a_{4,4} \quad (105)$$

$$\Sigma X_4^2 Y = 18a_0 + 16a_{1,1} + 16a_{2,2} + 16a_{3,3} + 18a_{4,4} \quad (101)$$

$$\Sigma X_1^2 Y - \Sigma X_4^2 Y = 0a_0 + 2a_{1,1} + 0a_{2,2} + 0a_{3,3} - 2a_{4,4} \quad (103)$$



$$\Sigma X_2^2 Y - \Sigma X_4^2 Y = 0a_0 + 0a_{1,1} + 2a_{2,2} + 0a_{3,3} - 2a_{4,4} \quad (104)$$

$$\Sigma X_3^2 Y - \Sigma X_4^2 Y = 0a_0 + 0a_{1,1} + 0a_{2,2} + 2a_{3,3} - 2a_{4,4} \quad (105)$$

$$18\Sigma Y + 38\Sigma X_1^2 Y + 38\Sigma X_2^2 Y + 38\Sigma X_3^2 Y - 139\Sigma X_4^2 Y = 0a_0 + 0a_{1,1} + 0a_{2,2} + 0a_{3,3} - 354a_{4,4} \quad (107)$$

$$a_{4,4} = 1/354(-18\Sigma Y - 38\Sigma X_1^2 Y - 38\Sigma X_2^2 Y - 38\Sigma X_3^2 Y + 139\Sigma X_4^2 Y) \quad (107)$$

$$a_{3,3} = 1/354(-18\Sigma Y - 38\Sigma X_1^2 Y - 38\Sigma X_2^2 Y + 215\Sigma X_3^2 Y - 38\Sigma X_4^2 Y) \quad (108)$$

$$2a_{2,2} = 1/354(-18\Sigma Y - 38\Sigma X_1^2 Y + 139\Sigma X_2^2 Y - 38\Sigma X_3^2 Y - 38\Sigma X_4^2 Y) \quad (109)$$

$$a_{1,1} = 1/354(-18\Sigma Y + 139\Sigma X_1^2 Y - 38\Sigma X_2^2 Y - 38\Sigma X_3^2 Y - 38\Sigma X_4^2 Y) \quad (103)$$

$$a_0 = 1/354(66\Sigma Y - 18\Sigma X_1^2 Y - 18\Sigma X_2^2 Y - 85.56\Sigma X_3^2 Y - 18\Sigma X_4^2 Y) \quad (101)$$

The solution of the system Equations (72-86) with respect to the coefficients  $a_0, a_1, a_2$  etc. could be determined by substitution. The general form of the solution will be:

$$a_0 = 1/354(66\Sigma Y - 18\Sigma X_1^2 Y - 18\Sigma X_2^2 Y - 85.56\Sigma X_3^2 Y - 18\Sigma X_4^2 Y)$$

$$a_1 = \Sigma X_1 Y / 18$$

$$a_2 = \Sigma X_2 Y / 18$$

$$a_3 = \Sigma X_3 Y / 18$$

$$a_4 = \Sigma X_4 Y / 18$$

$$a_{1,2} = \Sigma X_1 X_2 Y / 16$$

$$a_{1,3} = \Sigma X_1 X_3 Y / 16$$

$$a_{1,4} = \Sigma X_1 X_4 Y / 16$$

$$a_{2,3} = \Sigma X_2 X_3 Y / 16$$

$$a_{2,4} = \Sigma X_2 X_4 Y / 16$$

$$a_{3,4} = \Sigma X_3 X_4 Y / 16$$

$$a_{1,1} = 1/354(-18\Sigma Y + 139\Sigma X_1^2 Y - 38\Sigma X_2^2 Y - 38\Sigma X_3^2 Y - 38\Sigma X_4^2 Y)$$

$$2a_{2,2} = 1/354(- 18\Sigma Y - 38\Sigma X_1^2 Y + 139\Sigma X_2^2 Y - 38\Sigma X_3^2 Y - 38\Sigma X_4^2 Y)$$

$$a_{3,3} = 1/354(- 18\Sigma Y - 38\Sigma X_1^2 Y - 38\Sigma X_2^2 Y + 215\Sigma X_3^2 Y - 38\Sigma X_4^2 Y)$$

$$a_{4,4} = 1/354(- 18\Sigma Y - 38\Sigma X_1^2 Y - 38\Sigma X_2^2 Y - 38\Sigma X_3^2 Y + 139\Sigma X_4^2 Y)$$

(110-124)

From the experimental information (yield of metabolites determined by HPLC and yield of biomass) and Table 17 the necessary 15 sums were evaluated (Table 18).

Table 18. Sums Necessary for Evaluation of the Coefficients of Equations (2-7) Shown in Chapter IV.

Run	Equation (2)	Equation (3)	Equation (4)	Equation (5)	Equation (6)	Equation (7)
$\Sigma Y$	1341	598.5	193.8	263.1	246.1	34.64
$\Sigma X_1 Y$	-745.1	241.9	102.2	144.9	-	-
$\Sigma X_2 Y$	-85.00	-26.94	0.6756	14.14	51.87	3.200
$\Sigma X_3 Y$	22.36	-19.21	-18.13	-47.10	106.3	13.04
$\Sigma X_4 Y$	-99.71	16.51	-1.647	59.16	4.190	0.2200
$\Sigma X_1 X_2 Y$	-68.48	-27.57	-2.272	1.537	-	-
$\Sigma X_1 X_3 Y$	21.61	-15.39	-17.49	-30.17	-	-
$\Sigma X_1 X_4 Y$	-71.02	4.459	-0.7146	36.81	-	-
$\Sigma X_2 X_3 Y$	-33.19	-27.02	1.9718	80.89	41.95	3.120
$\Sigma X_2 X_4 Y$	7.547	-26.24	-14.81	88.93	61.76	-6.460
$\Sigma X_3 X_4 Y$	24.81	-36.53	-5.539	-99.44	-8.210	0.5800
$\Sigma X_1^2 Y$	1055	241.9	102.2	144.9	-	-
$\Sigma X_2^2 Y$	998.4	271.0	97.85	166.4	0.07200	-0.1970
$\Sigma X_3^2 Y$	998.4	271.0	97.85	166.4	-0.06100	-0.04100
$\Sigma X_4^2 Y$	998.4	271.0	97.85	166.4	-0.01200	-0.02700

where:  $X_1, X_2, X_3, X_4$  - factors (time of biotransformation, medium compositions)

Y - response variable (yield)

The yield of biomass is evaluated only after 120 h, therefore the time of growth  $X_1$  is not included in the equations (6) and (7) and the sums involving  $X_1$  are not presented.

From these sums the coefficients  $a_0$ ,  $a_1$ ,  $a_2$  etc. were determined by substitution of the values from Table 18 in Equations (110-124) and the results are shown in Table 19.

Table 19. Coefficients of Equations (2-7) Shown in Chapter IV.

Run	Equation (2)	Equation (3)	Equation (4)	Equation (5)	Equation (6)	Equation (7)
$a_0$	28.3	44.4	10.3	10.5	20.5	2.89
$a_1$	-41.4	13.4	5.67	8.05	-	-
$a_2$	-4.72	-1.50	0.0375	0.786	6.48	0.400
$a_3$	1.24	-1.07	-1.01	-2.62	13.3	1.63
$a_4$	-5.54	0.917	-0.0915	3.29	0.764	0.312
$a_{1.2}$	-4.28	-1.72	-0.142	0.0961	-	-
$a_{1.3}$	1.35	-0.962	-1.09	-1.89	-	-
$a_{1.4}$	-4.44	0.279	-0.0447	2.30	-	-
$a_{2.3}$	-2.07	-1.69	0.123	5.06	5.24	0.390
$a_{2.4}$	0.472	-1.64	-0.925	-5.56	- 7.72	- 0.808
$a_{3.4}$	1.55	-2.28	-0.534	-6.21	- 1.03	-0.00520
$a_{1.1}$	28.8	-29.2	0.340	-8.50	-	-
$a_{2.2}$	0.557	-14.6	-1.85	2.29	0.269	0.182
$a_{3.3}$	0.557	-14.6	-1.85	2.29	-	-
$a_{4.4}$	0.557	-14.6	-1.85	2.29	-	-

where:  $a_0$ ,  $a_1$ ,  $a_2$  - coefficients

### A.3 Significant Coefficients

Once the coefficients  $a_0, a_1, a_2$  in the mathematical model

$$Y_{\text{calc}} = a_0 + a_1X_1 + a_2X_2 + a_3X_3 + a_4X_4 + a_{1,2}X_1X_2 + a_{1,3}X_1X_3 + a_{1,4}X_1X_4 + a_{2,3}X_2X_3 + a_{2,4}X_2X_4 + a_{3,4}X_3X_4 + a_{1,1}X_1^2 + a_{2,2}X_2^2 + a_{3,3}X_3^2 + a_{4,4}X_4^2 \quad (1)$$

were evaluated their significance was determined and the coefficients which were statistically not significant were eliminated. After substitution of normalized factors with real values (Table 6 and 10, Chapter IV) were obtained the following equations:

$$Y_1 = 99.7 - 2.52X_1 + 0.195X_2 + 0.0619X_3 - 0.148X_4 - 0.0125X_1X_2 + 0.00494X_1X_3 - 0.00649X_1X_4 - 0.0287X_2X_3 + 0.0107X_3X_4 + 0.0222X_1^2 \quad (2)$$

$$Y_2 = -10.1 + 1.34X_1 + 0.950X_2 + 1.24X_3 + 0.543X_4 - 0.00482X_1X_2 - 0.00337X_1X_3 - 0.0224X_2X_3 - 0.00870X_2X_4 - 0.0151X_3X_4 - 0.0126X_1^2 - 0.0265X_2^2 - 0.0414X_3^2 - 0.00662X_4^2 \quad (3)$$

$$Y_3 = -3.54 + 0.164X_1 + 0.511X_2 + 0.596X_3 + 0.285X_4 - 0.00380X_1X_3 - 0.00488X_2X_4 - 0.00352X_3X_4 - 0.000250X_1^2 - 0.0195X_2^2 - 0.0304X_3^2 - 0.00487X_4^2 \quad (4)$$

$$\begin{aligned}
Y_4 = & - 4.66 + 0.450 \cdot X_1 - 0.257 \cdot X_2 - 0.390 \cdot X_3 + 0.310 \cdot X_4 - \\
& 0.00454 \cdot X_1 \cdot X_2 + 0.00222 \cdot X_1 \cdot X_4 + 0.0461 \cdot X_2 \cdot X_3 - 0.0203 \cdot X_2 \cdot X_4 \\
& - 0.0283 \cdot X_3 \cdot X_4 - 0.00432 \cdot X_1^2 + 0.0167 \cdot X_2^2 + 0.0261 \cdot X_3^2 + \\
& 0.00417 \cdot X_4^2
\end{aligned} \tag{5}$$

$$\begin{aligned}
Y_f = & 20.50 + 6.48 \cdot X_2 + 13.3 \cdot X_3 + 5.24 \cdot X_2 \cdot X_3 - 7.72 \cdot X_2 \cdot X_4 - 1.026 \cdot X_3 \cdot X_4 \\
& + 1.269 \cdot X_2^2
\end{aligned} \tag{6}$$

$$\begin{aligned}
Y_d = & 2.89 + 0.400 \cdot X_2 + 1.63 \cdot X_3 + 0.390 \cdot X_2 \cdot X_3 - 0.808 \cdot X_2 \cdot X_4 - \\
& 0.182 \cdot X_2^2
\end{aligned} \tag{7}$$

where:

$Y_1$  = Recovered Triptophenolide (**12**), (%)

$Y_2$  = Triptoquinone (**114**), (%)

$Y_3$  = 5 $\alpha$ ,14-Dihydroxytryptophenolide (**115**), (%)

$Y_4$  = 14-Glucosyl Triptophenolide (**116**), (%)

$X_1$  = Time (h)

$X_2$  = Glucose (g/L)

$X_3$  = Nutrient broth (g/L)

$X_4$  = Malt extract (g/L)

$Y_f$  = yield of biomass after 144 hours (fresh weight), (g/L)

$Y_d$  = yield of biomass after 144 hours (dry weight), (g/L)

#### A.4 Optimization Procedure

The completed mathematical model was used to predict the outcome of the process at different conditions (within the studied range -

i.e., within the range of parameter variation during the experiment). It was then used to find the optimum values of the parameters which will gave maximum  $Y_{\text{calc}}$ .

To find the optimum of  $Y_{\text{calc}}$  the method of scanning was used. This simple method consist of calculation and comparison the values of  $Y_{\text{calc}}$  while varying  $X_1$ ,  $X_2$ ,  $X_3$  and  $X_4$ . The variations of  $X_1$  are done by selecting minimum value for  $X_1$ ,  $X_2$ ,  $X_3$  and  $X_4$  and then using appropriate increment  $X_1$  was increased until its maximum value was reached. Then  $X_2$  was increased and the procedure is repeated until maximum value for all X was reached. To determine more precisely the optimum values of the parameters after the first scanning small part of the range of each parameter around the found optimum was selected and the scanning was repeated in this smaller range.

After the optimum conditions (Table 8, Chapter IV) are determined it is required to perform one single experiment at this conditions in order to confirm the calculated result. This experiment was the verification experiment.

#### **A.5 Linear Regression for the Equations of the Standard Curves**

Linear regression is the application of the least squares method to describe experimental data with a linear equation and it was used to convert the standard curves of the HPLC to linear equations:

$$Y_{\text{calc}} = a_0 + a_1 X_1 \quad (9)$$

where

$a_0$ ,  $a_1$  are coefficients of the equation (constants)

$X_1$  is a factor (parameter) value

$Y_{\text{calc}}$  is the calculated (predicted value) for the response variable.

Applying the least squares method (similar to the method used to determine the coefficients in the model of the factorial design experiment) gave:

$$(Y_{\text{exp}} - Y_{\text{calc}}) \Rightarrow \text{minimum} \quad (125)$$

where

$Y_{\text{exp}}$  is an experimentally determined value

After substitution of  $Y_{\text{calc}}$  with a linear expression

$$Y_{\text{calc}} = a_0 + a_1 X_1 \quad (126)$$

will be obtained

$$(Y_{\text{exp}} - a_0 + a_1 X_1) \Rightarrow \text{minimum} \quad (127)$$

The best values of the coefficients ( $a_0$  and  $a_1$ ) are determined by the following transformations:

$$\Sigma(Y_{\text{exp}} - a_0 + a_1 X_1)^2 \Rightarrow \text{minimum} \quad (128)$$

where  $\Sigma$  is the sum of the experimental results used for the standard curve. Solving this equation for each parameter will give the following system of equations:

$$\begin{aligned}\Sigma d(Y_{\text{exp}} - Y_{\text{calc}})^2 / da_0 &= 0 \\ \Sigma d(Y_{\text{exp}} - Y_{\text{calc}})^2 / da_1 &= 0\end{aligned}\quad (129-130)$$

$$\begin{aligned}\Sigma d(Y_{\text{exp}} - a_0 + a_1 X_1)^2 / da_0 &= 0 \\ \Sigma d(Y_{\text{exp}} - a_0 + a_1 X_1)^2 / da_1 &= 0\end{aligned}\quad (131-132)$$

This can be converted to:

$$\begin{aligned}\Sigma Y &= na_0 + a_1 \Sigma X_1 \\ \Sigma X_1 Y &= a_0 \Sigma X_1 + a_1 \Sigma X_1^2\end{aligned}\quad (133-134)$$

and then the necessary sums  $\Sigma Y$ ,  $\Sigma X_1 Y$ ,  $\Sigma X_1$ ,  $\Sigma X_1^2$  and the number of experimental results  $n$  can be used to evaluate the coefficients in the equation:

$$\Sigma Y = na_0 + a_1 \Sigma X_1 \quad (133)$$

$$\Sigma X_1 Y - (\Sigma X_1 / n) \Sigma Y = a_0 \Sigma X_1 + a_1 \Sigma X_1^2 - \{(\Sigma X_1 / n) na_0 + (\Sigma X_1 / n) a_1 \Sigma X_1\} \quad (135)$$

$$\Sigma Y = na_0 + a_1 \Sigma X_1 \quad (133)$$

$$\Sigma X_1 Y - \Sigma X_1 \Sigma Y / n = a_0 (\Sigma X_1 - \Sigma X_1) + a_1 (\Sigma X_1^2 - \Sigma X_1 \Sigma X_1 / n) \quad (136)$$

$$\Sigma Y = na_0 + a_1 \Sigma X_1 \quad (133)$$

$$\Sigma X_1 Y - \Sigma X_1 \Sigma Y / n = a_0 0 + a_1 (\Sigma X_1^2 - \Sigma X_1 \Sigma X_1 / n) \quad (137)$$

$$\Sigma Y = na_0 + a_1 \Sigma X_1 \quad (133)$$

$$\Sigma X_1 Y - \Sigma X_1 \Sigma Y / n = a_1 (\Sigma X_1^2 - \Sigma X_1 \Sigma X_1 / n) \quad (138)$$

$$a_1 = (\Sigma X_1 Y - \Sigma X_1 \Sigma Y / n) / (\Sigma X_1^2 - \Sigma X_1 \Sigma X_1 / n) \quad (139)$$



$$a_0 = (a_1 \Sigma X_1 - \Sigma Y) / n \quad (140)$$

After  $a_0$  and  $a_1$  were evaluated, the equation was used for conversion of HPLC results into linear functions:

$$Y_{\text{calc}} = a_0 + a_1 X_1 \quad (9)$$

All calculations were done by Nikolay Stoykov (Department of Chemistry, UBC), using SigmaPlot 5 Program for Windows. His help in calculating the results is highly appreciated.

## References

- Aoyama, Y., Yoshida, Y. & Sato, O. 1984. Yeast cytochrome P-450 catalyzing lanosterol 14 $\alpha$ -Demethylation. II. Lanosterol metabolism by purified P-450<sub>14DM</sub> and by intact microsomes. J. Biol. Chem. 259:1661-1666.
- Biellmann, J. F., Wenning, R., Daste, P. & Raynaud, M. 1968. Microbial degradation of diterpene acids. Chem. Commun. 168-169.
- Biellmann, J. F., Wenning, R., Daste, P. & Faure-Raynaud, M. 1970. Microbial degradation of dehydroabietic acid. Chem. Commun. 346-347.
- Biellmann, J. F., Branlant, G., Gero-Robert, M. & Poiret, M. 1973a. Degradation bacterienne de l'acide dehydroabietique par *Flavobacterium retinovorum*. Tetrahedron 29:1227-1236.
- Biellmann, J. F., Branlant, G., Gero-Robert, M. & Poiret, M. 1973b. Degradation bacterienne de l'acide dehydroabietique par un *Pseudomonas* et une *Alcaligenes*. Tetrahedron 29:1237-1241.
- Bocks, S. M. 1967. Fungal metabolism - III. The hydroxylation of anisole, phenoxyacetic acid, phenylacetic acid and benzoic acid by *Aspergillus niger*. Phytochemistry 6:785-789.
- Brannon, D. R., Boaz, H., Wiley, B. J., Mabe, J. & Horton, D. R. 1968. Hydroxylation of some dehydroabietanes with *Corticium sasakii*. J. Org. Chem. 33:4462-4466.
- Cerniglia, C. E. & Gibson, D. T. 1979. Oxidation of benzo[a]pyrene by filamentous fungus *Cunninghamella elegans*. J. Biol. Chem. 254:12174-12180.

- Cerniglia, C. E., Hebert, R. L., Szaniszlo, P. J., & Gibson, D. T. 1978. Fungal transformation of naphthalene. Arch. Microbiol. 117:135-143.
- Cerniglia, C. E., Pothuluri, J. V., Freeman, J. P. & Evans, F. E. 1992a. Fungal metabolism of acenaphthene by *Cunninghamella elegans*. Appl. Environ. Microbiol. 3654-3659.
- Cerniglia, C. E. 1992b. Biodegradation of polycyclic aromatic hydrocarbons. Biodegradation 3:351-368.
- Cerniglia, C. E., Sutherland, J. B., Fu, P. P., Yang, S. K., von Tungeln, L. S., Casillas, R. P. & Crow, S. A. 1993. Enantiomeric composition of the *trans*-dihydrodiols produced from phenanthrene by fungi. Appl. Environ. Microbiol. 2145-2149.
- Chang, J. 1981. Studies on suppressive action of total glycosides in *Tripterygium wilfordii* to humoral immunity. Symposium on Experimental and Clinical Studies of the Total Glycosides in Tripterygium wilfordii Hook F., Experimental section. 69-74.
- Chen, K-C., Yang, R-Z. & Wang, C-B. 1986. The lactone compounds in Hubei *Tripterygium wilfordii*. Chinese Tradition. Herb. Med. 17:242-245.
- Chen, K., Shi, Q., Fujioika, T., Zhang, D-C., Hu, C-Q., Jin, J-Q., Kilkuskie, R.E. & Lee, K-H. 1992. Anti-AIDS agents, 4. Tripterifordin, a novel anti-HIV principle from *Tripterygium wilfordii*: isolation and structural elucidation. J. Nat. Prod. 55:88-92.
- Cheng, Y-L., Ye, J-R., Lin, D-J., Lin, L-J. & Zhu, J-N. 1981. Some toxicities of triptolide in mice and dogs. Chung-kuo Yao Li Hsueh Pao. 2(1):70-72.

- Chibata, I. 1978. Immobilized Enzymes - Research and Development. John Wiley & Sons, Inc., New York.
- Chibata, I., Tosa, T & Sato, T. 1983a. Immobilized cells in the preparation of fine chemicals. Adv. Biotechnol. Processes. 10:203-222.
- Chibata, I & Wingard, L. B., Jr. 1983b. Immobilized microbial cells. Appl. Biochem. Bioeng. 4:1-349.
- Chibata, I., Tosa, T. & Sato, T. Methods of cell immobilization. Ch. 18. In Demain, A. L. & Solomon, N. A., Eds., 1986. Manual of Industrial Microbiology and Biotechnology. American Society for Microbiology, Washington, D.C., pp. 217-249.
- Davies, D. 1963. The Design and Analysis of Industrial Experiment. Oliver & Boyd, London.
- Deming, S. N. & Morgan, S. L. 1987. Data Handling in Science and Technology. Vol. 3. Experimental Design a Chemometric Approach. Elsevier, Amsterdam.
- Deng, F-X., Zhou, B. N., Wang, Z-D., Ma, G-G., Song, G-Q. & Chen, Z-X. 1981. Structural determination of triptonolide, a new diterpenoid lactone. Acta Pharmaceutica Sinica 16:155-157.
- Deng, F-X., Huang, S-Q., Song, G-Q. & Hu, C-Q. 1982. The isolation and structure of two new diterpenoid lactones, triptophenolide methyl ether and neotriptophenolide. Acta Pharmaceutica Sinica 17:146-150.
- Deng, F-X., Huang, S-Q., Cao, J-H., Xia, Z-L., Lin, S., Zhu, D-Y., Jiang, S-H. & Zhu, Y-L. 1985. The isolation and structure of three new diterpenes from *Tripterygium wilfordii*. Acta Botanica Sinica 27:516-519.

- Deng, F-X., Cao, J-H., Xia, Z-L., Lin, S., Zhu, D-Y. & Jiang, S-H. 1987. The isolation and structure of triptonoterpenol. Acta Pharmaceutica Sinica 22:377-379.
- Deng, F-X., Xia, Z-L., Xu, R-Q. & Chen, J-Y. 1992. The structure of triptotetraolide and wilforjine. Acta Botanica Sinica 34:618-621.
- Dunn, G. M. 1985. Ch.7. Nutritional requirements of Microorganisms. In Moo-Young, M. Ed. Comprehensive Biotechnology. A. Wheaton & Co. Ltd., Exeter, Great Britain, pp. 113-126.
- Duppel, W., Lebeault, J-M., & Coon, M. J. 1973. Properties of a yeast cytochrome P-450-containing enzyme system which catalyzes the hydroxylation of fatty acids, alkanes, and drugs. Eur. J. Biochem. 36:583-592.
- Finkelstein, D. B. & Ball, C. H. 1991. Biotechnology of Filamentous Fungi, Technology and Products. Butterworth-Heinmann, Boston, pp. 68, 76, 157-187
- Frieze, D. M., Berchtold, G. E. & Blount, J. F. 1978. Studies on the total synthesis of triptolide. II. The C-ring functionality of triptonide. Tetrahedron Lett. 47:4607-4610.
- Garcia-Ochoa, F., Santos, V. E. & Fritsch, A. P. 1992. Nutritional study of *Xanthomonas campestris* in xanthan gum production by factorial design experiments. Enzyme Microb. Technol. 4:991-996
- Gibson, D. T. & Cerniglia, C. E. 1977. Metabolism of naphthalene by *Cunninghamella elegans*. Appl. Environ. Microbiol. 34:363-370.
- Gibson, D. T., Cerniglia, C. E., Herbert, R. L., & Szaniszló, P. J. 1978. Fungal transformation of naphthalene. Arch. Microbiol. 117:135-143.

- Gilman, A. G., Rall, T. W., Nies, A. & Taylor, P. 1990. The Pharmacological Basis of Therapeutics. 8<sup>th</sup> ed. Pergamon Press, New York. 1264-1266.
- Greasham, R. & Inamin, E. 1986. Manual of Industrial Microbiology and Biotechnology. Demain, A & Solomon, N., Eds. American Society for Microbiology, Washington, D.C.
- Gu, W-Z., Banerjee, S., Rauch, J. & Brandwein, S. R. 1992a. Suppression of renal disease and arthritis, and prolongation of survival in MRL-*lpr* mice treated with an extract of *Tripterygium wilfordii* Hook F. Arthritis Rheum. 35:1381-1386.
- Gu, W-Z., Brandwein, S. R. & Banerjee, S. 1992b. Inhibition of type II collagen induced arthritis in mice by an immunosuppressive extract of *Tripterygium wilfordii* Hook F. J. Rheumatol. 19:682-688.
- Guengerich, F. P. 1991. Reactions and significance of cytochrome P-450 enzymes. J. Biol. Chem. 266:10019-10022.
- Guo, J., Yuan, S., Wang, X., Xu, S. & Li, D. 1981. *Tripterygium wilfordii* Hook F in rheumatoid arthritis and ankylosing spondylitis. Chin. Med. J. 7:405-412.
- Haaland, P. D. 1989. Experimental Design in Biotechnology. Marcel Dekker Inc., New York, pp. 29-35, 85-98.
- Han, K. 1995. Studies with Plant Cell Cultures of *Tripterygium wilfordii* - Isolation of Metabolites and Biotransformation. Ph.D. Thesis, University of British Columbia.
- Hattory, T. & Furusaka, C. 1960. Chemical activities of *Escherichia coli* adsorbed on a resin. J. Biochem. 48:831-837

- Hattory, T & Furusaka, C. 1961. Chemical activities of *Azotobacter agilis* adsorbed on a resin. J. Biochem. 50:312-315
- Hawker, L. E. & Linton A., Eds. 1975. Microorganisms, Functions, Form and Environment. Edward Arnold, London, pp. 70, 93.
- Hawksworth, D. 1977. Mycologist's Handbook. Commonwealth Mycological Institute, Surrey, England.
- Holland, H. L., Kinderman, M., Kumaresan, S. & Stefanac, T. 1993. Side chain hydroxylation of aromatic compounds by fungi. Part 5. Exploring the benzylic hydroxylase of *Mortierella isabellina*. Tetrahedron Asymmetry 4:1353-1364.
- Hou, D. H., Chen, H. G., Li, L. & Xu, L. F. 1980. Effect of total glycosides of Lei Gong Teng on experimental paw edema in rats and its mechanism of action. J. Nanjing College of Pharmacy 2:44-48.
- Huang, M. T., Johnson, E. F., Muller-Eberhard, U., Koop, D.R., Coon, M. J. & Conney, A. H. 1981. Specificity in the activation and inhibition by flavonoids of benzo[a]pyrene hydroxylation by cytochrome P-450 isozymes from rabbit liver microsomes. J. Biol. Chem. 256, 10897-10901.
- Huang, S. [Ed.] 1982. The Saint Peasant's Scripture of Materia Medica. Publishing House for Chinese Medical Classics, Beijing, pp. 309-310.
- Jack, T. R. & Zajic, J. E. 1977. The enzymatic conversion of L-histidine to urocanic acid by whole cells of *Micrococcus luteus* immobilized on carbodiimide activated carboxymethyl cellulose. Biotechnol. Bioeng. 19:631-648.

- Kalb, V. F., Woods, C. W., Turi, T. G., Dey, C. R., Sutter, T. R. & Loper, J. C. 1987. Primary structure of the P-450 lanosterol demethylase gene from *Saccharomyces cerevisiae*. DNA 6, 529-537.
- Kao, N. L., Richmond, G. W. & Moy, J. N. 1993. Resolution of severe lupus nephritis associated with *Tripterygium wilfordii* Hook F ingestion. Arthritis Rheum. 36:1751-1756.
- Kluger, M. J., Oppenheim, J. J. & Powanda, M. C. 1985. The physiologic, metabolic and immunologic actions of interleukin-1. Alan R. Liss., Inc., New York.
- Kupchan, S. M., Court, W. A., Dailey, R. G., Gilmore, C. J. & Bryan, R. F. 1972. Triptolide and triptdiolide, novel anti-leukemic diterpenoid epoxides from *Tripterygium wilfordii*. J. Am. Chem. Soc. 94:7194-7195.
- Kupchan, S. M. & Schubert, R. M. 1974. Selective alkylation: a biomimetic reaction of the antileukemic triptolides. Science 185:791-793.
- Kuri-Brena, F. 1992. Studies on Plant Cell Cultures of *Podophyllum peltatum* and *Tripterygium wilfordii* for Biosynthesis of Biologically Active Compounds, Ph. D. Thesis, University of British Columbia, Ch. 2.
- Kutney, J. P., Hewitt, G. M., Kurihara, T., Salisbury, P. J., Sindelar, R. D., Stuart, K. L., Townsley, P. M., Chalmers, W. T. & Jacoli, G. G. 1981a. Cytotoxic diterpenes triptolide, triptdiolide, and cytotoxic triterpenes from tissue cultures of *Tripterygium wilfordii*. Can. J. Chem. 59:2677-2683.
- Kutney, J. P., Singh, M., Hewitt, G., Salisbury, P. J., Worth, B. R., Servizi, J. A., Martens, D. W. & Gordon, R. W. 1981b. Studies



- related to biological detoxification of Kraft pulp mill effluent. I. The biodegradation of dehydroabietic acid with *Mortierella isabellina*. Can. J. Chem. 59:2334-2341.
- Kutney, J. P., Singh, M., Dimitriadis, E., Hewitt, G. M., Salisbury, P. J., Worth, B. R., Servizi, J. A., Martens, D. W. & Gordon, R. W. 1981. Studies related to biological detoxification of Kraft pulp mill effluent. II. The biotransformation of isopimaric acid with *Mortierella isabellina*. Can. J. Chem. 59:3350-3355.
- Kutney, J. P., Dimitriadis, E., Hewitt, G. M., Singh, M. & Worth, B. R. 1982a. Studies related to biological detoxification of Kraft pulp mill effluent. III. The biodegradation of abietic acid with *Mortierella isabellina*. Helv. Chim. Acta 65:661-670.
- Kutney, J. P., Dimitriadis, E., Hewitt, G. M., Salisbury, P. J., Singh, M., Servizi, J. A., Martens, D. W. & Gordon, R. W. 1982b. Studies related to biological detoxification of Kraft pulp mill effluent. IV. The biodegradation of 14-chlorodehydroabietic acid with *Mortierella isabellina*. Helv. Chim. Acta 65:1343-1350.
- Kutney, J. P. & Dimitriadis, E. 1982c. Studies related to biological detoxification of Kraft pulp mill effluent. V. The synthesis of 12- and 14-chlorodehydroabietic acids and 12,14-dichlorodehydroabietic acid, fish-toxic diterpenes from Kraft pulp mill effluent. Helv. Chim. Acta 65:1351-1358.
- Kutney, J. P., Choi, L. S. L., Duffin, R., Hewitt, G., Kawamura, N., Kurihara, T., Salisbury, P., Sindelar, R., Stuart, K. L., Townsley, P. M., Chalmers, W. T., Webster, F. & Jacoli, G. G. 1983a. Cultivation of *Tripterygium wilfordii* tissue cultures for the

- production of the cytotoxic diterpene triptolide. Planta Medica 48:158-163.
- Kutney, J. P., Dimitriadis, E., Hewitt, G. M., Salisbury, P. J., Singh, M., Servizi, J. A., Martens, D. W., and Gordon, R. W. 1983b. Studies related to biological detoxification of Kraft pulp mill effluent. VI. The biodegradation of 12,14-dichlorodehydroabiatic acid with *Mortierella isabellina*. Helv. Chim. Acta 66:921-928.
- Kutney, J. P., Hewitt, G. M., Salisbury, P. J., Singh, M., Servizi, J. A., Martens, D. W. & Gordon, R. W. 1983c. Studies related to biological detoxification of Kraft pulp mill effluent. VII. The biotransformation of 12-chlorodehydroabiatic acid with *Mortierella isabellina*. Helv. Chim. Acta 66:2191-2197.
- Kutney, J. P., Choi, L. S. L., Hewitt, G. M., Salisbury, P. S. & Singh, M. 1985. Biotransformation of dehydroabiatic acid with resting cell suspensions and calcium alginate-immobilized cells of *Mortierella isabellina*. Appl. Environ. Microbiol. 49:96-100.
- Kutney, J. P., Berset, J. D., Hewitt, G. M. & Singh, M. 1988. Biotransformation of dehydroabiatic, abiatic, and isopimaric acids by *Mortierella isabellina* immobilized in polyurethane foam. Appl. Environ. Microbiol. 54:1015-1022.
- Kutney, J. P., Hewitt, G. M., Lee, G., Piotrowska, K., Roberts, M. & Rettig, S. J. 1992. Studies with tissue cultures of the Chinese herbal plant, *Tripterygium wilfordii*. Isolation of metabolites of interest in rheumatoid arthritis, immunosuppression, and male contraceptive activity. Can. J. Chem. 70: 1455-1480.

- Kutney, J. P. 1993. Plant cell culture combined with chemistry: A powerful route to complex natural products. Acc. Chem. Res. 26(10): 559-566.
- Lai, C.K., Buckanin, R. S., Chen, S. J., Zimmerman, D. F., Sher, F. T. & Berchtold, G. E. 1982. Total synthesis of racemic triptolide and triptonide. J. Org. Chem. 47:2364-2369.
- Lan, Z-J., Gu, Z-P., Lu, R-F. & Zhuang, L-Z. 1992. Effects of multiglycosides of *Tripterygium wilfordii* (GTW) on rat fertility and Leydig and Sertoli cells. Contraception 45:249-261.
- Levinson, A. S., Carter, B. C. & Taylor, M. L. 1968. Microbial degradation of methyl dehydroabietate. Chem. Commun. 1344.
- Li, L. S., Zhang, X., Chen, H.P., Y.; Ji, D. X., Zhang, J. H., Hou, F. F., & Chen, P. D. 1982. Effect of *Tripterygium wilfordii* in the treatment of nephritis. Nat. Med. J. China 62: 581-585.
- Li, X. W. & Weir, M. R. 1990. Radix *Tripterygium wilfordii* - A Chinese herbal medicine with potent immunosuppressive properties. Transplantation 50:82-86.
- Li, X-Y. 1993. Anti-inflammatory and immunosuppressive components of *Tripterygium wilfordii* Hook F. Int. J. Immunotherapy 3:181-187.
- Lu, X-Y., Ma, P-C., Chen, Y., Zhang, C-P., Zhang, Y-G., Zhang, Z-X., Sheng, L-S., Li, S-Z., An, D-K., He, C-H. & Zheng Q-T. 1990. The isolation and structure of tripchlorolide (T<sub>4</sub>) from *Tripterygium wilfordii*. Acta Academiae Medicinae Sinicae 12(3):157-161.
- Ma, P-C., Lu, X-Y., Yang, J-J. & Zheng, Q-T. 1991. Structural study of triptriolide isolated from *Tripterygium wilfordii*. Acta Pharmaceutica Sinica 26:759-763.

- Manly, B. F. J. 1992. The design and analysis of research studies. Cambridge University Press, Cambridge.
- Matlin, S. A., Belenguer, A., Stacey, V. E., Qian, S. Z., Xu, Y., Zhang, J. W., Sanders, J. K. M., Amor, S. R. & Pearce, C. M. 1993. Male antifertility compounds from *Tripterygium wilfordii* Hook F. Contraception 47:387-400.
- Mead, R., Curmow, R. N. & Hasted, A. M. 1993. Statistical Methods in Agriculture and Experimental Biology. Chapman and Hall, London, pp.111-119, 183-210.
- Milanova, R. & Moore, M. 1993. The hydroxylation of plant diterpene analogues by the fungus *Syncephalastrum racemosum*. Arch. Biochem. Biophys. 303:165-171.
- Milanova, R., Hirai, Y. & Moore, M. 1994. Hydroxylation of synthetic abietane diterpenes by *Aspergillus* and *Cunninghamella* species: novel route to the family of diterpenes isolated from *Tripterygium wilfordii*. J. Nat. Prod. 57:882-889.
- Milanova, R., Han, K. & Moore, M. 1995. Oxidation and glucose conjugation of synthetic abietane diterpenes by *Cunninghamella* sp. II. Novel routes to the family of diterpenes from *Tripterygium wilfordii*. J. Nat. Prod. in press
- Miyazaki, N., Sato, K., Goto, M., Sasano, M., Natsuyama, M., Inoue, K. & Nishioka, K. 1988. Augmented interleukin-1 production and HLA-DR expression in the synovium of rheumatoid arthritis patients. Arthritis Rheum. 31:480-486.
- Mori, K. & Aki, S. 1993. Synthesis of the racemic form of tripterifordin, a novel anti-HIV diterpene lactone from *Tripterygium wilfordii*. Liebigs Ann. Chem. 97-98.

- Moser, A. 1988. Bioprocess Technology, Kinetics and Reactors. Springer-Verlag, New York, pp. 1.
- Navarro, J. M. & Durand, J. 1977. Modification of yeast metabolism by immobilization onto porous glass. Eur. J. Appl. Microbiol. 4:243-254.
- Ortiz de Montellano, P. & Matthews, J. M. 1981. Autocatalytic alkylation of the cytochrome P-450 prosthetic hem group by 1-aminobenzotriazole. Biochem. J. 195:761-764.
- Pelczar, M. J. Jr., Chan, E. C. S., Krieg, N. R., Edwards, D. D. & Pelczar, M. F. 1993. Microbiology: Concepts and Applications. MacGraw-Hill, New York.
- Petersen, R. 1985. Design and Analysis of Experiments. Marcel Dekker, Inc., New York.
- Pirt., S. J., 1975. Principles of Microbe and Cell Culture. Blackwell, Oxford.
- Qian, S-Z., Zhong, C-Q. & Ye, X. 1986a. Effect of *Tripterygium wilfordii* Hook F on the fertility of rats. Contraception 33(2):105-110.
- Qian, S-Z., Zhong, C-Q., Xu, Y., Ni, L-Q. & Feng, G-Z. 1986b. Antifertility effect of *Tripterygium wilfordii* in men. Adv. Contracep. 2:253-254.
- Qian, S-Z., Zhong, C-Q. & Xu, Y. 1986c. Studies on the reversibility of the antifertility effect of *Tripterygium wilfordii*. Adv. Contracep. 2:298.
- Qian, S-Z. 1987a. *Tripterygium wilfordii*, a Chinese herb effective in male fertility regulation. Contraception 36(3):335-345.

- Qian, S-Z. 1987b. In Diczfalusy, E. & Bygdeman, M. [Eds.] Fertility Regulation Today and Tomorrow. Raven Press, New York, pp. 217-232.
- Qin, W. Z. 1981. Advances in clinical studies on *Tripterygium wilfordii* and *Tripterygium hypoglaucum*. Shanghai J. Chin. Med. 5:46-48.
- Quenouille, M. H. 1953. The Design and Analysis of Experiment. Hafner Publishing Company, New York.
- Raktoe, B. L., Hedayat, F. & Federer, W. T. 1981. Factorial Designs John Willey & Sons, New York.
- Roberts, M. 1989. Studies with Tissue Cultures of *Tripterygium wilfordii*. Isolation of Metabolites and Biotransformation Studies. Ph. D. Thesis, University of British Columbia.
- Rosazza, J. P. & Smith, R. V. 1974. Microbial models of mammalian metabolism. Aromatic hydroxylation. Arch. Biochem. Biophys. 161:551-558.
- Rosazza, J. P. 1982. Microbial Transformations of Bioactive Compounds. Vol. II CRC Press, Inc., Boca Raton, Florida pp. 7-10.
- Sanglard, D., & Loper, J. C. 1989. Characterization of the alkane-inducible cytochrome P-450 (P-450 alk) gene from the yeast *Candida tropicalis*: identification of a new P-450 gene family. Gene 76:121-136.
- Santen, R. J., van den Bossche, H., Symoens, H. Brugmans, J. & Decoster, R. 1983. Site of action of low dose ketoconazole on androgen biosynthesis in men. J. Clin. Endocrin. Metab. 57:732-736.

- Sara, M., Redin, I., Ochin, F., Godia, F. & Casas, C. 1993. Application of factorial design to the optimization of medium composition in batch cultures of *Streptomyces lividans* TK21 producing a hybrid antibiotic. Biotechnol. Lett. 15:559-564.
- Shen, J. H. & Zhou, B. N. 1992. Studies on diterpene-quinones of *Tripterygium regelii* Sprague. Chin. Chem. Lett. 3:113-116.
- Sheng, J-H. 1990. Studies on isolation and structural elucidation of metabolites derived from *Tripterygium wilfordii* var. *regelii*. Ph.D. thesis, Shanghai Institute of Materia Medica, Chinese Academy of Sciences.
- Shishido, K., Goto, K., Miyoshi, S., Takaishi, Y. & Shibuya, M. 1993. Total synthesis of (+/-)-Triptoquinone A. Tetrahedron Lett. 34:339-340.
- Shishido, K., Nakano, K., Wariishi, N., Tateishi, H., Omodani, T., Shibuya, M., Goto, K., Ono, Y. & Takaishi, Y. 1994. Diterpene quinoides from *Tripterygium wilfordii* var. *regelii* which are interleukin-1 inhibitors. Phytochem. 35:731-737.
- Takaishi, Y., Aihara, F., Tamai, S., Nakano, K., & Tomimatsu, T. 1992a. Sesquiterpene esters from *Tripterygium wilfordii*. Phytochem. 31:3943-3947.
- Takaishi, Y., Shishido, K., Wariishi, N., Shibuya, M., Goto, K., Kido, M., Takai, M. & Ono, Y. 1992b. Triptoquinone A and B, novel interleukin-1 inhibitors from *Tripterygium wilfordii* var. *regelii*. Tetrahedron Lett. 33:7177-7180.
- Tao, X., Davis, L. S. & Lipsky, P. E. 1991. Effect of an extract of the Chinese herbal remedy *Tripterygium wilfordii* Hook F. on human immune responsiveness. Arthritis Rheum. 34:1274-1281.

- Tokoroyama, T., Koike, H., Kondo, A., Hirotsu, K. & Ezaki, Y. 1981. Tennen Yuki Kagobutsu Toronkai Koen Yoshishu, 24th, pp. 330-339.
- Tortora, G. J., Funke, B. R. & Case, C. L. 1989. Microbiology, An Introduction. The Benjamin/Cummings publishing Co., Inc., Redwood City, CA.
- Tripterygium* Study Group, Institute of Dermatology, Chinese Academy of Medical Sciences. 1982. Chin. J. Dermatol. 15(4):199.
- Van den Bossche, H., Lauwers, W., Willemsens, G., Marichal, P., Cornelissen, F. & Cools, W. 1984. Molecular basis for the antimycotic and antibacterial activity of N-substituted imidazoles and triazoles: the inhibition of isoprenoid biosynthesis. Pesticide Sci. 15:188-198.
- VanEtten, H. D., Matthew, D. E. & Smith, D. A. 1982. In Bailey, J. A. & Mansfield, J.W. [Eds.] Phytoalexins. Blackie, Glasgow, London, pp. 181-217.
- VanEtten, H. D., Matthews, D. E. & Matthews, P. S. 1989. Phytoalexin detoxification: importance for pathogenicity and practical implications. Ann. Rev. Phytopathol. 27:143-164.
- Wang, Y. S. Ed. 1983. The Pharmacology and Application of Chinese Traditional Medicine. People's Med. Publishing House, Beijing, pp.1186-1196
- Willemsens, G., Cools, W. & van den Bossche, H. 1980. In van den Bossche, H. [Ed.] The Host Invader Interplay. Elsevier/North Holland, Amsterdam, pp. 691-694.



- Wu, D-G., Sun, X-C. & Li, F. 1979. Novel diterpene lactones hypolide and tripterolide isolated from *Tripterygium hypoglaucum*. Acta Botanica Yunnanica 1:29-35.
- Xu, W. Y. 1981. The clinical use of *Tripterygium wilfordii* in various diseases. Symposium on *Tripterygium wilfordii*, Nanjing.
- Xu, W. Y., Zhang, J. R. & Lu, X. Y. 1985. *Tripterygium wilfordii* in dermatologic therapy. Int. J. Dermatol. 2:152-157.
- Xu, W., Rumin, Z. & Zhengji, H. 1993. Aneuploidy induction by water extract from *Tripterygium hypoglaucum* (Level) Hutch in mouse bone marrow cells. Mutagenesis 8:395-398.
- Yu, D. Y. 1983. Clinical observation of 144 cases of rheumatoid arthritis with glycoside of radix *Tripterygium wilfordii*. J. Trad. Chin. Med. 3:125-129.
- Zhang, T-M., Chen, Z-Y. & Lin, C. 1981. Antineoplastic action of triptolide and its effect on immune function in mice. Zhongguo Yaou Xuebao 2(2):128-131.
- Zhang, L., Zhang, Z-X., An, D-K. & Kong, C. 1991. Studies on the chemical constituents of *Tripterygium hypoglaucum* (Level) Hutch. Acta Pharmaceutica Sinica 26:515-518.
- Zhang, L., Zhang, Z-X., Sheng, L-S. & An, D-K. 1992a. Chemical constituents of *Tripterygium hypoglaucum* II. Chinese Tradition. Herb. Med. 23(7):339-340, 360.
- Zhang, X-M., Wang, C-F. & Wu, D-G. 1992b. The abietane type diterpenes from the root of *Tripterygium hypoglaucum*. Acta Botanica Yunnanica 14:319-322.
- Zhang, C-P., Lu, X-Y., Ma, P-C., Chen, Y., Zhang, Y-G., Yan, Z., Chen, G-F., Zheng, Q-T., He, C-H. & Yu, D-Q. 1993. Studies on

- diterpenoids from leaves of *Tripterygium wilfordii*. Acta Pharmaceutica Sinica, 28:110-511.
- Zheng, J., Xu, L., Ma, L., Wang, D. & Gao, J. 1983a. Studies on pharmacological effects of total glycosides of *Tripterygium wilfordii*. Acta Acad. Med. Sinica 5(1):1-8.
- Zheng, J., Liu, J., Hsu, L., Gao, J. & Jiang, B. 1983b. Studies on toxicity of total glycosides in *Tripterygium wilfordii*. Acta Acad. Med. Sinica 5(2):73-78.
- Zheng, J. R., Fang, J. L., Xu, L. F., Gao, G. W., Guo, H. Z., Li, Z. R. & Sun, H. Z. 1985a. Effect of total glycosides of *Tripterygium wilfordii* on animal reproductive organs. I. Experiments in male rats. Acta Acad. Med. Sinica 7:1-5.
- Zheng, J. R., Fang, J. L., Xu, L. F., Gao, J. W., Guo, H. Z., Li Z. R. & Sun, H. Z. 1985b. Effect of total glycosides of *Tripterygium wilfordii* on animal reproductive organs. II. Experiments in female rats. Acta Acad. Med. Sinica 7:256-259.
- Zheng, J., Fang, J., Gu, K., Xu, L., Gao, J., Guo, H., Yu, Y. & Sun, H. 1987a. Screening of active anti-inflammatory immunosuppressive and antifertility compounds from *Tripterygium wilfordii*. I. Screening of 8 components from total glucosides of *Tripterygium wilfordii* (T<sub>II</sub>). Acta Acad. Med. Sinica 9(5):317-322.
- Zheng, J., Fang, J., Gu, K., Yin, Y., Xu, L., Gao, J., Guo, H., Yu, Y. & Sun, H. 1987b. Screening of active anti-inflammatory immunosuppressive and antifertility compounds from *Tripterygium wilfordii*. II. Screening of 5 monomers from the total glucosides of *Tripterygium wilfordii* (T<sub>II</sub>). Acta Acad. Med. Sinica 9(5):323-328.

Zhou, B-N., Zhu, D-Y., Deng, F-X., Huang, C-G., Kutney, J. P. & Roberts, M. 1988. Studies on new components and stereochemistry of diterpenoids from *Tripterygium wilfordii*. Planta Medica 54:330-332.